Centro Brasileiro de Pesquisas Físicas

Isadora Barbosa Lima Veeren

Micro vs Macro:
Probing the frontiers between quantum and classical regimes
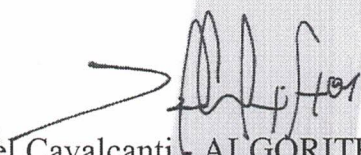
Rio de Janeiro, RJ
2023

"MICRO VC MACRO: PROBING THE FRONTIER BETWEEN QUANTUM AND CLASSICAL REGIMES"
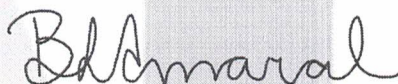
ISADORA BARBOSA LIMA VEEREN

Tese de Doutorado em Física apresentada no
Centro Brasileiro de Pesquisas Físicas do
Ministério da Ciência Tecnologia e Inovação.
Fazendo parte da banca examinadora os seguintes
professores:

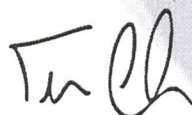Fernando da Rocha Vaz Bandeira de Melo - Orientador/CBPF

Daniel Cavalcanti - ALGORITHMIQ

Barbara Lopes Amaral - USP

Rafael Chaves Souto Araújo – IIP/UFRN

Marcelo Terra Cunha - UNICAMP

Rio de Janeiro, 30 de maio de 2023.

Isadora Barbosa Lima Veeren

Micro vs Macro:
Probing the frontiers between quantum and classical regimes

Centro Brasileiro de Pesquisas Físicas

Orientador: Dr. Fernando de Melo

Rio de Janeiro, RJ
2023

Abstract

In this work, we present a collection of results obtained from different research projects. In the first part, we investigate the so-called quantum-to-classical transition under the lens of coarse-grained measurements. We show that imprecision is a key ingredient for such transition to take place, and establish a critical value for imprecision, above which it is possible to prepare a state with magnetization in two perpendicular directions simultaneously well-defined. We also explore how irreversible dynamics can arise from reversible closed-system dynamics, when one only has partial access to the degrees of freedom of the physical system being studied. Using coarse-graining methods, we indicate what are the conditions that determine whether the emerging dynamics are reversible or not.

On the second part, we explore several areas of quantum information foundations. We first develop a method to characterize quantum contextuality when dimension restrictions are imposed on the system, a problem that could not, so far, be tackled efficiently. We also introduce a semi-device independent procedure to certify, in a bipartite steering scenario, that one of the parties is able to perform at least a certain number of measurements. Finally, we explore the framework of process matrices to investigate scenarios of indefinite causal order and shine light on the role of signaling in imposing limitations to what processes are physical and what are not possible.

Keywords: coarse-graining, entropic uncertainty relation, steering, contextuality

Resumo

Nesse trabalho, apresentamos uma coleção de resultados obtidos de diferentes projetos de pesquisa. Na primeira parte, investigamos a chamada transição clássico-quântico sob a lente de medições em *coarse-graining*. Mostramos que imprecisão é um ingrediente chave para que tal transição ocorra, e estabelecemos um valor crítico para a imprecisão, acima do qual é possível preparar um estado com magnetização em duas direções perpendiculares simultaneamente bem befinidas. Também exploramos como dinâmicas irreversíveis podem emergir de dinâmicas de sistemas fechados (e portanto, reversíveis), quando só se tem acesso parcial aos graus de liberdade do sistema de interesse. Usando métodos de coarse-graining, indicamos quais as condições para determinar se a dinâmica emergente é reversível ou não.

Na segunda parte, exploramos diversas áreas de fundamentos da mecânica quântica. Primeiro, desenvolvemos um método para caracterizar contextualidade quântica quando restrições de dimensão são impostas ao sistema, um problema até então sem solução eficiente. Também introduzimos um procedimento *semi-device independent* para certificar, em um cenário bipartido de *steering*, que uma das partes é capaz de realizar pelo menos um certo número de medições. Finalmente, exploramos o uso de matrizes de processo para investigar cenários de ordem causal indefinida e iluminar o papel de sinalização em impor limitações físicas a processos, definindo quais são possíveis e quais não.

Palavras-chave: coarse-graining, relações entrópicas de incerteza, steering, contextualidade

Contents

Agradecimentos

Introduction

When I meet new people and go through that initial exchange of basic information, I usually get the same reaction upon stating that I am PhD candidate in physics, specifically in the field of quantum mechanics: they either state something about how they hated physics in high school or they actually get somewhat interested and start making questions. Sooner or later in the conversation they realize there is a huge gap between Hollywood blockbuster quantum mechanics and what I actually do in my research, and get a bit disappointed or, to my dismay, even bored (though I have intentionally picked my research topics in order to maximize their "conversa de bar" potential). Time travel in outer space, multiverse quantum realm, or the infamous flux capacitor aren't really quantum mechanics, I argue, and the dreaded question usually follows: "OK, so what is quantum mechanics?". And the answer is... well, I don't know either.

Any undergrad student by the end of their program can tell you about the postulates of quantum mechanics, or apply Schrödinger's equation in a range of scenarios, and yet, in a sense, I have spent the last four years trying to answer this very question (without hopes, or even the ambition, of actually doing so). To me, the complexity of this matter is made more evident if one evaluates the complementary question: what *isn't* quantum mechanics?

If one takes the atomic hypothesis and accepts that every physical system is emerging as the result of a microscopic world, then it must be that understanding our everyday domain should boil down to the characterization of this underlying system (as complex as this description may be). If one admits this universality argument, then, in a sense, everything is quantum and quantum mechanics can be applied to systems on any size scale, at least in principle.

Stating that "everything is quantum" and calling it a day, however, is somewhat unsatisfactory, as it sure does not seem that everything is quantum. Where is everyday non-locality, measurement incompatibility or contextuality in our lives? Quantum mechanics has so many unique aspects to it when compared with classical physics, that it takes extra steps to make the universality argument compatible with the seemingly non-quantum experience with have of the world.

In this work, I tried to approach the dichotomy between quantum and classical regimes by two fronts. The first one, presented in part I is by gliding the abstract quantum-classical frontier and using coarse-grained measurements to explore the descriptions that arise. In chapter 1, we directly tackle the transition that must take place between a quantum and a classical description of a system. We investigate how performing macroscopic measurements can make it possible to prepare a state that has two simultaneously well-defined quantities even if their associated observables do not commute. This feat, notoriously prohibited in a usual microscopic scenario, is achieved by making the model for macroscopic measurements more realistic and considering imprecision in our evaluations. In chapter 2, we investigate how having only coarse-grained access to a physical system can make irreversible effective dynamics emerge from a closed microscopic evolution. We show what is the necessary interplay between coarse-graining maps and microscopic evolutions that yields reversible dynamics on the effective level, and propose a quantifier for uncertainty in such scenarios that physically motivates which dynamics will be reversible or not.

On the second front, presented in part II, we explore some of the very features that make quantum mechanics unique, highlighting a contrast with classical regimes. In chapter 4 we provide a method to characterize the set of d-quantum behaviors, that is, the probability distributions that can result from a quantum realization with a system of dimension d. Additionally, we improve former methods to evaluate non-contextuality inequalities when a dimension restriction must be observed. In chapter 5 we construct a set of increasingly strong criteria to establish, in a bipartite steering scenario, a lower bound to the number of incompatible measurements to which Alice has access. In a one-way-device-independent fashion, Bob can construct a series of semidefinite programs that test these conditions by only using the information to which he has access. Finally, in chapter 6, we presently the preliminary results obtained

from studying geometrical properties of the space of process matrices, the main tool used to investigate scenarios of indefinite causal order. We explore the role of signaling in determining which processes are physical and simplify a series of tasks from a semidefinite program into a set of linear equations.

Before we move on, I must highlight that this document is the physical manifestation of four years of hard work but not only from my side. I owe a share of this thesis to the collaborators that contributed to these projects, either directly by doing themselves part of the calculations or indirectly by discussing my results with me. The projects presented in part I were developed under the supervision of my advisor, Fernando de Melo, at CBPF, and our work in chapter 1 is already published [1]. In chapter 2, we present the work we developed alongside Raul Vallejos (who was also responsible for a great deal of the calculations, to which I made minor adaptions for more specific cases) and Frederico Borges de Brito, now at its final stages before being compiled in a definite manuscript. The projects in part II result from external collaborations. In chapter 4, we present a project conducted online with Xiaodong Yu and Otfried Gühne, available as a pre-print [2] and awaiting peer-review. Chapter 5 features the outcome of a research project conducted during my period as a visitor at University of Siegen, in collaboration with Martin Plávala and Otfried Gühne. This project is concluded and a manuscript pre-print will follow shortly. Finally, in chapter 6 we present a work in progress still on earlier stages, whose development started during my visit to the Young Independent Research Group at Vienna, in collaboration with Yelena Guryanova and Fionnuala Curran.

Part I

Coarse-graining approach to effective descriptions

Chapter 1

Entropic uncertainty relations and the quantum-to-classical transition

As far as our scientific knowledge goes, the world is fundamentally quantum. Figuring among science's most successful theories, quantum mechanics can make astonishingly precise predictions concerning increasingly small systems. Indeed, scientists can, for instance, describe the mechanism behind the Casimir effect and measure forces with ridiculous precision [3]. As impressive as these developments are, however, they only push the boundaries of quantum mechanics in one direction, namely the microscopic realm. We have no evidence disputing its validity in small-scale systems, nevertheless the universality of quantum mechanics is not a consensus among scientists: the weakest link to its universal application are macroscopic systems.

If instead of looking downwards toward progressively small orders of magnitude we shift our gaze to bigger, macroscopic systems, we find that in fact quantum mechanics is not an apparent key constituent of our everyday lives. Of course, macroscopic effects of quantum mechanics can be found [4, 5, 6], but its most distinctive and intriguing features are loudly absent. To name a few, we do not routinely experience entanglement or tunneling in our everyday lives, neither do we endure quantum superpositions or collapses of wave functions.

The question that naturally arises is: can one characterize this transition? Where is the cut between the quantum and the classical realm, if there is a cut at all? The contrast between these two extreme paradigms is indisputable, and yet not enough is known about what lies in the middle even though this matter has been tackled since the dawn of the field. Schrödinger, for instance, presented us with his "cat paradox" [7], illustrating the odd scenarios that come up when we naively push quantum mechanics into macroscopic descriptions.

As old as the pioneering attempts of translating quantum mechanics into our everyday lives are, this whole endeavor is far from being out-dated. Enticing more than foundational interest (as if it was not enough), the need for establishing the frontiers between quantum and classical is an increasingly pressing matter. Experimental efforts made it possible to investigate physical systems of considerable size [8, 9, 10, 11], and recent developments [12, 13, 14] suggest that soon a quantum computer of mesoscopic dimension may be achievable.

Setting the quantum-classical boundary is particularly relevant for the latter, since it would help preserve the very "quantumness" of bigger physical systems, a matter that must be addressed if one expects a quantum computer to be able to significantly outperform classical computation. On one hand, outlining this transition is fundamental to understand the mechanism through which physical systems lose their quantum properties in the macroscopic limit; on the other, it prescribes attributes to preserve if one wants to actually retain quantum features in a macroscopic system.

To that end, much has been expanded since the times of Schrödinger. For instance, the understanding that quantum systems should not be treated as completely isolated has sparked the decoherence argument [15, 16, 17], since Schrödinger's equation can only be used to describe isolated systems. In a similar direction, quantum Darwinism [18] highlights the essential role played by the interaction between the physical system and its environment in generating decoherence, as well as the vanishing of quantum features [19, 20]

Decoherence alone, however, does not settle the mystery of the quantum-to-classical transition. As a theory designed to address the consistency between the dynamics and statistics of open quantum systems and the predictions of classical physics, it says nothing about closed systems (which we would likewise

expect to exhibit classical features when large enough). In fact, as pointed out for instance in [21], the "quantumness" of the system of interest leaks to the environment and the total system remains quantum. It seems that the decoherence argument, in some aspects, defers the question of the quantum-to-classical transition by redefining where to look, and thus does not completely answer it. Further criticism of its claims of solving the measurement problem and the collapse of the wave-function can be found in [22, 23, 24].

A major contribution to solving the classical enigma is provided by the more recently developed field of quantum information, namely the coarse-graining method. In this approach, it is argued that the resolution of the description of the physical system will dictate whether quantum features are preserved or not: with access to highly precise measurements one can still observe genuine quantum behavior, while coarse-grained measurements may cause such traits to vanish [25, 26, 27]. Some pieces of this huge puzzle are already in the game: it is known, for instance, that imprecise measurements might render the violation of both Bell and Leggett-Garg inequalities unachievable [28, 29, 30]. Likewise, it is shown that if one only has access to coarse-grained descriptions then entanglement and superposition might also vanish [31, 32, 33, 34].

A main piece still missing, nevertheless, concerns the preparation of macroscopic quantum systems. Among the typical quantum element absent in our ordinary macroscopic life, preparation uncertainty relations are perhaps one of the most distinctive. Even though both classical and quantum scenarios can be described through the formalism of observables, a striking feature of the latter is that they must additionally obey such uncertainty relations. Unlike classical systems, a quantum system cannot be prepared in such a way that it will have both position and momentum simultaneously well-defined [35].

With these motivations in mind, we will follow the direction given by coarse-graining arguments and use the formalism to explain why macroscopic systems don't seem to obey preparation uncertainty relations, or rather, why these relations only impose restrictions that are trivially obeyed. In particular, we will employ entropic uncertainty relations to show a mechanism through which one may prepare a macroscopic quantum system that has total magnetization in perpendicular directions simultaneously well defined, a feat that would be prohibited for microscopic systems. This chapter will report the results presented in [1] and adopt the following outline: first, we discuss preparation uncertainty relations and motivate the use of entropic uncertainty relations in spite of Heisenberg's uncertainty principle; next, we examine the preparation of macroscopic states and suggest we focus our efforts on studying the particular subclass of spin-coherent quantum states; finally, we propose a model for macroscopic measurements that successfully yields the emergence of classical behavior in macroscopic quantum systems.

Figure 1.1: On top of having central relevance in physics, preparation uncertainty relations also figures among the main quantum features that have reached pop-culture [36]

1.1 Preparation uncertainty relations

1.1.1 Heisenberg uncertainty principle

Consider the following scenario: in a lab, a quantum state ρ is prepared. Two observables, A and B can me measured, and one wants to determine how well-defined these two quantities are for ρ. To gather statistics, many runs of an experiment must be performed, where one prepares ρ and measures A. The resulting outcomes of each run are recorded and presented in a probability distribution. The very same procedure is adopted for B, and one ends up with two distributions, one for each observable.

A common measure for how well-defined the properties associated to A and B are is the spread of the outcome distributions. Intuitively, a well-defined quantity should yield precise results producing narrow distributions with small spread, and bigger spreads are associated to poorly defined properties whose outcomes are more uncertain. To capture this notion, we are virtually always introduced to Heisenberg's uncertainty principle [37] on quantum mechanics courses, usually presented in the form

$$\Delta_p \Delta_x \geq \frac{\hbar}{2}, \tag{1.1}$$

where Δ_Q is the variance of an operator Q with respect to the state ρ, calculated as

$$\Delta_Q = \sqrt{\langle Q^2 \rangle - \langle Q \rangle^2}. \tag{1.2}$$

$\langle Q \rangle = \text{Tr}[Q\rho]$ is, in turn, the mean value of Q with respect to ρ. This relation was extended to any two observables by Robertson [38] and reads, for a pure state $|\psi\rangle$, as

$$\Delta_A \Delta_B \geq \frac{1}{2} |\langle \psi | [A, B] | \psi \rangle |. \tag{1.3}$$

Mathematically, this expression states that there is a lower bound for the product of variances of any two observables given a fixed state preparation. Physically, this preparation uncertainty relation restricts how precise two properties can be, and we can only prepare a state with A and B simultaneously well-defined if these observables commute, or if $|\psi\rangle$ is a common eigenstate of A and B.

This imprecision of the outcomes of a measurement are at the core of our quest for a better understanding of the quantum-to-classical transition, as its origins are twofold. The first source is a plain, classical one, namely the restrictions one faces in a lab. There will always be experimental limitations, and finding the exact value of a physical quantity is a hopeless task, though it is possible to achieve astonishing precision. The second source stems in the very nature of quantum mechanics, and determining the true value of any quantity is impossible because they are fundamentally undetermined. Part of the imprecision lies in the technology to which one has access and can be reduced with clever designs of experiments, but another part lies in the nature of quantum physics and cannot be circumvented.

Heisenberg-like uncertainty relations (HUR) play an important role in the debate over the essence of quantum imprecision, a topic that we will explore to investigate the quantum-to-classical transition. More generally, preparation uncertainty relations are a tool that can be used to study certain aspects of an experiment and state whether they are consistent with a scenario operating in a classical or a quantum regime. In a classical paradigm (unlike a quantum one) one would presume such uncertainty relations to play no significant role, since there is no restriction to the preparation of physical systems and their well-defined properties. Hence, the expectation is that as we deal with increasingly bigger systems and approach the macroscopic limit, then the lower bound on the uncertainty of its properties should progressively decrease, eventually reaching zero. Only if such a behavior is verified can we explain why classical observables no longer seem to abide by the rules that govern quantum observables, as in fact they are automatically satisfied, imposing no further restrictions on classical systems.

The relation presented in eq. (1.3) can be used to that end. Suppose one wants to evaluate the restrictions over preparing a state with observables A_N and B_N simultaneously well-defined. A_N and B_N are defined considering N, the number of particles in the physical system. For low N, if the observables do not commute then the r.h.s. of eq. (1.3) will be different from zero, meaning they cannot be simultaneously well-defined. However, as $N \to \infty$ this lower bound should also approach zero, allowing the state to be prepared in a way that both A_N and B_N are determined, as it is in classical regimes.

Nevertheless, we will argue that alternative preparation uncertainty relation should be employed instead, as Heisenberg-like uncertainty relations have a few limitations and will pose some major inconveniences, from which we highlight the three most relevant.

We start by pointing out that the bound in HURs is state dependent. The main issue it causes is that increases or decreases in the variance associated to A do not necessarily impose any restrictions on B, since these can be easily compensated by accordingly changing $|\psi\rangle$. If one wants HUR to make a statement about the observables, one could perhaps consider a minimization over all possible states

$$\Delta_A \Delta_B \geq \min_{|\psi\rangle} \frac{1}{2} |\langle \psi | [A, B] | \psi \rangle |. \tag{1.4}$$

However, choosing $|\psi\rangle$ to be in the kernel of A will always make this lower bound vanish. In fact, the l.h.s. would also vanish and not much is learned.

Secondly, HUR is not defined for the most general measurement operators. A positive operator valued measure (POVM) is a set of n operators E_i (POVM elements) obeying $E_i \geq 0$ (positivity) and $\sum_i E_i = \mathbb{1}$ (completeness). With HUR one could only analyze quantities associated to projective measurements, where the elements must additionally be orthogonal.

Finally, Heisenberg-like uncertainty relations are sensitive to re-scaling. Since the uncertainty around an observable is measured by the variance of the probability distribution of its outcomes, a simple change of eigenvalues will tamper with the product of Δ_A and Δ_B, an undesired feature, as the eigenvalues of A and B are somewhat arbitrary. If A and B do not commute one can still change their eigenvalues and make the norm of their commutator approach zero, even if no alterations are made to their eigenvectors (so A and B still do not commute. As a result, the only meaning we can draw from HURs is whether the lower bound it imposes on $\Delta_A\Delta_B$ is zero or not, since non-zero values can be inter-exchanged freely by a re-scaling that has no concrete effects.

Let us look into the example of measurements of total magnetization in the perpendicular directions x and z. In a quantum regime, these measurements depict a notorious example of the impossibility of preparing a state with two well-defined characteristics. However, there is no restriction to these quantities in macroscopic systems: both are simultaneously well-defined for a single preparation in the classical world. Somewhere in the middle a transition must take place, and von Neumann [39] had already suggested that , for the case of position and momentum, macroscopic observables are commuting versions of the "true" quantum observables. It is not uncommon to have the quantum-to-classical transition laid out to us in a simplistic way in introductory quantum mechanics courses, where merely taking the limit $N \to \infty$ should get the job done. Indeed, an inattentive reader might agree with this claim. Take the normalized, dimensionless observables of total magnetization in three orthogonal directions

$$X_N = \frac{1}{N}\sum_{i=1}^{N}\frac{\sigma_x^{(i)}}{2}, \quad Y_N = \frac{1}{N}\sum_{i=1}^{N}\frac{\sigma_y^{(i)}}{2}, \quad Z_N = \frac{1}{N}\sum_{i=1}^{N}\frac{\sigma_z^{(i)}}{2}, \qquad (1.5)$$

where N is the number of 1/2-spin particles and $\sigma_k^{(i)}$, with $k \in \{x,y,z\}$, is the k-th Pauli matrix acting on the i-th particle. These observables are defined for different numbers of particles, and as N increases we approach a description of a macroscopic measurement of total magnetization. If we evaluate the commutator between, say, X_N and Z_N, we get

$$[X_N, Z_N] = \frac{-iY_N}{N}, \qquad (1.6)$$

and in the macroscopic limit we, indeed, get

$$\lim_{N\to\infty}||[X_N, Z_N]|| = 0. \qquad (1.7)$$

Now, plug this result into the r.h.s. of HUR in eq. (1.3) and we see that the lower bound on the product $\Delta_{X_N}\Delta_{Z_N}$ tends to zero, as expected in the classical limit.

One might be tempted to dismiss it as a case-closed, but it is necessary to point out that for no finite value of N will this limit actually reach zero nor will X_N, Z_N share a common eigenvector. Given HUR's sensitivity to re-scalings, the fact that the lower bound will never be zero cannot be overlooked and thus this proposed solution does not solve much.

It is necessary, then, to find more reliable uncertainty relations that will not be susceptible to these shortcomings, constructed from objects more sturdy than the ones employed in HURs. Following Deutsch's approach [40], a good measure of the uncertainty of measuring observables A and B on a state ψ should hold a couple relevant properties.

First, it should reach a global minimum if and only if A and B have a shared eigenstate. This is not the case for HUR, since by picking $|\psi\rangle$ in the kernel of A will make the lower bound vanish regardless of the value of $[A,B]$. Second, relabeling the eigenvalues of A and B should have no physical effects. As already discussed, this makes HUR sensitive to re-scaling and not functional in many crucial scenarios.

All things considered, it is clear that an alternative to Heisenberg-like uncertainty relations must be employed. It should maintain all the main features of HURs and have a sound physical interpretation, while being free of its limitations.

1.1.2 Entropic uncertainty relations

In this section we present entropic uncertainty relations (EUR) [41], a set of well established tools we will use instead of Heisenberg-like uncertainty relations to analyze the transition from a quantum into a

classical regime when preparing a physical system.

The main ingredient in EURs is, naturally, entropy. Though somewhat elusive, the concept of entropy tends to revolve around the notion of randomness or diversity in a system. Particularly in information theory, it indicates how much one can learn from a measurement or yet how uncertain a state is before performing such measurement [42].

Take the Shannon entropy of a random variable Q with n possible outcomes $\{o_1, \ldots, o_n\}$ and respective probabilities given by the vector $P = \{p_1, \ldots, p_n\}$ with $\sum_i p_i = 1$ and $p_i \geq 0 \ \forall i$:

$$H(Q) = -\sum_{i=1}^{n} p_i \log p_i. \tag{1.8}$$

We can make a connection to quantum mechanics by associating P to outcomes of a measurement Q, an observable with eigenvectors $|q_i\rangle$, on a state $|\psi\rangle$

$$H(Q|\psi) = -\sum_{i=1}^{n} |\langle\psi|q_i\rangle|^2 \log|\langle\psi|q_i\rangle|^2. \tag{1.9}$$

The Shannon entropy is a logical candidate to compose our desired measure of uncertainty. It naturally encompasses the notion of indeterminacy, but in a more robust way than the variance. Like the latter, it is a quantity that increases when the spread of a distribution is larger and decreases when it is smaller. In fact, the Shannon entropy is only maximal when the probability distribution is a uniform one, and it is zero if and only if the distribution has a single outcome associated to probability 1. This behavior reflects our expectation when trying to guess an outcome, we make a blind guess if we assume nothing about the probability distribution and have absolute certainty when only one result is possible.

A very similar behavior is obtained from analyzing the variance of a probability distribution but entropies have the major advantage of being unresponsive to re-scaling, since the only relevant quantities to is evaluation are probabilities themselves and eigenvalues play no role in it. For this reason, using entropy-based uncertainty relations is preferable to employing HURs. Accordingly, it is only logical to pick the sum of the Shannon entropies of measuring A and B on a state $|\psi\rangle$ as our measure of uncertainty[1]. Indeed, well-established entropic uncertainty relations already exist, among which we highlight the following [40, 43, 44].

$$H(A|\psi) + H(B|\psi) \geq -2 \log \max_{j,k} |\langle a_j|b_k\rangle|. \tag{1.10}$$

The proof of this inequality is presented in appendix A. Mathematically, this expression states that the sum of these entropies is bounded from below by a quantity that depends on the maximal overlap of eigenvectors of A and B.

Much like HURs, the inequality above sets a lower bound to the uncertainty the properties associated to observables A and B, and physically imposes a restriction to the preparation of a state with both these properties simultaneously well-defined. It also has an analogous interpretation of the quantum-to-classical transition: we expect that the lower bound on the r.h.s. should approach zero as we get closer to a classical regime, meaning there would be no restriction on the preparation of states.

This uncertainty relation is, however, more suited to our task than the one presented in eq. (1.3). The r.h.s. will only be zero if A and B share a common eigenstate, recovering Robertson's prediction that commuting observables should yield an inequality with trivial lower bound. Nevertheless, this EUR strictly outperforms Robertson's uncertainty relation because is does not fall into the pits that HUR does, namely it is not state dependent and does not rely on eigenvalues. A point worth emphasizing is that, as a result, the lower bound in EURs has physical meaning beyond being zero or not.

We can now revisit the naive solution given to the preparation of X_N and Z_N, where one simply takes the macroscopic limit and expects to witness a smooth transition from quantum to classical regime. As discussed, the fact that the lower bound in HUR approaches zero (but never actually reaches it) is not enough to argue that a state can be prepared in such a way that X_N and Z_N are simultaneously well-defined. We can now analyze the same scenario with eq. (1.10). Since the maximal overlap between its eigenvectors is $2^{-N/2}$, it is straight-forward to show that

$$H(X_N|\psi) + H(Z_N|\psi) \geq N. \tag{1.11}$$

---

[1] Notice that evaluating their product would not be very useful if, for instance, the Shannon entropy of A tends to zero

We see that, contrary to what HURs suggest, the uncertainty around the total magnetization in two orthogonal direction actually increases with the size of the state. Blindly taking the limit of $N \to \infty$ does not explain how one can prepare a classical system with X_N and Z_N simultaneously well-defined.

Now that we have a reliable tool to measure uncertainty, we can proceed to exploit it in different scenarios trying to understand how classical behavior emerges from fundamentally quantum systems. In the following sections, we will provide physically motivated adjustments to our descriptions of macroscopic preparations and measurements, constructing a model that successfully reproduces a smooth quantum-to-classical transition. For simplicity, we will restrict our analysis to the paradigmatic case of total magnetization in the $x-$ and $z-$directions, exhibiting notorious non-classical behavior in quantum regimes.

1.2 Preparing macroscopic states

When looking for a description of the quantum-to-classical transition, there is more than one ingredient that one must have in mind. In our particular task, two elements play a relevant role: the measurements we perform and the physical states we prepare. Classicality emerges not only from one or the other, and thus we must construct models for both preparation and measurements that faithfully represent our macroscopic experience. In this section we cover the former, and in what follows we will cover the latter.

A first step is to determine to which states we should restrain ourselves when studying classical, macroscopic systems. In the bosonic case [45], coherent states have the spotlight, since Schrödinger showed how a quantum harmonic oscillator resembles a classical one [7], a pioneering example of a situation where the expected behavior is recovered when taking the classical limit. A reasonable choice for us, then, is to consider generalized spin-coherent states [46], the fermionic analogous to the bosonic case, defined as

$$|\Psi_N\rangle = |\Psi_1\rangle^{\otimes N}, \tag{1.12}$$

where $|\Psi_1\rangle = \sqrt{p}|0\rangle + e^{i\phi}\sqrt{1-p}|1\rangle$ is the state of a single spin, parameterized by $p \in [0,1]$ and $\phi \in [0, 2\pi[$. The power $\otimes N$ indicates the tensor product of N copies of $|\Psi_1\rangle$ and $\{|0\rangle, |1\rangle\}$ are the eigenvectors of σ_z, corresponding to a spin-up and a spin-down particle respectively. Let the eigenvectors of σ_x be $\{|+\rangle, |-\rangle\}$, with $|\pm\rangle = (|0\rangle \pm |1\rangle)/\sqrt{2}$, and notice that the states in the set $\{|0\rangle^{\otimes N}, |1\rangle^{\otimes N}, |+\rangle^{\otimes N}, |-\rangle^{\otimes N}\}$ saturate the bound in eq. (1.11).

We can further sustain the promotion of product states by invoking its relevance in the emergence of classicality, namely in quantum Darwinism. In this approach, it is argued that different observables agree on the values of properties of macroscopic systems because information is redundantly encoded in physical states, which are selected by nature to have the form in eq. (1.12).

With this restriction in mind, we can once again evaluate the uncertainty around X_N and Z_N, now setting the physical state to be in a product form. We can calculate the Shannon entropy associated to a measurement in the $z-$direction

$$H(Z_N|\Psi_N) = -\sum_{k=1}^{N} \binom{N}{k} p^k(1-p)^{N-k} \log p^k(1-p)^{N-k}. \tag{1.13}$$

An analogous calculation for the $x-$direction yields

$$H(X_N|\Psi_N) = -\sum_{k=1}^{N} \binom{N}{k} q^k(1-q)^{N-k} \log q^k(1-q)^{N-k}, \tag{1.14}$$

where $q = (\sqrt{p} + e^{i\phi}\sqrt{1-p})/\sqrt{2}$. The derivation of these expressions can be found in appendix B.

Finally, the expression capturing the overall uncertainty of X_N and Z_N considering a state in product form is

$$H(X_N|\Psi_N) + H(Z_N|\Psi_N) = N\left(h(p) + h(q)\right), \tag{1.15}$$

where $h(p) = -p \log p - (1-p) \log(1-p)$ is Shannon's binary entropy for p, and similarly for $h(q)$.

The result in eq. (1.15) shows us that making adjustments only on the side of macroscopic preparations is not enough to witness a transition from quantum to classical regimes, because the sum of these entropies

grows with N when it should in fact decrease when approaching the classical limit. It is in accordance with other results, as in [47] where it is shown that considering coherent states is not enough to explain classical behavior (in this case, the non-violation of Leggett-Garg inequalities).

Since exploring macroscopic preparations is not enough, we move on to provide modifications to macroscopic measurements, so that these two sides combined can help explain the quantum-to-classical transition.

1.3 Macroscopic measurements

Throughout our preliminary analyses, we have assumed that we have access to perfect macroscopic measurements of total magnetization. In this section we provide a realistic versions of X_N, Y_N and Z_N, considering the nature of these observables and experimental limitations.

1.3.1 Measurement degeneracy

Up to this point, we have represented the measurement of total magnetization in a given direction through eq. (1.5). What it basically describes is a process where one measures every single spin in a system and then adds them all up. This presumes an unbelievable control of the quantum state and an unreal level of access to its properties. To say the very least, performing this measurement on a state with N spins would require a POVM with 2^N outcomes, making it not only impractical but downright impossible for macroscopic systems.

Apart from being absolutely non-functional, such measurement would be unnecessary. Since we are only concerned with the total magnetization of a system, the individual value of each spin on a state is not relevant, only the sum thereof. This gives us a hint that a realistic description of these measurements should be highly degenerate, after all many different spin configurations will yield the same total magnetization. We can make this degeneracy explicit in these measurements, so we define the observables for total magnetization in the $x-$, $y-$ and $z-$directions as

$$\tilde{X}_N = \frac{1}{N} \sum_{j_x=-N/2}^{N/2} j_x \Pi_x(j_x), \quad \tilde{Y}_N = \frac{1}{N} \sum_{j_y=-N/2}^{N/2} j_y \Pi_y(j_y), \quad \tilde{Z}_N = \frac{1}{N} \sum_{j_z=-N/2}^{N/2} j_z \Pi_z(j_z). \tag{1.16}$$

Here, $\Pi_k(j_k)$ with $k \in \{x, y, z\}$ is the projector onto the subspace of total spin j_k, in the direction k.

This description is greatly inspired by the method of types, an approach to statistics where one dismisses the complete knowledge about a system in favor of a particular characterization of it. It can be found in works of probability theory [48] and statistical physics [49], and was systematic developed in the lingo of information theory in [50].

Notice that what these observables are describing is an entirely different process than the one in eq. (1.5). Unlike, say, Z_N, $\tilde{Z}_N$ has no access to the unnecessary information about the complete spin configuration of the state, only to its total sum. It is a vastly less invasive model of measurement, while the traditional one shows itself to be an overkill. As a consequence, one goes from having to deal with an exponential number of outcomes in Z_N to the more tractable amount of $N+1$ in $\tilde{Z}_N$.

We can now evaluate the behavior of entropic uncertainty relations combining our new model for these macroscopic measurements and the assumption of states in form eq. (1.12), hoping that the uncertainty around $\tilde{X}_N$ and $\tilde{Z}_N$ decreases as a function of N, indicating that one can prepare a quantum state in product form with total magnetization in both $x-$ and $z-$direction well-defined in the macroscopic limit. In appendix B, we show that the probability of obtaining outcome j_z/N when measuring $\tilde{Z}_N$ is given by

$$\Pr(j_z|\Psi_N) = \binom{N}{\frac{N}{2}+j_z} p^{\frac{N}{2}+j_z} (1-p)^{\frac{N}{2}-j_z}. \tag{1.17}$$

This is a binomial function, with mean $\langle \tilde{Z}_N \rangle_{\Psi_N} = p - 1/2$ and standard deviation $\Delta^2(\tilde{Z}_N|\Psi_N) = p(1-p)/N$. As a result, the distribution of eigenvalues of $\tilde{Z}_N$ concentrates around the mean value with $1/\sqrt{N}$, such that for bigger and bigger systems it will increasingly tend to a delta function.

Let us now use this probability distribution to evaluate the Shannon entropy of the measurement of $\tilde{Z}_N$. It reads

$$H(\tilde{Z}_N|\Psi_N) = -\sum_{j_z=-N/2}^{N/2} Pr(j_z|\Psi_N)\log Pr(j_z|\Psi_N)$$

$$= \binom{N}{\frac{N}{2}+j_z} p^{\frac{N}{2}+j_z}(1-p)^{\frac{N}{2}-j_z}\log\binom{N}{\frac{N}{2}+j_z}p^{\frac{N}{2}+j_z}(1-p)^{\frac{N}{2}-j_z}. \tag{1.18}$$

Since we are mostly interested in the behavior of this function in the classical limit, we can take $N \to \infty$ and use the de Moive-Laplace theorem to approximate the binomial distributions with a Gaussian one. By calling $\mu = \langle \tilde{Z}_N \rangle_{\Psi_N}$ and $\sigma^2 = \Delta^2(\tilde{Z}_N|\Psi_N)$, we reach the expression

$$H(\tilde{Z}_N|\Psi_N) \cong -\int_{-\infty}^{\infty} dj_z \frac{1}{\sqrt{2\pi\sigma^2}}\exp\left[-\frac{(j_z-\mu)^2}{2\sigma^2}\right]\log\left(\frac{1}{\sqrt{2\pi\sigma^2}}\exp\left[-\frac{(j_z-\mu)^2}{2\sigma^2}\right]\right)$$

$$= \int_{-\infty}^{\infty} dj_z \frac{1}{\sqrt{2\pi\sigma^2}}\exp\left[-\frac{(j_z-\mu)^2}{2\sigma^2}\right]\left(\log\sqrt{2\pi\sigma^2}+\frac{(j_z-\mu)^2}{2\sigma^2}\log e\right) \tag{1.19}$$

$$= \log\sqrt{2\pi\sigma^2} + \frac{\log e}{2} = \frac{1}{2}\log 2\pi e N p(1-p).$$

A completely analogous calculation can be followed for $\tilde{X}_N$ such that at the end of the day we get

$$H(\tilde{X}_N|\Psi_N) + H(\tilde{Z}_N|\Psi_N) \cong \frac{1}{2}\log 4\pi^2 e^2 N^2 pq(1-p)(1-q)$$

$$= \log N + \frac{1}{2}\log 4\pi^2 e^2 pq(1-p)(1-q). \tag{1.20}$$

This result shows that, even when considering these modifications to the model of macroscopic measurements and restricting ourselves to product states, the uncertainty around orthogonal measurements of total magnetization still increases with the system size N (though at a lower rate when compared to eqs. (1.11) and (1.15)).

Considering that the probability distributions in eq. (1.17) gather around the mean value as N grows, one might be surprised that the resulting entropy does not tend to zero, after all more concentrated distributions describe less uncertain scenarios. However, we must point out that the number of outcomes is not fixed, in fact it grows linearly with N, while the distribution concentrates with $1/\sqrt{N}$. Such realization points the direction of the additional modifications that are still necessary to make these measurements more realistic.

1.3.2 Measurement imprecision

Despite the adjustment of considering the natural degeneracy of total magnetization measurements, further adjustments must be taken into consideration. The fact that the observables $\tilde{X}_N$ and $\tilde{Z}_N$ have $N+1$ outcomes is still not at par with the reality in the lab.

First of all, this is still a ridiculously high number when considering the macroscopic limit. Measuring the total magnetization in a single direction of a system of roughly 10^{23} spins would require absurd precision. On top of that, even if this number was reasonable, it has the drawback of being a function of N. A usual measurement apparatus will function the same way regardless of the system size, and will typically have fixed precision in any case.

It is not reasonable to expect a measuring device to be able to tell apart states with very close values of total magnetization. As a result, there should be a gap within which the device is inexact, and the notion of imprecision should be considered when modeling macroscopic measurements.

To that end, a binned measurement can be introduced, where we group neighboring values of total magnetization under the same bin of width δ, incorporating both our inability of distinguishing similar outcomes and the fact that devices have fixed number of outcomes and precision. Instead of evaluating, for instance, the probability of a state having total magnetization j_z/N in the $z-$direction, one evaluates its probability of having total magnetization falling on an interval $[j_z/N - \delta/2, j_z/N - \delta/2[$. In this case, the number of outcomes is simply given by the number of bins N_b, tied to the bin width as $N_b = N/\delta$.

In terms of the number of outcomes (number of bins), the n-th bin will cover total magnetizations in the interval $[-\frac{1}{2}+\frac{n-1}{N_b}, -\frac{1}{2}+\frac{n}{N_b}[$, with $n \in \{1,\ldots,N_b\}$. The resulting observables for total magnetization in the x- and z-directions are

$$X'_N = \frac{1}{N} \sum_{n_x=1}^{N_b} j_{n_x} \left(\sum_{\frac{j_x}{N} \in [-\frac{1}{2}+\frac{n_x-1}{N_b}, -\frac{1}{2}+\frac{n_x}{N_b}[} \Pi_x(j_x) \right),$$

$$Z'_N = \frac{1}{N} \sum_{n_z=1}^{N_b} j_{n_z} \left(\sum_{\frac{j_z}{N} \in [-\frac{1}{2}+\frac{n_z-1}{N_b}, -\frac{1}{2}+\frac{n_z}{N_b}[} \Pi_z(j_z) \right).$$

(1.21)

Here, j_{n_k}/N is the eigenvalue associated to bin n_k, given direction k, a value we do not have to trouble ourselves with specifying since they play no role in entropic uncertainty relations. These observables are simply grouping together neighboring values of total magnetization under a single outcome, ensuring that N_b and the device precision are fixed.

With X'_N and Z'_N at hand, we can finally analyze the sum of their associated entropies when dealing with macroscopic systems, and compare that to what is expected from classical behavior. The results are presented in the next section.

1.4 Results and discussion

We start by obtaining the probability distributions associated to the outcomes of eq. (1.21), as always restricting ourselves to the case of spin-coherent states. These observables represent a measurement where one evaluates if the system has total magnetization within an interval by grouping neighboring outcomes, their associated probability distributions will follow the same organization. This way, the probability of obtaining the outcome associated to the n-th bin (or yet, the probability of the system having total magnetization within a certain interval) is the sum of the probabilities associated to the values of total magnetization that fall within that bin. Put mathematically, the probability of getting a click on the n_z-th bin when evaluating the total magnetization along the z-axis is

$$\Pr(n_z|\Psi_N) = \sum_{\frac{j_z}{N} \in [-\frac{1}{2}+\frac{n_z-1}{N_b}, -\frac{1}{2}+\frac{n_z}{N_b}[} \Pr(j_z|\Psi_N)$$

$$= \sum_{\frac{j_z}{N} \in [-\frac{1}{2}+\frac{n_z-1}{N_b}, -\frac{1}{2}+\frac{n_z}{N_b}[} \binom{N}{\frac{N}{2}+j_z} p^{\frac{N}{2}+j_z}(1-p)^{\frac{N}{2}-j_z}$$

(1.22)

Similarly, for the x-direction we have

$$\Pr(n_x|\Psi_N) = \sum_{\frac{j_x}{N} \in [-\frac{1}{2}+\frac{n_x-1}{N_b}, -\frac{1}{2}+\frac{n_x}{N_b}[} \binom{N}{\frac{N}{2}+j_x} p^{\frac{N}{2}+j_x}(1-p)^{\frac{N}{2}-j_x}.$$

(1.23)

To investigate the behavior of these probabilities in the macroscopic limit, where we can evaluate whether or not it complies with the expected classical results, one can make $N \to \infty$ and once again use the continuous approximation of a Gaussian. If once again $\mu = \langle \tilde{Z}_N \rangle_{\Psi_N}$ and $\sigma^2 = \Delta^2(\tilde{Z}_N|\Psi_N)$, the resulting probability distribution reads

$$\Pr(n_z|\Psi_N) \approxeq \int_{-\frac{1}{2}+\frac{n_z-1}{N_b}}^{-\frac{1}{2}+\frac{n_z}{N_b}} d(\frac{j_z}{N}) \frac{1}{\sqrt{2\pi\sigma^2}} \exp\left[-\frac{(\frac{j_z}{N}-\mu)^2}{2\sigma^2}\right].$$

(1.24)

In words, when measuring total magnetization along the z-direction the probability of obtaining the outcome associated to the n_z-th bin is evaluated by computing the integral of the curve given by the continuous limit of eq. (1.17) withing the corresponding boundaries of the bin.

If we recall that the integrand of the expression above concentrates around the mean value of $1/2 - p$ with $1/\sqrt{N}$, it is clear that as the size of the system grows the probability $\Pr(n_z|\Psi_N)$ will also concentrate around the same value. For large enough N, this integrand will be a Gaussian distribution so concentrated that it will be mostly restricted to the bin that contains the mean value, given by $\bar{n}_z = \lfloor N_b p \rfloor + 1$ if $0 \leq p < 1$ and $\bar{n}_z = N_b$ if $p = 1$. Consequently, as N approaches the macroscopic limit the probability

$\Pr(\bar{n}_z|\Psi_N)$ associated to the bin containing the mean value will tend to the maximal value of 1, while the remaining bins will have probabilities decreasing exponentially with N. Put simply, in the limit of $N \to \infty$ $\Pr(n_z|\Psi_N)$ will tend to a delta function fully contained in a single bin.

As already discussed, the fact that probability distributions concentrate around a single value is not enough to ensure that the their associated entropies will vanish, as evidenced by eq. (1.20). There, the caveat was that the number of outcomes was increasing with N, surpassing the rate of $1/\sqrt{N}$ at which the distribution concentrated. Fortunately, we are now faced with a different scenario, as our endeavor of modeling realistic macroscopic measurements has resulted in observables that in fact have a fixed number of outcomes N_b (as evidenced here by the fact that the limits of integration in eq. (1.24) do not depend on N). Therefore, one can make a direct connection between the probability distribution in eq. (1.24) concentrating around the mean value and the uncertainty around this measurement decreasing.

Following this argument, one can see that the entropy $H(Z'_N|\Psi_N)$ associated to the measurement of Z'_N on a product state will vanish, and that a similar line of thought can be followed for $H(X'_N|\Psi_N)$. As a result, we at last observe a classical behavior in the macroscopic limit, as

$$\lim_{N \to \infty} H(X'_N|\Psi_N) + H(Z'_N|\Psi_N) = 0. \tag{1.25}$$

As a matter of fact, such an effect would still be observed even if the number of outcomes did increase, provided it does not grow faster than the rate of $\sqrt{N}$, so that it balances out with the concentration of the probability distribution in eq. (1.24). The fact that this classical signature is recovered is numerically evidenced in figs. 1.2a and 1.2b.

We point out that the sum of entropies never actually reaching exactly zero is not an issue, as for macroscopic dimensions this value will be so low that it cannot be detected. We also recall that the value of this sum being very low has absolute meaning, as its decrease cannot, unlike in HURs, be attributed to a change of scale.

The only pathological cases where this sum does not vanish is when the state is prepared in such a way that the mean value $\langle \tilde{Z}_N \rangle$ lies precisely at a border between bins, in which case the probability distribution does not concentrate in a single bin. This happens if one prepares Ψ_N with $p = -\dfrac{1}{2} + \dfrac{m-1}{N_b}$, with $m \in \{1, \ldots, N_b\}$. These cases, however, represent a volume zero subset of all states that can be prepared, and thus will never occur in the lab.

Our result is portraying a very clear transition from a quantum to a classical rule. As the size of the system increases, the uncertainty associated to the observables X'_N and Z'_N (once significant, for small N) asymptotically tends to zero. This means that for large enough N one can prepare a spin-coherent state with total magnetization in the x- and z-directions simultaneously well defined, a feat not possible in the quantum regime.

When trying to understand the quantum-to-classical transition, it is clear that one must look beyond commutation relations between observables. By employing entropic uncertainty relations, one is assured to make reliable assessment, without having to dismiss everything that Heisenberg has already established at the dawn of quantum mechanics. We could then propose a model for macroscopic measurements that, combined with a well-motivated restriction of macroscopic state preparations, was enough to describe the emergence of classical features on a quantum system.

We showed that imprecision plays a decisive role on what kind of attributes a macroscopic system will display: quantum features fade away if apparatuses are imprecise; conversely, one needs to be able to perform highly precise measurements if one wishes to still observe such features on a macroscopic system. More than a qualitative analysis, we provided a clear frontier between these two scenarios, the turning point being that where the number of outcomes (directly connected to the imprecision of the measurement device) N_b grows faster than $1/\sqrt{N}$. This is a particularly relevant result if the scientific community hopes to construct quantum computer in the near future that can outperform classical computations, since it should have macroscopic dimensions while keeping quantum attributes.
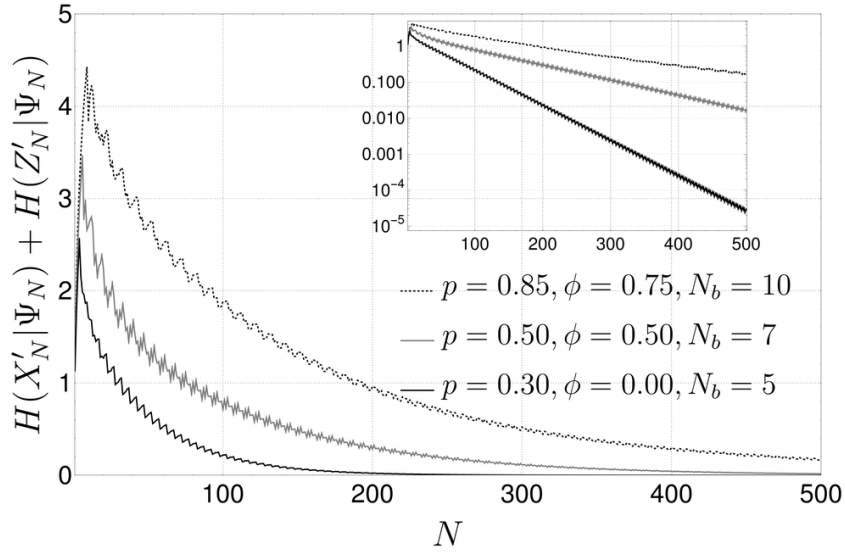
(a) Sum of entropies for increasing system size
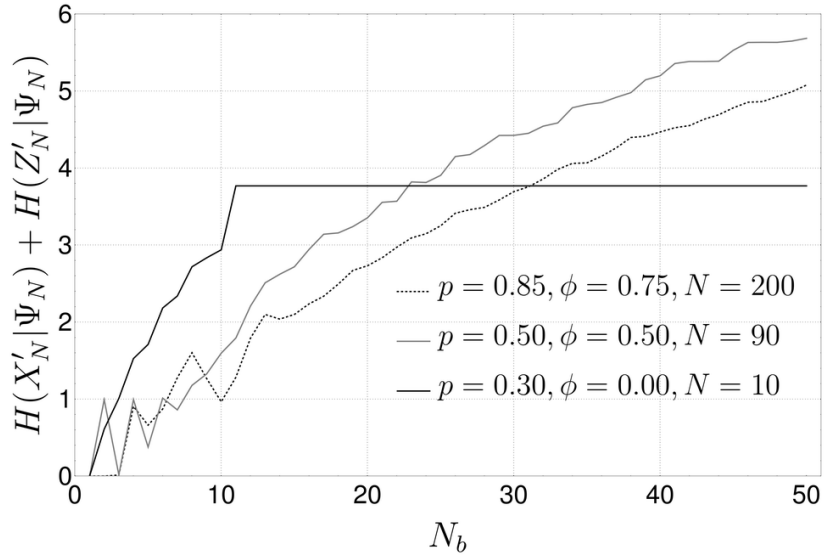
(b) Sum of entropies for increasing number of bins

Figure 1.2: **Sum of entropies as the system grows for different choices of preparation.** Numerically, one can see the behavior of the sum of entropies (and by proxy, of the uncertainty) of measuring total magnetization in two perpendicular directions, for different preparations of a spin-coherent state. In (a), we also evaluate different choices of N_b (assigning varied precisions to the measurement device) and see that the sum approaches zero as the size of the system increases. The inset highlights its exponential behavior. In (b), we show that increasing the number of bins (and consequently the number of outcomes) makes the sum of these entropies increase. If $N_b \geq N$ it is possible to observe quantum features even in larger systems. The sum of entropies stagnates for $N_b > N$ because the maximal uncertainty for a given N is already reached, since each possible outcome will be assigned to a different bin and the remaining bins will contain no possible outcome.

Chapter 2

Characterization of effective reversibility criteria

In the last chapter, we have dedicated ourselves to investigating the different behaviors displayed by quantum systems, as opposed to classical ones. Focusing our efforts specifically on the preparation of quantum states, we analyzed the uncertainty relations that govern this process and ended up with an enhanced understanding of the transition that must occur from one regime to the other, from systems of microscopic dimensions to those of macroscopic size.

According to our results, what enables this particular aspect of the quantum-to-classical transition to take place is the use of an effective description of the macroscopic measurements that are performed. This characterization has the final goal of providing a realistic model of what actually happens in a lab, and eventually boils down to describing what kind of information we can access. The research present in the last chapter suggest that it is our ignorance that, at the end of the day, makes our essentially quantum world seem classical.

Adopting effective descriptions of both systems and measurements, often an unavoidable necessity, has further consequences on our perception of the world. Of particular interest to this work, we can mention how our access to information affects the reversibility of physical processes.

Consider, for instance, a closed quantum system, described initially by a state ψ. All one needs to know in order to predict the whole future (or past, for that matter) of such system is the Hamiltonian H that governs its dynamics. If that is known, then one can, at least in principle, determine the new state of the system after some time has passed using Schrödinger's equation.

As a consequence, one can also move backwards in time and find out the past state of the physical system, all under the assumption that it undergoes some unitary evolution $\mathcal{U}_t$: if $\psi(t) = \mathcal{U}_t[\psi(0)]$, it is also the case that $\psi(0) = \mathcal{U}_{-t}[\psi(t)]$. Because of this feature, reversibility is a built-in feature of closed quantum dynamics, meaning the initial state can be recovered from the final state without any loss.

However, as we will see, when resorting to effective descriptions this feature fades away, in general. Even though one still assumes that the system is isolated from its environment and ruled by closed, unitary dynamics, if one's knowledge of it is not perfect and coarse-graining methods are applied, then the resulting effective dynamics may not be reversible, ultimately meaning one cannot recover the initial state from the final state.

This direct relation between information and reversibility is neatly captured by the second law of thermodynamics. It states that the entropy of closed systems cannot decrease, usually expressed mathematically as

$$\Delta S \geq 0, \tag{2.1}$$

meaning that if one evaluates the entropy S of the system and then again after some time has passed, it must be that S has increased, or at the very least not changed. Common reading of the second law states that the "disorder" of a system tends to increase, that the information it encodes can only change through losses, or yet that the arrow of time always points towards the future.

The second law of thermodynamics is regarded by many as one of the most fundamental laws of physics [51]. It regulates what processes are viable, regardless of the microscopic details of the system in question, or the nuances of the dynamics that they undergo. It is regarded as universally valid, being applied to scenarios in varied scales, ranging from subatomic collisions to cosmology [52], not shying

away from venturing even into the analysis of living organisms [53]. Consequently, the second law has an almost sacred aura around it. As Eddington put it,

> The law that entropy always increases holds, I think, the supreme position among the laws of Nature. If someone points out to you that your pet theory of the universe is in disagreement with Maxwell's equations – then so much the worse for Maxwell's equations. If it is found to be contradicted by observation – well, these experimentalists do bungle things sometimes. But if your theory is found to be against the second law of thermodynamics I can give you no hope; there is nothing for it but to collapse in deepest humiliation [54].

Even though this statement makes it clear that everyone agrees that the second law is paramount, it is nevertheless unclear exactly *to what* we are all agreeing. On its original formulation, derived heavily from the empirical findings of the 19th century, the second law states simply that heat cannot spontaneously be transferred from a colder to a hotter body [55, 56, 57], but since then we have strayed further from a clear interpretation of it, mainly because of the elusiveness of the concept of entropy.

Traditionally, entropy is presented in introductory statistical mechanics and thermodynamics courses as a state function, defined in terms of macroscopic quantities as

$$dS = \frac{\delta Q}{T}, \tag{2.2}$$

where δQ is the heat transferred to the system and T is its temperature. However, the so-called thermodynamical entropy is but one possible definition of this quantity, among many others suited for different applications.

To be called an entropy, an object must obey a few requirements, namely being an additive function of extensive variables (that is, variables that scale proportionally to the system's size), be positive, and reach maximum value for a given internal energy when the system is at equilibrium [51]. While the definition in eq. (2.2) considers only macroscopic properties, one can, alternatively, consider an equivalent formulation of entropy, where one takes into account the different microscopic states available to the system, at a given internal energy. It is the so-called Gibbs entropy, given by

$$S = -k_B \sum_i p_i \ln p_i, \tag{2.3}$$

k_B being Boltzmann's constant and p_i the probability associated to the i-th microstate, obeying $\sum_i p_i = 1$ and $p_i \geq 0$ for all i.

This other construction encourages a direct connection between entropy and information, encoded in the probability distribution p. The Gibbs entropy is known for being constant over time for closed systems [58], that is, when the system is subjected to Hamiltonian dynamics. This fact is consistent with the second law of thermodynamics while also tapping into our physical intuition that closed systems do not lose nor gain information.

While intuitive, this notion of entropy fails to recover other familiar behaviors of physical systems. It does not outright contradict the second law of thermodynamics, as the entropy does not decrease, but it also does not tend to increase. One would expect that even isolated systems undergoing closed dynamics should, with time, tend to more 'disordered' states, a process which would result in a spontaneous increase in entropy.

Another disadvantage of this approach is that it does not take into account our limited access to p and its corresponding microstates [1]. As we have discussed in more depth in the last chapter, complete knowledge of a state is generally neither possible not desirable, since the only tools we have to explore a physical system are the measurements we can perform. Thus, the unavoidable experimental limitations shaping these measurement further constrain the information one can obtain.

To realistically characterize the partial access one has to a physical state, it is useful to employ coarse-grained descriptions of measurements. As a result, instead of a heavy detail-oriented portrayal of a system, one deals with an effective description of a state and its dynamics. If one wants to travel down this road, a suitable option is to employ the Boltzmann entropy, defined for a macroscopic system as

$$S = k_B \ln \Omega. \tag{2.4}$$

The Boltzmann entropy emerges from scenarios where one performs coarse-grained measurements on a state, thus obtaining only partial information about it. As a consequence, one does not really know to

---

[1]In fact, there is a rich discussion on what p actually means [58]

what microscopic state their system should be assigned, only that there is a whole set of such states that are consistent with the effective description yielded by the coarse-grained measurements. Here, Ω is the number of microstates in the set of states that are compatible with observations, or yet the volume of this set.

This formulation of entropy also provides an intuitive interpretation for the role of information in measurements. Notice that the lower Ω is, the lower S itself becomes, and the other around for high Ω. This means that when there are many microstates compatible with the observed macroscopic state, a situation achieved when the coarse-graining of the measurements is very rough, there is little information about the underlying physical system. Compare it with a situation where the measurements are fine-grained, such that the effective description of the macroscopic system could only have emerged from a smaller set of microstates, and notice that the corresponding Boltzmann entropy would be lower than in the previous case. This relation between S and Ω depicts our ignorance of the underlying, microscopic state, as the more possibilities we have, the less sure we can be.

An additional feature of the Boltzmann entropy of a state is that, unlike the Gibbs entropy, it is not fixed throughout its evolution, not even if the system it describes is closed. It allows evolving macroscopic states to be compatible with sets of microscopic states whose volume varies with time, being associated to larger and larger Ω. Consequently, our ignorance about the microstate also increases, culminating on an increase of entropy.

We now take a step back from entropies and look at the broader picture painted by the second law of thermodynamics, only to see that a conflict is set. Micro- and macroscopic descriptions of states are not independent, and are closely connected under the assumption that one should emerge from the other, so it seems contradictory that the Gibbs entropy is constant but the Boltzmann entropy can vary in the same scenario. Furthermore, the universality of the second law dictates that it should govern both the micro- and the macroscopic realm, but when comparing the predictions yielded by the usage of these two different entropies we see a divergence, particularly when it comes to the reversibility of processes.

If it is the case that the entropy of a closed system undergoing any process cannot decrease, then the increase of S has direct consequences on the reversibility of dynamics. Indeed, a process can only be reverted if it does not alter the entropy of the state, otherwise reversing it would produce dynamics that decrease the entropy, a feat forbidden by the second law of thermodynamics. Thus, two different analyses derive from evaluating the second law from the Gibbs or from the Boltzmann perspective: one may impose no constraint on the reversibility of the microscopic process while the other dictates that the effective dynamics should be irreversible.

The unease caused by this inconsistency (after all, the effective dynamics is supposed to emerge from the microscopic process) can be placated by realizing that effective measurements are, in their nature, connected to irreversibility. Indeed, it is clear from the construction of coarse-grained measurements that not all information about the state is harvested, and one only has access to a fraction of its degrees of freedom. Consequently, upon performing an effective macroscopic measurement, some information is inevitably lost, which means that even a closed system have increasing entropy. Though the evolution to which the underlying physical system is subject is reversible, the construction of the effective state is not, a fact reflected on the uncertainty one has around what the microstate actually is.

Throughout this whole discussion on the second law and the concept of entropy, notice that quantum mechanics has not even been mentioned. Though talking about uncertainty triggers lengthy arguments for quantum physicists, it has been the case, so far in this passage, that uncertainty simply means ignorance, in its most classical meaning: there is an underlying microscopic state, I just cannot access it. However, the universality of the second law imposes that the entropy of closed *quantum* systems also cannot increase, and consequently the reversibility of quantum dynamics is equally defined by it: only evolutions that do not increase the entropy can be reversed.

If one wants to study the behavior of quantum dynamics through a similar analysis, then, it is necessary to investigate the interplay between microscopic reversibility and its effective counterpart. Fortunately, some parallels can be traced between quantum and classical microscopic entropy, made evident with the advent of quantum information. Given a density matrix ρ describing some quantum state, the von Neumann entropy reads [59]

$$S = -\operatorname{Tr}[\rho \ln \rho]. \tag{2.5}$$

Notice how this object also quantifies one's ignorance about a quantum system: pure states (around which there is no classical ignorance) yield null entropy, and the less pure ρ is, the higher S is in turn. In fact, if ρ is a mixture of perfectly distinguishable states then the von Neumann entropy reduces to the Shannon entropy [42], whose interpretation in terms of uncertainty has been discussed in chapter 1.

Just like Gibbs entropy, von Neumann's remains constant for states under closed dynamics, analogously signifying the conservation of information.

The natural next step in this argument would be to introduce a quantum entropy that, like Boltzmann's, can increase even when describing closed systems. The frustrating fact is that there is no consensus to which object should take this place, though many candidates do exist [58, 60, 61, 62, 63].

In this work, we have drawn inspiration from the classical Boltzmann entropy and quantified the uncertainty arising in effective descriptions of quantum systems. Under the light of coarse-grained measurements, we analyze the emergent macroscopic dynamics and investigate how their reversibility connects with the information one can actually access from the underlying quantum state. We highlight the interplay between micro- and macroscopic reversibility, and build a general framework for this type of analysis. We finally carry out two pedagogical examples, and trace parallels with well-known scenarios. We start by laying the necessary background to support our work.

2.1 Preliminary concepts

2.1.1 Coarse-graining maps and the average assignment map

Measurements are the main tool we can use to interact with the physical world. Upon each realization of an experiment we have an opportunity to learn something about the system we have in hands, and with some patience one might gather enough statistics in order to safely assign a state to that system. There are, however, many limitations to how much we can actually learn with measurement, as discussed in the previous chapter. Because of experimental and technological constraints, restricted access to resources, or simply limited interest, one does not typically exhaust all the knowledge about a system. The process of gaining information is then more similar to that of assembling a puzzle, with pieces provided by measurements, while having to accept the final picture will have missing pieces and some areas of sheer uncertainty[2]. Optimistically, one can still make sense of the finished image but the details will be lost.

This *effective* description of the system is the only one to which we have access. It is only natural to wonder how to relate the underlying physical system and our incomplete characterization of it, a task that can be carried out by employing coarse-grained measurements.

A coarse-graining map is a quantum channel connecting microscopic states to its effective description. It captures the degrees of freedom to which one has access, and models the measurement performed on the physical system. To formally define it, consider the Hilbert spaces $\mathcal{H}_D$ and $\mathcal{H}_d$, of dimensions D, d with $D > d$, and its respective linear operators $\mathcal{L}(\mathcal{H}_D), \mathcal{L}(\mathcal{H}_D)$. A coarse-graining map Λ is then

$$\Lambda : \mathcal{L}(\mathcal{H}_D) \to \mathcal{L}(\mathcal{H}_d), \tag{2.6}$$

such that the effective description $\rho \in \mathcal{L}(\mathcal{H}_d)$ of a microscopic state $\psi \in \mathcal{L}(\mathcal{H}_D)$ is given by

$$\Lambda[\psi] = \rho. \tag{2.7}$$

The most iconic example of a coarse-graining map is the partial trace operation. It is commonly applied in situations where an agent has access to only a share of the total physical system, in which case their part is described by a reduced state. If we rephrase it in terms of a system in $\mathcal{L}(\mathcal{H}_S)$ of dimension d_S, under one's control, subjected to an environment in $\mathcal{L}(\mathcal{H}_E)$ of dimension d_E, about which one cannot assume much, the partial trace is a coarse-graining map $\Lambda_{\mathrm{PT}} : \mathcal{L}(\mathcal{H}_S \otimes \mathcal{H}_E) \to \mathcal{L}(\mathcal{H}_S)$. Through its action, the agent is able to describe their system of interest on an effective level, but must permanently loose the information encoded in the environment.

Another example of a coarse-graining map, of particular interest to us, is the one describing the measurements performed on an imperfect detector. Consider the usual setup of a lattice of cold atoms, trapped in an optical cavity [64]. Consider the individual atoms as 3-level systems, which can be in states $|0\rangle, |1\rangle$ or $|2\rangle$. In a very simplified model, the apparatus that performs the corresponding measurements may not be able to resolve, for instance, the levels $|1\rangle$ and $|2\rangle$, being only able to ascertain whether the atom is in the ground state or not. This inherent imprecision in the measurements will result in a coarse-grained description of the system in terms of only two effective levels $|0\rangle$, to which atoms in the ground state are assigned, and $|1\rangle$, to which the two remaining states are assigned.

To describe the action of this imperfect device, one can follow an analogous procedure as the one outlined in [33, 25], where the authors analyze a detector that cannot differentiate neighboring atoms

---

[2]Even harder to accept is the realization that perhaps there is no fundamental picture to which this puzzle would correspond, as the nature of underlying physical systems is a source of great debate.

and has extremely poor resolution of energy levels above a given limit, thus being dubbed a blurred and saturated detector. Following their steps, it is not hard to construct the Kraus operators [42] characterizing the coarse-graining map Λ_D that describes our imperfect detector. We recall that in the Kraus formulation the action of a completely positive map Φ on any quantum state ρ can be characterized in terms of operators $\{K_i\}_i$ satisfying $\sum_i = K_i^\dagger K_i = \mathbb{1}$ such that

$$\Phi[\rho] = \sum_i K_i \rho K_i^\dagger. \tag{2.8}$$

Thus, the Kraus operators that describe Λ_D are

$$K_1 = \begin{bmatrix} 1 & 0 & 0 \\ 0 & 1/\sqrt{2} & 1/\sqrt{2} \end{bmatrix}, \quad K_2 = \begin{bmatrix} 0 & 0 & 0 \\ 0 & 1/\sqrt{2} & -1/\sqrt{2} \end{bmatrix}. \tag{2.9}$$

The action of this coarse-graining map is, alternatively, given by

$$\Lambda_D[|0\rangle\langle 0|] = |0\rangle\langle 0|$$
$$\Lambda_D[|0\rangle\langle 1|] = \tfrac{1}{\sqrt{2}}|0\rangle\langle 1|$$
$$\Lambda_D[|0\rangle\langle 2|] = \tfrac{1}{\sqrt{2}}|0\rangle\langle 1|$$
$$\Lambda_D[|1\rangle\langle 0|] = \tfrac{1}{\sqrt{2}}|1\rangle\langle 0|$$
$$\Lambda_D[|1\rangle\langle 1|] = |1\rangle\langle 1|$$
$$\Lambda_D[|1\rangle\langle 2|] = 0$$
$$\Lambda_D[|2\rangle\langle 0|] = \tfrac{1}{\sqrt{2}}|1\rangle\langle 0|$$
$$\Lambda_D[|2\rangle\langle 1|] = 0$$
$$\Lambda_D[|2\rangle\langle 2|] = |1\rangle\langle 1|$$

Notice that the map reflects the fact that coherence terms within the excited subspace (that is, the space spanned by $\{|1\rangle, |2\rangle\}$) must vanish, since they cannot be discriminated after the coarse-grained mapped has been applied.

Coarse-graining maps are a powerful tool to characterize the effective states emerging from measurements that do not allow us to get complete information about the quantum system. It is a "bottom-to-up" assignment, where we obtain the effective description after stating what is the microscopic state. But what about the other direction, that is, given this effective description, to which state should we assign the underlying physical system? Let us not forget that, at the end of the day, the effective descriptions are all that one can actually access, and thus any approach that sets out to explain a phenomenon in terms of observations should not take the microscopic state as a given.

The immediate problem that one has to face is the ambiguity concerning the underlying state. If we emphasize the coarse-graining nature of measurements, or if we recall the examples thereof that we provided, it is clear that different microscopic states yield the same effective description. This is only intuitive, since in the measurement process one has discarded information that cannot be retrieved, thus it is, in general, not possible to determine the precise state that one is measuring, only some aspects of it.

Let us be more precise. Given a coarse-graining map Λ and an effective description $\rho \in \mathcal{L}(\mathcal{H}_d)$, one can define the set of all microscopic pure states that are consistent with ρ as

$$\Omega_\Lambda(\rho) = \{\psi \in \mathcal{L}(\mathcal{H}_D) | \Lambda[\psi] = \rho, \ \psi = |\psi\rangle\langle\psi|\}. \tag{2.10}$$

In words, this is the set of all pure microstates that could have generated the effective state that one observes. It can also be formulated explicitly in terms of the set $\mathcal{O} = \{o_i\}_i$ of observed quantities, resulting from measuring observables $\{O_i\}_i$, such that

$$\Omega_\Lambda(\mathcal{O}) = \{\psi \in \mathcal{L}(\mathcal{H}_D) | \mathrm{Tr}[O_i\Lambda[\psi]] = o_i\}, \tag{2.11}$$

and the two approaches are equivalent if $\mathcal{O}$ is tomographically complete.

Once Ω_Λ defines the set of possible microscopic pure states, all that is left is to determine to which state one should assign the underlying physical system. Following [65], one can argue for picking the average state of this set, representing our best guess. Given the observed quantities $\mathcal{O}$, one can then define the average assigned state as

$$\mathcal{A}_\Lambda(\mathcal{O}) = \int d\mu_\psi \mathrm{Pr}_\Lambda(\psi|\mathcal{O})\psi, \tag{2.12}$$

where $d\mu_\psi$ is a Haar measure, and $\mathrm{Pr}_\Lambda(\psi|\mathcal{O})$ is the probability of having the microscopic state ψ given that $\mathcal{O}$ was observed. The microscopic state $\bar\psi$ obtained from this procedure is the average state one gets after many preparations of the effective state.

In [65], the authors find a closed form for the average assigned state in the case of the partial trace over the degrees of freedom of the environment. Given the effective state ρ, it reads

$$\mathcal{A}_{\Lambda_{\mathrm{PT}}}(\rho) = \rho_S \otimes \frac{\mathbb{1}_E}{d_E}. \tag{2.13}$$

Intuitively, the best guess one can produce is given by assuming the system to be in state ρ and the environment, from which we know nothing, to be maximally mixed.

Following a similar procedure to the one used in [65] to obtain a closed form for the average assigned state on their other example, one can also write out the corresponding expression for the case when the coarse-graining map is given by Λ_D, the imperfect detector we discussed earlier in the text. In terms of the effective state ρ, with density matrix elements given by

$$\rho = \begin{bmatrix} \rho_{00} & \rho_{01} \\ \rho_{01}^* & \rho_{11} \end{bmatrix}, \tag{2.14}$$

we have

$$\mathcal{A}_{\Lambda_D}(\rho) = \begin{bmatrix} \rho_{00} & \rho_{01}/\sqrt{2} & \rho_{01}/\sqrt{2} \\ \rho_{01}^*/\sqrt{2} & \rho_{11}/2 & \frac{|\rho_{01}|^2}{\rho_{00}} - \frac{\rho_{11}}{2} \\ \rho_{01}^*/\sqrt{2} & \frac{|\rho_{01}|^2}{\rho_{00}} - \frac{\rho_{11}}{2} & \rho_{11}/2 \end{bmatrix}. \tag{2.15}$$

The detail of the calculation can be found in appendix C.

2.1.2 Effective dynamics

With the map $\mathcal{A}_\Lambda$, one now has an assignment that is complementary to a coarse-graining map: while the latter is a "bottom-to-up" assignment, yielding an effective description if one knows the microscopic state, the former goes in the other direction and allows one to pick the best guess for the state of the underlying physical system, given that some quantities were observed. This allows us to transit between the microscopic the and effective levels of quantum states, and an advantage of this new mobility is that one can derive the dynamics of effective states using only the information available from coarse-grained measurements, without having to assume access to the microscopic states.

Let us set the scenario we will explore. In a lab, one can measure the effective state of a quantum system at any moment, given by $\rho(t) \in \mathcal{L}(\mathcal{H}_d)$. One also knows how to characterize the coarse-graining map $\Lambda : \mathcal{L}(\mathcal{H}_D) \to \mathcal{L}(\mathcal{H}_d)$. Finally, one can control the evolution $\mathcal{U}_t : \mathcal{L}(\mathcal{H}_D) \to \mathcal{L}(\mathcal{H}_D)$ that will govern the unknown microscopic state, which we assume to be unitary. Then, following [65], the effective evolution channel $\Gamma_t : \mathcal{L}(\mathcal{H}_d) \to \mathcal{L}(\mathcal{H}_d)$ is given by a composition of these maps

$$\Gamma_t = \Lambda \circ \mathcal{U}_t \circ \mathcal{A}_\Lambda, \tag{2.16}$$

as shown in fig. 2.1. Let us take moment to understand this construction.

Consider a simple experiment, where on each run one prepares the effective state $\rho(0)$. On the underlying level, what one is doing is a sampling process, randomly picking a state from $\Omega_\Lambda(\rho(0))$, the set of all possible microstates compatible with $\rho(0)$. For the i-th run, let the sampled microstate be $\psi^i(0)$ with probability $\mathrm{Pr}_\Lambda(\psi^i(0)|\rho(0))$. Then, one lets the unknown $\psi^i(0)$ evolve according to $\mathcal{U}_t$, yielding $\mathcal{U}_t[\psi^i(0)] = \psi^i(t)$. Finally, upon applying the coarse-graining map Λ on the evolved microscopic state one can obtain the effective evolved state of the i-th run, as

$$\rho^i(t) = (\Lambda \circ \mathcal{U}_t)[\psi^i(t)]. \tag{2.17}$$

After many runs, as shown in fig. 2.2, one will have performed enough measurements, and the induced averaging process defines the final effective state
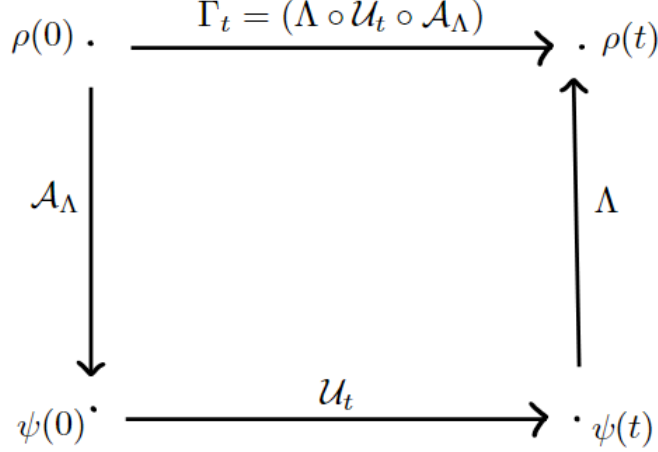
Figure 2.1: Γ_t *as a composition of maps.* On average, the effective evolution that a state $\rho(0)$ undergoes is given by the successive application of the average assignment map, the underlying unitary evolution and the coarse-graining map. No knowledge of the physical system, represented by the microscopic state $\psi(0)$, is necessary to construct Γ_t.

$$\rho(t) = \int d\mu_{\psi(0)} \mathrm{Pr}_\Lambda(\psi(0)|\rho(0))\psi(t) \tag{2.18}$$

$$= \int d\mu_{\psi(0)} \mathrm{Pr}_\Lambda(\psi(0)|\rho(0))(\Lambda \circ \mathcal{U}_t)[\psi(0)] \tag{2.19}$$

$$= (\Lambda \circ \mathcal{U}_t) \left[\underbrace{\int d\mu_{\psi(0)} \mathrm{Pr}_\Lambda(\psi(0)|\rho(0))\psi(0)}_{\mathcal{A}_\Lambda[\rho(0)]} \right] \tag{2.20}$$

$$= (\Lambda \circ \mathcal{U}_t \circ \mathcal{A}_\Lambda)[\rho(0)]. \tag{2.21}$$
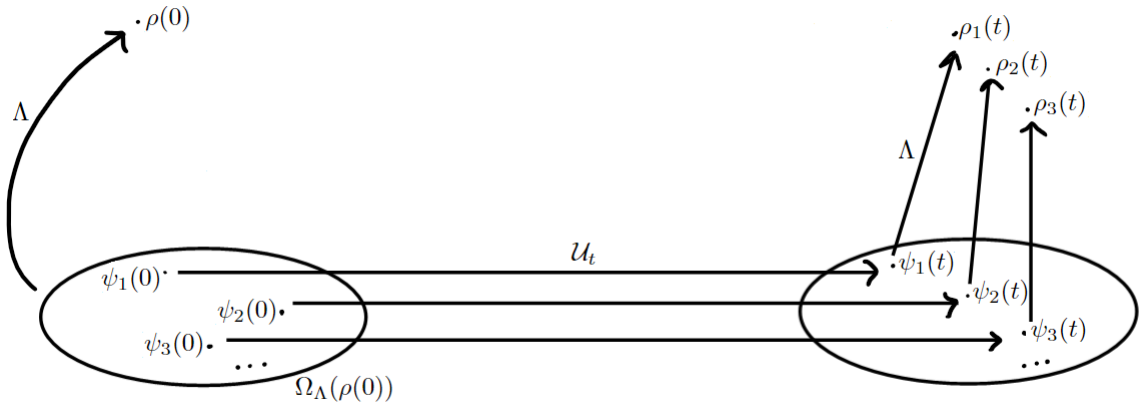
Figure 2.2: *A series of runs of a simple experiment.* By preparing an effective state $\rho(0)$, one is in fact sampling microscopic states from $\Omega_\Lambda(\rho(0))$. Upon letting them evolve according to $\mathcal{U}_t$ and applying the coarse-graining map Λ, one obtains potentially distinct effective evolved states, which can then be averaged to yield $\rho(t)$.

A simple example can be provided by evaluating the effective dynamics that emerge from a partial trace coarse-graining, from which we already know the closed form of average assigned states, yielding

$$\rho(t) = (\mathrm{Tr}_E \circ \mathcal{U}_t) \left[\rho(0) \otimes \frac{\mathbb{1}_E}{d_E} \right]. \tag{2.22}$$

2.2 Effective reversibility

Notice that even though the effective dynamics in eq. (2.22) are linear and completely positive, there is no guarantee that it should always be so. Given the construction of Γ_t, it is not surprising that qualitative differences between the effective and the underlying dynamics may appear, all despite one's assumption that the unknown microscopic state is evolving unitarily. Furthermore, it is generally the case that the effective dynamics are not reversible.

On the microscopic level, the evolution that the system undergoes is, by assumption, unitary. Consequently, one can promptly revert the action of any dynamics: the microscopic state at time t is given in terms of the initial state as $\psi(t) = \mathcal{U}_t[\psi(0)]$, and we recover the initial state in terms of the final state by simply applying the evolution map in the other direction as $\psi(0) = \mathcal{U}_{-t}[\psi(t)]$. Going backwards in time is, conceptually, no different from going forwards, and the concept of reversibility seems plain enough: if one always recovers the initial state when advancing and then regressing in time, then the evolution is reversible. For more complex scenarios, however, defining reversibility requires more caution.

Just like in the uncomplicated microscopic case, we want to characterize effective reversibility by comparing a forward and a backward process. The challenge lies, though, in two aspects of this quest, namely the statistical nature of effective descriptions (which, unlike evolutions given by the Schrödinger equation, are not deterministic) and the conceptual looseness of what is the appropriate reverse process.

Many approaches to this problem have been proposed, of which we must mention the works of Jarzynski [66] and Crooks [67], where fluctuation relations are constructed comparing a forward, physical process and a corresponding backward process, whose definition has been a source of debate (in particular in the quantum case) [68]. Particularly, in [69], the authors advocate for investigating reversibility not in terms of a backward evolution but rather a retrodiction process, where one tries to guess the initial state rather than physically recover it. We also point out recent advances towards making fluctuation relations suitable for quantum analyses [70, 52, 71].

None of these approaches, however, make the connection to the coarse-grained essence of realistic measurements clear, neither do they make the duality between microscopic and effective evolution central, highlighting their contrasting nature in terms of reversibility. In this direction, we invite the reader to once again consider the plain experiment we analyzed in the last section, were we have described an effective (forward) evolution while comparing what is happening on the effective and the microscopic level.

Let us now define the reverse process, after having let the initial state $\rho(0)$ effectively evolve to $\rho(t)$. If we take the final state $\rho(t)$ as our new starting point, just like in the forward process, we are in fact sampling a microscopic state from $\Omega_\Lambda(\rho(t))$. To revert the process, we let this state evolve according to $\mathcal{U}_{-t}$, and then obtain the effective reversed state $\rho'(0)$ by applying the coarse-graining map, see fig. 2.3 for clarity. Given the conceptual similarities between the forward and the backward process, it is straightforward to see that the effective reverse evolution is obtained by

$$\Gamma_{-t} = \Lambda \circ \mathcal{U}_{-t} \circ \mathcal{A}_\Lambda. \tag{2.23}$$

After letting the initial effective state $\rho(0)$ evolve forward in time, measuring the final state $\rho(t)$, and then evolving backward to $\rho'(0)$, one can compare the initial and reversed states. In general, there is no guarantee that $\rho(0) = \rho'(0)$, but it might just be so. When considering several runs of this experiment, one might verify that upon preparing any initial effective state, letting it evolve according to Γ_t and then backwards with Γ_t, the initial state is always recovered. If that is the case, then we say the effective dynamics is reversible.

It is worth stressing that, as illustrated in fig. 2.3, it is generally not the case that Γ_t is reversible, that is, the initial effective state $\rho(t)$ is not typically recovered after being let evolve forward and backward in time. Situations where Γ_t is reversible are rather the exception than the rule, and in the next section we will explore what are the conditions that determine which is the case.
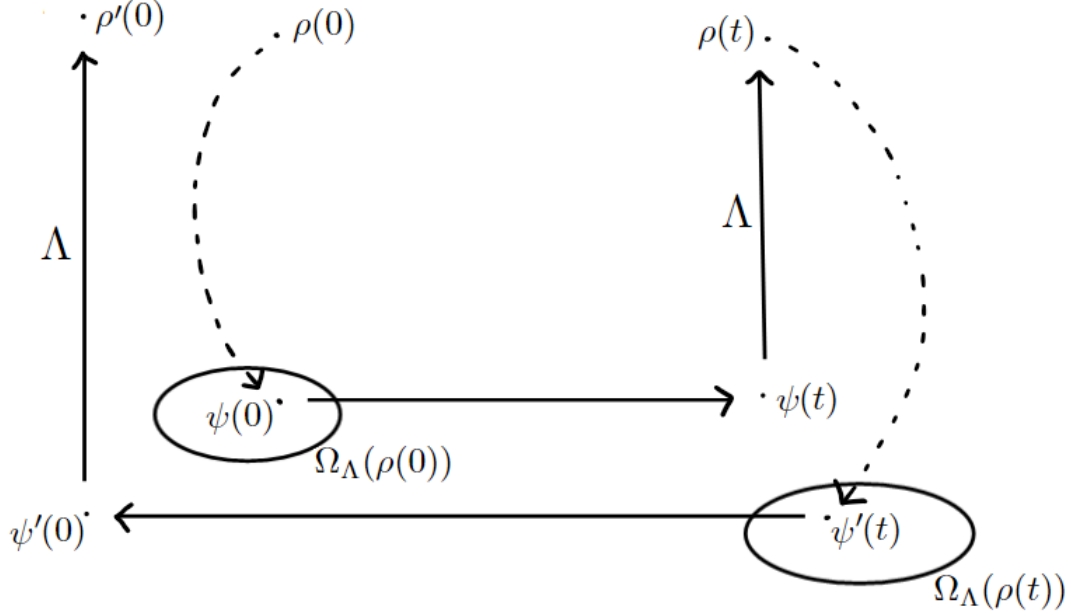
Figure 2.3: *Experimental scenario.* Upon preparing an effective state $\rho(0)$ in the lab (which corresponds to sampling a microstate $\psi(0)$ from $\Omega_\Lambda(\rho(0)))$, one applies the unitary evolution $\mathcal{U}_t$ on the microscopic system, and obtain the final effective state $\rho(t)$ after a coarse-grained measurement. To revert the evolution, one can see the measurement of $\rho(t)$ as a sampling process from $\Omega_\Lambda(\rho(t))$, where the microstate $\psi'(t)$ is picked, then let evolve backwards in time with $\mathcal{U}_{-t}$. Finally, the reversed effective state $\rho'(0)$ is obtained by applying the coarse-graining map.

2.3   Reversibility conditions

As pointed out, Γ_t emerges as a result of both the coarse-graining map and the microscopic unitary evolution. It is only natural, then, that whether or not the effective dynamics is reversible should be a consequence of an interplay between Λ and $\mathcal{U}_t$. One can set conditions for Λ and $\mathcal{U}_t$ that, when satisfied, ensure that the emerging effective dynamics is reversible.

Let us analyze the scenario we laid out with more care. To say that Γ_t is reversible is, according to the definition we adopted, the same as stating that any initial effective preparation $\rho(0)$ can be recovered from $\rho(t)$.[3] Mathematically, it is required that $\rho(0) = (\Gamma_{-t} \circ \Gamma_t)[\rho(0)]$, or yet

$$\rho(0) = (\Lambda \circ \mathcal{U}_{-t} \circ \mathcal{A}_\Lambda \circ \Lambda \circ \mathcal{U}_t \circ \mathcal{A}_\Lambda)[\rho(0)]. \tag{2.24}$$

In words, one is requiring that the action of Γ_t followed by Γ_{-t} is trivial on any initial effective state $\rho(0)$. Whenever this requirement is met, then the effective dynamics is reversible.

At a first glance, one might be tempted to conclude that eq. (2.24) is always satisfied, for any choice of coarse-graining map Λ and microscopic evolution $\mathcal{U}_t$. Given the complementary essence of Λ and $\mathcal{A}_\Lambda$, one being a bottom-to-up assignment and the other its "reversed" operation, one might get the feeling that the action of $(\mathcal{A}_\Lambda \circ \Lambda)$ is trivial. If that was the case, the channel in eq. (2.24) would indeed reduce to the identity, with $\mathcal{U}_{-t}$ and $\mathcal{U}_t$ canceling out and likewise for $(\Lambda \circ \mathcal{A}_\Lambda)$. This is however not true in general.

Let us first take a closer look at the action of $(\Lambda \circ \mathcal{A}_\Lambda)$. It is true that the result of applying the average assignment map on any effective state followed by the corresponding coarse-graining map is trivial. The microscopic state $\mathcal{A}_\Lambda[\rho(0)]$ clearly obeys $\Lambda[\mathcal{A}_\Lambda[\rho(0)]] = \rho(0)$, it is simply the average state of the set $\Omega_\Lambda(\rho(0))$. Consequently, applying the coarse-graining map Λ will recover $\rho(0)$, and one concludes that, indeed, the following statement holds for any $\rho(0)$

$$\rho(0) = (\Lambda \circ \mathcal{A}_\Lambda)[\rho(0)]. \tag{2.25}$$

---

[3]Here, we stress that, just like in the forward process, the recovered state can only be determined after many runs of the experiment where many measurements are performed at the end

It is important to stress at this point that the set $\Omega_\Lambda(\rho)$ is constituted solely of *pure* states that yield the same effective description ρ. The average assigned state $\bar\psi = \mathcal{A}_\Lambda[\rho]$ does not, in general, belong to this set, as it is not a pure state, but it does belong to the set $\Omega_\Lambda^M(\rho)$, which we define as

$$\Omega_\Lambda^M(\rho) = \{\psi \in \mathcal{L}(\mathcal{H}_D) | \Lambda[\psi] = \rho\}, \tag{2.26}$$

that is, $\Omega_\Lambda^M(\rho)$ is the set of *all* microscopic states compatible with the effective description ρ, regardless of being pure or mixed.

Interestingly enough, even though mixed states are constructed through the convex mixture of pure states, the convex hull of $\Omega_\Lambda(\rho)$ (which we denote $\Omega_\Lambda^{CH}(\rho)$) is not equivalent to $\Omega_\Lambda^M(\rho)$ (corresponding to simply allowing both pure and mixed states in the original definition of $\Omega_\Lambda(\rho)$). To see an example illustrating this difference, consider the partial trace and let ρ be the maximally mixed state. Then, $\Omega_\Lambda(\mathbb{1})$ is the set of maximally entangled states, and $\Omega_\Lambda^{CH}(\rho)$ is the set of states spanned by the Bell basis. Consider now the microscopic state

$$\psi = \frac{1}{2}\mathbb{1} \otimes |0\rangle\langle 0|. \tag{2.27}$$

It is easy to see that $\Lambda_{PT}[\psi] = \mathbb{1}$, so ψ belongs to the set $\Omega_\Lambda^M(\rho)$ of *mixed* states that yield the maximally mixed state as its effective description, and yet it does not belong to the convex hull of maximally entangled states, that is, it is not in $\Omega_\Lambda^{CH}(\mathbb{1})$.

After this short digression, one can re-visit eq. (2.25) and justify its validity in this new lingo: the average assigned state $\mathcal{A}_\Lambda[\rho(0)]$ clearly belongs to $\Omega_\Lambda^M(\rho)$, so applying the coarse-graining map naturally recovers $\rho(0)$.

One must be more careful, however, when evaluating the result of applying $(\mathcal{A}_\Lambda \circ \Lambda)$ on a microscopic state. Consider the action of Λ on a general microscopic state ψ, resulting on some effective state ρ. Clearly, $\psi \in \Omega_\Lambda^M(\rho)$. The subsequent application of $\mathcal{A}_\Lambda$, however, will not take ρ back to ψ, but rather to the average state of the set $\Omega_\Lambda(\rho)$, which will generally be another completely different state, see fig. 2.4 for clarity. Thus, $(\mathcal{A}_\Lambda \circ \Lambda)$ only acts trivially on a microscopic state ψ if it was an average assigned state to begin with.
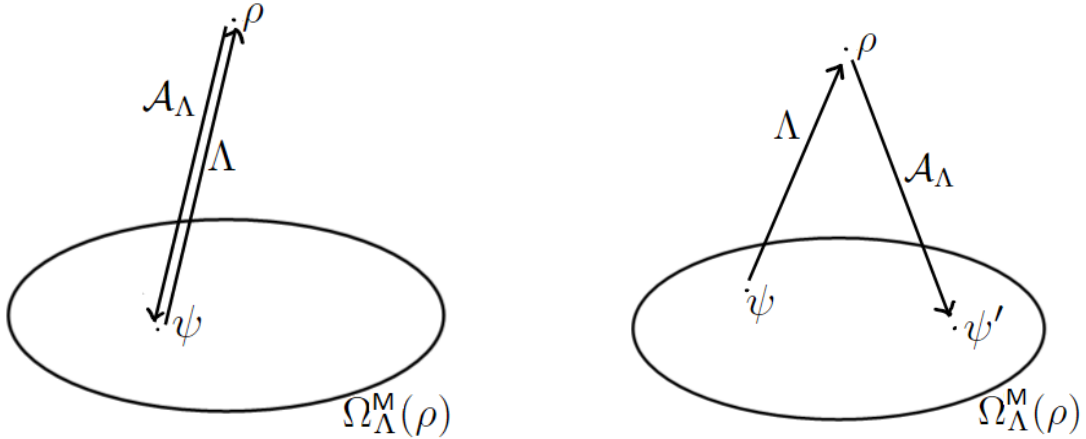
(a) $(\Lambda \circ \mathcal{A}_\Lambda)[\rho] = \rho$ for any prepared effective state, since $\mathcal{A}_\Lambda[\rho]$ is the average assigned state, which obviously belongs to $\Omega_\Lambda^M(\rho)$.

(b) The action of $\mathcal{A}_\Lambda$ on ρ will always yield the average assigned state. Thus, ψ' will only coincide with ψ if ψ was the average assigned state to begin with.

Figure 2.4: $(\Lambda \circ \mathcal{A}_\Lambda)$ is simply the trivial channel, but $(\mathcal{A}_\Lambda \circ \Lambda)$ will only act trivially on average assigned states.

Looking back at eq. (2.24), one can then see that the condition for effective reversibility is not, in fact, automatically satisfied. Moreover, we conclude that, in order for $(\mathcal{A}_\Lambda \circ \Lambda)$ to be trivial and the whole channel $(\Gamma_{-t} \circ \Gamma_t)$ to be the identity, one needs $(\mathcal{U}_t \circ \mathcal{A}_\Lambda)[\rho(0)]$ to be an average assigned state. Once that is true, it follows that

$$\rho(0) = (\Lambda \circ \mathcal{U}_{-t} \circ \mathcal{A}_\Lambda \circ \Lambda \circ \underbrace{\mathcal{U}_t \circ \mathcal{A}_\Lambda)[\rho(0)]}_{\text{average assigned state}} \tag{2.28}$$

$$= (\Lambda \circ \mathcal{U}_{-t} \circ \mathcal{U}_t \circ \mathcal{A}_\Lambda)\rho(0) \tag{2.29}$$

$$= (\Lambda \circ \mathcal{A}_\Lambda)\rho(0) \tag{2.30}$$

$$= \rho(0). \tag{2.31}$$

Put another way, the condition for the effective dynamics to be reversible, stated in eq. (2.24), is equivalently to demanding that $(\mathcal{U}_t \circ \mathcal{A}_\Lambda)[\rho(0)]$ be an average assigned state. Now, notice that $\mathcal{A}_\Lambda[\rho(0)]$ is, by construction, an average assigned state itself. This means that, ultimately, the microscopic evolution $\mathcal{U}_t$ must be such that it maps average assigned states into average assigned states.

We can finally express the condition for an effective dynamics Γ_t to be reversible: if ψ is an average assigned state, then the evolved state $\mathcal{U}_t[\psi]$ is also an average assigned state. Or yet,

$$\mathcal{U}_t[\psi] = (\mathcal{A}_\Lambda \circ \Lambda \circ \mathcal{U}_t)[\psi] \tag{2.32}$$
$$\text{whenever} \quad \psi = (\mathcal{A}_\Lambda \circ \Lambda)[\psi].$$

The requirement above reflects the fact that reversibility is not a feature automatically present in effective dynamics, being rather the result of a consonance between the coarse-graining map and the microscopic evolution. Only if these two maps are somehow fine-tuned to each other can Γ_t be reversible, and any initial state $\rho(0)$ can be recovered from $\rho(t) = \Gamma_t[\rho(0)]$ by applying the reverse effective evolution Γ_{-t}.

Let us take a moment to understand, from the physical perspective, why such dynamics are reversible. Consider an initial preparation of some state $\rho(0)$, where one is sampling an unknown microscopic state that, on average, is given by the average assignment map as $\bar{\psi}(0) = \mathcal{A}_\Lambda[\rho(0)]$. We let it evolve according to Γ_t, meaning that $\bar{\psi}(0)$ will evolve into $\bar{\psi}(t) = \mathcal{U}_t[\bar{\psi}(0)]$, which in the lab will correspond to $\rho(t) = \Lambda[\bar{\psi}(t)]$, on the effective level. Now, let us assume that the condition in eq. (2.32) is indeed satisfied, i.e., the microscopic evolution is such that it yields an average assigned state whenever it is applied on an average assigned state. Applying the reverse map $\Gamma_{-t} = (\Lambda \circ \mathcal{U}_t \circ \mathcal{A}_\Lambda)$ on the final effective state starts with applying $\mathcal{A}_\Lambda$ on $\rho(t)$ to find some microscopic state $\psi'(t)$, which is in general not the same as $\bar{\psi}(t)$. However, since $\bar{\psi}(0)$ is, by construction, an average assigned state, then so is $\psi'(t)$, as we have just assumed that $\mathcal{U}_t$ displays the desired property of taking average assigned states into average assigned states. If $\bar{\psi}(t)$ is an average assigned state, then, it satisfies condition that $\bar{\psi}(t) = (\mathcal{A}_\Lambda \circ \Lambda)[\bar{\psi}(t)]$, which means $\psi'(t) = \bar{\psi}(t)$. Consequently, evolving $\bar{\psi}(t)$ backwards with $\mathcal{U}_{-t}$ yields $\bar{\psi}(0)$, which corresponds to $\rho(0)$ after the coarse-graining map. See fig. 2.5 for clarity.

Thus, one can ascertain that the dynamics of effective states will be reversible if the microscopic evolution $\mathcal{U}_t$ and the coarse-graining map Λ satisfy eq. (2.24), which can only be achieved if the condition in eq. (2.32) is satisfied. $\mathcal{U}_t$ and Λ must be such that $\mathcal{U}_t$ takes average assigned states into average assigned states to ensure that, after gathering statistics from many runs of an experiment, one will conclude that the initial effective state $\rho(0)$ is always recovered, for any $\rho(0)$. This does not mean, however, that the initial state is always recovered, since the effective evolution channel Γ_t yields the average $\rho(t)$, obtained after analyzing the outcomes of many runs of the experiment.

If one wants to impose stronger conditions and require that the initial effective states be recovered on each run of the experiment, another analysis must be conducted, as demanding that eq. (2.24) is satisfied is too loose a condition. To derive that proper constraint, we must look at what is happening on the microscopic level of the experiment at each realization.

Following [25], we can explore a particular scenario where specially interesting reversibility is achieved, namely where the initial effective state is recovered not only on average but on every realization of the experiment. This situation is set when a stricter condition on $\mathcal{U}_t$ and Λ is satisfied, namely

$$(\Lambda \circ \mathcal{U}_t)[\psi(0)] = (\Lambda \circ \mathcal{U}_t)[\phi(0)] \tag{2.33}$$
$$\text{whenever} \quad \Lambda[\psi(0)] = \Lambda[\phi(0)].$$

What this condition is imposing is that whenever two microscopic states $\psi(0), \phi(0)$ are assigned to the same effective state, then the microscopic evolution $\mathcal{U}_t$ is such that the evolved states $\psi(t), \phi(t)$ will still be
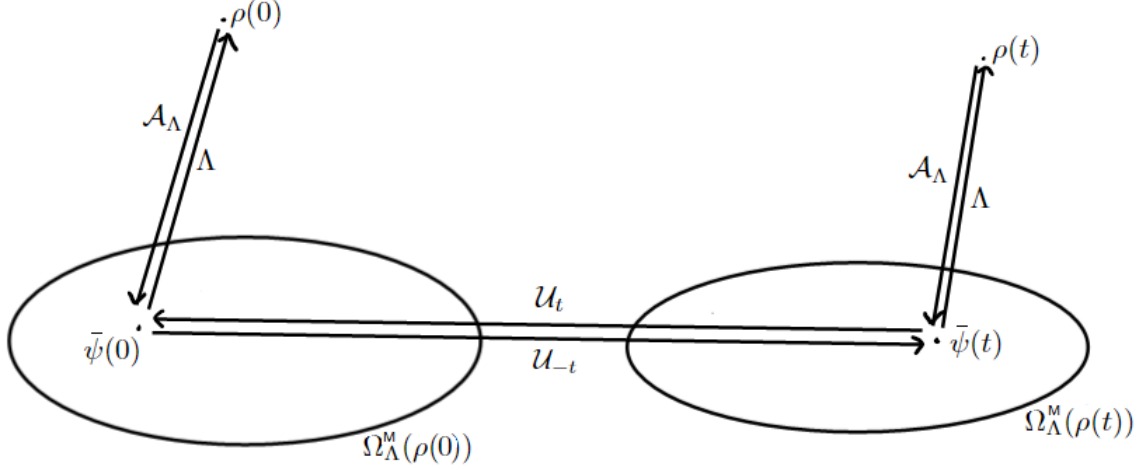
Figure 2.5: *Schematics of reversible effective dynamics.* Reversibility is assured whenever $\mathcal{U}_t$ takes the average state of some set $\Omega_\Lambda(\rho(0))$ into the average state of some other set $\Omega_\Lambda(\rho(t))$. Put another way, $(\mathcal{U}_t \circ \mathcal{A}_\Lambda)[\rho(0)] = \mathcal{A}_\Lambda[\rho(t)]$. Since the underlying unitary evolution is such that it takes average assigned states into average assigned states, it is guaranteed that, just as $\bar{\psi}(0)$, $\bar{\psi}(t)$ is an average assigned state. As a consequence, $\bar{\psi}(t) = (\mathcal{A}_\Lambda \circ \Lambda)[\bar{\psi}(t)]$ and the same path is followed by the forward and the backward evolution, assuring that the effective dynamics is reversible.

assigned to a single effective state. Put another way, $\mathcal{U}_t$ does not "split" the microscopic states compatible with the same effective description, even after the evolution they will still yield a single effective state: if $\psi(0), \phi(0)$ are both mapped to $\rho(0)$, then $\psi(t), \phi(t)$ are both mapped to $\rho(t)$. Mathematically, one could also state it as the requirement that the microscopic evolution take $\Omega_\Lambda^M(\rho(0))$ into $\Omega_\Lambda^M(\rho(t))$.

Let us now argue that the condition expressed above is indeed a particular case of the general condition for reversibility. Intuitively, this implication is a consequence of the linearity of $\mathcal{U}_t$: if the particular condition in eq. (2.33) imposes that $\Omega_\Lambda(\rho(0))$ evolves into $\Omega_\Lambda(\rho(t))$, the broader condition in eq. (2.32) is satisfied because the average state $\bar{\psi}(0)$ of $\Omega_\Lambda(\rho(0))$ evolves into the average state $\bar{\psi}(t)$ of $\Omega_\Lambda(\rho(t))$.

If this stricter condition on the microscopic evolution $\mathcal{U}_t$ and the coarse-graining map Λ is satisfied, then reversibility is assured, meaning that after many runs of the experiment one verifies that any initial effective preparation is recovered. Notice that one can only conclude that the dynamics is reversible after preparing $\rho(0)$ many times, and subsequently performing the forward and backward evolution protocols to infer $\rho(0)$ for instance with state tomography. In other words, the statistical nature of the measurement process only allows one to ascertain that the initial state is recovered on average. However, condition eq. (2.33) yields a particular scenario where reversibility is in fact achieved on every run of the experiment, and the initial effective state is recovered on every realization, not only on average (though one would still have to perform state tomography to determine the effective state).

To see why this is the case, we must take a moment to expand on the physics behind a scenario of what we dub "single-shot" reversibility, drawing from similar results in [25]. Suppose that, indeed, the condition in eq. (2.33) is satisfied and $\mathcal{U}_t$ takes all microscopic states associated with the same effective description into evolved microscopic states that are still compatible with a single effective description. Upon preparing a state $\rho(0)$ in the lab, one is in fact sampling some microscopic state $\psi(0) \in \Omega_\Lambda(\rho(0))$, which is then evolved into $\psi(t) = \mathcal{U}_t[\psi(0)]$. The effective evolved state is given by the coarse-graining map as $\rho(t) = \Lambda[\psi(t)]$. The reverse process is then performed, where this preparation of $\rho(t)$ corresponds to sampling $\psi'(t) \in \Omega_\Lambda(\rho(t))$, which is then evolved into $\psi'(0) = \mathcal{U}_{-t}[\psi'(t)]$. Notice now that both $\psi(t)$ and $\psi'(t)$ belong to $\Omega_\Lambda^M(\rho(t))$. If condition in eq. (2.33) is satisfied, as we assumed, this must mean both $\psi(0)$ and $\psi'(0)$ belong to $\Omega_\Lambda^M(\rho(0))$. Consequently, applying the coarse-graining map on $\psi'(0)$ yields the initial effective state $\rho(0)$, see fig. 2.6. In summary, $\rho(0)$ is recovered on every single run of the experiment if condition eq. (2.33) is satisfied.

The simplest instance of reversible dynamics can be seen as a special case of the scenario we described for single-shot reversibility. Consider that the condition in eq. (2.33) is satisfied, but in particular it holds that
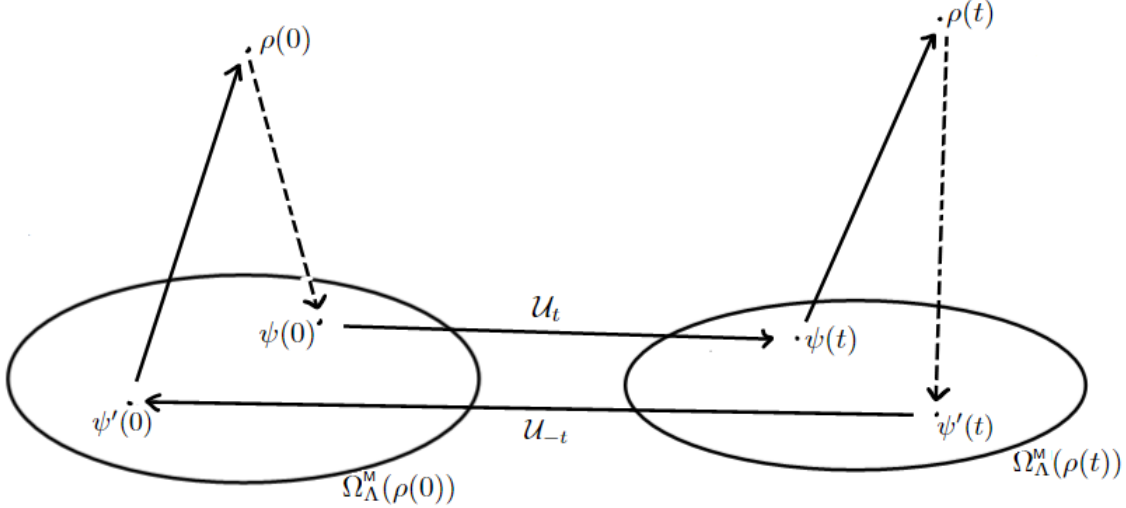
Figure 2.6: *Schematics of single-shot reversible dynamics* In a stricter scenario, single-shot reversibility is assured whenever $\mathcal{U}_t$ takes any state in $\Omega_\Lambda^M(\rho(0))$ into some state in $\Omega_\Lambda^M(\rho(t))$. When this condition is met, it is clear that $\psi(0)$ and $\psi'(0)$ will both belong to $\Omega_\Lambda^M(\rho(0))$, since clearly $\psi(t), \psi'(t) \in \Omega_\Lambda^M(\rho(0))$. This ensures that the initial state is recovered on every run of the experiment.

$$(\Lambda \circ \mathcal{U}_t)[\psi(0)] = \rho \qquad (2.34)$$
$$\text{whenever} \quad \Lambda[\psi(0)] = \rho.$$

In words, this even stricter conditions dictates that the microscopic evolution $\mathcal{U}_t$ takes all the microscopic states $\psi(0)$ compatible with an effective description ρ into evolved states $\psi(t)$ that are still compatible with the same initial effective state ρ. Put another way, $\mathcal{U}_t$ plays into the symmetries of the coarse-graining map and acts in such a way that states in $\Omega_\Lambda^M(\rho)$ remain in $\Omega_\Lambda^M(\rho)$ after being evolved.

Indeed, if the condition of eq. (2.34) is met the scenario is as follows. A preparation ρ corresponds to sampling some $\psi(0) \in \Omega_\Lambda(\rho)$, which evolves into $\psi(t) = \mathcal{U}_t[\psi(0)]$. However, it is imposed that $\Lambda[\psi(0)] = \Lambda[\psi(t)]$, meaning that the action of the coarse-graining map on the evolved microscopic state will yield ρ once again. As a result, only trivial dynamics are observed in the lab, and even though the microscopic state changes, no change is perceived on the effective level. Thus, the effective dynamics is trivially reversible, see fig. 2.7 for details.

Now that we have established the conditions on the microscopic evolution and the coarse-graining map that yield emerging dynamics that are reversible, we can move on to analyze a couple of examples.

2.3.1 Examples: $\Lambda_{\mathbf{PT}}$ and Λ_D

For Γ_t to be reversible, it is necessary that the condition expressed in eq. (2.24) is verified. Additionally, eqs. (2.33) and (2.34) impose even stricter constraints on $\mathcal{U}_t$ and Λ, which result in less general reversible dynamics on the effective level. Let us explicitly find the microscopic evolutions that satisfy each of these conditions for a couple of examples of coarse-graining maps: Λ_{PT} describing the partial trace, and Λ_D describing the imperfect detector.

Consider the partial trace map, acting on microscopic states $\psi \in \mathcal{L}(\mathcal{H}_S \otimes \mathcal{H}_E)$, composed of a system of interest interacting with an environment. We want to find which microscopic evolutions meet the reversibility condition eq. (2.24), that is, which $\mathcal{U}_t$ take average assigned states into average assigned states. Mathematically, this means that $\mathcal{U}_t$ must be such that there exist effective preparations ρ, ϕ satisfying

$$\mathcal{U}_t[\mathcal{A}_{\Lambda_{\mathrm{PT}}}(\rho)] = \mathcal{A}_{\Lambda_{\mathrm{PT}}}(\phi). \qquad (2.35)$$

Recall the expression one already has for the average assigned state of a general effective state, given in eq. (2.22), and the equation above can be re-written as

34
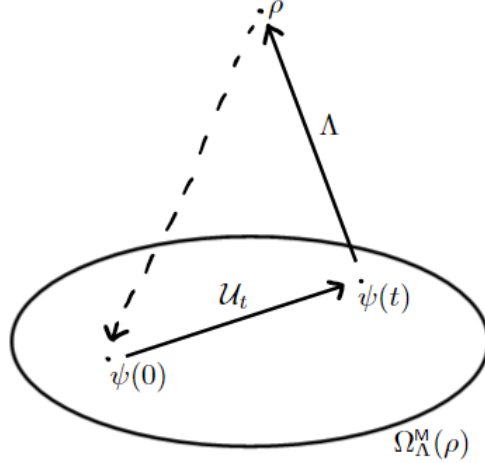
Figure 2.7: *Schematics of trivial effective dynamics.* Suppose an effective state ρ was prepared in the lab. Regardless to which underlying state $\psi(0) \in \Omega_\Lambda(\rho)$ it corresponds, single-run reversibility is assured whenever $\mathcal{U}_t$ is such that it takes states in $\Omega_\Lambda(\rho)$ into states in $\Omega_\Lambda^M(\rho)$, for any ρ. Even though the underlying physical state may change with the action of the unitary evolution, only trivial effective dynamics will be observed in the lab.

$$\mathcal{U}_t\left[\rho \otimes \frac{\mathbb{1}_E}{d_E}\right] = \phi \otimes \frac{\mathbb{1}_E}{d_E}. \tag{2.36}$$

One can then conclude that the microscopic evolution must act locally on the system and the environment. There must exist unitary operators $U_E \in \mathcal{H}_E$ and $U_S \in \mathcal{H}_S$, such that the action of $\mathcal{U}_t$ on any state ψ can be expressed as

$$\mathcal{U}_t[\psi] = (U_S \otimes U_E)\psi(U_S^\dagger \otimes U_E^\dagger). \tag{2.37}$$

Therefore, whenever $\mathcal{U}_t$ acts locally, then the effective dynamics induced by the partial trace satisfies eq. (2.24) and is thus reversible.

An interesting aspect to the partial trace is that the class of $\mathcal{U}_t$ that satisfy the most general condition for reversibility in eq. (2.24), requiring the initially prepared effective state to be recovered on average, also satisfy the more restricted condition in eq. (2.33), which implies that the initial state is recovered on every realization of the experiment. This means that if one's access to information about a physical system is described by the partial trace, reversible dynamics are always single-shot reversible.

Indeed, translating the condition expressed in eq. (2.33) in terms of the partial trace yields

$$\text{Tr}_E[\mathcal{U}_t[\psi(0)]] = \text{Tr}_E[\mathcal{U}_t[\phi(0)]] \tag{2.38}$$
$$\text{whenever} \quad \text{Tr}_E[\psi(0)] = \text{Tr}_E[\phi(0)],$$

which is clearly satisfied for microscopic evolutions that only act locally, that is, the set of $\mathcal{U}_t$ that satisfy the condition for general reversibility. Moreover, the simplest reversibility scenario, where the effective dynamics is trivial, is recovered when $U_S = \mathbb{1}_S$, and no change is perceived in the lab.

This is a peculiarity of this specific coarse-graining map and not a rule, as in general there will be microscopic evolutions that yield dynamics that are reversible (so, satisfying eq. (2.24)) but do not recover the initial effective state on every run of the experiment, only on average (meaning they do not satisfy the requirement in eq. (2.33)).

To show an example, let us now consider the coarse-graining described in section 2.1.1, modeling measurements performed by an imperfect detector. One can once again characterize the set of unitary microscopic evolutions that satisfy the conditions for reversibility in eq. (2.24), for single-shot reversibility in eq. (2.33), and trivial effective dynamics in eq. (2.34).

We can start with the simplest case. Let $\mathcal{S}_1$ be the set of unitary operators that describe the action of microscopic evolutions that satisfy eq. (2.34), that is, if $U \in \mathcal{S}_1$ then the evolution given by $\mathcal{U}_t[\psi] = U\psi U^\dagger$

yields trivial dynamics. It can be shown that, if one adopts Λ_D as the coarse-graining map, then the elements of $\mathcal{S}_1$ can be parameterized by $\alpha \in [0, 2\pi]$ as

$$U_1(\alpha) = \frac{1}{2} \begin{pmatrix} 2e^{-i\alpha} & 0 & 0 \\ 0 & (1 + e^{i\alpha}) & (1 - e^{i\alpha}) \\ 0 & (1 - e^{i\alpha}) & (1 + e^{i\alpha}) \end{pmatrix}. \tag{2.39}$$

Similarly, let $\mathcal{S}_2$ be the set of unitary operators that describe the action of microscopic evolutions that satisfy eq. (2.33) and yield single-shot reversible dynamics. The elements of $\mathcal{S}_2$ can be parameterized by $\alpha, \beta \in [0, 2\pi]$ as

$$U_2(\alpha, \beta) = \frac{1}{2} \begin{pmatrix} 2e^{-i(\alpha+\beta)} & 0 & 0 \\ 0 & (e^{i\alpha} + e^{i\beta}) & -(e^{i\alpha} - e^{i\beta}) \\ 0 & -(e^{i\alpha} - e^{i\beta}) & (e^{i\alpha} + e^{i\beta}) \end{pmatrix}. \tag{2.40}$$

Notice that, as expected, the unitary operators described in eq. (2.39) are a subset of those described in eq. (2.40), reflecting the observation that trivial dynamics are a particular case of single-shot reversible dynamics, and $\mathcal{S}_1$ can be obtained from $\mathcal{S}_2$ by setting $\beta = 0$.

Finally, let $\mathcal{S}_3$ be the set of unitary operators that describe the action of microscopic evolutions that satisfy the general reversibility condition in eq. (2.24). Its elements are expressed in terms of parameters $\theta_1, \theta_2, \theta_3 \in [0, \pi/2]$ and $\phi_1, \phi_2, \phi_3, \phi_4, \phi_5 \in [0, 2\pi]$ as

$$U_3(\theta_1, \theta_2, \theta_3, \phi_1, \phi_2, \phi_3, \phi_4, \phi_5) = \frac{1}{2} \begin{pmatrix} \cos\theta_1 \cos\theta_2 e^{i\phi_1} & \sin\theta_1 e^{i\phi_3} & \cos\theta_1 \sin\theta_2 e^{i\phi_4} \\ \chi_{21} & \cos\theta_1 \cos\theta_3 e^{i\phi_2} & \chi_{23} \\ \chi_{31} & \cos\theta_1 \sin\theta_3 e^{-i\phi_5} & \chi_{33} \end{pmatrix}, \tag{2.41}$$

with

$$\chi_{21} = \sin\theta_2 \sin\theta_3 e^{-i\phi_4 - i\phi_5} - \sin\theta_1 \cos\theta_2 \cos\theta_3 e^{i\phi_1 + i\phi_2 - i\phi_3}, \tag{2.42}$$

$$\chi_{23} = -\cos\theta_2 \sin\theta_3 e^{-i\phi_1 - i\phi_5} - \sin\theta_1 \sin\theta_2 \cos\theta_3 e^{i\phi_2 - i\phi_3 + i\phi_4}, \tag{2.43}$$

$$\chi_{31} = -\sin\theta_1 \cos\theta_2 \sin\theta_3 e^{i\phi_1 - i\phi_3 + i\phi_5} - \sin\theta_2 \cos\theta_3 e^{-i\phi_2 - i\phi_4}, \tag{2.44}$$

$$\chi_{33} = \cos\theta_2 \cos\theta_3 e^{-i\phi_1 - i\phi_2} - \sin\theta_1 \sin\theta_2 \sin\theta_3 e^{-i\phi_3 + i\phi_4 + i\phi_5}. \tag{2.45}$$

The parameters that define the elements of $\mathcal{S}_3$ have to obey the restrictions set by

$$0 \geq \frac{\sin\phi_5 - \phi_2}{\sin\phi_1 + \phi_2 + \phi_5} \geq 1 \tag{2.46}$$

$$\frac{\sin\phi_1 + 2\phi_2}{\sin\phi_1 + \phi_2 + \phi_5} \leq 0 \tag{2.47}$$

$$\phi_4 = \phi_3 \tag{2.48}$$

$$\frac{\theta_1}{\cos 2\theta_1} = \cos^2 2\theta_1 \left(\frac{\sin\phi_5 - \phi_2}{\sin\phi_1 + \phi_2 + \phi_5} \right) \tag{2.49}$$

$$\theta_2 = \arcsin\tan\theta_1, \quad 0 \leq \theta_1 \leq \pi/4 \tag{2.50}$$

$$\tan\theta_3 = -\cot^2\theta_1 \csc\phi_1 + \phi_2 + \phi_5 \sin\phi_1 + 2\phi_2 \tag{2.51}$$

The calculations leading to eqs. (2.39), (2.40) and (2.41) are presented in appendix D. There, we also show that a particular choice of parameters for $U_3(\theta_1, \theta_2, \theta_3, \phi_1, \phi_2, \phi_3, \phi_4, \phi_5)$ recovers the elements of $\mathcal{S}_2$, as expected. We point out that, unlike the scenario where one takes the partial trace as the coarse-graining map, the inclusion the set $\mathcal{S}_2$ in $\mathcal{S}_3$ is strict, meaning there are microscopic evolutions that will, indeed, yield reversible effective dynamics that are not single-shot reversible.

In this section, we have characterized the microscopic evolutions that, in composition with the coarse-graining maps Λ_{PT} or Λ_D, yield emerging effective dynamics that are reversible. We have also specified which subset of these microscopic evolutions additionally satisfy stricter restrictions, resulting in effective reversible dynamics that always recover the initial state (on every realization of the experiment, not only on average) or that describe a trivial effective evolution (where no change is perceived in the lab). We know move on to the next section, where we discuss how to characterize effective reversibility in terms of our ignorance about the physical system.

2.4 Uncertainty and reversibility

So far, what we have made clear is that, while not the norm, effective reversibility is achieved when some matching between the microscopic evolution $\mathcal{U}_t$ and the coarse-graining map Λ takes place. With this analysis, one can understand reversibility exclusively in terms of quantities and objects available during an experiment, and it is not necessary to assume any access to information that is not available (such as the actual microscopic state that is being prepared).

This is, however, a very descriptive analysis. It attests that reversibility is possible under certain conditions, but it does not touch the matter of *why* these specific dynamics are reversible. In this section, we want to address this aspect of the problem, and provide a physical meaning to reversibility on the effective level. To do that, we must revisit the discussion around the second law of thermodynamics (which ultimately should dictate which dynamics are reversible), and the difficulty around defining an adequate entropy.

As we have established, the object of interest for the second law is entropy, but it is very unclear *which* entropy should be at its core. In [39, 72], von Neumann argues for the central role that coarse-graining should have when analyzing thermodynamics systems, even in detriment of his eponymous entropy in eq. (2.5), which he deemed to be valid only in certain circumstances. Similarly, in [73], Einstein already argued that the entropy of a macroscopic state should be proportional to the log of the number of underlying quantum states compatible with the macroscopic description.

While the effort of defining the ultimate entropy to figure in the second law is beyond the scope of our work, we can surely take notes from the investigations of these researchers, as well as Boltzmann himself, and recognize the essential role that uncertainty must play. In all these approaches, what is established is that the entropy of an effective state is closely connected to the uncertainty around it. Although, upon preparing an effective state ρ, the actual microscopic state that is sampled is unknown, different degrees of uncertainty are associated to each effective state: the more microstates compatible with ρ there are, the more uncertainty one has, and the higher the entropy of ρ should be.

The physical implication that this realization has on the second law of the thermodynamics is that only dynamics where the uncertainty of an effective state decreases (or at least remains unchanged) are possible, since the entropy is constrained not to increase. In turn, an evolution is only be reversible if the entropy stays constant throughout the process, which means if the uncertainty associated to an effective state increases then reversibility can no longer be achieved.

The physical interpretation of this statement is that information that is lost should not be recovered. Starting with some effective state $\rho(0)$, with few compatible microscopic states and thus associated with low uncertainty, one lets it evolve to $\rho(t)$, with many compatible microscopic states. The result is an increase in uncertainty, which one should not expect to be reversible.

Motivated by this reasoning, we suggest that the relevant object that restricts the reversibility of effective dynamics is the volume of the set of microscopic states compatible with the effective description. This quantity assesses the uncertainty associated to a preparation, and its behavior throughout an effective evolution can rule out reversibility completely: if this volume increases, the process cannot be reversible.

Let ρ be an effective state in $\mathcal{H}_d$. Instead of constructing the set $\Omega_\Lambda(\rho)$ of pure microscopic states compatible with ρ, one can consider the set of pure microscopic states whose effective description is close enough to ρ. Let this set be defined as

$$\Omega_\Lambda^\epsilon(\rho) = \{\psi \in \mathcal{L}_D |\ ||\Lambda[\psi] - \rho|| \le \epsilon,\ \psi = |\psi\rangle\langle\psi|\}. \tag{2.52}$$

Here, one is simply including an imprecision parameter ϵ, determining how far the effective description of a microstate can be from the target effective state ρ. Of course, by taking the limit $\epsilon \to 0$ we promptly recover $\Omega_\Lambda(\rho)$.

We can, then, gauge the uncertainty of ρ by evaluating the volume of $\Omega_\Lambda^\epsilon(\rho)$, given by the following expression

$$\mathcal{V}_\Lambda^\epsilon(\rho) = \int d\mu_\psi\ \frac{1}{\epsilon}\mathrm{rect}\left(\frac{||\Lambda[\psi] - \rho||}{\epsilon}\right), \tag{2.53}$$

where $d\mu_\psi$ is the Haar measure over pure states in $\mathcal{H}_D$, and rect is the rectangular function, defined as

$$\mathrm{rect}\frac{t}{a} = \begin{cases} 0, & \text{if } |t| > \frac{a}{2} \\ 1, & \text{if } |t| < \frac{a}{2} \\ \frac{1}{2}, & \text{if } |t| = \frac{a}{2} \end{cases} \tag{2.54}$$

We are naturally interested in the situation where ϵ is very small, in which case the expression above is reduced to

$$\mathcal{V}_\Lambda(\rho) = \int d\mu_\psi \delta(\Lambda[\psi] - \rho). \tag{2.55}$$

Notice that, strictly speaking, evaluating eq. (2.55) yields zero. This result will be show in more detail further in the text, but it an expected and intuitive result: microscopic states that correspond *exactly* to ρ after a coarse-graining map is applied are in a hyperspace of volume zero. However, just as in standard statistical physics, one can evaluate $\mathcal{V}_\Lambda^\epsilon(\rho)$ in the limit of $\epsilon \ll 1$. Then, taking the first order approximation would confer a "thickness" ϵ to the set $\Omega_\Lambda(\rho)$, and $\mathcal{V}_\Lambda(\rho)$ is proportional to ϵ and no longer null.

For a generic Λ, the expression for the volume of the set of pure microscopic states compatible with ρ in eq. (2.55) can be quite tough to evaluate. Nevertheless, it is possible to find the uncertainty associated to an effective state in both our working examples, either analytically or at least numerically.

2.4.1 Examples: $\Lambda_{\mathbf{PT}}$ and Λ_D

Let us evaluate the uncertainty associated to an effective description $\rho \in \mathcal{H}_S$, emerging from choosing the partial trace over $\mathcal{H}_E$ as the coarse-graining map. We want to compute

$$\mathcal{V}_{\Lambda_{\mathrm{PT}}}(\rho) = \int d\mu_\psi \delta(\Lambda_{\mathrm{PT}}[\psi] - \rho), \tag{2.56}$$

where $d\mu_\psi$ is the Haar measure in $\mathcal{H}_S \otimes \mathcal{H}_E$. Recall the trick used in appendices C and D, where one uses the symmetries of the coarse-graining map to simplify the integral. Start by making the change of variable $|\psi\rangle \to U_S \otimes \mathbb{1}_E |\psi\rangle$, where U_S is an arbitrary unitary acting on $\mathcal{H}_S$. Since the Haar measure is invariant under unitary transformations, it follows that

$$\mathcal{V}_{\Lambda_{\mathrm{PT}}}(\rho) = \int d\mu_\psi \delta(U_S \Lambda_{\mathrm{PT}}[\psi] U_S^\dagger - \rho) \tag{2.57}$$

$$= \int d\mu_\psi \delta(\Lambda_{\mathrm{PT}}[\psi] - U_S^\dagger \rho U_S). \tag{2.58}$$

The choice of U_S is arbitrary, so let us choose it such that it diagonalizes ρ

$$\mathcal{V}_{\Lambda_{\mathrm{PT}}}(\rho) = \int d\mu_\psi \delta(\Lambda_{\mathrm{PT}}[\psi] - \mathrm{diag}[\lambda_1, \ldots, \lambda_{d_S}]), \tag{2.59}$$

and we assume that all $\lambda_i \neq 0$.[4]

Now, let us parameterize ψ as

$$|\psi\rangle = \sum_{i,j} c_{ij} |\phi_i\rangle_S |\gamma_j\rangle_E, \tag{2.60}$$

with $i = 1, \ldots, d_S$, $j = 1, \ldots, d_E$, and $\langle \phi_i | \phi_j \rangle = \langle \gamma_i | \gamma_j \rangle = \delta_{ij}$ such that the reduced state of the system is given by

$$\rho^S = \mathrm{Tr}_E[|\psi\rangle\langle\psi|] = \sum_{ijk} c_{ik} c_{jk}^* |\phi_i\rangle\langle\phi_j|, \tag{2.61}$$

and the element of the reduced density matrix are

$$\rho_{ij}^S = \sum_k c_{ik} c_{jk}^* \tag{2.62}$$

$$= \vec{c}_i \cdot \vec{c}_j^\dagger. \tag{2.63}$$

Consequently, the expression for the volume is now

---

[4]This assumption is aligned with the framework we are setting throughout this chapter. We are trying to deal with realistic scenarios, and quantum states with a null eigenvalue (that is, that are not full-rank) are never going to be exactly prepared in the lab

$$\mathcal{V}_{\Lambda_{\mathrm{PT}}}(\rho) = \int d\vec{c} \prod_{i=1}^{d_S} \delta(\vec{c}_i\vec{c}_i^\dagger - \lambda_i) \prod_{i\neq j}^{d_S} \delta(\vec{c}_i\vec{c}_j^\dagger), \tag{2.64}$$

where

$$d\vec{c} = \prod_{i=1}^{d_S} d\vec{c}_i \tag{2.65}$$

$$d\vec{c}_i = \prod_{k=1}^{d_E} dc_{ik}. \tag{2.66}$$

Let us once again make a change of variable $\vec{c}_i = \sqrt{\lambda_i}\vec{z}_i$, such that

$$d\vec{c}_i = \lambda_i^{d_E} d\vec{z}_i \tag{2.67}$$

$$d\vec{c} = (\det[\rho])^{d_E} d\vec{z} \tag{2.68}$$

$$\prod_i \delta(\vec{c}_i\vec{c}_i^\dagger - \lambda_i) = \prod_i \frac{1}{\lambda_i}\delta(\vec{z}_i\vec{z}_i^\dagger - 1) \tag{2.69}$$

$$\prod_{i\neq j} \delta(\vec{c}_i\vec{c}_j^\dagger) = \prod_{i\neq j} \frac{1}{\sqrt{\lambda_i\lambda_j}}\delta(\vec{z}_i\vec{z}_j^\dagger). \tag{2.70}$$

The resulting expression for the volume is

$$\mathcal{V}_{\Lambda_{\mathrm{PT}}}(\rho) = \det[\rho]^{d_E} \prod_i \frac{1}{\lambda_i} \prod_{i<j} \frac{1}{\lambda_i\lambda_j} \int d\vec{z} \prod_{i=1}^{d_S} \delta(\vec{z}_i\vec{z}_i^\dagger - \lambda_i) \prod_{i\neq j}^{d_S} \delta(\vec{z}_i\vec{z}_j^\dagger). \tag{2.71}$$

Moreover, one can see that

$$\prod_i \frac{1}{\lambda_i} = \det[\rho], \tag{2.72}$$

$$\prod_{i<j} \frac{q}{\lambda_i\lambda_j} = \frac{1}{(\det[\rho])^{d_S-1}}. \tag{2.73}$$

Finally, one reaches the final expression

$$\mathcal{V}_{\Lambda_{\mathrm{PT}}}(\rho) = \det[\rho]^{d_E-d_S} \underbrace{\int d\vec{z} \prod_{i=1}^{d_S} \delta(\vec{z}_i\vec{z}_i^\dagger - 1) \prod_{i\neq j}^{d_S} \delta(\vec{z}_i\vec{z}_j^\dagger)}_{K(d_S)}. \tag{2.74}$$

where the integral is a constant that does not depend on ρ, only on d_S, and $K(d_S)$ is simply the volume associated to identity matrix in d_S.

As expected, this expression reflects the uncertainty of ρ. One can see for instance that this volume is maximal for the maximally mixed state, which corresponds, intuitively, to the effective preparation where one knows the least about the possible microscopic state. On the other hand, effective states with very high purity, i.e., one eigenvalue very close to 1 and the remaining eigenvalues very close to 0, have a small corresponding uncertainty volume.

A few things must be noted about this result. First, it is expected that pure states should have the corresponding volume of uncertainty be zero. In fact, this holds for any state that is not full-rank, since its determinant would be zero. We point out, however, that such states would never be realistically prepared in the lab, since it would require infinite precision.

Second, eq. (2.74) predicts that all (full-rank) states would have the same volume of uncertainty if $d_E = d_S$. We argue that, once again, in a realistic scenario that would never be the case. First of all because the environment typically has more degrees of freedom than the system of interest, so $d_E > d_S$

usually holds. Furthermore, this whole calculation was carried out considering pure microscopic states. It can be easily generalized for mixed states by purifying them with the aid of some auxiliary system of dimension $d_B > 1$. As a result, the corresponding expression for the volume would be

$$\mathcal{V}_{\Lambda_{\mathrm{PT}}}^{d_B}(\rho) \propto \det[\rho]^{d_E d_B - d_S}. \tag{2.75}$$

This expression would only yield constant volume if $d_S > d_E$, which would be very atypical. If we stress again that pure states cannot be realistically prepared in the lab, considering the expression above combined with the usual scenario of $d_E > d_S$ is enough to argue that one will not face a situation where eq. (2.74) yields the not-so-useful result of constant volume for all states. In fig. 2.8, we provide a numerical analysis further supporting the use of $\mathcal{V}_{\Lambda_{\mathrm{PT}}}(\rho)$ as defined above.
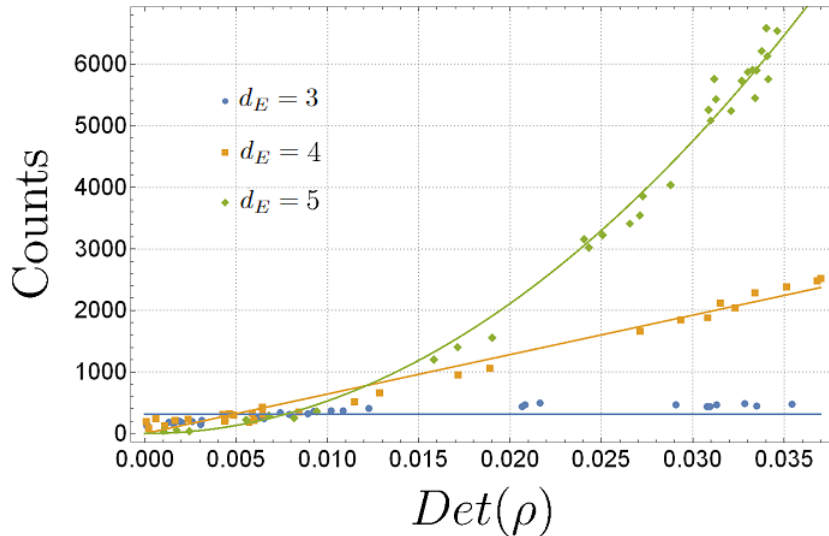
Figure 2.8: *Numerical analysis of the volume of uncertainty of effective states.* In this graph, we evaluate how well simulations fit with the prediction given by eq. (2.55). For a given effective qutrit states ρ, we sampled 10000 microscopic states $\psi \in \mathcal{L}(\mathcal{H}_3 \otimes \mathcal{H}_E)$ and checked how many of those satisfied the condition $||\Lambda_{\mathrm{PT}}[\psi] - \rho|| < \epsilon$, for $\epsilon = 0.3$, that is, how many of those were approximately compatible with ρ. Put another way, the count of microscopic states obeying this condition is a estimate of the volume $\mathcal{V}_{\Lambda_{\mathrm{PT}}}(\rho)$. By plotting the results against $\det(\rho)$ and superposing the fitted curves, we can confirm the expected behavior: for $d_E = 3$ (in blue), we see that the volume of uncertainty is constant, as $d_E = d_S$, for $d_E = 4$ it grows linearly with $\det(\rho)$; and for $d_E = 5$ it grows quadratically.

Once the calculation for the case of the partial trace have been done, one can similarly evaluate the uncertainty associated to an effective description ρ when the coarse-graining map is Λ_D, which yields

$$\mathcal{V}_{\Lambda_D}^{d_B}(\rho) = \frac{2^{4-3d_B}\pi^{1+4d_B}(1+z)^{-d_B}(1-x^2-y^2-z^2)^{2(d_B-1)}}{\Gamma[d_B]\Gamma[2d_B - 1]}, \tag{2.76}$$

where x, y, z are the Bloch vectors of ρ. Moreover, here we also consider mixed states, which are purified with an auxiliary system of dimension d_B. This calculation is significantly more complicated, and the details are presented in appendix E, where we have adapted a calculation lead in [74].

Now that we have these two expressions, we can move on to probe the relation between reversibility of effective dynamics and their consequences on the volume of uncertainty of the effective preparations.

2.5 Results and discussion

Let us once again consider the simple experiment we have described in earlier sections. An effective state $\rho(0)$ is prepared and let evolve according to the effective evolution Γ_t, given by the composition of the coarse-graining map Λ, the microscopic evolution $\mathcal{U}_t$ and the average assignment map $\mathcal{A}_\Lambda$. The resulting effective state is $\rho(t) = \Gamma_t[\rho]$. The same process is followed backwards, and the effective state $\rho'(0) = \Gamma_{-t}[\rho(t)]$ is obtained.

In this scenario, we can compare the initially prepared state $\rho(0)$ and the state that is obtained after the backwards evolution $\rho'(0)$ to assess the reversibility of Γ_t. If they always coincide, then Γ_t is, according to our definition, reversible.

Consider the example of the partial trace, applied on microscopic states composed of a 2-qubits system of interest and a 2-qubit environment. We already know that only microscopic evolutions that can be decomposed as local unitaries will yield reversible effective dynamics, any other construction of $\mathcal{U}_t$ will fail to recover the initial state. This can be visualized numerically in figs. 2.10 and 2.9, where we let random $\rho(0)$ evolve according to a given Γ_t for different time intervals, and then reversed back to $\rho'(0)$. We evaluate whether or not the initial state was recovered and how the volume of uncertainty of the effective state changed.

Figure 2.9: We sampled a random effective 2-qubits state $\rho(0)$, which we let evolve for different time intervals while keeping track of the uncertainty volume associated to it, here plotted in red. At any time t, the effective state is given by $\rho(t) = \Gamma_t[\rho(0)]$, and in this example Γ_t emerges from a microscopic evolution that does not act locally on the system of interest and the environment. In blue, we plot the trace distance between the initially prepared state $\rho(0)$ and the state that was recovered through $\rho'(0) = \Gamma_{-t}[\rho(t)]$. Given this choice for $\mathcal{U}_t$, the resulting effective dynamics is not reversible, which can be attested by the fact that the trace distance between $\rho(0)$ and $\rho'(0)$ is not zero (except for the points where the cyclic nature of $\mathcal{U}_t$ makes it the trivial evolution), meaning that the initial prepared state is not recovered after the backwards process. Consequently, we also see that the volume of uncertainty of the prepared state indeed changes with time, prohibiting these dynamics to be reversible. Qualitatively equivalent behaviors are observed when other initial states are sampled, or when other microscopic evolutions that do not satisfy the reversibility criterion are chosen. Here, the unitary evolution is given by the operator $U_t = e^{-iHt}$ with $H = \sigma_z \otimes \sigma_z \otimes \sigma_x \otimes \sigma_x$.

From these simple numerical examples we see instances of situations that corroborate the use of the volume of uncertainty to analyze the reversibility of effective dynamics. As expected, only when $\mathcal{V}_{\Lambda_{\mathrm{PT}}}(\rho(t))$ remains unaltered through the evolution do we observe that the initial state is recovered. The interpretation behind it is also clear, if we recall that reversible effective dynamics are only achievable if $\mathcal{U}_t$ acts locally on the system of interest and the environment, as stated in eq. (2.37). Γ_t acts on an effective state $\rho(0)$ as in eq. (2.22), and in the reversible case it reduces to

$$\rho(t) = U_S \rho(0) U_S^\dagger. \tag{2.77}$$

It comes at no surprise, then, that under these conditions $\mathcal{V}_{\Lambda_{\mathrm{PT}}}(\rho(t))$ does not change with time, since it depends only on the determinant of $\rho(t)$, which does not change under unitary transformations.

On the other hand, if the microscopic evolution does not act locally on the system and the environment, then the emerging dynamics is not reversible. This is compatible with the numerical results showing that $\mathcal{V}_{\Lambda_{\mathrm{PT}}}(\rho(t))$ increases, prohibiting Γ_t to be reversible. Indeed, it is always the case that microscopic evolutions that do not decompose into local unitaries should make $\mathcal{V}_{\Lambda_{\mathrm{PT}}}(\rho(t))$ increase, resulting in

Figure 2.10: As before, we sampled a random effective 2-qubits state $\rho(0)$, which we let evolve for different time intervals while keeping track of the uncertainty volume associated to it. In blue, we plot the trace distance between $\rho(0)$ and $\rho'(0)$. However, here we picked $\mathcal{U}_t$ such that eq. (2.37) is satisfied, i.e., the resulting dynamics is reversible. Consequently, we see that the trace distance between $\rho(0)$ and $\rho'(0)$ is always zero (meaning the initial state is recovered) and that the volume of uncertainty of $\rho(t)$ remains unaltered. Qualitatively equivalent behaviors are observed when other initial states are sampled, or when other microscopic evolutions satisfying the reversibility criterion are chosen. Here, the unitary evolution is given by the operator $U_t = e^{-iHt}$ with $H = \sigma_z \otimes \sigma_z \otimes \mathbb{1} \otimes \mathbb{1} + \mathbb{1} \otimes \mathbb{1} \otimes \sigma_x \otimes \sigma_x$.

irreversible effective dynamics. To see why it is so, first consider the following result from [75], stating that, for any two states σ_1, σ_2 of same dimension, it holds

$$T[\sigma_1] = \sigma_2 \iff \vec{\lambda}(\sigma_1) \succ \vec{\lambda}(\sigma_2), \tag{2.78}$$

where T is some unital transformation, and $\vec{\lambda}(\sigma_1) \succ \vec{\lambda}(\sigma_2)$ means that σ_1 majorizes σ_2, that is,

$$\sum_{i=1}^{k} \lambda_i^{\downarrow}(\sigma_1) \geq \sum_{j=1}^{k} \lambda_j^{\downarrow}(\sigma_2) \quad \forall\, k \geq 1 \tag{2.79}$$

where $\lambda_i^{\downarrow}(\sigma_1)$ are the eigenvalues of σ_1 organized in non-increasing order, and similarly for $\lambda_i^{\downarrow}(\sigma_2)$. Moreover, from [76] we know that

$$\vec{\lambda}(\sigma_1) \succ \vec{\lambda}(\sigma_2) \implies G(\sigma_1) \geq G(\sigma_2), \tag{2.80}$$

where G is defined as

$$G(x) = \sum_i g(x_i), \tag{2.81}$$

and g is any convex function. Putting these two results together, we see that, since Γ_t is unital,

$$\rho(t) = \Gamma_t[\rho(0)] \iff \rho(0) \succ \rho(t). \tag{2.82}$$

Then, by choosing $g(x) = -\log(x)$, as it is a convex function we have that

$$\rho(0) \succ \rho(t) \implies -\log(\det(\rho(0))) \geq -\log(\det(\rho(t))) \tag{2.83}$$

which in turn means that

$$\det(\rho(t)) \geq \det(\rho(0)). \tag{2.84}$$

42

Thus, the volume of uncertainty of an evolved effective state does not decrease. If $\mathcal{U}_t$ is appropriately chosen, $\mathcal{V}_{\Lambda_{\mathrm{PT}}}(\rho(t))$ does not change and Γ_t is reversible, otherwise $\mathcal{V}_{\Lambda_{\mathrm{PT}}}(\rho(t))$ will increase.

We can now follow the same analysis and compare the behavior of the volume of uncertainty of effective states when the coarse-graining map is Λ_D, numerical examples are provided in figs. 2.11 and 2.12. Once again, the observed behaviors strengthen our proposal of using $\mathcal{V}_{\Lambda_D}^{d_B}(\rho(t))$ to analyze effective reversibility: whenever the dynamics is reversible (that is, whenever $\rho(0) = \rho'(0)$ for any given time interval), it follows that the volume of uncertainty of $\rho(t)$ is constant.

We must point out, however, that this does not seem to be a two-way implication: reversible effective dynamics only take place when the volume of uncertainty of the effective state $\rho(t)$ is constant throughout time, but the fact that $\mathcal{V}_{\Lambda_D}^{d_B}(\rho(t))$ does not vary does not imply that the dynamics is reversible. In fig. 2.13, we provide a numerical analysis of a situation where the dynamics is not reversible (that is, it does not fit the requirements for reversibility set in eq. (2.41), and consequently $\rho(0) \neq \rho'(0)$) and yet the volume of uncertainty of $\rho(t)$ is constant.

The existence of such examples of irreversible effective dynamics with constant volume of uncertainty does not undermine our claim that $\mathcal{V}_{\Lambda_D}^{d_B}(\rho)(t)$ can be used to analyze effective reversibility. Having only one way of the implication hold is in fact aligned with the common analysis of the behavior of entropy in the context of the second law of thermodynamics. Let us recall that some scenarios yield constant entropy for closed systems regardless of the reversibility of the effective dynamics, such as when we choose to evaluate the von Neumann entropy of the system. As we have argued then for the von Neumann entropy, this result is not at all in contradiction with the second law, but it is rather useless as it does not directly link entropy and reversibility.

In our case there is also no direct link between $\mathcal{V}_{\Lambda_D}^{d_B}(\rho(t))$ and the reversibility of effective dynamics, but our result is still more useful than using the von Neumann entropy. First of all, the von Neumann entropy does not rule out any (closed) dynamics as irreversible, while our analysis prohibits dynamics that change $\mathcal{V}_{\Lambda_D}^{d_B}(\rho(t))$ to be reversible. Choosing to investigate volumes of uncertainty instead of the von Neumann entropy may, thus, be more conclusive in many instances, though it does not mean that the constancy of $\mathcal{V}_{\Lambda_D}^{d_B}(\rho(t))$ guarantees reversibility.

The second reason why evaluating the volume of uncertainty of the effective state throughout time is useful is because, as far as our numerical analyses go, a direct link between $\mathcal{V}_{\Lambda_D}^{d_B}(\rho(t))$ and the reversibility of the effective dynamics can be re-established if one considers $d_B > 1$, see fig. 2.14 for details. There, we have first shown that a given effective dynamics is irreversible and yet $\mathcal{V}_{\Lambda_D}^1(\rho(t))$ is constant, where stress that $d_B = 1$. Then, we show that by choosing $d_B > 1$ the expected behavior is obtained: the dynamics is irreversible but now $\mathcal{V}_{\Lambda_D}^{d_B}(\rho(t))$ is not constant anymore.

In other words, there is numerical evidence suggesting a direct link connecting $\mathcal{V}_{\Lambda_D}^{d_B}(\rho(t))$ and effective reversibility if $d_B > 1$. Consequently, a two-way implication between the volume of uncertainty of an effective state being constant throughout a given evolution and the initial state being effectively recovered can be envisioned. The restriction that one must, then, only consider $d_B > 1$ is neither nonphysical nor unmotivated: once again it comes to accepting that perfectly pure states cannot be prepared in real life, any realistic theoretic approach to this matter must take into account that the infinite precision required for such a feat is not achievable. This means that one should employ an auxiliary system to purify the (mixed) microscopic states that are compatible with a given effective preparation, that is, $d_B > 1$.

2.6   Concluding remarks

The second law of thermodynamics is taken as a tool whose comprehensive use universally dictates which dynamics are allowed in a physical scenario: do what you will as longs as you do not decrease the entropy of closed systems. Determining what exactly this entropy is constitutes a challenge for the field of quantum thermodynamics in particular, and different choices for the entropy can yield distinct predictions arising from the second law, specially when it comes to reversibility.

In this work, we have taken on the matter of effective reversibility, a subject that has both foundational and applied relevance. By trying to conciliate microscopic and effective descriptions of systems, we provide a framework that highlights the connections between these two approaches. We show how coarse-grained access to a physical systems results in irreversible effective dynamics, even though we have assumed that the underlying physical system is subject to a closed unitary evolution.

Once it was clear that reversible effective dynamics are the exception rather than the norm, we have established that reversibility is only achieved on the effective level if there is a certain consonance between the coarse-graining map Λ that describes one's access to the system and the microscopic evolution $\mathcal{U}_t$ to which the physical state is subjected. We then determined the constraints that Λ and $\mathcal{U}_t$ must
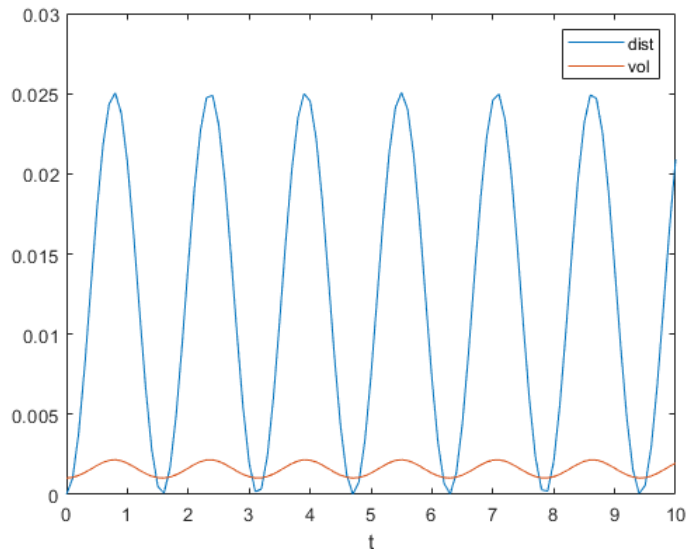
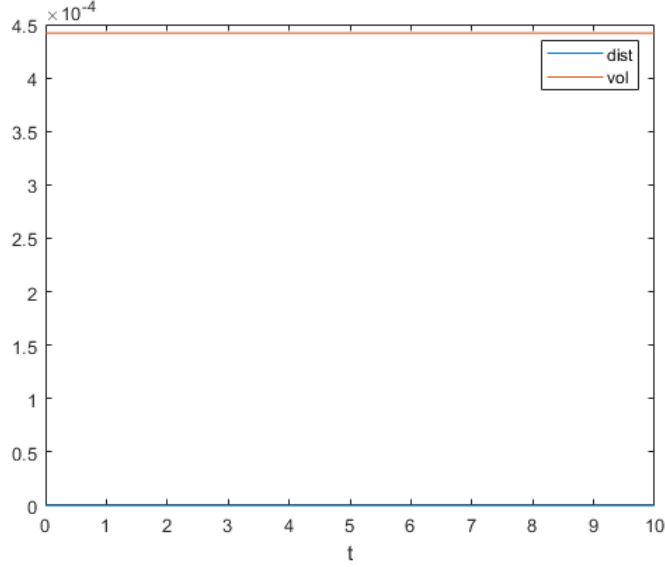Figure 2.11: Similarly, we sampled a random effective state $\rho(0)$, which we let evolve for different time intervals while keeping track of the uncertainty volume associated to it, here plotted in red. At any time t, the effective state is given by $\rho(t) = \Gamma_t[\rho(0)]$, and in this example Γ_t emerges from a microscopic evolution that does not fit eq. (2.41) and eqs. (2.46) to (2.51). In blue, we plot the trace distance between $\rho(0)$ and $\rho'(0) = \Gamma_{-t}[\rho(t)]$. Given this choice for $\mathcal{U}_t$, the resulting effective dynamics is not reversible, which can be attested by the fact that the trace distance between $\rho(0)$ and $\rho'(0)$ is not zero, meaning that the initial prepared state is not recovered after the backwards process. Consequently, we also see that the volume of uncertainty of the prepared state indeed changes with time, prohibiting these dynamics to be reversible. Qualitatively equivalent behaviors are observed when other initial states are sampled, or when other microscopic evolutions that do not satisfy the reversibility criterion are chosen. Here, the unitary evolution is given by the operator $U_t = e^{-iHt}$ with $H = \lambda_5$, where $\{\lambda_i\}_{i=1}^8$ are the Gell-Mann matrices.

satisfy in order for the emerging effective dynamics Γ_t to be reversible. We also explicitly obtained the corresponding microscopic evolutions that obey such constraints for two examples of Λ: the partial trace and an imperfect detector.

We then argued for the use of the volume of uncertainty of a given effective state $\rho(t)$ throughout its evolution to determine whether the dynamics is reversible or not. Taking inspiration from the Boltzmann entropy, we use our ignorance about an effective preparation (to whose degrees of freedom one only has partial access, modeled through the coarse-graining map) to re-phrase one of the main interpretations of the second law of thermodynamics: the information one has about a closed system cannot increase. In our framework, $\mathcal{V}_\Lambda(\rho(t))$ quantifies our ignorance about what is microscopic state was actually sampled when we prepare an effective state $\rho(t)$, and the more microscopic states compatible with observing $\rho(t)$ there are, the larger $\mathcal{V}_\Lambda(\rho(t))$ is.

The relation between reversibility and uncertainty can be encapsulated in the statement that reversible dynamics cannot alter our ignorance about a system. One cannot gain any information on a closed system in any case, thus if one actually *loses* information about it through time, then this evolution cannot be reversed as it would mean one would *gain* information in the backwards process, which is not allowed. In terms of the framework we constructed, if Γ_t is reversible then $\mathcal{V}_\Lambda(\rho(t))$ cannot vary with t.

We have put our construction to test with two examples, and showed that if Λ is the partial trace then we have a perfect correspondence between reversibility and the constancy of the volume of uncertainty of the effective states. When Λ describes the imperfect detector, we have provided robust numerical evidence that a similar correspondence exists.

Many paths are still open to continue this line of research. We can still go beyond numerical evidence and analytically show that the reversible effective evolution that emerge from Λ_D and the appropriate $\mathcal{U}_t$ do not change $\mathcal{V}_{\Lambda_D}^{d_B}(\rho(t))$, for $d_B > 1$. It would be even better to show that this implication holds for any coarse-graining map, though this feat might a considerably larger effort. On the other hand, it would also be very interesting to provide numerical methods to evaluate $\mathcal{V}_\Lambda(\rho(t))$, since finding an analytical
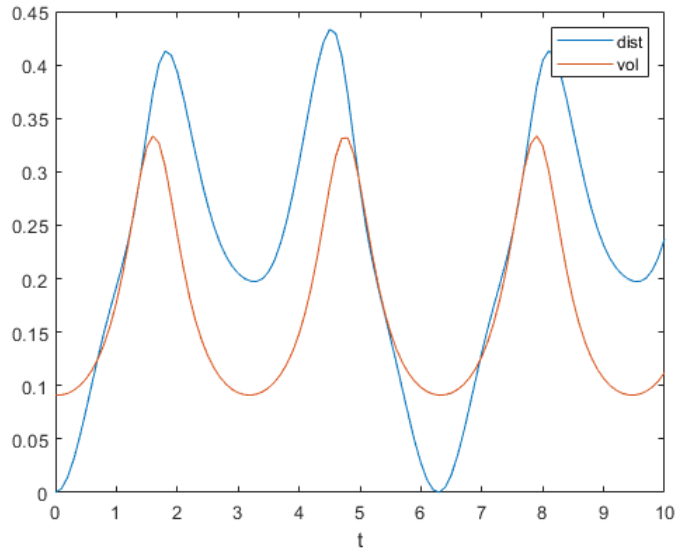
44
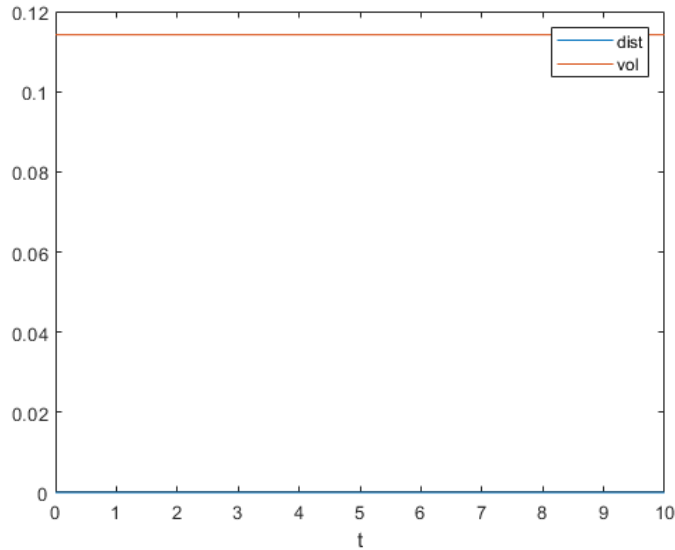
Figure 2.12: As before, we sampled a random effective state $\rho(0)$, which we let evolve for different time intervals while keeping track of the uncertainty volume associated to it. In blue, we plot the trace distance between $\rho(0)$ and $\rho'(0)$. However, here we picked $\mathcal{U}_t$ such that eq. (2.41) and eqs. (2.46) to (2.51) are satisfied, i.e., the resulting dynamics is reversible. Consequently, we see that the trace distance between $\rho(0)$ and $\rho'(0)$ is always zero (meaning the initial state is recovered) and that the volume of uncertainty of $\rho(t)$ remains unaltered. Qualitatively equivalent behaviors are observed when other initial states are sampled, or when other microscopic evolutions satisfying the reversibility criterion are chosen. Here, the unitary evolution is given by the operator $U_t = e^{-iHt}$ with $H = \lambda_6$, where $\{\lambda_i\}_{i=1}^8$ are the Gell-Mann matrices.

expression for it can prove itself challenging. One could also construct a measure of reversibility, a quantity that could reflect, for instance, how far from the initially prepared state $\rho(0)$ the recovered state $\rho'(0)$ is.

Though still under construction, we hope our work can foster a discussion over what effective reversibility means when one understands that effective dynamics must emerge from microscopic quantum dynamics. If nothing else, our contribution to the debate is that the scenarios with which we work must be physically motivated by realistic settings, and consequently one should evaluate effective phenomena without assuming knowledge about inaccessible objects, such as the microscopic states. With our work, what we confirm at the end of the day is that even when no unanimously accepted formulation of the second law of thermodynamics is available (such as it is in the scenario we have adopted), its aura is still to be felt, assuring that, indeed and quite poetically, uncertainty cannot decrease.
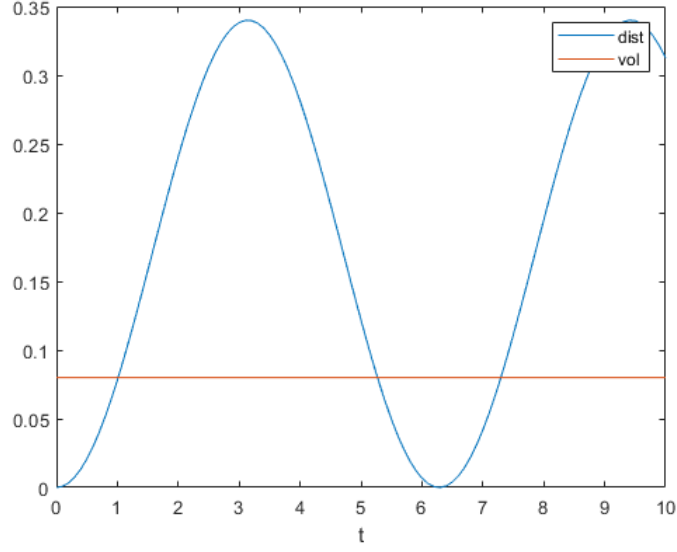
Figure 2.13: Numerical analysis of $\mathcal{V}^1_{\Lambda_D}(\rho(t))$ for a randomly sampled $\rho(0)$ in red, and the trace distance between $\rho(0)$ and the effective state $\rho'(0)$ that is recovered after letting $\rho(0)$ evolve effectively for a given time interval t and then evolve backwards for the same interval, in blue. Here, the specific choice of the underlying microscopic evolution yields irreversible dynamics (as evidenced by the fact that $\rho(0) \neq \rho'(0)$, as the trace distance is not zero) but the volume of uncertainty of $\rho(0)$ is nevertheless constant. Here, the unitary evolution is given by the operator $U_t = e^{-iHt}$ with $H = \lambda_3$, where $\{\lambda_i\}_{i=1}^8$ are the Gell-Mann matrices. We stress out that $d_B = 1$.
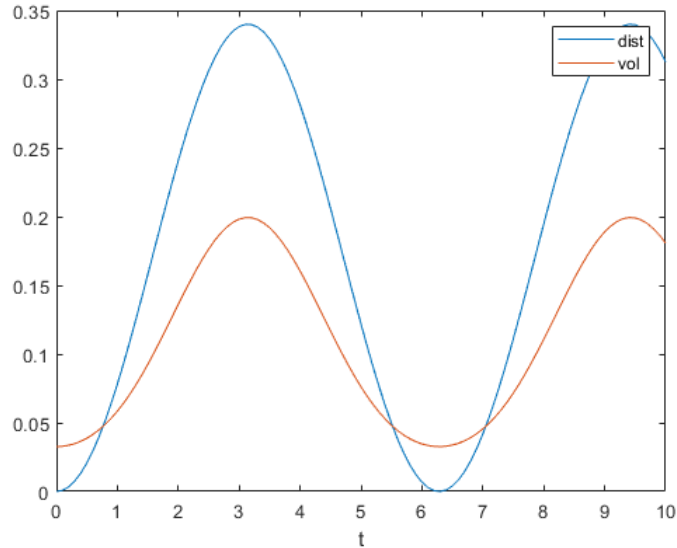
Figure 2.14: A similar numerical analysis, conducted for the same randomly sampled $\rho(0)$ as before, evolving according to the effective evolution given by the same underlying dynamics. Here, however, we have chosen $d_B = 3$ to evaluate $\mathcal{V}^{d_B}_{\Lambda_D}(\rho(t))$, that is, we are not considering only pure microscopic states anymore. As a result, the irreversibility of the effective dynamics is now matched by a change in the volume of uncertainty associated to $\rho(t)$.

Part II

Additional projects: Witnessing non-classicality

Chapter 3

Semidefinite programming

In this section we will provide a brief overview of semidefinite programming (SDP), a class of mathematical problems framed as optimization tasks. It is by no means a new concept, with an early paper discussing its theoretical properties dating back from 1963 [77], and the field has since been established as a domain of significant interest, with major contributions (both theoretical and applied) spanning the decades ever since.

The interest in the area is of course justified through the importance of optimization tasks themselves, which are central in physics, chemistry, engineering, economics, among others. Such tasks are in general exceedingly hard to perform, but semidefinite programs in particular display the wonderful characteristic of being solved with reasonable efficiency and precision.

Being defined as an optimization of a linear objective function over some variable constrained by a set of linear matrix inequalities, SDPs are much more general than linear programs (LP) while not being much harder to solve. On the other hand, as a particular class withing the widely studied field of conic programming (itself a sub-field of convex programming), SDPs also benefit from the many theoretical results and methods that have already been established. Additionally, actually applying semidefinite programming to a problem is fairly easy since many coding packages are available, from which we highlight CVX [78] and YALMIP [79] for MATLAB [80], and CVXPY [81] for Python [82], running numerical solvers (often offered for free) such as SCS [83] or MOSEK [84].

If its sound foundations helped establish semidefinite programming as an area on its own in computer science, at least part of its crescent popularity is due to a symbiotic relationship with quantum information. SDPs deal, at its core, with positive semidefinite matrices, used canonically to represent quantum states and measurements, and thus dwelling basically in the backyard of quantum information. Connections between one another are promptly made in any problem where one wants to find states, observables or even channels featuring some specific property, as often is the case in the fields of Bell non-locality [85], quantum steering [86], quantum contextuality [87] or measurement incompatibility [88] (often grouped under the umbrella term "quantum correlations").

The results that will be presented in later chapters do not stray far from the quantum correlations field and benefited immensely from their usage of semidefinite programming. For that reason, before we can move on and discuss our remaining projects we must establish a base knowledge of what SDPs are. In what follows we will present a couple of original results, but most of the content will be a simple adaptation from previous works. For in depth discussions on semidefinite programming we refer to [89, 90, 91, 92, 93], from which we adapted different passages to produce the next section, a brief introduction to SDPs.

3.1   Basic notions and usage

Semidefinite programming concerns itself with tasks where one optimizes a linear function of interest over a matrix variable within a spectrahedron (i.e., the intersection of the cone of positive semidefinite matrices with the affine space delimited by a set of matrix inequalities). It is a special instance of convex optimization, which have the generic formulation

$$\begin{aligned} \textbf{maximize} \quad & g(X) \\ \textbf{subject to} \quad & X \in \mathcal{C} \,. \end{aligned} \tag{3.1}$$

While X is the *variable*, g is called the *objective function* of the problem, assumed to be concave and $g(X)$ is assumed to be real. The set $\mathcal{C}$, a subset of the domain of g, is the *feasibility region* of the problem. This program represents the task of maximizing the function g over all values of X that obey the restrictions that define the set $\mathcal{C}$, and the value the objective function assumes in this case is called the *optimal solution* of the problem.

An inviting aspect of convex optimization tasks is that local maxima of the objective function are also global maxima, an appealing feature when formulating a problem. A not so inviting side of convex optimization is that it is, in general, not efficiently solved [94]. If one can re-formulate a convex optimization problem such that the variable X is further restricted to the positive semidefinite cone, however, one enters the realm of SDPs and many efficient algorithms can be used to solve it.

Semidefinite programs fit the general form

$$
\begin{aligned}
\textbf{maximize} \quad & \text{Tr}[AX] \\
\textbf{subject to} \quad & \Lambda_i(X) = B_i, \quad i = 1, \ldots, m \\
& \Gamma_j(X) \leq C_j, \quad j = 1, \ldots, n \\
& X \geq 0 \,.
\end{aligned}
\tag{3.2}
$$

The variable X is a Hermitian matrix (since $X \geq 0$), and so are $A, \{B_i\}_{i=1}^m$ and $\{C_j\}_{j=1}^n$, given by the problem one wants to solve. $\{\Lambda_i\}_{i=1}^m$ and $\{\Gamma_j\}_{j=1}^n$ are hermiticity-preserving linear maps, such that we have a set of $m+n$ affine constraints on X, which together with the positivity constraint define the feasibility region $\mathcal{F}_p$ and synthesize the essence of an SDP. We point out that equally valid formulations can be constructed for minimization problems or even feasibility problems (where one simply wants to find any point in the feasibility region). Furthermore, one could take the inequality constraints in eq. (3.2) to be the other way around and nothing would substantially change.

A simpler subset of SDPs are linear programs (LP), which can be stated as

$$
\begin{aligned}
\textbf{maximize} \quad & \vec{a} \cdot \vec{x} \\
\textbf{subject to} \quad & \vec{\lambda}_i \cdot \vec{x} = b_i, \quad i = 1, \ldots, m \\
& \vec{\gamma}_j \cdot \vec{x} \leq c_j, \quad j = 1, \ldots, m \\
& \vec{x} \geq 0 \,,
\end{aligned}
\tag{3.3}
$$

where the variable $\vec{x}$, as well as $\vec{a}$, $\{\vec{\lambda}_i\}_{i=1}^m$ and $\{\vec{\gamma}_j\}_{j=1}^n$, are now real vectors. Linear programs can be obtained from SDPs if $A, B_1, \ldots, B_m, C_1, \ldots, C_n$ are diagonal matrices. Notice that LPs pose linear constraints on the elements of $\vec{x}$, while SDPs generally pose non-linear constraints on the elements of X, making them substantially more versatile.

The way the optimization programs were laid out in eqs. (3.1), (3.2) and (3.3) are referred to as the *primal formulation* of the problem. It has a closely related form, namely its *dual formulation*, connected to the primal through the Lagrangian of the problem. Let us take the prototype of an SDP eq. (3.2) and associate a dual variable to each of its constraints: each equality will be associated to Y_i, $i = 1, \ldots, m$, each inequality will be associated to Z_j, $j = 1, \ldots, n$, and the positivity constraint will be associated to W. Let us also require these variables to obey the restrictions

$$
\begin{aligned}
Y_i &= Y_i^\dagger, \quad i = 1, \ldots, m \\
Z_j &= Z_j^\dagger \geq 0, \quad j = 1, \ldots, n \\
W &= W^\dagger \geq 0 \,.
\end{aligned}
\tag{3.4}
$$

The Lagrangian of the problem is defined as

$$
\mathcal{L} = \text{Tr}[AX] + \sum_i \text{Tr}[Y_i(B_i - \Lambda_i(X))] + \sum_j \text{Tr}[Z_j(C_j - \Gamma_j(X))] + \text{Tr}[WX].
\tag{3.5}
$$

This object depends on both the primal variable X and the dual variables $Y_1, \ldots, Y_m, Z_1, \ldots, Z_m, W$. Notice that the original objective function is a lower bound for the Lagrangian whenever X is in the

feasibility region of the primal problem[1]. This is easily verified, since the conditions we imposed on the dual variables ensure that each term on the r.h.s. of eq. (3.5) is non-negative. Mathematically, this means

$$\mathcal{L} \geq \mathrm{Tr}[AX]. \tag{3.6}$$

What we want at the end of the day is to construct a function that will be independent of X. To do that, let us first rearrange some terms in eq. (3.5) and make the dependence on X more explicit.

$$\mathcal{L} = \mathrm{Tr}[X \ (A - \sum_i \Lambda_i'(Y_i) - \sum_j \Gamma_j'(Z_j) + W)] + \sum_i \mathrm{Tr}[Y_i B_i] + \sum_j \mathrm{Tr}[Z_j C_j]. \tag{3.7}$$

Here, the objects $\{\Lambda_i'\}_{i=1}^m$ and $\{\Gamma_j'\}_{j=1}^n$ are the dual maps of $\{\Lambda_i\}_{i=1}^m$ and $\{\Gamma_j\}_{j=1}^n$, obeying by definition the duality relation

$$\mathrm{Tr}[\Lambda_i(X)Y] = \mathrm{Tr}[X\Lambda_i'(Y)], \quad \forall X, Y \tag{3.8}$$

for all $i = 1, \ldots, m$, and similarly for $\{\Gamma_j\}_{j=1}^n$. Let us additionally impose

$$W = \sum_i \Lambda_i'(Y_i) + \sum_j \Gamma_j'(Z_j) - A \geq 0 \tag{3.9}$$

and get rid of X, such that the Lagrangian now reads

$$\mathcal{L} = \sum_i \mathrm{Tr}[Y_i B_i] + \sum_j \mathrm{Tr}[Z_j C_j]. \tag{3.10}$$

To achieve the tight bound in eq. (3.6), one must minimize $\mathcal{L}$ over the dual variables. By doing that and taking into consideration the restrictions we made in eqs. (3.4) and (3.9), we finally get the dual formulation of the problem in eq. (3.2)

$$
\begin{aligned}
\textbf{minimize} \quad & \sum_i \mathrm{Tr}[Y_i B_i] + \sum_j \mathrm{Tr}[Z_j C_j] \\
\textbf{subject to} \quad & \sum_i \Lambda_i'(Y_i) + \sum_j \Gamma_j'(Z_j) - A \geq 0 \\
& Y_i = Y_i^\dagger, \quad i = 1, \ldots, m \\
& Z_j = Z_j^\dagger \geq 0, \quad j = 1, \ldots, n \, .
\end{aligned}
\tag{3.11}
$$

Notice that any point in the feasibility region $\mathcal{F}_p$ of the primal SDP provides a lower bound to the optimal value of its objective function, since the task is a maximization. Similarly, any point in the feasibility region $\mathcal{F}_d$ of the dual SDP provides an upper bound to the optimal value of the dual objective function. We also know that, because of eq. (3.6), the dual objective function of the problem is lower bounded by the primal objective function, implying that *the optimal solution of the dual SDP is an upper bound to the optimal solution of the primal SDP*. This last statement is known as *weak duality*, and it further implies that any point in the dual feasible region provides an upper bound to the optimal primal solution (since it is an upper bound to the dual optimal solution). The difference between these two optimal solutions is often called the *duality gap*.

Because of these properties, both the primal and the dual formulation of a problem can be used to find upper and lower bounds to the optimal solution of a task. In fact this strategy is at the core of how numerical solvers tackle the problem, using the so-called interior-point methods such as [95], that have worst-case polynomial complexity [90]. Furthermore, it is often the case where the primal and the dual optimal values coincide (a feature present in all SDPs we constructed in this thesis). This happens, as proven in Slater's theorem [96], whenever the primal and the dual SDPs are said to be *strictly feasible*, meaning that there exists at least one point in their respective feasibility regions that is not at its border, i.e., obeying

$$
\begin{aligned}
\Gamma_j(X) &< C_j, \quad j = 1, \ldots, n \\
X &> 0
\end{aligned}
\tag{3.12}
$$

---

[1]Notice that, unlike Z_j or W, Y_i does not need to be positive semidefinite for the Lagrangian to be lower bounded by the objective function. Since Y_i is associated to an equality constraint, it's corresponding term in $\mathcal{L}$ is always equal to zero when X is a feasible point

for the primal variable X and

$$\sum_i \Lambda'_i(Y_i) + \sum_j \Gamma'_j(Z_j) - A > 0$$
$$Z_j > 0, \quad j = 1, \dots, n \tag{3.13}$$

for the dual variables $\{Y_i\}$ and $\{Z_j\}$.

An interesting geometric interpretation, which has a close connection to quantum information, can be given to the primal and the dual formulations of a problem, as shown in fig. 3.1. If one considers the space of matrices, the primal feasible region is delimited by a set of constraints and the primal objective function defines a direction. The primal program will search the point as far as possible in the direction set by the objective function while staying in the feasibility region. The dual program, in turn, will play around with the dual variable W, which can be seen as a hyperplane separating the space in two: one part containing the whole convex set of feasible points, and another with no feasible points. The optimal instance of W is a hyperplane tangent to the optimal primal points. Any similarity with the concept of witnesses is not a coincidence. In fact, such analogy is often exploited to look for optimal entanglement and steering witnesses in different scenarios [97, 98, 99].
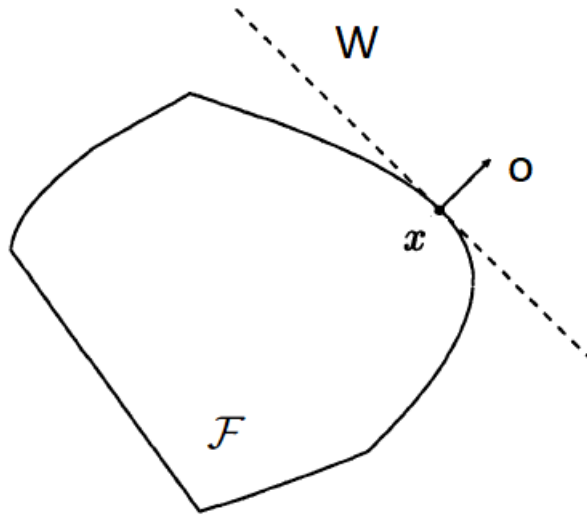
Figure 3.1: A geometrical visualization of the primal and dual formulations of an SDP, adapted from [90]. The feasibility region $\mathcal{F}$ is set by the constraints given by the primal SDP. The objective function, in turn, defines a direction o, and the primal task is to find the optimal point x furthest along this direction while still inside $\mathcal{F}$. The dual program optimizes over all hyperplanes, and the optimal instance W is a hyperplane tangent to x.
.

Given the general approach we adopted in this brief introduction to semidefinite programming, it is clear how broad its applications can be. It would be wonderful if one could say the only limitation to its usage is the researcher's imagination, but we already know that SDP simply cannot be employed in problems with constraints that do not fit into the model in eq. (3.2). Fortunately, motivated mainly by how practical semidefinite programming can be, many different approaches to such problems have been developed. In the next sections we will present the ones that are most relevant to this thesis.

3.2 Overcoming limitations of SDPs and alternative strategies

As we have seen, only a subset of optimization problems can be framed as an SDP. Whenever we end up with a non-linear objective function or constraints that cannot be expressed as linear matrix inequalities, there is no guarantee that an SDP can be established. This is utterly disappointing, because, even though many problems in quantum information can be cast as an SDP, many others end up requiring some non-convex (or not linear) condition.

Many strategies can be employed to re-frame an optimization problem as an SDP, though there must always be a cost to it. For instance, one can instead compute not just one but a series of SDPs organized in hierarchical order. Examples of such strategy are the Naváscues-Pironio-Acín (NPA) hierarchy [100] to approximate the quantum set or [101] to tackle the quantum marginal problem. Alternatively, one can employ see-saw algorithms, where one iteratively computes two distinct SDPs to find a lower (or upper) bound to the optimal solution, as in [102] to find dimension witnesses. Other approaches include bluntly dropping the non-convex restriction and solve a relaxed version of the original problem [103], or even imposing such conditions after finding a generic solution [104].

In this chapter, we explain in detail how three of these alternative strategies work, laying out the previous knowledge the reader must have to understand our results in the next chapters. In section 3.2.1, we present an SDP hierarchy to tackle the separability problem, and in section 3.2.2 another hierarchy to overcome rank constraints in optimization problems. In section 3.2.3 we present a heuristic procedure commonly known as "see-saw method". After these approaches have been dissected, we move on to the next chapter, where we employ them to efficiently solve physical problems that are otherwise intractable.

3.2.1 The DPS separability hierarchy

In this section we expose the optimization hierarchy brought forward by Doherty, Parrilo and Spedalieri (or shortly, DPS) in [105], that will be particularly useful to us in chapter 5. This method allows one to tackle the problem of deciding whether a state is separable or entangled by framing it as a family of SDPs, though the price one has to pay is that the analysis may be inconclusive.

This sort of inquiry plays a central role in many problems in quantum information, since entanglement itself is a main quantum feature and a resource to numerous protocols: without entanglement one cannot violate any Bell inequalities [106] or observe steering [107], to name a few. For such tasks, preserving, transforming and manipulating entanglement is crucial, but in any case it all starts with detecting it.

The definition of entanglement is, actually, constructed from its absence. A bipartite state is said to be separable (or rather, not entangled) if it can be expressed as a convex sum of pure, product states. For a state ρ acting on $\mathcal{H}_A \otimes \mathcal{H}_B$, this means

$$\rho = \sum p_i \left| \psi_i \right\rangle \left\langle \psi_i \right| \otimes \left| \phi_i \right\rangle \left\langle \phi_i \right|, \tag{3.14}$$

where p is a probability distribution with elements obeying $p_i \geq 0$, $\sum_i p_1 = 1$, while $\left| \psi_i \right\rangle$ is a state in $\mathcal{H}_A$ and $\left| \phi_i \right\rangle$ in $\mathcal{H}_B$. If a state can be written in the form above, it is separable. If these is no choice of p, $\{\left| \psi_i \right\rangle\}$ and $\{\left| \phi_i \right\rangle\}$ that satisfies this relation, then the state is entangled.

Despite the simple setting, answering this question is remarkably hard. In fact, it's NP-hard [108], which means there is no hope of ever finding an efficient algorithm to decide whether a given mixed state admits the decomposition in eq. (3.14). In particular, it means there is no way to pose the separability problem as a convex optimization task in the form of an SDP.

This does not mean, however, that the task cannot be tackled at all. Alternative methods based on separability criteria exist and are extensively used [109, 110, 111, 112], from which we highlight the PPT criterion [113]. Like any criterion, it is based on finding a property that all separable states must hold; consequently, if one can certify that a given state lacks this feature it must mean the state is entangled. Nothing can be said of the state if the property is indeed verified, since it may be present in both separable and entangled states. This way, a test based on separability criteria can only yield two answers: either the state is entangled or the test is inconclusive.

In particular, the characteristic that the PPT criterion exploits is the fact that every separable state must remain positive semi-definite (i.e., have only non-negative eigenvalues) under partial transposition of one of its subsystems. Given a general bipartite state Ψ in $\mathcal{H}_A \otimes \mathcal{H}_B$, expressed as

$$\Psi = \sum_{ijkl} \gamma_{ijkl} \left| i \right\rangle \left\langle j \right| \otimes \left| k \right\rangle \left\langle l \right|, \tag{3.15}$$

the partial transposition of subsystem A is given by

$$\Psi^{T_A} = \sum_{ijkl} \gamma_{ijkl} (\left| i \right\rangle \left\langle j \right|)^T \otimes \left| k \right\rangle \left\langle l \right| = \sum_{ijkl} \gamma_{ijkl} \left| j \right\rangle \left\langle i \right| \otimes \left| k \right\rangle \left\langle l \right|. \tag{3.16}$$

To check whether the criterion applies, one must evaluate the eigenvalues of the resulting matrix and verify that they are non-negative. Looking at definition of separable states in eq. (3.14), it is easy to see that any state ρ admitting such a decomposition will obey $\rho^{T_A} \geq 0$, since the (total) transposition

of a matrix does not alter its eigenvalues. The same cannot be assured for entangled states, thus the separability criterion. Notice that the choice of subspace to be transposed is irrelevant, as $\Psi^{T_A} = (\Psi^{T_B})^T$. However, even though a state ρ being PPT does not assure its separability, this implication holds in the special cases where the state is composed of two qubits or a qubit and a qutrit.

Separability criteria can also be formulated in terms of the so-called entanglement witnesses. An observable $\mathcal{W}$ is said to be a witness if $\text{Tr}[\mathcal{W}\rho_{sep}] \geq 0$ for any separable state ρ_{sep} and $\text{Tr}[\mathcal{W}\rho_{ent}] < 0$ for at least one entangled state ρ_{ent}. A separability criterion is established where measuring $\text{Tr}[\mathcal{W}\rho] < 0$ assures that ρ is entangled, but nothing is learned otherwise. These witnesses have a geometrical meaning, representing hyperplanes in the set of all states that split the space in two parts: one contains only entangled states, and the other contains all separable states (and possibly some entangled states). See fig. 3.2 for more details.
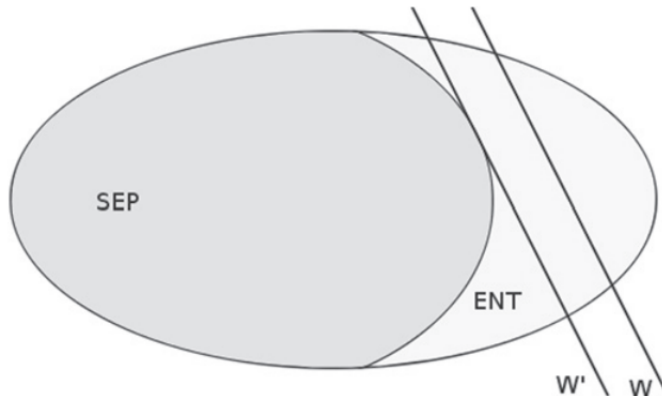
Figure 3.2: A geometrical visualization of entanglement witnesses, taken from [114]. Both hyperplanes W and W' are valid entanglement witnesses, W' however can detect more entangled states than W.

Concerning entanglement witnesses, it is important to notice that even though a specific witness may not be able to single-out a certain state as entangled (since measuring $\text{Tr}[\mathcal{W}\rho] \geq 0$ is inconclusive), there is always a witness capable of detecting any entangled state, since the set of separable states is convex. In this sense, some witnesses are better for some tasks than others, as they identify different sets of entangled states. This "completeness of witnesses" was proven in [115], and justifies a whole branch of quantum information that is finding good entanglement witnesses for different situations.

The method we will expose in this section heavily relies both in the PPT criterion and in the concept of entanglement witnesses in general. The core idea is to build a generalization of PPT, considering extensions of a quantum state to many copies of its subsystems, where the more copies one considers the better the witness constructed is. Let ρ acting on $\mathcal{H}_A \otimes \mathcal{H}_B$ be a bipartite separable state, thus obeying eq. (3.14). From ρ one can construct the following state $\tilde{\rho}$ in $\mathcal{H}_A \otimes \mathcal{H}_B \otimes \mathcal{H}_C$, with $\mathcal{H}_C = \mathcal{H}_A$

$$\tilde{\rho} = \sum p_i \, |\psi_i\rangle\langle\psi_i| \otimes |\phi_i\rangle\langle\phi_i| \otimes |\psi_i\rangle\langle\psi_i|. \tag{3.17}$$

This state is said to be a PPT symmetric extension of ρ to two copies of $\mathcal{H}_A$, because it obeys a set of three requirements.

First, it is an extension of ρ to three parties, meaning

$$\text{Tr}_C[\tilde{\rho}] = \rho, \tag{3.18}$$

where Tr_C is the partial trace over the third party. Second, it is symmetric under swapping of $\mathcal{H}_A$ and $\mathcal{H}_C$. If P_{AC} is the swap operator acting on the first and third parties, it means

$$P_{AC} \, \tilde{\rho} \, P_{AC} = \tilde{\rho}. \tag{3.19}$$

Finally, it obeys the PPT criterion and remains positive under partial transpositions, or yet

$$\tilde{\rho}^{T_A}, \tilde{\rho}^{T_B}, \tilde{\rho}^{T_C} \geq 0. \tag{3.20}$$

Since $\tilde{\rho}$ was constructed from ρ, a separable state, one can use the existence of a state satisfying eqs. (3.18), (3.19) and (3.20) as a separability criterion. Given some state Ψ, can one find a PPT symmetric extension of Ψ to two copies? If so, nothing can be said about Ψ, but if the answer is negative

then Ψ must be entangled. Notice that this inquiry is only non-trivial if the state Ψ in question is PPT, otherwise one would already know it is entangled.

A completely analogous line of thought can be followed to establish similar separability criteria where one in fact considers more than just two copies of a subsystem. Consider a state $\tilde{\rho}$ in $\mathcal{H}_A \otimes \mathcal{H}_B \otimes \mathcal{H}_A^{\otimes n-1}$, an n-copy symmetric extension of ρ, such that

$$\tilde{\rho} = \sum p_i \, |\psi_i\rangle\langle\psi_i| \otimes |\phi_i\rangle\langle\phi_i| \otimes |\psi_i\rangle\langle\psi_i|^{\otimes n-1} \,. \tag{3.21}$$

$\tilde{\rho}$ satisfies similar properties to eqs. (3.18), (3.19) and (3.20): when tracing out any $n-1$ copies of subsystem A we recover ρ; it is preserved under swapping of any two copies of subsystem A; and it remains positive under any partial transposition of a subsystem. Just as before, the existence of such a state $\tilde{\rho}$ is a criterion for the separability of ρ.

This way, for each number of copies n a test is established. A good thing about them is that they are not independent: it is easy to see that if a state has a n-copy PPT symmetric extension it must also have a $(n-1)$-copy PPT symmetric extension. These criteria form a family of tests organized in a hierarchical order, where each level is as least as strong as the previous one. The first level of the hierarchy corresponds to the original PPT criterion (which can be seen as a "single-copy" analysis), while the second corresponds to finding a two-copy PPT symmetric state, and so on [2]. On top of that, as proven in [105], such hierarchy is complete, in the sense that every entangled state will be singled out by tests above some value of n.

At the end of the day, these separability tests boil down to trying to find the n-copy PPT symmetric extension, and this is where SDPs are crucial. This task can be put in the form of a convex optimization problem and be efficiently solved by an SDP. Given a state ρ, one wants to find a state $\tilde{\rho}$ such that the requirements in eqs. (3.18), (3.19) and (3.20) are met. Put mathematically, the optimization task for the second level of the DPS hierarchy is

$$
\begin{aligned}
\textbf{given} \quad & \rho \\
\textbf{find} \quad & \tilde{\rho} \\
\textbf{subject to} \quad & \mathrm{Tr}_C[\tilde{\rho}] = \rho \\
& P_{AC}\, \tilde{\rho}\, P_{AC} = \tilde{\rho} \\
& \tilde{\rho}^{T_A} \geq 0, \ \tilde{\rho}^{T_B} \geq 0, \ \tilde{\rho}^{T_C} \geq 0, \ \tilde{\rho} \geq 0 \,.
\end{aligned}
\tag{3.22}
$$

This task can be directly implemented the way it is, but some simple modifications can be made to improve computation. First, one can realize that performing the partial trace on subspace A or on its copy C should be equivalent. Moreover, we already know that $\tilde{\rho}^{T_A} \geq 0$ implies $\tilde{\rho}^{T_B} \geq 0$, which we can use to simplify the last condition.

Additionally, because of the difficulty of dealing with imprecision and numerical error, solvers do not tend to cope well with the task of finding a solution, but rather prefer performing minimizations or maximizations. For instance, a feasible point with eigenvalue zero might be overlooked because it was identified as having very small but negative eigenvalues. To avoid that, one can translate eq. (3.22) into a maximization problem by introducing an auxiliary parameter t as follows

$$
\begin{aligned}
\textbf{given} \quad & \rho \\
\textbf{maximize} \quad & t \\
\textbf{subject to} \quad & \mathrm{Tr}_C[\tilde{\rho}] = \rho \\
& P_{AC}\, \tilde{\rho}\, P_{AC} = \tilde{\rho} \\
& \tilde{\rho}^{T_A} \geq t\mathbb{1}, \ \tilde{\rho} \geq 0 \,.
\end{aligned}
\tag{3.23}
$$

This way, if $t \geq 0$ we know we have found a solution to eq. (3.22), where not much can be said about ρ, but if $t < 0$ the task is infeasible and ρ must be entangled.

Of course completely analogous formulations can be written out for tests corresponding to higher levels of this hierarchy, i.e., considering PPT symmetric extensions to more than two copies of a subsystem of ρ. This concept can also be generalized to the multipartite case to comprise states with more than two subsystems.

---

[2]Let there be no confusion: when we say a state $\tilde{\rho}$ is a n-copy extension of ρ we mean it has $n-1$ additional parties

The DPS hierarchy method allows one to circumvent the issue of efficiently deciding whether a state is separable, by instead implementing some separability criteria a finite amount of times. We stress, however, that even though each level of the hierarchy can be efficiently solved by an SDP, the dimension of the problem grows exponentially with the hierarchy level. As a result, the computational cost of going beyond the first few levels of the hierarchy is prohibitively high. Nevertheless, at the price of giving up on establishing a decision protocol (where one would always a have a definite answer), one can often find a good enough answer by running a couple of SDPs. This method will be central in chapter 5, where we will use it to certify the number of incompatible measurements to which a party has access in a steering scenario.

3.2.2 A complete SDP hierarchy for rank constrained problems

Among the types of constraints that render an optimization problem unfit for an SDP formulation, a kind of special relevance are rank constraints. Frequently, an optimization is performed over the set of all quantum states, but one would like to restrain the search only to, say, pure states. Consider, for instance, the scenario laid out in [116], where one performs a set of $\{M_i\}_{i=1,...,n}$ measurements on an unknown (but pure) state in the lab, with outcomes $\{m_i\}_{i=1,...,n}$. Suppose one wants to find a quantum state compatible with these outcomes that also maximizes some physical property encoded in observable X. This task can be framed as an optimization problem, as in

$$
\begin{aligned}
\textbf{given} \quad & \{M_i\}, \{m_i\} \\
\textbf{maximize} \quad & \mathrm{Tr}[X\rho] \\
\textbf{subject to} \quad & \mathrm{Tr}[M_i\rho] = m_i \\
& \mathrm{Tr}[\rho] = 1 \\
& \rho \geq 0 \\
& \mathrm{rank}(\rho) = 1 \, .
\end{aligned}
\tag{3.24}
$$

Because of the last constraint, this optimization is not an SDP. In the remaining of this section, we will report the results of Yu et al [117], where they re-frame rank constraints in terms of the separability problem, which can, then, be tackled by an adapted DPS method.

Consider the following task, a generic optimization problem

$$
\begin{aligned}
\textbf{maximize} \quad & \mathrm{Tr}[X\rho] \\
\textbf{subject to} \quad & \mathrm{Tr}[\rho] = 1 \\
& \rho \geq 0 \\
& \Lambda(\rho) = \Upsilon \\
& \mathrm{rank}(\rho) \leq k \, ,
\end{aligned}
\tag{3.25}
$$

where ρ and X are $n \times n$ Hermitian matrices, Υ is a complex matrix in $m \times m$ and Λ is a map taking matrices in $\mathbb{C}^{n \times n}$ to matrices in $\mathbb{C}^{m \times m}$. k is some number in $\{1, \ldots, n\}$.

The set of all $n \times n$ Hermitian matrices compatible with the constraints in eq. (3.25), denoted by $\mathcal{F}$, is

$$
\mathcal{F} = \{\rho | \Lambda(\rho) = \Upsilon, \mathrm{Tr}[\rho] = 1, \rho \geq 0, \mathrm{rank}(\rho) \leq k\}.
\tag{3.26}
$$

We can re-define this feasibility region in terms of purifications of ρ. Consider the Hilbert spaces $\mathcal{H}_1 = \mathbb{C}^n$ and $\mathcal{H}_2 = \mathbb{C}^k$, and notice that $\mathrm{rank}(\rho) \leq k$ means ρ must have a purification in $\mathcal{H}_1 \otimes \mathcal{H}_2$, i.e., there must be a pure state $|\phi\rangle \in \mathbb{C}^{n+k}$ such that $\mathrm{Tr}_2[|\phi\rangle\langle\phi|] = \rho$, and vice versa [42].

The optimization in eq. (3.25) is performed over the feasibility region described in eq. (3.26). Alternatively, one can consider $\mathcal{P}$, the set of purifications of states in $\mathcal{F}$

$$
\mathcal{P} = \{|\phi\rangle\langle\phi| \, | \tilde{\Lambda}(|\phi\rangle\langle\phi|) = \Upsilon, \langle\phi|\phi\rangle = 1\},
\tag{3.27}
$$

where $|\phi\rangle \in \mathbb{C}^{n+k}$ and $\tilde{\Lambda}(\cdot) = \Lambda(\mathrm{Tr}_2[\cdot])$. Notice how $\mathcal{F}$ is simply $\mathrm{Tr}_2[\mathcal{P}]$. This way, performing a maximization of $\mathrm{Tr}[X\rho]$ over $\mathcal{F}$ is equivalent to performing a maximization of $\mathrm{Tr}[\tilde{X} |\phi\rangle\langle\phi|]$ over $\mathcal{P}$, where $\tilde{X} = X \otimes \mathbb{1}_k$, i.e., applying the original observable X on subsystem $\mathcal{H}_1$ and the identity operator $\mathbb{1}_k$ on subsystem $\mathcal{H}_2$, which will be traced out.

However equivalent, this new formulation does not correspond directly to an SDP, since $\mathcal{P}$ only considers pure states, meaning it is not convex. This can be easily solved by realizing that the extreme values of a linear objective function will be achieved by extreme points of the feasibility region, so we can consider the convex hull of $\mathcal{P}$ without any losses. As a consequence, the original optimization problem eq. (3.25) can be translated as

$$\max_{\rho \in \mathcal{F}} \text{Tr}[X\rho] = \max_{\Phi \in \text{conv}(\mathcal{P})} \text{Tr}[\tilde{X}\Phi]. \tag{3.28}$$

It might seem we have simply made it six and two threes, since we had to fully characterize $\mathcal{F}$ and now have to likewise fully characterize $\text{conv}(\mathcal{P})$. However, while we did not know how to cope with the rank restriction in eq. (3.25) we do now how to characterize $\text{conv}(\mathcal{P})$, namely in terms of the set of its symmetric extensions to two parties. Consider the following set

$$\mathcal{S}_2 = \text{conv}(\{|\phi\rangle\langle\phi|_A \otimes |\phi\rangle\langle\phi|_B \,||\phi\rangle\langle\phi| \in \mathcal{P}\}), \tag{3.29}$$

where we recall that $|\phi\rangle$ belongs to $\mathcal{H}_1 \otimes \mathcal{H}_2 = \mathbb{C}^n \otimes \mathbb{C}^k$. The elements of $\mathcal{S}_2$, in turn, belong to $\mathcal{H}_A \otimes \mathcal{H}_B$, where $\mathcal{H}_A = \mathcal{H}_B = \mathcal{H}_1 \otimes \mathcal{H}_2$.

Notice, first of all, how $\text{Tr}_B[\mathcal{S}_2] = \text{conv}(\mathcal{P})$. This means that if one can fully characterize $\mathcal{S}_2$ the problem is solved. Then, as maybe this whole endeavor makes a bell ring in the reader's mind, we call attention to the many similarities this approach has to the DPS method, introduced in section 3.2.1.

If we recall that there is no direct SDP formulation to rank-constrained optimization problems, it is only natural to expect there should be no SDP formulation to any problem that is perfectly equivalent to eq. (3.25), as we have done so far. Thus, inspired by the DPS method, the authors in [117] establish an SDP hierarchy whose $N-$th level corresponds to an optimization over $\mathcal{S}_N$, the set of N-copy symmetric extensions of $\text{conv}(\mathcal{P})$, the convex hull of the purifications of ρ. Let the variable $\Phi_{AB\ldots Z}$ belong to $\mathcal{H}_A \otimes \mathcal{H}_B \otimes \ldots \otimes \mathcal{H}_Z$, composed of N subsystems, each obeying $\mathcal{H}_A = \mathcal{H}_B = \cdots = \mathcal{H}_Z = \mathcal{H}_1 \otimes \mathcal{H}_2$. Then, since $\text{Tr}_{B\ldots Z}[\mathcal{S}_N] = \text{conv}(\mathcal{P})$, the optimization problem reads

$$
\begin{aligned}
\textbf{maximize} \quad & \text{Tr}[(\tilde{X}_A \otimes \mathbb{1}_{B\ldots Z})\Phi_{AB\ldots Z}] \\
\textbf{subject to} \quad & \text{Tr}[\Phi_{AB\ldots Z}] = 1 \\
& \Phi_{AB\ldots Z} \geq 0 \\
& P_N \Phi_{AB\ldots Z} P_N = \Phi_{AB\ldots Z} \\
& (\tilde{\Lambda}_A \otimes \textbf{id}_{B\ldots Z})\Phi_{AB\ldots Z} = \Upsilon \otimes \text{Tr}_A[\Phi_{AB\ldots Z}],
\end{aligned}
\tag{3.30}
$$

Let us dissect this SDP step by step.

$\tilde{X}_A$ is the observable $\tilde{X} = X \otimes \mathbb{1}_k$ acting on subsystem A, and maximizing the above objective function over $\mathcal{S}_N$ is manifestly equivalent to maximizing $\text{Tr}[\tilde{X}\Phi]$ over $\text{conv}(\mathcal{P})$ or, as we originally set out, $\text{Tr}[X\rho]$ over $\mathcal{F}$.

The first two constraints in the SDP are simply demanding that $\Phi_{AB\ldots Z}$ be a state. They are equivalent to the first two constraints in the original prototype SDP eq. (3.25).

Next, we scrutinize the remaining constraint, assuring that the solution will be invariant under exchanges of subsystems. For that, we define the projector P_N onto the symmetric subspace of $\mathcal{H}_A \otimes \mathcal{H}_B \otimes \ldots \otimes \mathcal{H}_N =: \mathcal{H}^{\otimes N}$, to which the variable $\Phi_{AB\ldots Z}$ must belong. This object is basically the sum of the operators performing all possible permutations of subsystems of $\mathcal{H}^{\otimes N}$,

$$P_N = \frac{1}{N!}\sum_\sigma V_\sigma, \tag{3.31}$$

where V_σ are the aforementioned operators performing the permutation σ.

Finally, let us look into the last constraint. $\tilde{\Lambda}_A$ is the channel $\tilde{\Lambda}(\cdot) = \Lambda(\text{Tr}[\cdot])$ applied on subsystem A and $\textbf{id}_{B\ldots Z}$ is the identity channel on the remaining subsystems. This constraint recovers $\Lambda(\rho) = \Upsilon$ in the original.

Together, these constraints establish the N-th instance of the SDP hierarchy, and by considering symmetric extensions to different numbers N of copies of subsystem A we can formulate different optimization tasks. As proved on the original work [117], these different instances correspond indeed to separate levels of a complete SDP hierarchy: if ξ is the optimal value of the original rank-constrained problem eq. (3.25) and ξ_N is the optimal value of the N-th level SDP in eq. (3.30), then

$$\xi_{N+1} \leq \xi_N, \quad \lim_{N \to \infty} \xi_N = \xi. \tag{3.32}$$

This means that by considering higher and higher levels of the hierarchy one obtains tighter upper bounds to the optimal solution, and in the limit of $N \to \infty$ one actually reaches the exact solution to eq. (3.25).

As a simple application of this method, we can revisit the optimization task eq. (3.24) posed in the beginning of this section, where the rank constraint comes from performing the maximization exclusively over pure states. The SDP corresponding to the second level of this hierarchy is

$$
\begin{aligned}
&\textbf{given} \quad \{M_i\}, \{m_i\} \\
&\textbf{maximize} \quad \text{Tr}[(\tilde{X}_A \otimes \mathbb{1}_B)\Phi_{AB}] \\
&\textbf{subject to} \quad \Phi_{AB} \geq 0 \\
&\qquad\qquad\quad \text{Tr}[\Phi_{AB}] = 1 \\
&\qquad\qquad\quad P_2 \Phi_{AB} P_2 = \Phi_{AB} \\
&\qquad\qquad\quad \text{Tr}_A[(M_i \otimes \textbf{id}_B)\Phi_{AB}] = m_i \, \text{Tr}_A[\Phi_{AB}] \, .
\end{aligned}
\tag{3.33}
$$

In summary, by mapping rank-constrained optimization problems into a search for symmetric extensions of quantum states, the authors manage to circumvent the non-convexity of a class of computation tasks. This method will be particularly useful to us in chapter 4, where we will use it do deal with restrictions to the dimension of quantum states.

3.2.3 See-saw methods

Another sub-class of optimization problems of interest, closely related to rank-constrained problems as we will see, is that of bi-linear objective functions. This type of task cannot be put in SDP form, but since they figure in many relevant problems in quantum information it is interesting to find alternative approaches.

One of such approaches is to employ a so-called see-saw method. Apart from bi-linear problems, it can be used to solve so-called *min-max* problems (where one minimizes over one variable and maximizes over another) [91]. It can also be applied to problems with constraints formulated in terms of a product of two variables as in [118], where the authors want to find the most incompatible measurements over a set, a task that requires optimizing over all measurements and all quantum states; or in [119, 120] where one finds multiple counter-examples to the Peres conjecture [121], stating that bound entangled states always admit a local hidden variable model.

In general, see-saw methods are a class of algorithms where one iteratively solves two sub-tasks and feeds one with the optimal answer found from the other, repeating a cycle until some convergence criteria is met. The point achieved by such a method is a local extreme of the objective function and provides an upper (lower) bound to the original minimization (maximization) problem. In particular, we will focus on solving rank-constrained optimization problems, following a method that will incur in computation tasks with bi-linear objective function. Take the following feasibility task, optimized over all $(n+1) \times (n+1)$ Hermitian matrices

$$
\begin{aligned}
&\textbf{find} \quad X \\
&\textbf{subject to} \quad X_{ij} = \mu_{ij}, \quad i, j \in \{0, \dots, n\} \\
&\qquad\qquad\quad X \geq 0 \\
&\qquad\qquad\quad \text{rank}(X) \leq d \, .
\end{aligned}
\tag{3.34}
$$

Here, one is basically looking for any matrix X with specific matrix elements that obeys some extra restrictions. Some elements may be tied such that some values of $\{\mu_{ij}\}$ are specified, but others are free parameters that one can optimize over. For instance, maybe the diagonal elements and the first column and row are fixed ($\{\mu_{ii}\}$, $\{\mu_{0i}\}$ and $\{\mu_{i0}\}$ are known) but the other elements are not, and one can vary the free elements to find an instance of X that is positive semidefinite and has lower or equal to d. This kind of problem will be particularly useful in chapter 4.

Even though rank-constrained problems cannot, in general, be solved efficiently by SDPs, there are some particular instances of it that do admit a closed form for the optimal solution. The goal of the method we will illustrate, generally outlined in [89] and applied to this problem by us in [2], is to convert

the rank-constrained problem in eq. (3.34) into one of such problems with known solution, bypassing the need of framing the rank constraint in an SDP altogether. First, one can translate eq. (3.34), a feasibility problem, into a minimization problem. The optimization in eq. (3.34) is feasible if and only if the following optimization task has solution zero

$$
\begin{aligned}
\textbf{minimize}_{\{X,P\}} \quad & \text{Tr}[XP] \\
\textbf{subject to} \quad & X \geq 0, \quad X_{ij} = \mu_{ij} \\
& P \geq 0, \quad P^2 = P \\
& \text{rank}(P) = n - d + 1,
\end{aligned}
\tag{3.35}
$$

where now one has a minimization over two variables, X and P being $(n+1) \times (n+1)$ Hermitian matrices. The equivalence between eq. (3.34) and eq. (3.35) is not hard to conceive if one recalls the rank-nullity theorem, stating that for a matrix M it holds that

$$
\dim(M) = \text{rank}(M) + \text{null}(M),
\tag{3.36}
$$

where $\text{null}(M)$ is the dimension of its kernel space. If the optimal value of eq. (3.35) is zero, then $\text{null}(X) \geq \text{rank}(P)$ or $\text{null}(P) \geq \text{rank}(X)$. Either way, since $\text{rank}(P) = n - d + 1$, the rank-nullity theorem imposes that $\text{rank}(X) \leq d$, and we recover the original optimization eq. (3.34). Likewise, the other direction of the correspondence follows directly.

Now, one is left with the minimization of a bi-linear objective function over variables X and P. One can then establish two optimization tasks and perform them alternatingly, using a see-saw algorithm. Start by choosing a random rank-$(n - d + 1)$ projector P_* as a starting point and perform the following SDP

$$
\begin{aligned}
\textbf{minimize}_{\{X\}} \quad & \text{Tr}[XP_*] \\
\textbf{subject to} \quad & X \geq 0, \quad X_{ij} = \mu_{ij}.
\end{aligned}
\tag{3.37}
$$

It will yield some optimal X_*. One then feeds this solution to a second optimization problem

$$
\begin{aligned}
\textbf{minimize}_{\{P\}} \quad & \text{Tr}[X_*P] \\
\textbf{subject to} \quad & P \geq 0, \quad P^2 = P \\
& \text{rank}(P) = n - d + 1.
\end{aligned}
\tag{3.38}
$$

This is not an SDP, namely because of the rank constraint. However, it can be efficiently solved because it has known solution [89]. Let X_* be decomposed in its eigenbasis as

$$
X_* = \sum_{i=0}^{n} \lambda_i \, |\phi_i\rangle\langle\phi_i| \, ,
\tag{3.39}
$$

with its eigenvalues ordered non-increasingly as $\lambda_0 \geq \lambda_1 \geq \ldots \geq \lambda_n$. Then, a solution to eq. (3.38) is given by

$$
P_* = \sum_{i=d}^{n} |\phi_i\rangle\langle\phi_i| \, ,
\tag{3.40}
$$

namely the sum of the eigenvectors of X_* associated to its $(n - d + 1)$ smallest eigenvalues. One can immediately see that P_* is in the feasibility region of eq. (3.38) since it clearly obeys its restrictions. Furthermore, it minimizes the objective function because it basically selects the $(n - d + 1)$ smallest eigenvalues of X_*, which is the best a rank-$(n - d + 1)$ orthogonal projection matrix can do.

After finding P_*, one can re-feed it into eq. (3.37) to find yet another X_*, which is re-fed to eq. (3.38) and so on. After each round of iterations, one can take the pair X_*, P_* and evaluate $\tau = \text{Tr}[X_*P_*]$. If one keeps track of this result, it can be used as a halting condition to this loop of alternating optimizations: if there is no significant change between rounds and τ converges to some value one ends the algorithm. We point out that this should always happen sooner or later and τ will indeed converge to some value, since successive iterations cannot increase its value, and $\text{Tr}[X_*P_*]$ is lower bounded by zero because $X_*, P_* \geq 0$.

After halting the algorithm all that is left is to interpret the final result. If $\tau = 0$, as discussed, one has found a solution to eq. (3.35) and consequently solved the original feasibility problem in eq. (3.34). If τ converges to some other value then nothing can be concluded, as an optimal solution may exist while this heuristic method was simply not capable of finding it. Notice that the possibility of such inconclusive answer is to be expected from this strategy. The original problem eq. (3.34) is not an SDP and cannot be efficiently solved, so neither should any of its equivalent formulations.

After introducing this final strategy to overcome particular difficulties when dealing with optimization problems, we can finally conclude this chapter. A basic understanding of how semidefinite programming works, plus familiarity with some specific methods, is the background knowledge one needs in order to be able to thoroughly follow what will be presented in the following chapters, where SDPs are extensively used to investigate different aspects of quantum information.

Chapter 4

Complete characterization of finite contextuality

In the field of quantum foundations, there is no denying that the differences displayed by quantum and classical systems are a main source of query. These phenomena challenge our intuition that has been trained since birth in a classical world, and we can firmly say that there is no shortage of such phenomena, some of which are approached in this thesis.

Among them figures the field of quantum contextuality. In few words, it shows us that one cannot think of a measurement as simply revealing a property of a quantum state independently of the set of measurements one chooses to perform (the *context* of an experiment). This is of course at clash with what we would expect from our classically conditioned intuition, where systems are well-defined before any (typically non-disturbing) measurement, and efforts to conciliate the contextual claim with a classical reasoning have proven to be futile, as we will see.

It is clear that quantum contextuality must be deeply understood if one hopes to ever bridge the fundamental gap between classical and quantum regimes, but the importance of the field to science does not restrict itself to that. More than foundational relevance, contextuality has major practical applications in quantum information processing, such as quantum cryptography [122], random number generation [123, 124], as well as being a key ingredient to achieve quantum advantage in a range of tasks [125, 126, 127].

How to certify that such a peculiar feature is indeed manifesting itself in the lab? The path has already been set by the study of Bell non-locality: one must establish a theory independent test. Given the probabilistic nature of quantum mechanics, our classical intuition would tell us to explain the weird statistics one gets in a contextual scenario with classical ignorance, claiming there is simply a "hidden variable", unknown to us, that would set everything right.

To completely kill this hopeful vision, the theory is abundant with so-called "non-contextuality inequalities", expressions setting an upper bound to expectations values of a set of measurements. To achieve these inequalities, one accepts the non-contextual hypothesis (stating that the outcomes of a given measurement are independent of whatever other measurements are performed jointly), and thus the violation of these bounds means one is dealing with a contextual scenario. This is known as the Kochen-Specker theorem [128], and, put simply, it takes a set of probabilities obtained from joint measurements and tells us whether these correlations can be reproduced by a hidden variable model.

Given its multifaceted relevance, certifying contextuality is an important task in quantum information. The good news is that non-contextuality inequalities are often formulated in such a way that their violation can be investigated with semidefinite programming. The bad news is that some of its most noteworthy instances cannot, namely when one adds dimension restrictions.

Knowing the dimension of the physical system one is dealing with is central in many tasks, such as characterizing a device or ensuring the security of protocols in quantum key distribution [129, 130]. To discover this attribute, one can employ *dimension witnesses* [131], an approach where one set a lower bound on the dimension a system must have given the statistics one obtains from experiments. The idea behind it is that some behaviors can only be reproduced by systems with dimension at least d (though one does not necessarily find out the exact dimension of the system).

This type of query can be formulated in terms of an optimization problem that unfortunately contains a rank restriction, and thus is not an SDP. Given the importance of characterizing quantum contextuality, the fact that these problems cannot be efficiently tackled poses a huge drawback to the field of quantum

information. Many advances have been made in this sense [132, 102, 133], but a reliable and efficient approach is still lacking.

In this section we will present our work [2], where we provide systematic methods to answer the two main questions one asks when characterizing dimension-restricted contextuality. First, do the statistics obtained in the lab belong to the set of d-dimension quantum behaviors, or put another way, can these probabilities be reproduced by a d-dimensional system in a contextual scenario? Second, what is the maximum violation a d-dimension system can achieve at a general non-contextuality inequality? With these answers one can assure a probability distribution admits no hidden variable model and certify contextuality in a theory independent way, as well as construct a dimension witness.

4.1 Preliminary concepts

In what follows we will present the concept of quantum contextuality as well as lay out relevant notions in graph theory, so that we can then present our results. These will be brief introductions to complex and prolific themes, for in-depth discussions we redirect the reader to the work that served as main reference when writing this section, namely [87, 132, 102, 134, 135, 136, 137].

4.1.1 Contextuality

Classical mechanics is built upon the ubiquitous and silent assumption that physical systems display intrinsic properties with well-defined values. Measurements are thought of as simply revealing these properties, and whatever discrepancy observed in the outcome statistics is merely the result of the fact that one cannot completely control an experiment. If within an acceptable range, these fluctuations are then overlooked and not much thought must be dispensed on it. The same cannot be said of quantum mechanics, where state preparation and measurement has to be dealt with much more care. Quantum contextuality is one of the many instances where this classical reasoning just does not apply.

Let us consider a set of 9 measurements, labeled $\{A, a, \alpha, B, b, \beta, C, c, \gamma\}$. For simplicity, let them be dichotomic measurements with possible outcomes labeled by $+1, -1$. These measurements are related to each other in a way that some of their subsets are compatible, i.e., it is possible to jointly measure them. To pictorially visualize such relation, we can arrange them in a square

$$\begin{bmatrix} A & B & C \\ a & b & c \\ \alpha & \beta & \gamma \end{bmatrix}. \tag{4.1}$$

This is knows as the Peres-Mermin square [138, 139, 140, 141], and it provides an example of a situation where contextuality manifests itself. Let us assume that all measurements on the same row or the same column are jointly measurable. This means, for instance, that $\{A, a, \alpha\}$ can be measured in a way that one does not disturb the other, and the same goes for $\{A, B, C\}$. Such sets of compatible measurements are called a *context*. The *non-contextual* hypothesis consists in assuming that each of these measurements reveals a well-defined property of the system, regardless of their context.

Let $\langle Aa\alpha \rangle$ denote the expectation value of a joint measurement of A, a, α, and similarly for other sets of measurements. It is then easy to see that the following inequality must hold

$$\langle ABC \rangle + \langle abc \rangle + \langle \alpha\beta\gamma \rangle + \langle Aa\alpha \rangle + \langle Bb\beta \rangle - \langle Cc\gamma \rangle \leq 4. \tag{4.2}$$

If one can find measurements fitting the Peres-Mermin square that violate the bound above, it must then mean the non-contextual assumption does not hold and one cannot think of measurements the same way as when dealing with classical mechanics. As in [142], let us consider measurements performed on a two spin-1/2 particles, obtained by locally applying the Pauli operators $\{\sigma_x, \sigma_y, \sigma_z\}$. Let the corresponding Peres-Mermin square be

$$\begin{bmatrix} \sigma_z \otimes \mathbb{1} & \mathbb{1} \otimes \sigma_z & \sigma_z \otimes \sigma_z \\ \mathbb{1} \otimes \sigma_x & \sigma_x \otimes \mathbb{1} & \sigma_x \otimes \sigma_x \\ \sigma_z \otimes \sigma_x & \sigma_x \otimes \sigma_z & \sigma_y \otimes \sigma_y \end{bmatrix}. \tag{4.3}$$

Notice how every row and column forms a context. Moreover, the product of the elements in each context is $ABC = \mathbb{1}$, and similarly for all other contexts, except for $Cc\gamma = -\mathbb{1}$. This means that the expectation values of measurements in these contexts are state independent, and plugging them back in eq. (4.2) we obtain a clear violation of the upper bound. Since the inequality in eq. (4.2) was obtained

under the assumption of the non-contextual hypothesis, the fact that it can be violated (incidentally, by any quantum state) implies that one cannot consistently assign a value to these measurements regardless of their context.

The Peres-Mermin square provides a simple example of contextual behavior. In the lingo of quantum information, eq. (4.2) provides a contextuality witness, certifying that a set of measurements displays quantum features. A broader approach to proving that contextuality cannot be understood in classical terms is the Kochen-Spekker theorem [128]. It considers specific context arrangements and shows that one cannot assign values to the outcomes of measurements without incurring in contradictions. It is a rather long proof, using a contextuality scenario to construct a 120-vertex graph and showing that it cannot be colored in accordance to a specific set of rules. Later, simpler proofs following a similar reasoning have been found, until an 18-vertex proof was developed in [143], which was then proven to be minimal in [144], meaning no proof of the Kochen-Specker theorem can be found that uses graphs with less than 18 vertices.

Now that we have established the core idea behind contextuality, namely that there is more to quantum measurements than one can grasp solely with classical theory, we can move on to describe how contextuality can be explored and studied.

4.1.2 Graph theory applied to contextuality

Kochen-Specker proofs give us an interesting hint of how to analyze contextuality, and the fact that contextuality scenarios can be translated into graphs is a meaningful addition to the field. More than pure mathematical worth, graphs can be applied to a vast range of problems, including quantum information, which means one can take advantage of the many already established results and developments in graph theory. Particularly in quantum contextuality, one can use graphs to describe events and measurements in a way that the contextual nature of a scenario can be assessed with properties of the graph. We start by introducing some relevant definitions.

A graph is a way to represent the relationship between entities in terms of vertices (or nodes) and edges. The graph $\mathcal{G} = (V, E)$ is composed of a set V of vertices and a set E of edges, which in turn are unordered pairs of vertices (i, j), with $i, j \in V$. Whenever two vertices are connected by an edge, they are said to be *adjacent*. A set of mutually adjacent vertices is a *clique*, while a set of vertices is called *independent* if none of its vertices are connected.

Now, consider a measurement M with possible outcomes $\{a_i\}$, so and *event* is a pair $e_i = (a_i|M)$. We say two events are *exclusive* if they correspond to different outcomes of the same measurement. For multiple measurements, an event is a set of n compatible measurements and its corresponding outcomes, then two events $e_i = (a_{i_1}, \ldots, a_{i_n}|M_{i_1}, \ldots, M_{i_n})$ and $e_j = (a_{j_1}, \ldots, a_{j_n}|M_{j_1}, \ldots, M_{j_n})$ are exclusive if there exists i, j, k such that $M_{i_k} = M_{j_k}$ but $a_{i_k} \neq a_{j_k}$. This situation corresponds to two events with at least one common measurements but different outcomes of this specific measurement.

In an *exclusivity graph* $\mathcal{G}_{ex}$ the vertices are associated to events and exclusive events are connected by an edge, as shown in fig. 4.1. To each event e_i one can associate a probability $p_i \in [0, 1]$. The condition that must be respected is that for two exclusive events e_i, e_j we must have $p_i + p_j \leq 1$, since they correspond to different outcomes of a same measurement. For an exclusivity graph of n events, the set of probabilities $p = \{p_1, \ldots, p_n\}$ is called a behavior.

Exclusivity graph can hence describe scenarios where one performs a series of measurements in a lab and obtains some outcome statistics. As such, some properties of this graph will reflect characteristics of the experimental setting itself, and one can use concepts in graph theory to analyze phenomena like quantum contextuality. To introduce this approach, we must dig deeper in the fields of both contextuality and graph studies.

We start by defining *deterministic non-contextual behavior*, a sub-class of behaviors where events are associated either to probability 1 or 0. If the probability distribution p obeys $p_i \in \{0, 1\}$ for all i while not contradicting the exclusivity condition that adjacent vertices e_i, e_j have probabilities $p_i + p_j \leq 1$, the behavior is deterministic non-contextual. If we think of p as a vector, we can define the *non-contextual polytope* $\mathcal{P}_{NC}(\mathcal{G}_{ex})$ as the convex hull of all deterministic non-contextual behaviors that can be assigned to the exclusivity graph $\mathcal{G}_{ex}$. All behaviors that do not belong to $\mathcal{P}_{NC}(\mathcal{G}_{ex})$ are called *contextual*.

Thus, non-contextual behaviors are consistent probability distributions that follow the classical reasoning, where one can simply assign outcomes to measurements regardless of their context (and convex combination thereof). Contextual behaviors, in contrast, are those distributions where this is not possible. When an exclusivity graph admits no non-contextual behavior it must mean we are dealing with a contextuality scenario, and for this reason, characterizing $\mathcal{P}_{NC}(\mathcal{G}_{ex})$ is such a relevant task.
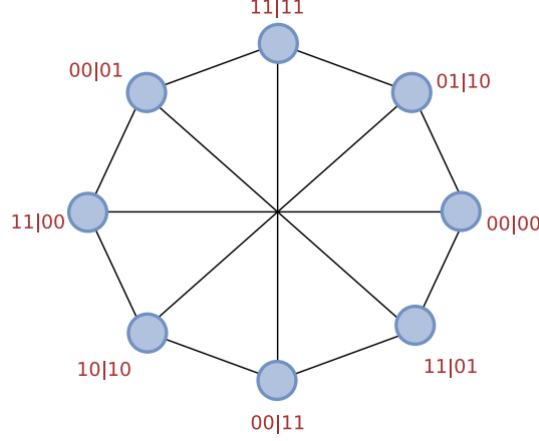
Figure 4.1: The exclusivity graph of the events in a bipartite Bell scenario, adapted from [145]. Each event $(a_i b_j | A_i B_j)$ corresponds to performing dichotomic measurements A_i on Alice's side and B_j on Bob's side with $i, j \in \{0, 1\}$, and obtaining the respective outcomes a_i, b_j. For more details, see appendix F .

Let behaviors be vectors in $\mathbb{R}^n_+$. For deterministic behaviors, the exclusivity condition dictates that for every pair of exclusive events at the most one event can have probability 1. This way, one can mathematically express the set of non-contextual behaviors as

$$\mathcal{P}_{NC}(\mathcal{G}_{ex}) = \text{conv}\{p \in \{0, 1\}^n \,|\, p_i p_j = 0 \text{ if } (i, j) \in E\}. \tag{4.4}$$

This is precisely the definition of STAB($\mathcal{G}_{ex}$), the *stable set polytope* of a graph, the convex hull of the set of probability vectors that assign 1 to all vertices of an independent set and 0 to all other vertices. The vectors p are said to be *orthogonal representations* of the graph.

Moreover, p is said to be a *quantum behavior* if it admits a *quantum realization*, i.e. there exist a quantum state $|\psi\rangle$ and projectors $\Pi_1, \dots, \Pi_n$ that obey

$$p_i = \langle \psi | \Pi_i | \psi \rangle, \ i = 1, \dots, n \quad \text{and} \quad \text{Tr}[\Pi_i \Pi_j] = 0 \text{ if } (i, j) \in E. \tag{4.5}$$

This means that the statistics of the events can be reproduced by measurements on quantum states[1]. The set of quantum behaviors of a given exclusivity graph is denoted $\mathcal{P}_Q(\mathcal{G}_{ex})$. As shown in [132], $\mathcal{P}_Q(\mathcal{G}_{ex})$ is precisely the *theta body* of the graph, defined as

$$TH(\mathcal{G}_{ex}) = \{p \in \mathbb{R}^n_+ | \exists Y \in \mathbb{S}^{1+n}_+ : Y_{00} = 1, Y_{ii} = Y_{0i} = p_i \ \forall i \in \{1, \dots, n\}, \text{ and } Y_{ij} = 0 \text{ if } (i, j) \in E\}, \tag{4.6}$$

where $\mathbb{S}^{1+n}_+$ is the set of positive semidefinite $(n + 1) \times (n + 1)$ matrices.

The fact that $\mathcal{P}_{NC}(\mathcal{G}_{ex})$ corresponds to $STAB(\mathcal{G}_{ex})$ means we can characterize the set of non-contextual behaviors with techniques already established in graph theory. Since $STAB(\mathcal{G}_{ex})$ is a polytope, the maximum value of the sum $\sum_i p_i$ over non-contextual behaviors (a linear function) is achieved by one of its extreme points. If one recalls the definition of $\mathcal{P}_{NC}(\mathcal{G}_{ex})$, it is clear that the maximum is achieved by a deterministic behavior. For these behaviors, the exclusivity conditions implies that the sum $\sum_i p_i$ equals the number of vertices in the independent set they define, and the maximum value of the sum is then the number of vertices of the largest independent set of $\mathcal{G}_{ex}$. This is precisely the definition of the *independence number* of the graph, $\alpha(\mathcal{G}_{ex})$. Thus, we come to the following inequality

$$\sum_{i=1}^n p_i \leq \alpha(\mathcal{G}_{ex}), \ \forall \, p \in \mathcal{P}_{NC}(\mathcal{G}_{ex}). \tag{4.7}$$

This is a non-contextuality inequality, and whenever it is violated by some behavior p it means there is no non-contextual model that can explain these correlations. It serves as a contextuality witness, delimiting the facet of the non-contextual polytope.

---

[1]One may go further and also consider mixed states and non-projective measurements, but this would go beyond the scope of our work. For more details, see [146]

Indeed, quantum behaviors are capable of violating this inequality. If one wants to find the maximum violation of eq. (4.7), one must perform an search over all possible behaviors, not only the deterministic ones. This problem can be stated as an optimization task as

$$\textbf{maximize} \quad \sum_{i=1}^{n} p_i$$
$$\textbf{subject to} \quad p \in \mathcal{P}_Q(\mathcal{G}_{ex}). \tag{4.8}$$

If we recall that $\mathcal{P}_Q(\mathcal{G}_{ex})$ is $TH(\mathcal{G}_{ex})$ defined in eq. (4.6), we have

$$\textbf{maximize} \quad \sum_{i=1}^{n} p_i$$
$$\textbf{subject to} \quad p_i = X_{ii} = X_{0i}, \quad \forall\, i$$
$$X_{ij} = 0, \quad \text{if } (i,j) \in E$$
$$X_{00} = 1$$
$$X \in \mathbb{S}_+^{1+n}. \tag{4.9}$$

This optimization happens to be precisely one of the many formulations of the famous Lovász number $\vartheta(\mathcal{G}_{ex})$, so we achieve an inequality that holds for all quantum behaviors, contextual or not

$$\sum_{i=1}^{n} p_i \leq \vartheta(\mathcal{G}_{ex}), \ \forall\, p \in \mathcal{P}_Q(\mathcal{G}_{ex}). \tag{4.10}$$

4.1.3 The Lovász number

The Lovász number was first formulated in [147] as an upper bound to the Shannon capacity of a channel, measuring how efficiently messages can be transmitted. Consider the following typical example scenario: one has access to a channel, across which one can choose to send 5 different signals, labeled by the code words '0', '1', '2', '3' and '4'. Now, suppose this channel is noisy, and when one sends a signal m the person at the other end gets $m + \xi \mod 5$, where $\xi \in\,]-1, 1[$ is random, so if one party sends the signal '2' the receiving party might actually get '1.8', or perhaps '2.3'. This means that if the receiver reads a signal 3.6 there is no way to know whether the original content was 3 or 4.

In such sub-optimal conditions, the fact is that one can only rely on two of the five total possible code words. It is only safe to send, for instance, the code words '1' and '3', so the receiver knows that any signal in the interval $]0, 2[$ corresponds to '1' and anything in the interval $]2, -4[$ corresponds to '3'. Sending anything else might lead to confusion, so the parties should agree to only use '1' and '3' in their messages. Over n steps, one has the possibility of sending 2^n different messages, or 1 out of 2 code words per step. To express this situation one can construct a confusion graph, where nodes are code words and edges connect signals that cannot be distinguished as in fig. 4.2. It suffices to find a set of non-connected vertices to establish which code words to pick, as they represent signals that cannot be confused.

A clever strategy is to perhaps use bigger code words composed of more than one signal. Consider the code words '11', '23', '35', '54', '42'. It would take two steps to send a single code word, but the advantage is that they are all distinguishable now: if there is any confusion over the true value of the first signal, the second signal necessarily clarifies it. This means that over n steps one can send $5^{n/2}$ different messages, or $\sqrt{5}$ per step, a huge improvement from the previous approach.

The Shannon capacity is the concept that measures the efficiency of the channel that it describes, i.e., the best ratio between the number of possible different messages and the number of steps needed. It is easy to see that the independence number of the confusion graph is a lower bound to the Shannon capacity, as it describes precisely the largest subset of non-adjacent vertices, i.e., largest subset of vertices that cannot be confused with each other. This quantity corresponds to the naive strategy of using single signals as code words, but, as we have seen, more efficient strategies can be employed. Given a graph $\mathcal{G}$, to compute the independence number $\alpha(\mathcal{G})$ one can resort to an optimization task, namely
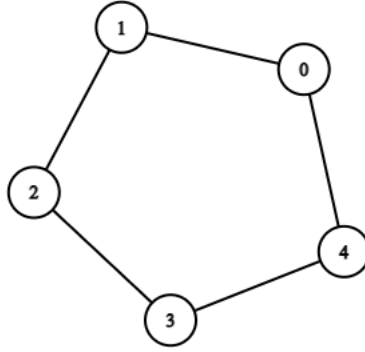
Figure 4.2: The confusion graph associated to the scenario where one can send 5 code words over a noisy channel that makes some of them indistinguishable to the receiver. Vertices 1 and 3 are not connected, so we can use them for communication.

$$
\begin{aligned}
\textbf{maximize} \quad & \sum_{i=1}^{n} x_i \\
\textbf{subject to} \quad & x_i^2 = x_i, \quad i = 1, \ldots, n \\
& x_i x_j = 0, \quad \text{if } (i,j) \in E \\
& x_i \geq 0.
\end{aligned}
\tag{4.11}
$$

The constraints dictate that x_i must be either 0 or 1, and that for every pair of adjacent nodes at most one vertex can be designated as 1. This problem is formulated in a way that the variable x is defining independent sets, by assigning 1 to mutually non-connected vertices and 0 to all other nodes. The objective function is simply the cardinality of these independent sets, so the solution of this task is the number of elements in the largest independent set, i.e., the independence number of the graph.

This problem is not a semidefinite program, but Lovász proposed in [147] a relaxed version of it that is and SDP. Given a graph $\mathcal{G}$, one optimizes over variables $x \in \mathbb{R}^n$ and $X \in \mathbb{S}_+^n$ the following problem

$$
\begin{aligned}
\textbf{maximize} \quad & \sum_{i=1}^{n} x_i \\
\textbf{subject to} \quad & X_{ii} = x_i, \quad i = 1, \ldots, n \\
& X_{ij} = 0, \quad \text{if } (i,j) \in E \\
& \begin{bmatrix} 1 & x^T \\ x & X \end{bmatrix} \geq 0.
\end{aligned}
\tag{4.12}
$$

This is yet another formulation of $\vartheta(\mathcal{G})$, equivalent to eq. (4.10) (one is the dual formulation of the other). It is easy to check that $\alpha(\mathcal{G}) \leq \vartheta(\mathcal{G})$, because any solution x to eq. (4.11) produces a feasible point in eq. (4.12), namely the pair $(x, X = xx^T)$. Moreover, it is proven in [147] that, in fact, the Shannon capacity of a graph is also upper bounded by $\vartheta(\mathcal{G})$.

With all these considerations, we can turn back to contextuality analyses. Given an exclusivity graph $\mathcal{G}_{ex}$ and a contextual behavior $p \notin \mathcal{P}_{NC}$, we have that

$$
\alpha(\mathcal{G}_{ex}) \leq \sum_{i} p_i \leq \vartheta(\mathcal{G}_{ex}).
\tag{4.13}
$$

This relation is at the core of contextuality studies. All behaviors have the sum of its probabilities upper bounded by the Lovász number, but only contextual behaviors can violate the classical bound given by

the independence number. Given a behavior p one can test whether it admits a non-contextual hidden variable model or not by comparing it to $\alpha(\mathcal{G}_{ex})$. Whenever there is a gap between this classical bound and the quantum bound (given by the Lovász number) it is possible to construct a non-contextuality inequality, or yet a contextuality witness.

As important as the relation in eq. (4.13) is, notice that the dimension of the states is completely left out. It reveals the contextual properties of a setting but nothing is said about this characteristic of the system, which we already argued to be of utmost relevance. If we want to include a discussion of dimensionality in our studies, we have to start by defining the set of d-quantum behaviors

$$\mathcal{P}_Q^d(\mathcal{G}_{ex}) = \{p \in \mathbb{R}_+^n \mid \exists \, |\psi\rangle \in \mathbb{C}^d : \, p_i = \langle\psi|\Pi_i|\psi\rangle, \text{Tr}[\Pi_i\Pi_j] = 0 \text{ if } (i,j) \in E\}, \qquad (4.14)$$

where $\{\Pi_i\}_{i=1}^n$ are projectors. In words, $\mathcal{P}_Q^d(\mathcal{G}_{ex})$ is the set of behaviors that admit a quantum realization with dimension d. Given the statistics of an experiment, one can put a lower bound d' on the dimension of the quantum system that was measured by checking whether it belongs to $\mathcal{P}_Q^{d'}(\mathcal{G}_{ex})$ (notice that if a behavior belongs to $\mathcal{P}_Q^{d'}(\mathcal{G}_{ex})$, it trivially also belongs to $\mathcal{P}_Q^{d'+1}(\mathcal{G}_{ex})$).

The main obstacle to the task of lower bounding the dimension of a system is the fact that even though $\mathcal{P}_Q(\mathcal{G}_{ex})$ is a convex set, $\mathcal{P}_Q^d(\mathcal{G}_{ex})$ is not. This means one cannot simply write a semidefinite program that will check if a behavior p belongs to the set of d-quantum behaviors, and all the firepower provided by convex optimization cannot be directly employed.

A common strategy that we will explore in depth in section 4.3 is to compute the finite-dimensional Lovász number $\vartheta^d(\mathcal{G}_{ex})$ of the graph. It is similar to eq. (4.10), but the maximization of $\sum_i p_i$ is now performed over the d-quantum behaviors. Then, one can use $\vartheta^d(\mathcal{G}_{ex})$ to witness the dimension of the physical system that was measured. The problems with this approach are, as we will see in more detail, twofold: first, $\vartheta^d(\mathcal{G}_{ex})$ does not admit an SDP formulation, precisely because this dimension restriction results in a rank constraint; second, as $\mathcal{P}_Q^d(\mathcal{G}_{ex})$ is not convex, $\vartheta^d(\mathcal{G}_{ex})$ is in fact a witness to the convex hull of d-dimension quantum behaviors, not to $\mathcal{P}_Q^d(\mathcal{G}_{ex})$ itself.

In the next sections, we will present our approach to this problem. In section 4.2, we show an efficient and reliable way to lower bound the dimension of a system by determining whether a behavior p belongs to $\mathcal{P}_Q^d(\mathcal{G}_{ex})$. Additionally, in section 4.3 we enhance the dimension witness method by providing an improved strategy to compute $\vartheta^d(\mathcal{G}_{ex})$.

4.2 Characterizing finite contextuality

In this section, we want to analyze a situation where one conducts a series of compatible measurements on an unknown pure quantum state $|\psi\rangle$. From the statistics obtained, one can describe the associated behavior p and from the data try to draw some information about $|\psi\rangle$, such as its dimension. This question can be mathematically translated as deciding whether $p \in \mathcal{P}_Q^d$, or equivalently whether this behavior could result from measurements on some quantum state of dimension d. If so, then d is a lower bound to the dimension of $|\psi\rangle$, and otherwise one knows it must have dimension at least $d+1$.

As easy as stating this problem might be, actually answering it is more laborious and inefficient than one would hope, since $\mathcal{P}_Q^d$ is not a convex set. In our work, we tackle this problem by performing two distinct tests: the first one checks if $p \in \mathcal{P}_Q^d$; the second one checks is $p \notin \mathcal{P}_Q^d$. In this approach, these two tasks are not equivalent! If one checks if $p \in \mathcal{P}_Q^d$, for instance, there are two possibilities: indeed, $p \in \mathcal{P}_Q^d$; or an inconclusive answer (and vice versa for checking if $p \notin \mathcal{P}_Q^d$). This happens because we use computational methods that rely on necessary, but not sufficient, conditions for $p \notin \mathcal{P}_Q^d$ or $p \in \mathcal{P}_Q^d$ to be true, respectively. What we do is check whether this necessary condition is satisfied, but an affirmative answer is not enough to assert anything.

Let us be more explicit. We claim that, given an exclusivity graph $\mathcal{G}_{ex} = (V, E)$ with n nodes, the corresponding behavior $p = (p_1, \ldots, p_n)$ is a d-dimension quantum behavior, i.e., $p \in \mathcal{P}_Q^d$ if and only if there exists an $(n+1) \times (n+1)$ Hermitian matrix X that satisfies

$$
\begin{align}
X_{0i} &= \sqrt{p_i}, \quad i = 1, \ldots, n \tag{4.15a} \\
X_{ii} &= 1, \quad i = 0, \ldots, n \tag{4.15b} \\
X_{ij} &= 0, \quad \text{if } (i,j) \in E \tag{4.15c} \\
X &\geq 0, \quad \text{rank}(X) \leq d. \tag{4.15d}
\end{align}
$$

Let us prove one way of the implication. Suppose $p \in \mathcal{P}_Q^d$, then the definition in eq. (4.14) implies there exists a state $|\psi\rangle$ and states $\{|\phi_i\rangle\}_{i=1}^n$ in $\mathbb{C}^d$ such that

$$\langle\phi_i|\phi_j\rangle = 0 \text{ if } (i,j) \in E \quad \text{and} \quad |\langle\psi|\phi_i\rangle|^2 = p_i, \tag{4.16}$$

by expressing the projectors in eq. (4.14) as $\Pi_i = |\phi_i\rangle\langle\phi_i|$. Then, if we make

$$|\tilde{\phi}_i\rangle = e^{-\gamma_i}|\phi_i\rangle, \quad \gamma_i = \arg\langle\psi|\phi_i\rangle, \tag{4.17}$$

and let

$$|\tilde{\phi}_0\rangle = |\psi\rangle, \tag{4.18}$$

we can define X as

$$X_{ij} = \langle\tilde{\phi}_i|\tilde{\phi}_j\rangle, \quad i,j = 0,1,\ldots,n. \tag{4.19}$$

X is known as the Gram matrix of $\{|\tilde{\phi}_i\rangle\}_{i=0}^n$ and clearly satisfies the conditions expressed in eqs. (4.15a – 4.15c). To show that conditions (4.15d) are also satisfies, we note that X can be expressed as

$$X = \sum_{i,j=0}^n X_{ij}|i\rangle\langle j| = \sum_{i,j}|i\rangle\langle\tilde{\phi}_i|\tilde{\phi}_j\rangle\langle j| = L^\dagger L, \tag{4.20}$$

where L is a $d \times (n+1)$ matrix. It follows, then, that X must be positive and $\text{rank}(X) \leq \text{rank}(L) \leq d$, so the final condition is satisfied.

To prove the other direction, we assume there exists a Hermitian X satisfying conditions (4.15a – 4.15d). One can write the unitary decomposition of X as

$$X = U\,\text{diag}(\lambda_0,\ldots,\lambda_{d-1},0,\ldots,0)\,U^\dagger \tag{4.21}$$

where U is some unitary matrix and $\text{diag}(\lambda_0,\ldots,\lambda_{d-1},0,\ldots,0)$ is the diagonal matrix with elements $(\lambda_0,\ldots,\lambda_{d-1},0,\ldots,0)$, for $\lambda_i \geq 0$, $i = 0,\ldots,d-1$. Now, let

$$|\phi_i\rangle = \sum_{k=0}^{d-1}\sqrt{\lambda_k}\,\langle k|U^\dagger|i\rangle\,|k\rangle, \; i = 1,\ldots,n \quad \text{and} \quad |\phi_0\rangle = |\psi\rangle. \tag{4.22}$$

One can directly verify that the conditions in eq. (4.14), or equivalently in eq. (4.16), are met. Indeed, if one lets the summation in eq. (4.22) range from $k = 0$ to $k = n$, with $\lambda_k = 0$ for $k > d-1$, one can write

$$\langle\phi_i|\phi_j\rangle = \left(\sum_{k=0}^n\sqrt{\lambda_k}\,\langle i|U|k\rangle\langle k|\right)\left(\sum_{l=0}^n\sqrt{\lambda_l}\,\langle l|U^\dagger|j\rangle|l\rangle\right) = \left(\sum_{k=0}^n\lambda_k\,\langle i|U|k\rangle\,\langle k|U^\dagger|j\rangle\right) = X_{ij}, \tag{4.23}$$

such that $|\psi\rangle$ and $|\phi_i\rangle$ obey eq. (4.16) and are thus a quantum realization of the behavior p.

Now we know that determining whether $p \in \mathcal{P}_Q^d$ is equivalent to finding X obeying the conditions stated in eqs. (4.15a – 4.15d). If there exists such Hermitian matrix, then the answer is affirmative, otherwise $p \notin \mathcal{P}_Q^d$. The complication resides in computing this feasibility problem, since the rank constraint makes it not suitable for SDPs. To undertake this task, we will face it on two fronts, namely an outer and an inner approximation of $\mathcal{P}_Q^d$.

4.2.1 Outer approximation

There is no way of directly formulating the conditions in eqs. (4.15a – 4.15d) as a semidefinite program, that would compute the feasibility of the task of finding X obeying the relevant restrictions. Fortunately, though, we do have a way of certifying that at least a necessary condition for the existence of such X, namely the SDP hierarchy method described in section 3.2.2.

What renders this problem not suitable for an SDP formulation is the rank constraint, as it makes the feasibility region of the problem not convex anymore. The complete SDP hierarchy from section 3.2.2 is then perfect to face the task: applying this method one can establish a series of programs that will check whether a necessary condition for $p \in \mathcal{P}_Q^d$ is present. These SDPs are ranked in a hierarchy, and one can compute its successive levels to certify stricter and stricter necessary conditions. If at any point the given

behavior p fails the test, we now for sure that $p \notin \mathcal{P}_Q^d$, since the necessary condition is not obeyed. If p passes the test one has to advance to the following level and perform yet another SDP.

Two things can happen in this process. In the first scenario, after implementing a few SDPs, p fails the test and one concludes that it is not a d-dimensional quantum behavior, so p must have dimension at least $d + 1$. In the second scenario, one implements a few SDPs but p passes all the tests. One runs out of computational power, as the SDPs become more costly up in the hierarchy, and is forced to stop. In this case, nothing can be said about the dimension of the system that generated the behavior p, since one might simply not have been able to go deep enough in the hierarchy to find a test at which p fails. We recall, however, that the SDP hierarchy in section 3.2.2 is complete, which in this specific scenario means that if $p \notin \mathcal{P}_Q^d$ then p will necessarily fail the test at some level, though one may not be able to compute it because of technical limitations.

Thus, this method can be seen as an outer approximation of the set $\mathcal{P}_Q^d$. After translating the task into a separability problem, each level of the hierarchy provides a set of witnesses that approximate the feasibility region. Much like when dealing with other witnesses, one can only draw any conclusion from it if the necessary condition is not fulfilled.

Let us now obtain the explicit formulation of the SDP hierarchy corresponding to the conditions in eqs. (4.15a – 4.15d). The original feasibility task is

$$
\begin{aligned}
\textbf{given} \quad & \{p_i\}_{i=1}^n, \mathcal{G}_{ex} = (V, E) \\
\textbf{find} \quad & X \text{ Hermitian} \\
\textbf{subject to} \quad & X_{ij} = \mu_{ij} \\
& \mathrm{Tr}[X] = n + 1 \\
& X \geq 0 \\
& \mathrm{rank}(X) \leq d \, .
\end{aligned} \tag{4.24}
$$

The conditions (4.15a – 4.15c) are condensed in the first constraint of the problem, with $\mu_{0j} = \sqrt{p_j}$, $\mu_{ii} = 1$ and $\mu_{ij} = 0$ if $(i, j) \in E$. The trace condition on X is redundant, but it we make it explicit for clarity since it will be relevant later on.

Implementing the method in section 3.2.2 yields an SDP hierarchy whose N-th level reads

$$
\begin{aligned}
\textbf{given} \quad & \{p_i\}, \mathcal{G}_{ex} \\
\textbf{find} \quad & \Phi_{A \ldots Z} \text{ Hermitian} \\
\textbf{subject to} \quad & \mathrm{Tr}[\Phi_{A \ldots Z}] = (n+1)^N & \text{(4.25a)} \\
& \Phi_{A \ldots Z} \geq 0 & \text{(4.25b)} \\
& P_N \Phi_{A \ldots Z} P_N = \Phi_{A \ldots Z} & \text{(4.25c)} \\
& \mathrm{Tr}_A[(|i\rangle\langle j| \otimes \mathbb{1}_d \otimes \mathbb{1}_{B \ldots Z})\Phi_{A \ldots Z}] = \frac{\mu_{ij}}{n+1} \mathrm{Tr}_A[\Phi_{A \ldots Z}] \, . & \text{(4.25d)}
\end{aligned}
$$

Let us dissect this SDP. We are looking for a Hermitian $d^N(n+1)^N \times d^N(n+1)^N$ matrix $\Phi_{A \ldots Z}$, an N-copy symmetric extension of a purification of X with an auxiliary system of dimension d. The trace condition in eq. (4.25a) reflects the fact that X itself is not normalized, so any purification of X has trace $(n+1)$ and its N-copy extension must have trace $(n+1)^N$. The remaining conditions result from the direct application of the necessary constraints, as discussed in section 3.2.2. Conditions (4.25c) and (4.25c) reflect positivity and symmetry requirements. Condition (4.25d) expresses the original constraint that $X_{ij} = \mu_{ij}$, but now translated as a function of $\Phi_{A \ldots Z}$ instead of X.

By performing this computation for different levels of the hierarchy, i.e., increasing values of N, one checks for the validity of necessary conditions for a behavior p to admit a d-dimensional quantum realization. If at some point this condition is not satisfied, then $p \notin \mathcal{P}_Q^d$. If the violation of this condition is not verified one cannot conclude anything, but not all is lost: one can still perform an inner approximation of the feasibility region of the original problem.

4.2.2 Inner approximation

Let us recall the original feasibility task we want to perform, stated in eqs. (4.15a – 4.15d), the necessary and sufficient condition for a behavior p to admit a d-dimension quantum realization. We state it once again below for clarity, but now explicitly as an optimization problem:

$$
\begin{aligned}
\textbf{given} \quad & \{p_i\}_{i=1}^n, \mathcal{G}_{ex} = (V, E) \\
\textbf{find} \quad & X \text{ Hermitian} \\
\textbf{subject to} \quad & X_{0i} = \sqrt{p_i}, \quad i = 1, \ldots, n \\
& X_{ii} = 1, \quad i = 0, \ldots, n \\
& X_{ij} = 0, \quad \text{if } (i,j) \in E \\
& X \geq 0, \quad \text{rank}(X) \leq d \,.
\end{aligned}
\tag{4.26}
$$

Recalling the discussions in section 3.2.3, rank-constrained optimization problems such as the above can be processed with a see-saw algorithm. Since the problem we want to solve is not originally an SDP, any alternative method to solving it will have to feature some downsides and one must pay a price for computing it. However, when using either an SDP hierarchy, as explained in the last section, or a see-saw method the disadvantages are luckily complementary.

The outer approximation method supplies necessary conditions for $p \in \mathcal{P}_Q^d$, so all it can do is attest that $p \notin \mathcal{P}_Q^d$ whenever it fails. Likewise, see-saw methods check a necessary condition for $p \notin \mathcal{P}_Q^d$, so the only conclusion one can draw from it is that $p \in \mathcal{P}_Q^d$. For this reason, the method we will expose can be seen as an inner approximation of $\mathcal{P}_Q^d$, since it can attest that a behavior indeed admits a d-dimensional quantum realization but remains inconclusive otherwise.

Since the particular see-saw method we will use here has already been laid out in section 3.2.3, we can simply apply it to eq. (4.26) by realizing that it has basically the same form as the prototype we introduced in eq. (3.34). As a consequence, the the behavior p admits a d-dimensional quantum realization if and only if the solution to the problem stated in eq. (3.35) equals zero, which we re-state here

$$
\begin{aligned}
\textbf{minimize}_{\{X,P\}} \quad & \text{Tr}[XP] \\
\textbf{subject to} \quad & X \geq 0, \quad X_{ij} = \mu_{ij} \\
& P \geq 0, \quad P^2 = P \\
& \text{rank}(P) = n - d + 1 \,,
\end{aligned}
\tag{4.27}
$$

A subset of the solutions to this equivalent optimization problem can be achieved with a see-saw method that iteratively solves the SDPs in eqs. (3.37) and (3.38). If at some point the iterations make the objective function of the problem converge to zero, we have found a solution to the task above, and by construction have found a d-dimensional quantum realization for p. If there is no convergence or if the objective function converges to a value other than zero, nothing can be said. Put another way, the solution *not* converging to zero is a necessary (but not sufficient) condition for $p \notin \mathcal{P}_Q^d$, and if indeed one finds X, P obeying the relevant restrictions such that $\text{Tr}[XP] = 0$ it means that $p \in \mathcal{P}_Q^d$.

With both the outer and the inner approximation methods, we have a reliable strategy to determine whether a behavior could be the result of measurements on a d-dimension quantum system. It is built upon equivalent optimization tasks that can be put into SDP form, and thus profit from all the advantages of this well-established field. Let us provide an example where the method we illustrated can be applied.

4.2.3 Our method in action

Consider the so-called G_{KK} graph, shown in fig. 4.3. It is an exclusivity graph introduced in [148] to describe a scenario with nine projective measurements yielding a non-contextuality inequality that is violated by almost all qutrit quantum states (the only exception is the maximally mixed state). It has independence number $\alpha(G_{KK}) = 3$ and the resulting non-contextuality inequality

$$
\sum_{i=1}^9 p_i \leq \alpha(G_{KK})
\tag{4.28}
$$

is saturated, for instance, if $p_1 = p_6 = p_7 = 1$. This upper bound can be violated by contextual behaviors up to the Lovász number of this graph, $\vartheta(G_{KK}) = 4.4704$. This gap between $\alpha(G_{KK})$ and $\vartheta(G_{KK})$ makes it possible to determine whether a given behavior p can result from a non-contextual scenario, i.e., $p \in \mathcal{P}_{NC}(G_{KK})$, or not. If there was no such gap and $\alpha(G_{KK}) = \vartheta(G_{KK})$, one could not attest that p is a contextual behavior, since the bound above would never be violated.

Consider, now, the following behaviors
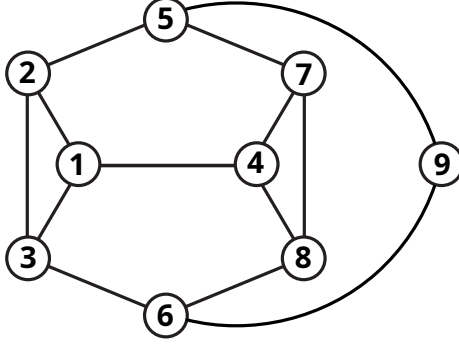
Figure 4.3: The G_{KK} exclusivity graph, where each node is associated to an event e_i, represented by a projective measurement Π_i. Vertices associated to exclusive events e_i, e_j (or equivalently, if $\Pi_i \Pi_j = 0$) share an edge.

$$p_\alpha = \left(\frac{1}{3}, \frac{1}{3}, \frac{1}{3}, \frac{1}{3}, \frac{1}{3}, \frac{1}{3}, \frac{1}{3}, \frac{1}{3}, \frac{1}{3} \right), \tag{4.29a}$$

$$p_\beta = \left(\frac{1}{2}, \frac{1}{4}, \frac{1}{4}, \frac{1}{2}, 0, 0, \frac{1}{4}, \frac{1}{4}, 1 \right), \tag{4.29b}$$

$$p_\gamma = \left(\frac{5}{12}, \frac{7}{24}, \frac{7}{24}, \frac{5}{12}, \frac{1}{6}, \frac{1}{6}, \frac{7}{24}, \frac{7}{24}, \frac{2}{3} \right). \tag{4.29c}$$

One can easily verify that $p_\gamma = (p_\alpha + p_\beta)/2$. With the inner approximation method one can show that both p_α and p_β admit a 3-dimensional quantum realization, i.e., that $p_\alpha, p_\beta \in \mathcal{P}_Q^3(G_{KK})$. Nevertheless, even though p_γ is a convex combination of two behaviors in $\mathcal{P}_Q^3(G_{KK})$, one can use the outer approximation method to show that $p_\gamma \notin \mathcal{P}_Q^3(G_{KK})$, since p_γ already fails the first level of the SDP hierarchy.

These easily obtained results, more than just illustrate the power of our method, also emphasize a crucial difference between quantum behaviors with and without dimension restrictions: for any exclusivity graph $\mathcal{P}_Q(\mathcal{G}_{ex})$ is convex, but its dimension restricted counterpart $\mathcal{P}_Q^d(\mathcal{G}_{ex})$ may not be. Here, we have shown that $\mathcal{P}_Q^3(G_{KK})$ is not convex, but when expanding our investigation to $d = 4$ we found no indication that $\mathcal{P}_Q^4(G_{KK})$ is not convex: applying the inner approximation method, we observed that $p_c \in \mathcal{P}_Q^4(G_{KK})$ (p_a and p_b naturally also belong to $\mathcal{P}_Q^4(G_{KK})$, since they belong to $\mathcal{P}_Q^3(G_{KK})$).

Motivated by how easy it is to check whether a behavior admits a d-dimension quantum realization, one can start wondering what singles out peculiar behaviors such as p_γ. Another curious feature we can attest in G_{KK} with the outer approximation method is that, even though the quantum bound $\vartheta(G_{KK})$ can be achieved by states with dimension at least 4, there are still many behaviors that do not admit a 4-dimension quantum realization, such as p_δ

$$p_\delta = \left(\frac{1}{3}, \frac{1}{3}, \frac{1}{3}, 0, \frac{2}{3}, \frac{1}{3}, 0, 0, \frac{1}{3} \right). \tag{4.30}$$

We see that unique quantum aspects can arise from the non-convexity of $\mathcal{P}_Q^d$, but one can only study them if contextuality is properly characterized, a task that until now lacked proper methodology precisely because of the non-convexity of the set of d-dimension quantum behaviors.

As already discussed, this analysis could not have been conducted by simply investigating contextuality witnesses and violations of non-contextuality inequalities. This does not mean that evaluating these inequalities is useless. Indeed, in the following section we will discuss how to calculate the maximum violation of a non-contextuality inequality given a dimension restriction.

4.3   Dimension witnesses

When dealing with scenarios where one is not interested in the dimension of a system, the standard method of characterizing the sets of non-contextual and contextual quantum behaviors is evaluating linear

inequalities such as the ones in eqs. (4.10) and (4.13), where the sum $\sum_i p_i$ is bounded from above or below by the independence number or the Lovász number.

If one wants to consider a more general scenario, where for instance the sum of probabilities attributes different weights to different p_i, one can resort to the weighted Lovász number $\vartheta(w, \mathcal{G}_{ex})$, defined for an exclusivity graph $\mathcal{G}_{ex}$ as the solution of the following semidefinite problem

$$
\begin{aligned}
\textbf{given} \quad & \{w_i\}_{i=1}^n, \mathcal{G}_{ex} = (V, E) \\
\textbf{maximize} \quad & \sum_{i=1}^n w_i |X_{0i}|^2 \\
\textbf{subject to} \quad & X_{ii} = 1, \quad i = 0, \dots, n \\
& X_{ij} = 0, \quad \text{if } (i,j) \in E \\
& X \geq 0 \,,
\end{aligned}
\tag{4.31}
$$

where the variable X is a $(n+1) \times (n+1)$ Hermitian matrix. Notice how similar this task is to the one of defining whether a behavior p is in $\mathcal{P}_Q$, but also mind the differences. There, p is given and one wants to find a quantum realization that explains the statistics associated to an exclusivity structure. Here, we are not interested in any specific behavior, we simply want to know what is the maximum value that any p can achieve in some function of $\{p_i\}$, given by $\sum_i w_i p_i$. To reflect the goal of this task, $\{p_i\}$ are now variables expressed as $|X_{0i}|^2$. The weights $\{w_i\}$ are chosen to reflect, for instance, the expectation value of some observable. See appendix appendix F for a detailed description of this approach (implemented in an example to evaluate the maximum violation of the CHSH inequality).

Because it can be formulated as an SDP, the evaluation of $\vartheta(w, \mathcal{G}_{ex})$ is quite straightforward and efficient. However, this is not true anymore when one additionally considers dimension restrictions. One may want to compute the maximum value that $\sum_i w_i p_i$ can achieve with d-dimensional quantum behaviors, so that this value can be used to witness the dimension of the quantum system that generated some given behavior. To do that, one typically resorts to the so-called d-dimension weighted Lovász number $\vartheta^d(w, \mathcal{G}_{ex})$, defined as

$$
\begin{aligned}
\textbf{given} \quad & \{w_i\}_{i=1}^n, \mathcal{G}_{ex} = (V, E) \\
\textbf{maximize} \quad & \sum_{i=1}^n w_i |X_{0i}|^2 \\
\textbf{subject to} \quad & X_{ii} = 1, \quad i = 0, \dots, n \\
& X_{ij} = 0, \quad \text{if } (i,j) \in E \\
& X \geq 0, \quad \text{rank}(X) \leq d \,,
\end{aligned}
\tag{4.32}
$$

which is of course simply the weighted Lovász number with the familiar rank restriction.

Recall the example we briefly exposed in the last section, where the graph G_{KK} was analyzed. We showed that even though the quantum bound $\vartheta(G_{KK})$ is already achieved by states of dimension 4, some behaviors do not admit a 4-dimension quantum realization. In the lingo of Lovász numbers, we can re-state our findings in a way that makes the disadvantages of the inequality method clear: even though $\vartheta(G_{KK}) = \vartheta^4(G_{KK})$, $\mathcal{P}_Q \neq \mathcal{P}_Q^4$. This goes to show how sub-optimal it is to characterize dimension-restricted sets of quantum behaviors with linear inequalities, $\vartheta(G_{KK})$ is enough to delimit set $\mathcal{P}_Q$, but $\vartheta^d(G_{KK})$ is not efficient in witnessing $\mathcal{P}_Q^d$ as there are behaviors, such as p_d, that cannot be detected by it.

To summarize, there are two main problems with using $\vartheta^d(\mathcal{G}_{ex})$ to witness the dimension of a quantum system. First, because the set of d-dimension quantum behaviors is not convex, linear inequalities cannot provide necessary and sufficient conditions to determine whether $p \in \mathcal{P}_Q^d$, and $\vartheta^d(\mathcal{G}_{ex})$ is in fact characterizing the *convex hull* of the behaviors in $\mathcal{P}_Q^d$.

Even though our approach can more thoroughly determine whether a behavior admits a d-dimension quantum realization, there are reasons to nevertheless adopt an inequality-based method. In particular, they are useful in lab, where one can experimentally determine expectation values and observe violations of quantum bounds. If that is the case, we bring up the second problem with employing $\vartheta^d(\mathcal{G}_{ex})$, namely that it cannot be formulated as an SDP.

To face this issue and evaluate the d-dimension weighted Lovász number, it was proposed in [102] to compute the following optimization, whose solution we denote by $\tilde{\vartheta}^d(\mathcal{G}_{ex}, w)$

$$
\begin{aligned}
\textbf{given} \quad & \{w_i\}_{i=1}^n, \mathcal{G}_{ex} = (V, E) \\
\textbf{maximize} \quad & \sum_{i=1}^n w_i X_{ii} \\
\textbf{subject to} \quad & X_{ii} = X_{0i}, \quad i = 0, \ldots, n \\
& X_{ij} = 0, \quad \text{if } (i, j) \in E \\
& X_{00} = 1, \quad X \geq 0, \quad \text{rank}(X) \leq d \,.
\end{aligned}
\tag{4.33}
$$

One can check that $\tilde{\vartheta}^d(\mathcal{G}_{ex}, w)$ is an upper bound for $\vartheta^d(\mathcal{G}_{ex}, w)$ by verifying that any feasible point of the task defining $\vartheta^d(\mathcal{G}_{ex}, w)$ is also in the feasibility region of $\tilde{\vartheta}^d(\mathcal{G}_{ex}, w)$, though it might not be the optimal solution. From there, the authors obtain a see-saw algorithm that, similar to the ones we have employed, that provides a lower bound for $\tilde{\vartheta}^d(\mathcal{G}_{ex}, w)$. Moreover, it is conjectured in the text in [102] that in fact $\tilde{\vartheta}^d(\mathcal{G}_{ex}, w) = \vartheta^d(\mathcal{G}_{ex}, w)$ whenever $\mathcal{P}_Q^d$ is not an empty set. If that is indeed the case, then applying a see-saw algorithm to evaluate the problem in eq. (4.33) actually provides a lower bound to $\vartheta^d(\mathcal{G}_{ex}, w)$ and can be used to attest that a given behavior indeed admits a d-dimension quantum realization.

Alternatively, one can use the same approach we explored before to tackle the task of evaluating $\vartheta^d(\mathcal{G}_{ex}, w)$. The outer approximation method provides an upper bound to $\vartheta^d(\mathcal{G}_{ex}, w)$, where each level of the hierarchy makes the gap between what is found and the actual solution smaller. The inner approximation method provides a lower bound to $\vartheta^d(\mathcal{G}_{ex}, w)$, since its solution corresponds to a point in the feasibility region of the maximization problem in eq. (4.32) which may still not be optimal. If the results obtained by these two complementary approaches coincide it means one has in fact found the actual value of $\vartheta^d(\mathcal{G}_{ex}, w)$, since it must be both an upper and a lower bound to the d-dimension weighted Lovász number.

One can in fact use this strategy to disprove the claim that $\tilde{\vartheta}^d(\mathcal{G}_{ex}, w) = \vartheta^d(\mathcal{G}_{ex}, w)$, by finding a counter example to it. Consider once again the G_{KK} graph and the specific scenario of $d = 3$. With our approach, one can assert that $\vartheta^3(G_{KK}) = 3.333$ by computing an upper and a lower bound and verifying that they coincide, up to numerical precision [2]. Now, when considering the task of determining $\tilde{\vartheta}^3(G_{KK})$, notice that any feasible point X obeys

$$
\sum_i X_{ii} \leq \vartheta^3(G_{KK}),
\tag{4.34}
$$

since $\vartheta^d(G_{KK})$ is the optimal value of a task of maximizing $\sum_i X_{ii}$.

If, on top of that, X is such that $\sum_i X_{ii}$ is strictly greater than $\vartheta^3(G_{KK})$, it implies that

$$
\vartheta^3(G_{KK}) < \sum_i X_{ii} \leq \tilde{\vartheta}^3(G_{KK}).
\tag{4.35}
$$

We have found an example of X in the feasibility region of problem eq. (4.33) such that $\sum_i X_{ii} = 3.3380 > \vartheta^3(G_{KK})$. With that, we conclude that, whatever the value of $\tilde{\vartheta}^3(G_{KK})$, it is strictly larger than $\vartheta^3(G_{KK})$ and $\tilde{\vartheta}^3(G_{KK}) \neq \vartheta^3(G_{KK})$.

4.4 Concluding remarks

We have formulated a strategy that allows us to check whether a behavior admits a d-dimension quantum realization, by translating a task that is not a convex optimization problem into a series of SDPs. With the outer approximation method one can certify that $p \notin \mathcal{P}_Q^d$, while the inner approximation method certifies that $p \in \mathcal{P}_Q^d$, two tasks that are not equivalent.

With these tools one can characterize the set of quantum behaviors, an enterprise of both foundational and practical relevance. On one hand, if one hopes to further investigate the differences between quantum and classical regimes, improving our understanding of contextuality is crucial, a task that can only benefit from better tools to probe the structure of quantum behaviors. On the other hand, characterizing such sets allows us to obtain a lower bound to the dimension of quantum states in the lab, another goal of central importance in information processing since many quantum protocols rely on it.

Furthermore, one can employ our methods to evaluate dimension-restricted contextuality inequalities, which can in turn be used to construct dimension witnesses. With more reliable methods of evaluating

---

[2] We point out that $\vartheta^d(\mathcal{G}_{ex})$ is simply a particular case of $\vartheta^d(\mathcal{G}_{ex}, w)$, with $w = (1, \ldots, 1)$.

the dimension restricted weighted Lovász number, one can additionally profit from the close connection between $\vartheta(G)$ and communication scenarios, as explored in [149], which may lead to improved efficiency and new applications in quantum information.

Chapter 5

Certifying the number of incompatible measurements in a steering scenario

Since its very dawn, quantum mechanics has built the tradition of challenging our physical intuition, this particular set of notions we have been developing since the day we are born. From quantizing energy [4] to questioning causality itself [150] (with an assortment of other major breakthroughs in-between), quantum theory puts in check the assumptions we hold most dear and fundamental about our world. It is, thus, no surprise that advances in the field of foundations are customarily met with great resistance. Unfortunately for those who keep a more conservative approach to physics, there is no denying that such odd features are genuine and ubiquitous throughout quantum mechanics. Or is there?

Indeed, many outstanding physicists have struggled to disprove what they believed to be sheer nonsense about quantum mechanics. Most prominently, Einstein, Podolsky and Rosen proposed a simple thought experiment that, according to them, implied that the theory could not be considered complete [151], an analysis that would be known as the EPR-paradox. In summary, they argued that the probabilistic nature of quantum mechanics cannot be any different from that of a classical scenario, and all uncertainty arising from it should be explained by hidden variables to which we have no access.

How could one be sure which was the case? Whether quantum mechanics was just like classical physics with some extra uncertainty thrown in the mix was a question that remained unanswered for the following decades, until Bell struck the final blow in [152]. By showing that some correlations simply cannot be reproduced by classical physics, the violation of so-called Bell inequalities forces physicists to let go of at least one core classical assumption: locality, reality or free-will.

What sets Bell approach apart from quantum theory as it was developed so far is that one does not need to "trust" anything in the process, not the devices, not the parties involved, only perhaps mathematics itself. This asset is crucial in the task of convincing skeptics of the genuinely odd features of quantum mechanics. In other words, the strength of Bell's theorem lies of the fact that it is theory-independent, meaning it does not take quantum mechanics (or any physical theory) as a starting point. By making no assumptions about how probabilities are obtained, Bell scenarios can be seen as black-box experiments, device-independent approaches where one does not need to trust the equipment or the parties involved[1].

A neat consequence of this formulation is that Bell's theorem can be put to test in a lab. This is no frivolous asset, first of all because testability is a cornerstone of physics as a science, and second because Bell non-locality is closely related to the notion of entanglement [85], which plays a central role in foundations of quantum mechanics. The experimental violation of a Bell inequality can be used to certify entanglement [154], a crucial resource in many informational tasks [155].

Notice that entanglement can alternatively be detected with straight-forward techniques such as state tomography [154], but from a foundational point of view there is a trade-off to be observed. Full tomography can theoretically be used to characterize entanglement in any state (though it is not easily applied to large systems [156]), but it is a device-dependent approach. The violation of a given Bell inequality does not detect every entangled state [157], but it results in a robust, theory-independent claim.

---

[1]This is of course easier said than done and there is a deep debate around it, but experimentalists have been making steady progress towards loop-hole free implementations [153].

Whether or not one is required to trust an apparatus, a colleague or even a theory is often a matter of central relevance in an enterprise. Take, for instance, the task of distributing a cryptography key while keeping it a secret from eavesdroppers: the less trust required, the safer the procedure. For these situations, protocols such as the E91 protocol [130] are ideal: one does not have to trust the other parties, since the secrecy of the key relies on observing the violation of a bipartite Bell inequality. The very security of the protocol lies on a fundamental distrust of the process.

But what about situations where perhaps partial distrust can be lifted? If one party (traditionally named Alice) corresponds to a bank user with an everyday computer while the another is the bank itself (here representing Bob), it may be reasonable to distrust only Alice's device while making reasonable assumptions about Bob's. Such scenarios are described by one-way-device-independent approaches and can be exploited with quantum steering.

Steering is a quantum phenomenon whose first description by Schrödinger dates from 1935 as a formalization of the EPR argument [158, 159], but has seen a modern revival after being reformulated in the lingo of quantum information [107] by Wiseman, Jones and Doherty. The trio originally described a scenario where Alice prepares a bipartite state and sends one part to Bob. Alice's goal is to convince Bob that she can "steer" his system by simply performing measurements on her side and communicating her results to him. Bob, in turn, does not trust Alice and will try to come up with classical models that explain the statistics he observes after performing measurements on his side of the shared state. In few words, whenever his results cannot be explained by plain classical ignorance, Bob must admit Alice's influence on his system. Much like Bell non-locality, steering can be certified through the violation of so-called steering inequalities [86].

As we will see in the following sections, steering manifests itself in asymmetric scenarios where Alice and Bob cannot be inter-exchanged. Bob's role is intrinsically different from that of Alice, since she is the one trying to convince her colleague, and thus cannot be trusted. Because of the way this scenario is designed, steering can be formulated in one-way-device-independent approaches. As a result, it can also be exploited for many practical applications, such as quantum key distribution [160], randomness certification [161] or secret sharing [162], where such asymmetry is an advantage.

Beyond its applications, steering has a considerable role in foundations of quantum mechanics. Though a completely distinct and independent phenomenon, it is closely related to Bell non-locality, entanglement and compatibility of measurements [86]. In fact, steering can only be observed if the shared state is entangled and the measurements performed by Alice are incompatible [163]. Such requirement makes the detection of steering a strategy to certify that these measurements are incompatible in a one-way-device-independent approach, a feat that is relevant on its own since incompatibility is central in many protocols [85].

In this work, we go beyond witnessing incompatibility of measurements through the violation of a steering inequality. Indeed, we provide a strategy to actually certify the *number* of incompatible measurements to which Alice has access. In a bipartite steering scenario, we develop a series of tests that Bob can perform with the information he has on his side of the experiment and conclude that his colleague must have performed at least k incompatible measurements on her part of the shared quantum state. Our method also displays the main advantage of admitting and SDP formulation.

This chapter is outlined as follows. In section section 5.1 we lay some relevant preliminary concepts, such as measurement compatibility, measurement simulability and steering itself, while also setting the notation we will use throughout the chapter. Then, in section 5.2 we introduce our method for certifying the number of incompatible measurements Alice can perform. Finally, in section 5.3 we apply our method to a paradigmatic example and discuss its qualities and limitations, as well as prospects for future research.

5.1 Preliminary concepts

5.1.1 Joint measurability and compatibility

The fact that some measurements are incompatible is yet another feature that sets quantum and classical physics apart. Two tasks are understood to be incompatible if they are mutually exclusive, i.e., they cannot be performed simultaneously on a single device. This does not seem to be a particularly relevant discussion in classical scenarios, as all classical measurements are compatible [164], but it is an unalienable part of quantum measurements. An instance of this phenomenon is given by the emblematic example of spin measurements in two perpendicular directions, represented for instance by the Pauli matrices σ_x and σ_z, notoriously incompatible. For projective measurements, compatibility is reduced to

the commutativity of observables, but it is known that for POVMs in general this equivalence does not hold, as there are non-commuting measurements that are nevertheless jointly measurable [165, 166].

Though it was mostly seen as an obstacle and a limitation, incompatibility of quantum measurements was recast as an advantage and a resource in quantum informational tasks [85, 167, 168, 169], being crucial to different protocols. It is known, for instance, that there is neither non-locality nor steering without incompatible measurements [85, 163], and that it is closely related to contextuality [87]. There is no denying, thus, that incompatibility of measurement plays a major role in both foundation and applications of quantum mechanics.

Let us formally define joint measurability[2]. Let the measurement assemblage $\mathcal{M} = \{M_{a|x}\}_{a,x}$ be a collection of POVM elements, with $x = 1, \ldots, N$ labeling the measurements and $a = 1, \ldots, l$ labeling their outcomes. This set of measurements is said to be *compatible* if it admits a *joint measurement*, i.e., there exist a POVM $\{G_\lambda\}_\lambda$ and probability distribution p such that

$$M_{a|x} = \sum_\lambda p(a|x,\lambda)G_\lambda, \tag{5.1}$$

where $\sum_\lambda G_\lambda = \mathbb{1}$, $G_\lambda \geq 0$ $\forall\lambda$ and $\sum_a p(a|x,\lambda) = 1$, $p(a|x,\lambda) \geq 0$ $\forall a, x, \lambda$. Physically, it means one can measure G_λ and obtain the same statistics of $M_{a|x}$ after some post-processing. Equivalently, joint measurability can be defined in terms of the existence of a N output measurement with effects $\{H_{a_1,\ldots,a_N}\}_{a_1,\ldots,a_N}$ obeying

$$M_{a|x} = H_a^{[x]} := \sum_{a_i,\; i \neq x} H_{a_1,\ldots,a_{x-1},a,a_{x+1},\ldots,a_N}. \tag{5.2}$$

In this formulation, measurements can be recovered by the marginalization over all but one output of H (in this case, the x-th output, to which we assign the outcome a). $H_a^{[x]}$ is often referred to as the x-th marginal of H. For instance, considering two observables A and B with l possible outcomes each, compatibility imposes the condition that

$$A_a = \sum_i H_{ia}, \quad a = 1, \ldots, l \tag{5.3}$$

$$B_b = \sum_j H_{bj}, \quad b = 1, \ldots, l. \tag{5.4}$$

A way to define compatibility is by considering measurements as black boxes with one input and one output [164], on an operational level. The input of such box is a physical system and the classical output is a label that designates different outcomes. Two observables A and B can thus be represented by two single-input, single-output boxes, and they are said to be jointly measurable if they can be equivalently described by a joint device C, defined as a black box with a single input and two outputs that reproduce the probability distributions yielded by the outcomes of A and B.
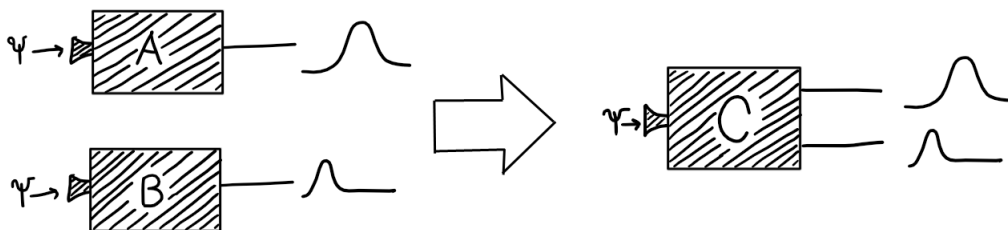
Figure 5.1: A black-box can describe a physical one-input-one-output device. Taking states as inputs and producing classical labels as outcomes, these black-boxes can be associated to measurements. If two devices A and B implement compatible measurements, then there exists a device C with a single input and two outputs that reproduces the statistics yielded by A and B. Figure adapted from [164].

This black-box formulation presents some interesting insight into the problem. With it one can, for instance, re-interpret impossibility statements such as no-cloning and no-information-without-disturbance

---

[2]In this text we use the terms compatibility and joint measurability interexchangely, though some subtleties might differ them [118]

as statements about incompatibility of devices [164, 170, 171]. It also provides an interpretation to what can be a good measure of incompatibility, as follows.

Consider, now, a black-box that yields the same probability distributions regardless of the state input. Physically, this could correspond, for instance, to a coin toss, and this trivial device would not actually need any input to correctly describe the corresponding observable: this box would have no input and a single outcome. It is easy to see, then, that a trivial box is compatible with any other box A: there is always a joint device, with one input (namely, that of box A) and two outputs (one from A and another from the trivial box), that reproduces their statistics. The fact that such a pair of observables is always compatible suggests that one can measure how incompatible two arbitrary measurements A and B are by evaluating their distance to a trivial box: if A and B are not compatible, how much more similar to a trivial box should they be in order for a joint measurement to be possible?

This measure is captured by the notion of robustness. Consider the depolarizing map Λ_η acting on some d-dimensional operator A as

$$\Lambda_\eta(A) = \eta A + (1 - \eta) \operatorname{Tr}[A]\frac{\mathbb{1}}{d}, \tag{5.5}$$

where $\eta \in [0, 1]$. Physically, this map models white noise in a measurement in terms of η. If $\eta = 1$ the measurement of A is noise-free, but the lower the value of η the closer the resulting measurement is to a trivial one, all the way up to $\eta = 0$ when one gets uniformly random outcomes. η captures how far A is from a trivial measurement and thus from being compatible with any other measurement. This suggests the usual definition of *incompatibility robustness* of an ensemble of measurements $\mathcal{M} = \{M_{a|x}\}_{a,x}$ [118]

$$\eta^* = \max\{\eta|\{\Lambda_\eta(M_{a|x})\} \in \mathrm{COMP}\}, \tag{5.6}$$

where COMP is the set of ensembles that admit a joint measurement. In words, η^* is the minimum amount of noise one must allow in the measurements in order for them to be compatible. Any value of η below this threshold already yields measurements that are noisy enough to be compatible, and the lower η^* the more incompatible the original ensemble.

Notice that the convex mixture of compatible measurements also yields compatible measurements, as this would correspond to a simple post-processing. This means the set COMP is convex and SDP formulations of the task of determining whether an assemblage is compatible can be established. Indeed, the corresponding program that assesses the compatibility of two measurements A and B with l possible outcomes, for instance, reads

$$
\begin{aligned}
\textbf{given} \quad & \{A_a\}_{a=1,\dots,l}, \{B_b\}_{b=1,\dots,l} \\
\textbf{maximize} \quad & \eta \\
\textbf{subject to} \quad & \Lambda_\eta(A_a) = \sum_i H_{ia}, \quad a = 1, \dots, l \\
& \Lambda_\eta(B_b) = \sum_j H_{bj}, \quad b = 1, \dots, l \\
& H_{ij} \geq 0, \quad \sum_{ij} H_{ij} = \mathbb{1}, \quad \eta \leq 1.
\end{aligned}
\tag{5.7}
$$

Here, H is a two-output joint observable for $\Lambda_\eta(A)$ and $\Lambda_\eta(B)$, and one can recover the original observables by taking the marginals of H over each output. Intuitively, one is asking how much noise must be added to A and B for a joint measurement H to exist.

k-compatibility of a set of measurements

We can now move on to define the more general concept of k-compatibility of an assemblage. If we were to try to implement a joint measurement of two incompatible observables A and B on a quantum state ρ the task would be futile, as no single device can, on a single run, implement both measurements at once. However, if we had access to *two* copies of ρ, then such device could promptly be idealized: it would simply perform measurement A on one copy and B on the other. What about a scenario with three incompatible measurements, A, B and C? Clearly, three copies of ρ would suffice to implement all of them at once even if such a task is impossible with a single copy, but what can one do with two copies of ρ?

This is the question that was explored in [172], where the authors introduce the concept of k-compatibility. Formally, a set of POVMs $\mathcal{M} = \{M_{a|x}\}_{a,x}$ is said to be k-compatible if it admits a k-copy joint measurement, that is, if there exists an observable H acting on k copies of the system such that the statistics of each $M_{a|x}$ can be recovered by marginalizing over H. Mathematically, it means there exists a POVM H such that

$$\text{Tr}[\rho M_{a|x}] = \text{Tr}[\rho^{\otimes k} H_a^{[x]}], \quad \forall \rho, a, x. \tag{5.8}$$

Notice that when a single copy of ρ is considered and $k = 1$, the usual concept of joint measurability is recovered. This way, a weaker notion of compatibility is established: perhaps one cannot devise a joint measurement for an assemblage, but if one has access to more copies, then other possibilities arise.

By looking at eq. (5.8) one might be lead to conclude that there is no SDP formulation for the task of determining whether an assemblage is k-compatible. Unlike for usual compatibility, this definition would imply on non-linear constraints, as both ρ and H would be variables. Luckily for us, the authors in [172] have already tackled this issue and concluded that eq. (5.8) can be equivalently stated in a more convenient way.

Let us first define the symmetrizer channel S_k acting on an operator A in $\mathcal{L}(\mathcal{H}^{\otimes k})$ as

$$S_k(A) = \frac{1}{k!} \sum_p \sigma(p) A \sigma(p)^*, \tag{5.9}$$

where $\sigma(p)$ are the possible permutation operators. Basically, this channel permutes the subspaces of A in every possible way and adds them all up. Now, the symmetric product of two operators A_1 in $\mathcal{L}(\mathcal{H}^{\otimes k_1})$ and A_2 in $\mathcal{L}(\mathcal{H}^{\otimes k_2})$ is

$$A_1 \odot A_2 = S_{k_1+k_2}(A_1 \otimes A_2). \tag{5.10}$$

Let us now introduce the main result of [172]: an assemblage of observables $\{M_{a|x}\}_{a,x}$ is k-compatible if and only if there exists an observable G such that

$$G_a^{[x]} = \mathbb{1}^{\otimes(k-1)} \odot M_{a|x}, \quad \forall a, x. \tag{5.11}$$

This result allows one to think of k-compatibility of an assemblage in terms of the regular compatibility of another, closely related assemblage. If one wants to know whether $\{M_{a|x}\}$ is k-compatible if suffices to take the symmetric product of each POVM effect with the identity operator acting on $(k-1)$ subspaces and check whether this new set of measurements admits a joint observable.

For instance, consider the spin-$1/2$ noisy observables in directions x, y and z, whose effects are defined in terms of the Pauli matrices as

$$X_\pm^\eta = \frac{\mathbb{1} \pm \eta \sigma_x}{2}, \quad Y_\pm^\eta = \frac{\mathbb{1} \pm \eta \sigma_y}{2}, \quad Z_\pm^\eta = \frac{\mathbb{1} \pm \eta \sigma_z}{2}, \tag{5.12}$$

where $\eta \in [0,1]$ is a noise parameter: high values of η result in sharper spin measurements, eventually recovering the original POVM elements for $\eta = 1$; low values of η result in noisy spin measurements, resulting in a trivial measurement for $\eta = 0$. For $\eta = 1$ this set of observables is not compatible. As a consequence, there is no joint observable acting on a single copy of an arbitrary qubit state ρ that can reproduce their results, but for $\eta \leq 1/\sqrt{3}$ these noisy spin observables are jointly measurable [173].

One might now wonder whether there is a 2-copy joint observable, acting on $\rho \otimes \rho$ that might, after a post-processing, recover the statistics of the noisy spin measurements. In other words, one want to check whether this set of measurements is 2-compatible. To answer this question, one must compute the regular compatibility of the following observables, resulting from the symmetric product of the corresponding POVM effects with the identity operator. By taking $k = 2$ in eq. (5.11),

$$\bar{X}_\pm^\eta = \mathbb{1} \odot X_\pm^\eta = \frac{1}{2}(\mathbb{1} \otimes X_\pm^\eta + X_\pm^\eta \otimes \mathbb{1}), \tag{5.13}$$

$$\bar{Y}_\pm^\eta = \mathbb{1} \odot Y_\pm^\eta = \frac{1}{2}(\mathbb{1} \otimes Y_\pm^\eta + Y_\pm^\eta \otimes \mathbb{1}), \tag{5.14}$$

$$\bar{Z}_\pm^\eta = \mathbb{1} \odot Z_\pm^\eta = \frac{1}{2}(\mathbb{1} \otimes Z_\pm^\eta + Z_\pm^\eta \otimes \mathbb{1}). \tag{5.15}$$

Now, all that is left is to check for what values of η the assemblage $\{\bar{X}_\pm^\eta, \bar{Y}_\pm^\eta, \bar{Z}_\pm^\eta\}$ admits a joint observable. As shown in [172], this happens whenever $\eta \leq \sqrt{3}/2$, in which case the set is 2-compatible.

Notice how this example makes it explicit that $(k+1)$-compatibility is a "weaker" property than k-compatibility. One needs to add more noise into a measurement in order to make it compatible than what is necessary to make it 2-compatible.

It is also worth mentioning that the possibility of translating the problem of determining whether an assemblage is k-compatible into a regular compatibility problem offers a great computational advantage. By looking at eq. (5.8), one can see that using this expression directly to impose constraints on a program would not result in an SDP. Indeed, such program would consist on looking for all possible observables G such that it is a k-copy joint observable for an assemblage $\{M_{a|x}\}_{a,x}$. Explicitly,

$$
\begin{aligned}
&\textbf{given} \quad \{M_{a|x}\},\ k \\
&\textbf{maximize} \quad \eta \\
&\textbf{subject to} \quad \mathrm{Tr}[\Lambda_\eta(M_{a|x})\rho] = \mathrm{Tr}[\rho^{\otimes k} \underbrace{\sum_{a_i,\, i \neq x} G_{a_1,\ldots,a_{x-1},a,a_{x+1},\ldots,a_N}}_{G_a^{[x]}}] \\
&\qquad\qquad G_{a_1,\ldots,a_N} \geq 0, \quad \sum_{a_1,\ldots,a_N} G_{a_1,\ldots,a_N} = \mathbb{1}, \quad \eta \leq 1.
\end{aligned}
\tag{5.16}
$$

This program is evaluating the minimum amount of noise one must add to the assemblage such that it admits a k-copy joint measurement. Whenever the solution is $\eta = 1$ one can conclude that $\{M_{a|x}\}$ is k-compatible, because it would mean no noise is necessary at all. Lower optimal values for η indicate that the set is not k-compatible.

Since the k-copy joint observable must recover the statistics of $\{M_{a|x}\}$ when the measurements are performed on any state ρ, both $\{G_{a_1,\ldots,a_N}\}$ and ρ are variables in this program, and thus it is not an SDP. However, if one re-formulates this task using to their advantage what we already know about k-compatibility translating into regular compatibility, an equivalent task can be written:

$$
\begin{aligned}
&\textbf{given} \quad \{M_{a|x}\},\ k \\
&\textbf{maximize} \quad \eta \\
&\textbf{subject to} \quad \Lambda_\eta(M_{a|x}) \odot \mathbb{1}^{\otimes(k-1)} = \underbrace{\sum_{a_i,\, i \neq x} \tilde{G}_{a_1,\ldots,a_{x-1},a,a_{x+1},\ldots,a_N}}_{\tilde{G}_a^{[x]}} \\
&\qquad\qquad \tilde{G}_{a_1,\ldots,a_N} \geq 0, \quad \sum_{a_1,\ldots,a_N} \tilde{G}_{a_1,\ldots,a_N} = \mathbb{1}, \quad \eta \leq 1.
\end{aligned}
\tag{5.17}
$$

Here, one is checking whether the symmetrized versions of $\{M_{a|x}\}$ admit a joint observable, and $\{\tilde{G}_{a_1,\ldots,a_N}\}$ are the only variables of the problem.

After this brief exposition of basic notions in joint measurability, we can move on to introduce the closely related concept of measurement simulability.

5.1.2 Measurement simulability

Compatibility is the property that defines whether the general statistics yielded by a set of measurements can be reproduced by the post-processing of the results from the measurement of a single POVM. One decides if an assemblage is compatible by determining whether there is a joint observable that can fulfill this task.

A closely related, yet complementary inquiry can be framed the other way around. In compatibility analyses, one wants to know if a given set of measurements can be reproduced. Alternatively, one can now wonder what measurements can be reproduced given the measurements to which one actually has access. To face such interrogations, one can dive into the field of measurement simulability [174, 175].

A set of measurements $\mathcal{M} = \{M_{a|x}\}$ is said to be simulated by another set of measurements $\mathcal{N} = \{N_{a|x}\}$ if there exists a protocol relying only on classical manipulations of $\mathcal{N}$ that can reproduce the statistics of $\mathcal{M}$ for any state ρ. Such classical manipulations are completely encompassed in two categories: pre-processing and post-processing [176]. Simulation protocols consist on classically mixing the measurements one has available in the lab (a pre-processing phase), followed by performing these measurements, and finally relabeling or coarse-graining the outcomes (the post-processing phase). Mathematically, this

means a set of measurements $\mathcal{M}$ can be simulated by $\mathcal{N}$ if there exist probability distributions p and q such that

$$M_{a|x} = \sum_{x'} p(x'|x) \sum_{a'} q(a|x, a', x') N_{a'|x'}, \tag{5.18}$$

with $p(x'|x) \geq 0 \ \forall x', \quad \sum_{x'} p(x'|x) = 1$ and $q(a|x, a', x') \geq 0 \ \forall a, \quad \sum_a q(a|x, a', x') = 1$. This way, the pre-processing phase is controlled by p while the post-processing is given by q. If the measurements in the set $\mathcal{N}$ (said to be simulators of $\mathcal{M}$) consist of k POVMs, that is, if $x' = 1, \ldots, k$, then $\mathcal{M}$ said to be k-simulable.

Notice that simulability and compatibility are closely related concepts. In fact, compatibility can be seen as the particular case of k-simulability where $k = 1$, i.e., a set of measurements is compatible when it can be simulated by a single POVM. Indeed, it is easy to see that if x' can assume only one value then the expression in eq. (5.18) reproduces the usual definition of compatibility. By wondering if a set of measurements can be simulated by more than one POVM, one is relaxing the notion of joint measurability.

Unfortunately, the problem of deciding whether a set of measurements is k-simulable does not seem to admit an SDP formulation [174]. Indeed, the constraint expressed by eq. (5.18) is non-linear, since p, q and $\{N_{a'|x'}\}$ would all be variables in the program, and no trick to overcome this issue is known. Even though this is a major draw-back from the computational perspective, we will show in section 5.2.2 that there is a close connection between the concepts of k-simulability and k-compatibility, and a necessary condition for k-simulability can be cast as an SDP.

5.1.3 Steering

Steering and entanglement are terms that were first introduced by Schrödinger in his 1935 work [158], following Einstein, Podolski and Rosen's famous EPR paper [151] criticizing quantum mechanics as a physical theory. The trio considered a thought experiment analyzing position and momentum of a bipartite system, and the argument was later reformulated by Bohm [177], which we can re-interpret in terms of qubits. Consider a scenario where Alice and Bob each hold half of a two-particle system in laboratories far away from each other. They share a singlet state, defined as

$$|\psi_{AB}\rangle = \frac{(|01\rangle - |10\rangle)}{\sqrt{2}}, \tag{5.19}$$

where $|0\rangle$ and $|1\rangle$ are the eigenstates of spin along the z-direction, with eigenvalues $\{+1, -1\}$ respectively. Notice that $|\psi_{AB}\rangle$ still preserves its anti-correlation if one were to instead use the basis $\{|+\rangle, |-\rangle\}$, where $|\pm\rangle = (|0\rangle \pm |1\rangle)/\sqrt{2}$ are the eigenvectors of spin along the x-direction, with eigenvectors $\{+1, -1\}$. As a consequence, Alice can predict Bob's outcomes of a spin measurement on either the x- or z-direction depending on her own choice of measurements: if she measures the spin of her particle in the z-direction and obtains the result $+1$ (or -1) she knows Bob's state must be $|1\rangle$ (or $|0\rangle$); similarly, if she measures the spin of her particle in the x-direction and obtains the result $+1$ (or -1) she knows Bob's state must be $|+\rangle$ (or $|-\rangle$).

Since the outcomes of these two spin measurements on Bob's side could, in principle, be predicted with certainty by Alice without disturbing his system (as the subsystems no longer interact), it was argued in the EPR paper that these observables corresponded to "elements of reality". Quantum mechanics dictates that one cannot assign simultaneously well-defined values for these observables, which leads to the conclusion that the theory is incomplete (or so it was claimed). To solve this apparent paradox, one could trivially consider local hidden variables and all was well again.

Schrödinger, in turn, believed quantum theory to provide a complete description of the whole physical system, rejecting the need of a local hidden variable to make sense of it. He pointed out that, even though Alice could not send any information to Bob by performing different measurements on her side (since his reduced state would not depend on her choice), she could indeed "steer" his share of the bipartite state into eigenvectors of spin along either direction, an effect he described as "magic".

However, even Schrödinger could not accept the possibility of steering actually happening on a lab, and thus deemed quantum mechanics to be incorrect in its description of delocalized entangled states. In his opinion, the parties where dealing with well-defined states even before measurements, and a local hidden state model should describe the bipartite system [107].

Following the formalism put forward in [107], one can frame a steering scenario as a quantum information task. Consider two parties, Alice and Bob, each having access to half of a bipartite physical system

previously prepared by Alice. On each run of the protocol, both parties can perform measurements on their share of the state in their respective far-away laboratories and communicate classically. Alice's task is to convince Bob that she can, by correctly choosing her measurements, collapse his system into different states, that is, she can *steer* his system. Bob is a particularly skeptical scientist, and will only yield if the correlations that he observes between his and Alice's results cannot be explained by sheer classical ignorance, otherwise Alice could simply be exploiting her knowledge about their shared physical system to tweak her results and fool him. In other words, Bob will only be convinced if the scenario admits no local hidden state explanation.

Let us introduce the mathematical notation we will use to explore such scenarios. Consider a quantum state ρ, such that $\text{Tr}[\rho] = 1$ and $\rho \geq 0$. An *ensemble* for ρ is a set $\mathcal{E} = \{\rho_a\}_a$ whose elements obey $\rho_a \geq 0$ and $\sum_a \rho_a = \rho$. In a classical scenario, it can be seen as a collection of states non-normalized , which physically correspond to a local hidden state (LHS) model for ρ. The same state admits different LHS models, and a collection of such ensembles is called a *state assemblage*, denoted $\mathcal{A} = \{\mathcal{E}_x\}_x$. The elements of this collection are now indexed by two labels, and $\sum_a \rho_{a|x} = \rho$, $\rho_{a|x} \geq 0$. A *measurement assemblage* $\mathcal{M} = \{M_{a|x}\}_{a,x}$ is a collection of POVMs, with $M_{a|x} \geq 0$ and $\sum_a M_{a|x} = \mathbb{1}$ for all x.

We denote the bipartite state shared by Alice and Bob ρ_{AB}. On her side, Alice has access to the measurement assemblage $\{M_{a|x}\}_{a,x}$, and can perform different measurements by choosing settings labeled by x yielding outcomes labeled by a. On his side, Bob is left with a state assemblage $\{\rho_{a|x}\}_{a,x}$ whose elements are given by

$$\rho_{a|x} = \text{Tr}_A[(M_{a|x} \otimes \mathbb{1})\rho_{AB}], \qquad (5.20)$$

where Tr_A is the partial trace operation over Alice's subsystem. Notice that whatever Bob's conditional states are, they must correspond to an assemblage for the reduce state $\rho_B = \text{Tr}_A[\rho_{AB}]$. Put mathematically,

$$\rho_B = \sum_a \rho_{a|x} \qquad (5.21)$$

for any setting x Alice may choose. This is of course a physical consequence of the pair only being allowed to communicate classically, and Bob's reduced state being independent of Alice's choice of measurement.

Finally, we say Bob's state assemblage admits a LHS model if there exist $p(a|x,\lambda) \geq 0$ and a set of positive operators $\{\sigma_\lambda\}$ obeying $\text{Tr}[\sum_\lambda \sigma_\lambda] = 1$ such that

$$\rho_{a|x} = \sum_\lambda p(a|x,\lambda)\sigma_\lambda, \quad \forall a, x. \qquad (5.22)$$

Whenever it is the case, we say Bob's state assemblage is unsteerable. This would mean Bob's assemblage could in fact corresponds to an unknown classical mixture of well-defined states, and all that changes with Alice's measurements is his knowledge about the probability distribution of the hidden states. On the other hand, if no such model exists then Bob must admit Alice can steer his share of the physical system.

Now that we have specified the kind of scenario with which we will be dealing throughout this work, we can discuss steering equivalent observables, a mathematical construction that will allows us to introduce out method to certify the number of incompatible measurements to which Alice has access.

Steering equivalent observables

After establishing what steering actually is, one is led to wonder how this phenomenon can be verified and what are necessary or sufficient conditions to ascertain that steering can manifest itself on a given scenario.

Indeed, one may detect steering from different fragments of information about a setup, but we will focus our analysis on a specific instance of special interest to our goals. For completeness, however, we mention some additional strategies. First, in close analogy to Bell inequalities certifying non-locality, steering inequalities can be employed to verify that certain correlations cannot be obtained from LHS models, a method that features the advantage of being experimentally applicable [178, 179, 180, 181]. Second, one can start from already having full knowledge of the shared state ρ_{AB} and examine whether there are measurements that Alice can perform that will reveal that the state is steerable. This question is harder than it may seem at first, particularly if one considers scenarios beyond two-qubit states and non-projective measurements [182, 183, 184]. Finally, one can analyze what Bob can conclude from the information to which he has access. When his state assemblage is known, it suffices to show that it admits

a LHS model to conclude that steering cannot take place, and fortunately this question can be decided with the aid of of an SDP [91, 185].

Still following this last line of research, one can apply the results in [186] to formulate yet another SDP that takes Bob's state assemblage as input and verifies whether or not it is steerable. Instead of looking for a LHS model for $\{\rho_{a|x}\}_{a,x}$, one constructs the set of *steering equivalent observables* (SEO) and checks whether it admits a joint measurement. This result is particularly relevant to understand our method when we present it in section 5.2.

Let us first define Π_B, the projector on the subspace $\mathcal{K}_{\rho_B} = \text{range}(\rho_B)$, that is, the subspace spanned by the columns of ρ_B. One can evaluate Bob's state assemblage and reduced state when restricted to the subspace $\mathcal{K}_{\rho_B}$, given by[3]

$$\tilde{\rho}_{a|x} = \Pi_B \rho_{a|x} \Pi_B^\dagger, \quad \tilde{\rho}_B = \Pi_B \rho_B \Pi_B^\dagger. \tag{5.23}$$

Since $\rho_{a|x}$ and ρ_B are positive, $\tilde{\rho}_{a|x}$ and $\tilde{\rho}_B$ are also positive and we can define Bob's steering equivalent observables as

$$B_{a|x} = (\tilde{\rho}_B)^{-1/2} \tilde{\rho}_{a|x} (\tilde{\rho}_B)^{-1/2}. \tag{5.24}$$

Since $B_{a|x} \geq 0$ for all a, x, and one can easily verify that $\sum_a B_{a|x} = \mathbb{1}_{\mathcal{K}_{\rho_B}}$, and each set $\{B_{a|x}\}_a$ for a fixed x forms a POVM.

We now state the main result in [186]: Bob's state assemblage $\{\rho_{a|x}\}_{a,x}$ is unsteerable if and only if its steering equivalent observables $\{B_{a|x}\}_{a,x}$ are jointly measurable. The proof of this statement is simple enough. The first implication is established by assuming the existence of a LHS model $\{\tilde{\sigma}_\lambda\}_\lambda$ for $\{\tilde{\rho}_{a|x}\}_{a,x}$ and explicitly constructing a joint measurement for $\{B_{a|x}\}_{a,x}$, namely

$$G_\lambda = (\tilde{\rho}_B)^{-1/2} \tilde{\sigma}_\lambda (\tilde{\rho}_B)^{-1/2}. \tag{5.25}$$

The other direction follows trivially if one realizes that a joint measurability problem is simply a steerability problem with ρ_B being the maximally mixed state. Indeed, if one assumes $\{B_{a|x}\}_{a,x}$ to be jointly measurable, that is,

$$B_{a|x} = \sum_\lambda p(a|x, \lambda) G_\lambda, \quad \forall a, x \tag{5.26}$$

for some p, G, then simply setting $\rho_B = \mathbb{1}$ in eq. (5.24) yields

$$\rho_{a|x} = \sum_\lambda p(a|x, \lambda) G_\lambda, \quad \forall a, x \tag{5.27}$$

so p and G form a LHS model for $\{\rho_{a|x}\}_{a,x}$, and consequently Bob's assemblage is not steerable.

This result makes the connection between steering and measurement compatibility even clearer [163], and in fact Bob's steering equivalent observables can be interpreted as the very measurements that must be performed by Alice to prepare $\{\rho_{a|x}\}_{a,x}$ [86] on Bob's side.

Now that all the pieces are available, we can start assembling the puzzle whose final picture is our strategy to determine the number of incompatible measurements on Alice's assemblage, using only the information to which Bob has access.

5.2 A method to certify how many incompatible measurements Alice performs

Following the tradition of cultivating distrust when performing quantum-informational tasks, we develop a straight-forward method to certify the number of incompatible measurements to which Alice has access in a steering scenario. As mentioned before, the very verification of steering is already enough to ensure that Alice has performed incompatible measurements, but nothing, so far, has been said about *how many* of these measurements there are.

By exploiting a chain of implications, we are able to construct a test that checks whether a necessary condition for Alice to perform k incompatible measurements is satisfied. Whenever this condition is

---

[3]If the reader is wondering what's the difference between ρ_B and $\tilde{\rho}_B$, we recall that ρ_B may not be full-rank, in which case $\tilde{\rho}_B$ and ρ_B will have different dimensions.

not met, we conclude with certainty that Alice, then, must have performed at least $k + 1$ incompatible measurements; if the condition is met, however, nothing can be ascertained.

As we will discuss, this necessary (but not sufficient) condition is that Bob's steering equivalent observables are k-compatible, with the additional restriction that the corresponding k-copy joint observable is in a product form. This criterion displays two central features, with both foundational and applied relevance: first, it depends only on the information that Bob can harvest, namely his state assemblage, and thus no trust has to be deposited in Alice; second, this test can be formulated in terms of a semidefinite program, and one can consequently profit from all the computational advantages that come with it.

In sections sections 5.2.1 and 5.2.2, we will introduce fragments of this chain of implications, and in section 5.2.3 we will tie them all together and construct the full criterion. We will, afterwards, frame this test as a hierarchy of SDPs, and finally put it to test in the last section of this chapter.

5.2.1 k-simulability of Alice's assemblage implies k-simulability of Bob's steering equivalent observables

In this section we are going to prove that if Alice's measurement assemblage is k-simulable, then Bob's steering equivalent observables are also k-simulable. This is the very first step in constructing a test that Bob can use to certify the number of incompatible measurements that Alice can perform, as we must create a link between the information to which Bob has access and the object we want to investigate, namely Alice's measurement assemblage.

We start by assuming that Alice's measurement assemblage $\mathcal{M} = \{M_{a|x}\}_{a,x}$ is k-simulable, that is, there exist probability distributions p, q and a set of k simulators $\{N_{b|y}\}_{b,y}^{y=1,\dots,k}$ satisfying eq. (5.18), the condition for k-simulability. Bob's steering equivalent observables are given by eq. (5.24), and one can expand this equation using the definition of Bob's state assemblage in eq. (5.20). Then, the expression for Bob's SEOs $\mathcal{B} = \{B_{a|x}\}_{a,x}$ reads

$$B_{a|x} = (\tilde{\rho_B})^{-1/2} \Pi_B \operatorname{Tr}_A[(M_{a|x} \otimes \mathbb{1})\rho_{AB}] \Pi_B^\dagger (\tilde{\rho_B})^{-1/2}. \tag{5.28}$$

Since $\mathcal{M}$ is k-simulable, one can substitute $M_{a|x}$ so that we have an expression for Bob's SEO in terms of the simulators of Alice's measurement assemblage. The corresponding equation is

$$B_{a|x} = \sum_{y=1}^k \sum_b p(y|x) q(a|b,x,y) (\tilde{\rho_B})^{-1/2} \Pi_B \operatorname{Tr}_A[(N_{b|y} \otimes \mathbb{1})\rho_{AB}] \Pi_B^\dagger (\tilde{\rho_B})^{-1/2}. \tag{5.29}$$

To show that $\{B_{a|x}\}_{a,x}$ is k-simulable it suffices to explicitly construct its simulators. Indeed, it is straight-forward to identify them in the equation above. We define

$$\tilde{N}_{b|y} = (\tilde{\rho_B})^{-1/2} \Pi_B \operatorname{Tr}_A[(N_{b|y} \otimes \mathbb{1})\rho_{AB}] \Pi_B^\dagger (\tilde{\rho_B})^{-1/2}, \tag{5.30}$$

and the set $\{\tilde{N}_{b|y}\}_{b,y}^{y=1,\dots,k}$, along with probability distributions p, q, fit into the definition of k-simulability given in eq. (5.18). All that is left is to show that $\{\tilde{N}_{b|y}\}_{b,y}$ are indeed observables. Since $\{N_{b|y}\}$ are themselves positive, it follows directly that $\tilde{N}_{b|y} \geq 0, \forall b, y$. One can also easily check that $\sum_b \tilde{N}_{b|y} = \mathbb{1}$. As $\sum_b N_{b|y} = \mathbb{1}$, we have

$$\sum_b \tilde{N}_{b|y} = (\tilde{\rho_B})^{-1/2} \Pi_B \operatorname{Tr}_A[\rho_{AB}] \Pi_B^\dagger (\tilde{\rho_B})^{-1/2} \tag{5.31}$$

$$= (\tilde{\rho_B})^{-1/2} \Pi_B \rho_B \Pi_B^\dagger (\tilde{\rho_B})^{-1/2} \tag{5.32}$$

$$= (\tilde{\rho_B})^{-1/2} \tilde{\rho}_B (\tilde{\rho_B})^{-1/2} \tag{5.33}$$

$$= \mathbb{1}. \tag{5.34}$$

Thus, we can conclude that if Alice's measurement assemblage is k-simulable, then so are the steering equivalent observables of Bob's state assemblage. Notice that the other way around does not hold: if Bob's SEOs are k-simulable there is no guarantee that Alice's measurements are k-simulable. Indeed, a counter-example can be constructed, for instance, if the state that the two parties share is separable. Whenever that is the case, it is easy to see that Bob's SEOs correspond to a trivial measurement and are, thus, k-simulable.

In this section, we have devised a way to check if Alice's measurement assemblage $\mathcal{M}$ is k-simulable using only the information to which Bob has access. After evaluating the k-simulability of his steering

equivalent observables, Bob can interpret the meaning of a negative answer. If his SEOs are not k-simulable, he can be sure that Alice's measurement assemblage is not k-simulable. Of course, as we have already discussed, if his SEOs are indeed k-simulable, then nothing can be stated.

We point out that the k-simulability of $\mathcal{M}$ is a telling feature: if this set of measurements is composed of k compatible observables then it must necessarily be k-simulable. This means that if this characteristic is not present, then $\mathcal{M}$ must consist of *at least $k + 1$* incompatible measurements.

Let us assert a couple of facts about k-simulability, proven in [172], that can nevertheless be easily verified.

- All assemblages of k measurements are k-simulable, since one could simply take each measurement as a simulator.

- If an assemblage is k-simulable, then it must also be $(k+1)$-simulable, as one can trivially add any measurement to the set of simulators and never actually use it.

Consequently, there is no alternative conclusion that can be drawn from the impossibility of constructing a set of k simulators for $\mathcal{M}$, other than that the assemblage must have at least $k + 1$ incompatible measurements. If $\mathcal{M}$ was composed of more than k compatible measurements, or composed of k or less incompatible measurements, the set would still be k-simulable.

Thus, if one wants to ensure that Alice's measurement assemblage consists of at least $k+1$ incompatible measurements, it suffices to show that it is not k-simulable. What we have achieved in this section was to find a way to check that $\mathcal{M}$ is not k-simulable while only assuming knowledge that Bob can obtain. In summary, by checking that his steering equivalent observables (obtained from his state assemblage) are not k-simulable, Bob can conclude that Alice must have access to at least $k + 1$ incompatible measurements.

5.2.2 k-simulability implies k-compatibility

In this section we will show that if a measurement assemblage is k-simulable, then it must also be k-compatible. Furthermore, the assemblage must admit a k-copy joint observable that is separable.

Let $\mathcal{B} = \{B_{a|x}\}_{a,x}$ be a set of POVM elements. Assume that is it k-simulable, that is, there exist an assemblage of k POVMs $\mathcal{N} = \{N_{b|y}\}_{b,y}^{y=1,\ldots,k}$ and probability distributions p, q that satisfy eq. (5.18). To show that $\mathcal{B}$ must also be k-compatible we will explicitly construct a k-copy joint observable.

Let us define the set $\{H_{b|y}\}_{b,y}^{y=1,\ldots,k}$, with POVM elements

$$H_{b|y} = \underbrace{\mathbb{1} \otimes \ldots \otimes \overbrace{N_{b|y}}^{\text{y-th term}} \otimes \ldots \mathbb{1}}_{\text{k terms}}. \tag{5.35}$$

That is, this measurement is performed on states in $\mathcal{L}(\mathcal{H}^{\otimes k})$, such as $\rho^{\otimes k}$. On the y-th copy one measures the y-th simulator of $\mathcal{B}$ obtaining outcome b, while a trivial measurement is performed on the other copies. It is easy to see that $\{H_{b|y}\}_b$ indeed form a POVM for each fixed y, since we assume $\{N_{b|y}\}_b$ are POVMs themselves.

Because of this block-structure of $H_{b|y}$, it naturally follow that

$$\text{Tr}[\rho B_{a|x}] = \sum_{y=1}^{k} \sum_b p(y|x) q(a|b, x, y) \text{Tr}[\rho^{\otimes k} H_{b|y}]. \tag{5.36}$$

We are already halfway to showing that eq. (5.8) is satisfied and $\mathcal{B}$ is k-compatible. In order to do that, we must clearly identify the k-copy joint observable. Let us first rearrange the expression above,

$$\text{Tr}[\rho B_{a|x}] = \text{Tr}[\rho^{\otimes k} \left(\sum_{y=1}^{k} \sum_b p(y|x) q(a|b, x, y) H_{b|y} \right)]. \tag{5.37}$$

It suffices to show that the onject in parenthesis indeed corresponds to a marginalization over all but one entry of some observable. To that end, notice that $H_{b|y}$ is the y-th marginal of $\{\tilde{H}_{b_1,\ldots,b_k}\}_{b_1,\ldots,b_k}$, with effects defined as

$$\tilde{H}_{b_1,\ldots,b_k} = N_{b_1|1} \otimes \ldots \otimes N_{b_k|k}. \tag{5.38}$$

Indeed, one can easily verify that

$$H_{b|y} = \tilde{H}_b^{[y]} = \sum_{b_i, i \neq y} N_{b_1|1} \otimes \ldots \otimes N_{b|y} \otimes \ldots \otimes N_{b_k|k}. \tag{5.39}$$

If we plug this result back into eq. (5.37), we get

$$\mathrm{Tr}[\rho B_{a|x}] = \mathrm{Tr}[\rho^{\otimes k} \left(\sum_{y=1}^{k} \sum_b p(y|x)q(a|b,x,y) \sum_{b_i, i \neq y} N_{b_1|1} \otimes \ldots \otimes N_{b|y} \otimes \ldots \otimes N_{b_k|k} \right)] \tag{5.40}$$

$$= \mathrm{Tr}[\rho^{\otimes k} \left(\sum_{y=1}^{k} \sum_{b_1, \ldots, b_y, \ldots, b_k} p(y|x)q(a|b_y,x,y) \, N_{b_1|1} \otimes \ldots \otimes N_{b_y|y} \otimes \ldots \otimes N_{b_k|k} \right)] \tag{5.41}$$

$$= \mathrm{Tr}[\rho^{\otimes k} \left(\sum_{y=1}^{k} \sum_{b_1, \ldots, b_k} p(y|x)q(a|b_y,x,y) \, \tilde{H}_{b_1, \ldots, b_k} \right)]. \tag{5.42}$$

All we did in between these equations was relabel the dummy index b as b_y, which made the expression somewhat simpler, and then explicitly including the k-copy joint measurement $\tilde{H}$. It is easy to verify that $\tilde{H}$ is indeed a POVM, i.e., $\tilde{H}_{b_1, \ldots, b_k} \geq 0 \,\forall b_1, \ldots, b_k$ and $\sum_{b_1, \ldots, b_k} \tilde{H}_{b_1, \ldots, b_k} = \mathbb{1}$, since $\{N_{b|y}\}_{b,y}$ are POVM elements themselves.

With that, we have explicitly constructed a k-copy joint measurement for $\mathcal{B}$. If one assumes the existence of a k-simulability protocol, then a k-copy joint observable can always be constructed through another closely related procedure, see fig. 5.2 for clarity. More than that, looking at eq. (5.38) we see that the joint POVM must be in a product form, separable with respect to a partition of k subspaces, one for each copy of a generic state ρ on which it will act.

Notice, however, that k-copy joint observables are not unique: more than one POVM can satisfy the definition in eq. (5.8). Yet, by showing that a k-copy joint measurement always exists in the form of eq. (5.38), we assure that at least one of all possible joint measurements is separable across this specific partition.

A result of the discussion we conducted in this section is that we have constructed a criteria for the k-simulability of a measurement assemblage. Given $\mathcal{B}$, one can simply determine whether the assemblage admits a separable k-copy joint measurement to conclude, if the answer is negative, that $\mathcal{B}$ is not k-simulable. This is once again an instance where a positive answer renders the test inconclusive: if no separable k-copy joint measurement exists, one knows for sure that $\mathcal{B}$ is not k-simulable; if there is such a measurement, however, nothing can be said.

The advantage of using this alternative approach is that, unlike k-simulability, the k-compatibility of a set of POVMs can be evaluated as an SDP, a valuable asset since SDP formulations benefit from solid computational support. The results we obtained in the last two sections can finally be linked together to build a test from which one can infer to how many incompatible measurements Alice has access.

5.2.3 Witnessing the number of incompatible measurements in Alice's assemblage

We recall the motivation behind investigating whether a set of POVMs is k-simulable: if Alice's measurement assemblage is not k-simulable, then it must consist of at least $k+1$ incompatible measurements. We want a strategy to check this property while only assuming access to the information that Bob can extract from his side of the experiment, and such method would preferably be cast as an SDP.

Let us go over what we already have achieved. If one want to check whether Alice's measurement assemblage is k-simulable, one can instead check if Bob's steering equivalent observables are k-simulable. If the answer is negative, then one knows Alice's assemblage is not k-simulable; a positive answer is inconclusive. By applying the result from the previous section to Bob's SEOs, we also know that to check whether Bob's steering equivalent observables are k-simulable it suffices to evaluate if they are k-compatible and admit a separable k-copy joint measurement.

Our combined results state that Bob can evaluate the k-compatibility of his SEOs to reach a conclusion about Alice's measurements: if Bob's steering equivalent observables do not admit a separable k-copy joint observable, then they cannot be k-simulable, which in turn imply Alice's measurement assemblage cannot be k-simulable, ultimately meaning it must consist of at least $k+1$ incompatible measurements.
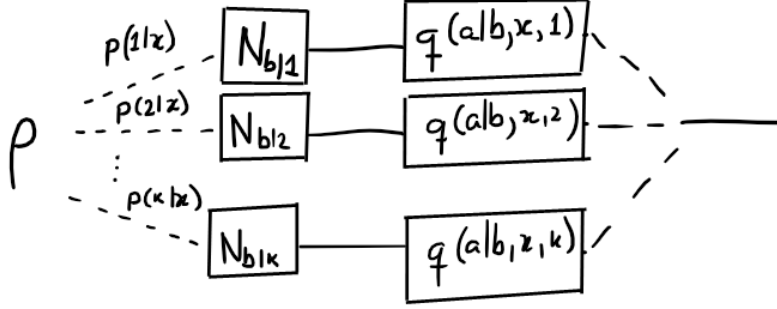
(a) Representation of a protocol where the measurement of $\{B_{a|x}\}_{a,x}$ could be simulated by $\{N_{b|y}\}_{b,y}$ and p, q. A pre-processing, given by p, selects which measurement will be performed on each run. Then, a post-processing, given by q, produces the final outcome.
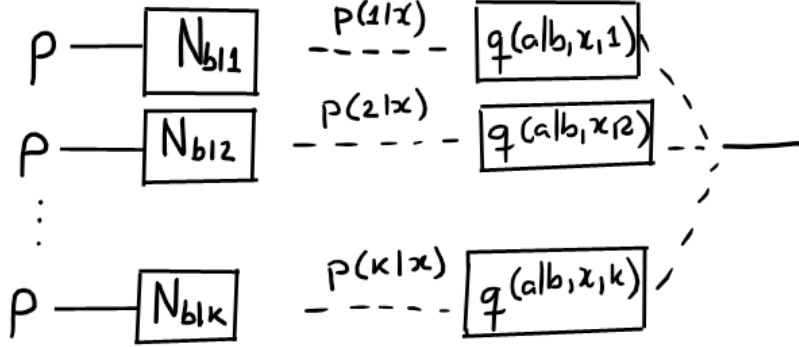
(b) Representation of a protocol where the one constructs a k-copy joint measurement of $\{B_{a|x}\}_{a,x}$, given that it admits a set of simulators with k elements. Each measurement $\{N_{b|y}\}$ will be performed on a single copy of ρ, out of k copies in total. The resulting outcomes are mixed according to p and post-processed according to q, to finally yield a single outcome.

Figure 5.2: **Construction of a k-copy joint measurement from the set of k simulators** If one assumes that a measurement assemblage $\mathcal{B} = \{B_{a|x}\}_{a,x}$ is k-simulable, then it is always possible to construct a k-copy joint observable for $\mathcal{B}$. Furthermore, this observable has a product structure, acting locally on each copy of ρ.

Thus, we now have a simple way to certify that Alice has access to, at least, $k + 1$ incompatible measurements on her side of the experiment. Given Bob's state assemblage $\{\rho_{a|x}\}_{a,x}$, he can construct his steering equivalent observables $\mathcal{B} = \{B_{a|x}\}_{a,x}$. A simple SDP can be written to check the existence of a k-copy joint observable G that is, furthermore, in a product form. If G exists nothing can be inferred, but if a program searching for it is infeasible then one can conclude that Alice must have access to at least $k + 1$ incompatible measurements.

As neat and straight-forward as it is, this test comes with a caveat. We note that separability cannot be directly translated as a SDP constraint, which means we must resort to alternative approaches, such as the DPS hierarchy introduced in section 3.2.1. In practice, our criterion is implemented as a hierarchy of SDPs, i.e., instead of imposing that the k-copy joint observable is separable, we demand it to admit a symmetric extension to N copies that is positive under partial transpose of its subsystems. Different levels of this hierarchy are constructed by testing extensions to higher and higher numbers of copies. If at any level such SDP is infeasible, either because there is no k-copy joint measurement or because such observable has no PPT symmetric extension to N copies (thus, it is not separable), one concludes that Alice's measurement assemblage consists of at least $k + 1$ incompatible measurements.

An explicit construction of the level $N = 2$ of this hierarchy of SDP tests can be implemented as follows. Let $\{\tilde{B}_{a|x}^k\}_{a,x}$ be the symmetrized versions of the POVM elements in $\mathcal{B}$, obtained by evaluating the symmetric product of Bob's SEOs and the identity. According to eq. (5.11), we can evaluate the compatibility of

$$\tilde{B}_{a|x}^k = \mathbb{1}^{\otimes(k-1)} \odot B_{a|x} \tag{5.43}$$

86

to infer the k-compatibility of $\mathcal{B}$. The resulting SDP will look for a corresponding joint observable G, acting on $\mathcal{H}_A \otimes \mathcal{H}_B$. Additionally, we impose that such observable admits a symmetric extension to $N = 2$ copies of subspace $\mathcal{H}_B$, which we call $\tilde{G}$, acting on $\mathcal{H}_A \otimes \mathcal{H}_{B_1} \otimes \mathcal{H}_{B_2}$. The final program is

$$
\begin{array}{lll}
\text{given} & \{\tilde{B}_{a|x}^k\}_{a,x} \\
\text{find} & \{\tilde{G}_\lambda\}_\lambda \\
\text{s.t.} \\
k\text{-compatibility} & \left\{ \begin{array}{l} \tilde{B}_{a|x}^k = \sum_\lambda p(a|x,\lambda)G_\lambda, \forall a, x \\ \sum_\lambda G_\lambda = \mathbb{1} \\ G_\lambda \geq 0, \forall \lambda \end{array} \right. & (5.44) \\
\text{second level of DPS} & \left\{ \begin{array}{l} \text{Tr}_{B_2}[\tilde{G}_\lambda] = G_\lambda \\ \tilde{G}_\lambda^{T_X} \geq 0, X = \{A, B_1, B_2\} \\ \tilde{G}_\lambda \geq 0. \end{array} \right.
\end{array}
$$

In summary, Bob can perform this hierarchy of tasks using only the information he has available. He can start with low levels of the separability hierarchy and keep testing whether his steering equivalent observables admit a k-copy joint observable that has a product form. If the test fails for given k and N, he concludes that Alice's measurement assemblage consists of at least $k + 1$ incompatible measurements. If the SDP is feasible, a similar program can be written for higher levels of the separability hierarchy and he can perform yet another test, perhaps now with k and $N + 1$. Bob can keep increasing the number of copies to which he extends G, until he either meets a breaking point where the SDP is infeasible, or the computational power required exceeds his resources.

5.3 Results and discussion

We can finally put our method to proof and test its efficiency in certifying a lower bound for the number of incompatible measurements in Alice's measurement assemblage. To do that, we will analyze the typical example of measurements in mutually unbiased bases (MUBs, for short). Two bases $\{|\psi_i\rangle\}_{i=1}^d$ and $\{|\phi_i\rangle\}_{i=1}^d$ for a d-dimensional Hilbert space are said to be mutually unbiased if they satisfy

$$
|\langle\psi_i|\phi_j\rangle|^2 = \frac{1}{d}. \tag{5.45}
$$

Measurements performed on these bases are maximally incompatible, and play an important role in many quantum information tasks [187]. For dimension $d = 2$, for instance MUBs correspond for instance to the eigenstates of Pauli operators. In general, finding MUBs for a given dimension is a difficult task, and even though it is known that there can be at most $d + 1$ of such bases [188], it is not clear when this bound is tight. For our purposes, it suffices to know that the complete set of MUBs is known for dimensions which are powers of prime numbers, i.e., if $d = p^r$ for p prime and r positive and integer [189].

Let Alice's measurement assemblage $\mathcal{M} = \{M_{a|x}\}_{a,x}$, with $x = 1, \ldots, m$, be composed of m measurements in mutually unbiased bases. We can define the noisy versions of these measurements in terms of a noise parameter t as in

$$
M_{a|x}^t = tM_{a|x} + (1-t)\frac{\mathbb{1}}{d}. \tag{5.46}
$$

We can then evaluate what is the lowest value of t for which the noisy assemblage $\mathcal{M}^t$ does not fail our test. In other words, we will look for critical values t_c such that whenever $t \geq t_c$ we can assure that Alice has access to at least $k + 1$ incompatible measurements. Notice that t_c is, of course, only an upper bound for the true critical value of noise in Alice's measurements. This correspondence cannot be perfect since we can only consider the first few levels of the separability hierarchy because of computational limitations.

Ideally, the values we find for t_c for each case (that is, considering different dimensions and different numbers of measurements) should reproduce the incompatibility robustness η^* of MUBs, as defined in eq. (5.6). If that is case, it means that our test is able to perfectly detect that Alice's measurements are incompatible, never yielding an inconclusive answer if Alice indeed has access to $k + 1$ incompatible measurements. The closer the two numbers t_c and η^* are, the more efficient our method is. A gap between these two values indicates a window where our test cannot act.

We considered dimensions $d = 2$ and $d = 3$ (that is, qubits and qutrits), with Alice's assemblage ranging from 2 to $d + 1$ MUBs. Out of this set of POVMs, we constructed Bob's steering equivalent observables and submitted them to the SDP defined in eq. (5.44).

We then evaluated the values of t_c for each case, looking for a k-copy joint observable for Bob's SEOs that admit a PPT symmetric extension to N copies, while considering that Alice and Bob share a maximally entangled state. Different values of N correspond to different levels of the hierarchy, with $N = 1$ corresponding simply to the PPT criterion. We also considered the case where no separability criterion is used, and only k-compatibility of Bob's SEOs is considered. Our findings are presented in tables 5.1, 5.2 and 5.3, along with known values of the incompatibility robustness η^* of MUBs in table 5.4.

n	k	$d = 2$	$d = 3$
2	1	$1/\sqrt{2}$	$(1 + \sqrt{3})/4$
3	1	$1/\sqrt{3}$	$\cos(\pi/18)/\sqrt{3}$
	2	$\sqrt{3}/2$	0.8553
4	1		$(1 + 3\sqrt{5})/16$
	2		0.7681
	3		0.9310

Table 5.1: Resulting t_c when one only demands that Bob's SEO are k-compatible. This is a first upper bound for the critical noise, which can be made tighter by considering different levels of a separability hierarchy. Notice that there is no set of 4 MUBs for qubits.

n	k	$d = 2$	$d = 3$
2	1	$1/\sqrt{2}$	$(1 + \sqrt{3})/4$
3	1	$1/\sqrt{3}$	$\cos(\pi/18)/\sqrt{3}$
	2	$\sqrt{2/3}$	0.7975
4	1		$(1 + 3\sqrt{5})/16$
	2		0.6959
	3		0.8959

Table 5.2: Resulting t_c when one demands that Bob's SEO are k-compatible and satisfy the first level of the separability hierarchy, corresponding to the PPT criterion. This is a stronger constraint than the one imposed for the values in table 5.1, so the values obtained there cannot be lower than the ones presented here.

n	k	$d = 2$	$d = 3$
2	1	$1/\sqrt{2}$	$(1 + \sqrt{3})/4$
3	1	$1/\sqrt{3}$	$\cos(\pi/18)/\sqrt{3}$
	2	$\sqrt{2/3}$	0.7393
4	1		$(1 + 3\sqrt{5})/16$
	2		0.6933
	3		0.859

Table 5.3: Resulting t_c when one demands that Bob's SEO are k-compatible and satisfy the second level of the separability hierarchy. This is a stronger constraint than the one imposed for the values in table 5.2, so the values obtained there cannot be lower than the ones presented here.

By comparing these results with the actual values of η^*, we can conclude a few things. Our upper bounds for the critical visibility are tight in trivial cases: t_c and η^* coincide for $k = 1$, because we are simply checking that Bob's SEO are compatible. If one remembers the construction of these objects, the incompatibility of SEO implies steering, and we already know that steering only happens if the measurement performed are incompatible. Thus, our results for these cases were to be expected, and whenever Bob's SEOs do not admit a joint measurement (i.e., it fails the test for $k = 1$) we conclude that Alice has access to at least 2 incompatible measurements.

We can now analyze more interesting results. We see immediately that our upper bounds are not tight, as even when considering the highest level of the separability hierarchy we were able to implement,

n	$d = 2$	$d = 3$
2	$1/\sqrt{2}$	$(1 + \sqrt{3})/4$
3	$1/\sqrt{3}$	$\cos(\pi/18)/\sqrt{3}$
4	-	$(1 + 3\sqrt{5})/16$

Table 5.4: Known values for the incompatibility robustness η^* of MUBs [190]

in table 5.3, there is still a gap between t_c and η^*. However, there is already a significant amount of noise one can add to Alice's measurements before our test starts performing poorly, i.e., before it does not detect the incompatibility of Alice's measurements. This gap can be made even smaller by considering higher values of N, but we do not believe this would be enough to make the upper bound tight. This is mainly because the improvement achieved by considering extensions to more copies in the DPS method decreases at each step. As one can see, there is good improvement between results from tables 5.1 and 5.2, and still significant improvement between those in tables 5.2 and 5.3, but taking it further would likely only produce only a modest decrease in t_c.

This means our research can still lead to prospective projects. Our method can be improved, for instance, by investigating further the contents of section 5.2.2, where we have explicitly constructed a (separable) k-copy joint observable for k-simulable measurement assemblages. One can investigate whether it is possible to construct more general joint observables, such that k-compatibility of a set of measurements, combined perhaps with another requirement, can be a stronger criterion for k-separability than the one we provided. Ultimately, this would result in a test that can detect the k-simulability of Alice's measurements more effectively.

Additionally, we conjecture that the implication proven in section 5.2.2 is actually valid in both ways, that is, if a measurement assemblage admits a separable k-copy joint observable, then it is k-simulable. We were however unable to prove this claim. If it is indeed the case, such a result will have a big impact on k-simulability investigations. As already discussed, there is no known SDP formulation for k-simulability tasks, but a class of measurements could be investigated probing their k-compatibility instead.

Finally, it would be interesting to use this method to construct an inequality similar to so many others used in quantum information, imposing an upper bound to the expected value of some operator, whose violation would indicate, in this case, that Alice has access to at least a certain amount of incompatible measurements.

In this chapter, we have constructed a method that can, through a series of criteria that can be implemented with semidefinite programming, determine a lower bound to the number of incompatible measurements that Alice can perform. To do that, Bob only needs the information he can access in his laboratory, from which he constructs a hierarchy of SDPs that indirectly checks a necessary condition for Alice to have at least $k + 1$ incompatible measurements in her assemblage. This test can be inconclusive, i.e., the necessary condition is satisfied and nothing can be concluded from it, but we have shown with our analysis of MUBs that our method can achieve promising results.

Chapter 6

Geometry of process matrices

One of the main goals of information processing is to enhance the quality of communication between parties, by way of increasing the amount of information that can be exchanged, reducing loss due to noise, or perhaps cutting down on the resources employed. The efficiency one can achieve at any of these fronts is subjected, of course, to physical limitations, but it is still unclear what is the ultimate barrier to communication, the final limit to efficiency that one simply cannot transpose.

Protocols such as teleporting [191] or superdense coding [192] have largely contributed to the hope that quantum information will drastically boost our communication power, and yet one might wonder if even better protocols could be constructed. The question that lies behind such an inquiry is of foundational relevance, as we are, in fact, questioning where the limits of a physical theory lie, and how close to this frontier one can actually get.

To push the boundaries of quantum mechanics to its limit, it is necessary to question the foundations upon which the theory is built. To strip it down to only the essentials, one must scrutinize the elusive and silent assumptions that permeate the theory and investigate their necessity. This is what is done in works such as [193], where the authors determine sets of fundamental axioms and derive corresponding inequalities whose violation signal the incompatibility of the assumptions. It is, of course, also the procedure behind fields such as Bell non-locality [85] or contextuality [87], from which one learns that many "innocent" assumptions can be questioned.

In this same direction, one identifies a pre-supposed definite causal order permeating quantum mechanics, that is, the sneaky assumption that one can always arrange a set of events such that it it clear which events precede the others. In [150], the authors spot this assumption and diagnose its consequences. They introduce the formalism of process matrices, objects that describe the most general physical scenario where one is not building upon a well-defined causal structure, and more general scenarios can be constructed. The result is a construction where one can go beyond the formulation of usual quantum mechanics, while still in the realm of a physical theory.

Of particular interest to our project, the notion of signaling is deeply connected to the type of causal order that a scenario admits. Roughly speaking, the ability to signal is the possibility of sending information through some channel, and scenarios that admit less orthodox causal structures also allow for broader possibilities when it comes to signaling.

In this on-going project, we explore the limits that are imposed on information exchange in this broader framework. With the aid of the newly-developed resource theory of causal connection [194], we explore the validity of processes in this extended scenario and their relation to physical constraints imposed on signaling. Though new possibilities for signaling are accessible in scenarios without a definite causal order, it is to be expected that even in such situation there must be limits to how much signaling is allowed. We show a preliminary numerical analysis of how one can "tweak" the amount of signaling permitted before rendering the process invalid, and try to sketch a picture of the geometry of the space of process matrices.

In the following section we introduce some already established concepts, namely the process matrix formalism itself and a selection of notions drawn from the resource theory of causality. Then, we present some preliminary results that point in the direction of a fundamental relation between signaling and the validity of a physical process. Finally, we outline the future of our research, the goals we want to achieve and the expected relevance of this project.

6.1 Preliminary concepts

6.1.1 Process matrices

We will briefly present the main results from [150], where the authors derive causal inequalities and provide examples of processes that violate them. Using the framework of process matrices, one can investigate situations where all that is assumed is the validity of quantum mechanics on a local level, but no further restriction is imposed when it comes to the scenario as a whole.

Consider the following task, dubbed the "OCB game", after Oreshkov, Costa and Brukner. Alice and Bob share a physical system, with which they can interact on their respective laboratories, separated from each other. Each of them receives a classical binary input, such as the result of a coin toss, a for Alice and b for Bob. Additionally, Bob receives an extra input $b' = \{0, 1\}$ that defines the task of the duo: if $b' = 0$ Alice must guess Bob's input b, and if $b' = 1$ Bob must guess Alice's input a. Upon receiving their share of the physical system, Alice and Bob can perform operations on it, and their closed laboratories will be opened just once, either to send the system out or to receive the system sent by the colleague.

Notice how there is a restriction to the signaling between the parties. Indeed, if Alice manages to send her system to Bob (and signal to him), then Bob cannot signal to Alice since the labs only open once. Consequently, effects on the probability of correctly guessing each other's inputs will appear. Let us denote x, y the guesses produced by Alice and Bob, respectively, and assume that these guesses are made regardless of which of the two tasks is being performed. Then, by also assuming a, b, b' are uniformly distributed, the probability of successfully completing the task is expressed as follows

$$P_{OCB} = \frac{1}{2}[p(x = b|b' = 0) + p(y = a|b' = 1)], \tag{6.1}$$

where $p(x = b|b' = 0)$ is the probability of Alice guessing Bob's input correctly (that is, producing a guess x that matches his input b), given that this is the task that was randomly picked ($b' = 0$), and similarly for $p(y = a|b' = 1)$.

The goal of the duo is to think of a strategy that maximizes this probability, and it is easy to see that

$$P_{OCB} \leq \frac{3}{4}, \tag{6.2}$$

Indeed, either Alice or Bob will not be able to signal to the other, so let us assume that Alice can signal her input to Bob. Then, $p(y = a|b' = 1) = 1$ because Bob will always guess her input correctly, but Alice must blindly guess his input and $p(x = b|b' = 0) = 1/2$. As a result, the probability of success of the whole scenario is 3/4.

In the original paper a lengthy proof of this upper bound is formally obtained, where three assumptions are openly made. First, it is assumed that a causal structure governs the scenario. In words, a causal structure is a set of events equipped with a partial order determining which events precede others events, resulting in only some directions of signaling being possible. By writing $A \prec B$ one denotes that event A is preceded by event B, or that A is in the causal past of B. Second, it is assumed that the variables a, b, b' are random and can only be correlated to events in their causal future, a assumption often referred to as "free will". Finally, it is assumed that the laboratories are closed at all times, except for the single moment they open to send or receive a system, implying that Alice's guess x can only be correlated to Bob's input b if x was generated in the causal past of Bob's system entering Alice's lab (and vice-versa for y and a).

In the main text, the authors however show that the upper bound for *eq.* (6.2) can be theoretically violated if one describes the operation performed (locally) in the laboratories with quantum mechanics but makes no assumptions regarding a global causal structure. Since nothing leads one to suspect the validity of the assumptions of free will and closed laboratories, it is suggested that one cannot assume the existence of an underlying causal structure.

To describe the most general possible scenarios that abide by local validity of quantum mechanics, one can use the process matrix formalism. In this framework, probabilities are obtained from the Born rule in terms of the operation that each party can perform on their physical system in the lab, as

$$p(a, b|x, y) = \text{Tr}[(M_{a|x}^{A_I A_O} \otimes M_{b|y}^{B_I B_O})W], \tag{6.3}$$

where $M_{a|x}^{A_I A_O} \in \mathcal{H}^{A_I} \otimes \mathcal{H}^{A_O}$ represent Alice's instruments, with input space $\mathcal{H}^{A_I}$ and output space $\mathcal{H}^{A_O}$, and similarly for Bob and $M_{b|y}^{B_I B_O} \in \mathcal{H}^{B_I} \otimes \mathcal{H}^{B_O}$, with input space $\mathcal{H}^{B_I}$ and output space $\mathcal{H}^{B_O}$.

As showed in [195], process matrices can be defined through the following linear restrictions

$$W \geq 0, \tag{6.4a}$$

$$\mathrm{Tr}[W] = d_{A_O} d_{B_O}, \tag{6.4b}$$

$$_{B_I B_O} W = {}_{A_O B_I B_O} W \tag{6.4c}$$

$$_{A_I A_O} W = {}_{A_I A_O B_O} W \tag{6.4d}$$

$$W = {}_{B_O} W + {}_{A_O} W - {}_{A_O B_O} W, \tag{6.4e}$$

where

$$_{A_I} W = \frac{\mathbb{1}_{A_I}}{d_{A_I}} \otimes \mathrm{Tr}_{A_I}[W] \tag{6.5}$$

denotes the trace-and-replace operation of Alice's input space, and similarly for the remaining spaces.

The first two constraints arise naturally from demanding the process matrix to yield a valid probability distribution according to eq. (6.3), that is, $p(a, b|x, y)$ are non-negative and normalized. Equation (6.4c) ensure that the events in Alice's lab are causally ordered and there can be no signaling from her output space to her input space. Similarly, eq. (6.4d) has an analogous interpretation for the events in Bob's lab.

Equation (6.4e) sets the relation between the types of signaling in process. Notice how $_{B_O} W$ cannot encode any signaling from Bob to Alice, as Bob's output space is trivial. Similarly, $_{A_O} W$ cannot encode any signaling from Alice to Bob. If one wants, then, to decompose a generic process W in terms of processes that only contain one-way signaling, one must account for the double counting of processes where not signaling at all in encoded, since they fit both $_{B_O} W$ and $_{A_O} W$. Thus, one must subtract the term $_{A_O B_O} W$, as both Alice's and Bob's output spaces are trivial and no signaling takes place.

Moreover, the three last constraints can be combined into a single one as

$$L_v[W] = W, \tag{6.6}$$

where L_v is the projection operator

$$L_v[W] = {}_{B_O} W + {}_{A_O} W - {}_{A_O B_O} W - {}_{B_I B_O} W + {}_{A_O B_I B_O} W - {}_{A_I A_O} W + {}_{A_I A_O B_O} W. \tag{6.7}$$

Though not being an *a priori* assumption, a process may admit a well-defined causal order, in which case bi-directional signaling is not allowed. Denote by $W^{A \prec B}$ a process where Alice can signal to Bob, and by $W^{B \prec A}$ a process in where signaling can take place in the opposite direction. A process W is said to be *causally separable* if there are $t \in [0, 1]$ and $W^{A \prec B}, W^{B \prec A}$ such that

$$W = t W^{A \prec B} + (1 - t) W^{B \prec A}, \tag{6.8}$$

that is, W is a convex combination of processes where only only party can signal to the other. If no decomposition as in eq. (6.8) is admitted, then the process is *non-separable*, and cannot be understood in a scenario where global causality prohibits bi-directional signaling. Such processes are the only ones that can violate causal inequalities, such as eq. (6.2) [196].

6.1.2   Signaling robustness

Let us now present some of the concepts used in [194] to construct a resource theory of causal connection. Following the usual steps in resource theory approaches [197, 198], the authors define free objects and transformations, as well as a measure for their resource, and incidentally construct objects that are useful to our research.

Let the set of valid process, that is, the set of matrices that satisfy eq. (6.4), be denoted by $\mathcal{W}_{proc}$. A subset of $\mathcal{W}_{proc}$ is $\mathcal{W}_{sep}$, the set of processes that admit a decomposition in the form of eq. (6.8), while $\mathcal{W}_{cns}$ denotes the processes that are causally non-separable.

Moreover, let $\mathcal{W}_{A \prec B}$ denote the processes where Alice precedes Bob, and $\mathcal{W}_{B \prec A}$ similarly for when Bob precedes Alice. The restrictions imposed on these sets is that Bob cannot signal to Alice if the process is in $\mathcal{W}_{A \prec B}$, and Alice cannot signal to Bob if the process is in $\mathcal{W}_{B \prec A}$. From this, two things can be concluded. First, from the definition of a separable process in eq. (6.8), we see that $\mathcal{W}_{sep}$ is the convex hull of the union of $\mathcal{W}_{A \prec B}$ and $\mathcal{W}_{B \prec A}$, that is, all possible convex combinations of processes where only one party can signal to the other. Second, one sees that the intersection of $\mathcal{W}_{A \prec B}$ and $\mathcal{W}_{B \prec A}$ defines the processes where no signaling is allowed, neither in one direction or the other, and one denotes the set of such processes by $\mathcal{W}_{par}$ (for parallel processes), see figure fig. 6.1 for clarity.
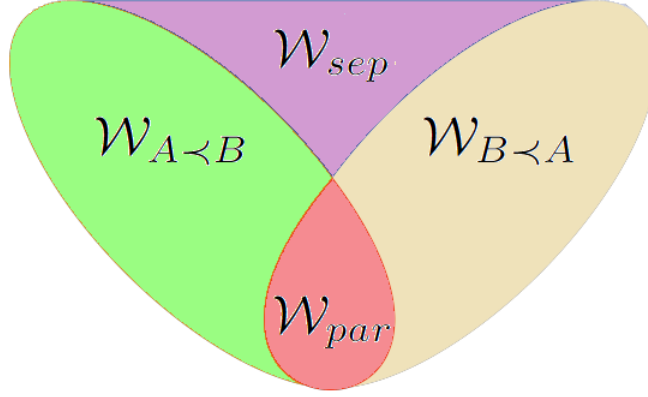
Figure 6.1: Graphical representation of the relation between the sets of causally ordered process matrices. From eq. (6.8), we know that the convex hull of $\mathcal{W}_{A \prec B}$ and $\mathcal{W}_{B \prec A}$ is $\mathcal{W}_{sep}$, and their intersection is $\mathcal{W}_{par}$. Every process represented in this figure belongs to the set $\mathcal{W}_{sep}$ of causally separable processes. Processes that do not admit a decomposition as in eq. (6.8) belong instead to $\mathcal{W}_{cns}$, not represented in the figure above. Graphic adapted from [194]

The authors of [194], then, propose using the robustness against worst-case noise as a measure of causal connection, that is, of how much signaling there is in a given process. We have already used similar concepts of robustness in this thesis, namely in chapter 5 for evaluating the incompatibility of a set of measurements, and in a similar way the signaling robustness of a process W is defined as

$$\mathcal{R}_s(W) = \min_{T \in \mathcal{W}_{proc}} \left\{ s \geq 0 \,\middle|\, \frac{W + sT}{s + 1} \in \mathcal{W}_{par} \right\}. \tag{6.9}$$

What the definition above is measuring is the distance between W and the set of processes where no signaling take place, by checking how much one has to convexly mix W with some other process T to make the resulting object non-signaling. If $\mathcal{R}_s(W) = 0$, then W is itself a non-signaling process, and any positive value for $\mathcal{R}_s(W)$ is a measure of how much signaling there is in W.

Notice how this procedure is similar to adding noise into W until is becomes non-signaling, except one also allows the optimization to consider different kinds of noise other than white (which here would correspond to a process matrix proportional to the identity operator). Putting this task in the form of an optimization problem yields

$$
\begin{aligned}
\textbf{given} \quad & W \\
\textbf{minimize} \quad & s \\
\textbf{subject to} \quad & \frac{W + sT}{s + 1} = \rho_{A_I B_I} \otimes \mathbb{1}_{A_O B_O} \\
& L_v[T] = T \\
& \mathrm{Tr}[T] = d_{A_O} d_{B_O} \\
& \mathrm{Tr}[\rho_{A_I B_I}] = 1 \\
& T \geq 0, \quad \rho_{A_I B_I} \geq 0, \quad s \geq 0.
\end{aligned}
\tag{6.10}
$$

Let us clarify some of the constraints in this task. As shown in [194], any process $W^{A \prec B}$ in $\mathcal{W}_{A \prec B}$ should have the form $W^{A \prec B} = W_{A_I A_O B_I} \otimes \mathbb{1}_{B_O}$. Intuitively, since these are the processes where Bob cannot signal to Alice, Bob's action on his output space should be trivial. A similar argument follows to show that processes where Alice cannot signal to Bob must have the form $W^{B \prec A} = W_{A_I B_I B_O} \otimes \mathbb{1}_{A_O}$. Then, since non-signaling processes are both in $\mathcal{W}_{A \prec B}$ and $\mathcal{W}_{B \prec A}$, one concludes that any process W^{par} in $\mathcal{W}_{par}$ must have the form $W^{par} = W_{A_I B_I} \otimes \mathbb{1}_{A_O B_O}$. It also follows from the normalization and

93

positivity constraints imposed on any process that $W_{A_I B_I}$ is a quantum state, that is, $W_{A_I B_I} \geq 0$ and $\text{Tr}[W_{A_I B_I}] = 1$.

In summary, the optimization in eq. (6.10) charges itself with two tasks. The first is demanding the process resulting from the mixing of W and T to be non-signaling, and the second is ensuring that T is itself a process matrix.

It is important to notice that the problem above is not in SDP form, since one optimizes over both s and T. However, a simple trick can be employed to circumvent this issue. Make $\tilde{T} = sT$, $\tilde{\rho}_{A_I B_I} = (1+s)\rho_{A_I B_I}$, and substitute $\tilde{T} = \tilde{\rho}_{A_I B_I} \otimes \mathbb{1}_{A_O B_O} - W$, and some quick algebra yields

$$
\begin{aligned}
\textbf{given} \quad & W \\
\textbf{minimize} \quad & \text{Tr}[\tilde{\rho}_{A_I B_I}] - 1 \\
\textbf{subject to} \quad & \tilde{\rho}_{A_I B_I} \otimes \mathbb{1}_{A_O B_O} - W \geq 0 \\
& \tilde{\rho}_{A_I B_I} \geq 0.
\end{aligned}
\tag{6.11}
$$

The authors in [194] also find the dual formulation of this SDP

$$
\begin{aligned}
\textbf{given} \quad & W \\
\textbf{minimize} \quad & \text{Tr}[WS] - 1 \\
\textbf{subject to} \quad & \mathbb{1}_{A_I B_I} - \text{Tr}_{A_O B_O}[S] \geq 0 \\
& S \geq 0.
\end{aligned}
\tag{6.12}
$$

In fact, it is further argued that the first constraint of the dual SDP can be substituted by an equality constraint without loss of generality. Indeed, for any optimal S (that is, S maximizes the objective function and satisfies the constraints), one can define

$$
S' = S + D \otimes \frac{\mathbb{1}_{A_O B_O}}{d_{A_O} d_{B_O}},
\tag{6.13}
$$

where

$$
D = \mathbb{1}_{A_I B_I} - \text{Tr}_{A_O B_O}[S] \geq 0.
\tag{6.14}
$$

S' clearly is also a feasible point, and one can see that $\text{Tr}[WS'] \geq \text{Tr}[WS]$, so it is also optimal.

The final result in [194] that is relevant to our work is the upper bound on $\mathcal{R}_s(W)$ that the authors find, that is, the maximum amount of signaling that a process can have. In the text of the paper, it is shown that

$$
\mathcal{R}_s(W) \leq d_O^2 - 1, \quad d_O := \max(d_{A_O} d_{B_O}).
\tag{6.15}
$$

This bound is saturated by processes such as

$$
W_{sat} = \frac{1}{d_{A_I}} \rho_{A_I} \otimes \Phi^+_{A_O B_I} \otimes \mathbb{1}_{B_O},
\tag{6.16}
$$

where $\Phi^+ = \sum_{ij} |ii\rangle\langle jj|$ is the Choi matrix of the identity channel. Such causally ordered processes can be interpreted as Alice preparing an initial state in her lab, sending it to Bob through a perfect channel, and Bob discarding his output.

We can finally move on to the findings we have achieved in our research.

6.2   Geometry of process matrices

In the following section we will present our unfinished work where we investigate what kind of physical restrictions are imposed on the amount of signaling a process allows. We come up with models that describe specific classes of process matrices, given in terms of parameter that can be associated to the amount of signaling that the process encodes. The goal is to explore the possibilities that employing the broader framework of process matrices brings, and we show that scenarios governed by standard causality structures yield an upper bound for the amount of signaling that can be overcome with processes that do not admit a global causal order. Employing other signaling measures inspired by $\mathcal{R}_s$, we draw relations between the distance of any process to the subsets $\mathcal{W}_{A \prec B}, \mathcal{W}_{B \prec A}, \mathcal{W}_{par}$, contributing to a geometrical interpretation of the whole set $\mathcal{W}_{proc}$

To explore our results, let us first dive a bit deeper into the process matrix formalism.

6.2.1 Decompositions of process matrices

In order to say anything about generic processes, it would be interesting to find a universal model of these objects, capable of parameterizing all possible processes, upon which one could impose restrictions and study its effects. If approached at this level of generality, this task is quite overwhelming, as too many parameters and non-linear constraints arise. Instead, one can investigate a subset of all possible processes, employing models that simplify the problem and render them somewhat more tractable.

This choice for a model may be well-motivated but it is in general far from simple, and studying good models can improve our understanding of what a valid process is, as well as its relation to signaling. Take for instance the decomposition induced by the restrictions that define what a process matrix is, which we re-write here for clarity. From eq. (6.4), we have

$$W = {}_{B_O}W + {}_{A_O}W - {}_{A_O B_O}W. \tag{6.17}$$

These individual terms can be shown to be process matrices themselves, that is, if W is a valid process then so are ${}_{B_O}W, {}_{A_O}W, {}_{A_O B_O}W$. One can, then, analyze the physical properties of each of these terms and extrapolate them to W. In ${}_{B_O}W$, Bob's output space is trivial, meaning there is no signaling from Bob to Alice, and vice-versa for ${}_{A_O}W$, while ${}_{A_O B_O}W$, in turn, is a non-signaling process.

Given a matrix W, one can easily determine whether or not it corresponds to a valid process, it suffices to check for positivity and the correct normalization, as well as ensuring that $L_v[W] = W$. Then, one can apply the suitable trace-and-replace operations to obtain the terms in eq. (6.17), which contain information about the signaling in the process.

However, building a valid process matrix starting from a given decomposition is a much harder task. Take valid ${}_{B_O}W, {}_{A_O}W, {}_{A_O B_O}W$, and combining them according to eq. (6.17) does not necessarily yield a W that obeys all the restrictions in eq. (6.4). This shows that a process matrix is a complex object, and not any scenario is physically possible.

To explore the restrictions that are imposed on valid processes, we investigate some specific models. Take $d_{A_I} = d_{A_O} = d_{B_I} = d_{B_O} = 2$ and let ${}_{B_O}W, {}_{A_O}W, {}_{A_O B_O}W$ assume the form

$$\begin{aligned}
{}_{B_O}W_p &= \frac{\mathbb{1}_{A_I B_O}}{2} \otimes \left[p\Phi^+_{A_O B_I} + (1-p)\frac{\mathbb{1}_{A_O B_I}}{2} \right], \\
{}_{A_O}W_q &= \frac{\mathbb{1}_{A_O B_I}}{2} \otimes \left[q\Phi^+_{A_I B_O} + (1-q)\frac{\mathbb{1}_{A_I B_O}}{2} \right], \\
{}_{A_O B_O}W &= \frac{\mathbb{1}_{A_I A_O B_I B_O}}{4}.
\end{aligned} \tag{6.18}$$

These are not the most general form that these terms can assume, but they are enough to model a great range of processes by tweaking the parameters $p, q \in [0, 1]$.

Recall that ${}_{B_O}W$ is interpreted as an object that encodes the signaling from Alice to Bob. In the model above, this term describes a process where Alice has a one-way imperfect channel to Bob, subject to noise parameterized by p. For $p = 1$ she can perfectly signal to Bob using an identity channel, while for $p = 0$ the resulting channel is trivial. Thus, p is a quantifier for the signaling that happens from Alice to Bob. A similar reasoning can be followed to conclude that q quantifies the signaling from Bob to Alice.

One may now wonder what values of p, q will yield ${}_{B_O}W_p$ and ${}_{A_O}W_q$ that, when combined according to eq. (6.17), result in a matrix that satisfies the necessary restrictions in eq. (6.4), that is, that result is a valid process. In a sense, what is being asked is how much signaling can one allow in either direction before the resulting process is no longer physical.

This kind of question can, fortunately, be answered with SDPs. One constructs W resulting from this modeling of ${}_{B_O}W_p, {}_{A_O}W_q, {}_{A_O B_O}W$ in terms of p, q and looks for the maximum values that the parameters can assume while W still satisfy eq. (6.4). The result is not surprising, as we get that valid processes are generated whenever

$$p + q \leq 1. \tag{6.19}$$

Notice how any process described by this model is inevitably causally separable, as it is simply a combination of two one-way noisy channels. This result, then, reinforces the intuition that these mundane processes do not showcase any extraordinary relation between the signaling from Alice to Bob and from Bob to Alice. Both p and q are upper bounded by 1, which is interpreted as an upper bound for one-way signaling, and this same upper bound is shared by their sum, such that there is a trade-off to how much

signaling each party is allowed: Alice and Bob cannot surpass the upper bound of 1 to the total amount of signaling in the whole process.

But what about processes that do not admit a decomposition such as eq. (6.8), that is, processes that are causally non-separable? These processes may violate causal inequalities and correspond to protocols where advantages in communication can be achieved, so it would be reasonable to expect that somehow signaling can be enhanced is such scenarios.

Looking back at the protocol explored in section 6.1.1, where two parties try to guess each other's input, it is known from [150] that the following process matrix surpasses the success probability of $P_{suc} = 3/4$ and violates a causal inequality

$$W_{OCB} = \frac{1}{4}\left[\mathbb{1}_{A_I A_O B_I B_O} + \frac{1}{\sqrt{2}}(\mathbb{1}_{A_I} \otimes Z_{A_O} \otimes Z_{B_I} \otimes \mathbb{1}_{B_O} + Z_{A_I} \otimes \mathbb{1}_{A_O} \otimes X_{B_I} \otimes Z_{B_O})\right], \qquad (6.20)$$

where X, Z are the Pauli operators in the x and z-directions, respectively. One can take inspiration from this process to construct yet another model for a class of process matrices, now defined in terms of parameters p, q and a decomposition given by

$$\begin{aligned} {}_{B_O}W_p &= \frac{1}{4}\mathbb{1}_{A_I A_O B_I B_O} + \frac{p}{4}\mathbb{1}_{A_I} \otimes Z_{A_O} \otimes Z_{B_I} \otimes \mathbb{1}_{B_O}, \\ {}_{A_O}W_q &= \frac{1}{4}\mathbb{1}_{A_I A_O B_I B_O} + \frac{q}{4}Z_{A_I} \otimes \mathbb{1}_{A_O} \otimes X_{B_I} \otimes Z_{B_O}, \\ {}_{A_O B_O}W &= \frac{\mathbb{1}_{A_I A_O B_I B_O}}{4}. \end{aligned} \qquad (6.21)$$

The model above, just like the previous one, is quantifying the signaling from Alice to Bob through p and the signaling from Bob to Alice through q. In ${}_{B_O}W_p$, the lower p is the closer this term corresponds to the trivial channel, and similarly for ${}_{A_O}W_q$ and q. It is easy to realize how this model describes processes that are completely different from the previous one. Furthermore, one can easily see that setting $p = q = 1/\sqrt{2}$ recovers W_{OCB}.

If one takes ${}_{B_O}W_p, {}_{A_O}W_q, {}_{A_O B_O}W$ in the form above and construct a matrix using eq. (6.17), one can once again use an SDP to check which values of p and q will yield valid processes. Surprisingly enough, the restriction that the parameter must abide is now

$$p^2 + q^2 \leq 1. \qquad (6.22)$$

It is important to highlight how qualitatively different this restriction is from the one imposed on eq. (6.19), since here Alice and Bob can, together, overcome the boundary of total signaling, coded by the sum $p + q$, amounting to 1. Indeed, just like before, the maximum value for signaling achieved by employing only one-way signaling is still $p = 1$ or $q = 1$, meaning either Alice or Bob having access to a perfect channel with which one of them can signal to the other. However, unlike in eq. (6.19), there is still room for more signaling in the other direction. In other words, it is suggested that, for processes that can be modeled as in eq. (6.21), it is possible to have more overall signaling than in processes described by eq. (6.18), a feat mathematically expressed by the possibility of $p + q > 1$.

Quite intuitively, this difference on the nature of the restriction that is imposed on signaling in eqs. (6.18) and (6.21) is not the only thing that set these two models apart. In fact, while eq. (6.18) described a class of causally separable processes (that is, processes that belong to $\mathcal{W}_{sep}$), the processes modeled by eq. (6.21) do not admit the decomposition into a convex mixture of causally ordered processes in eq. (6.8), and are thus causally non-separable (and belong to $\mathcal{W}_{cns}$). It is reasonable to expect processes in $\mathcal{W}_{csn}$ to be able to encode more signaling than those in $\mathcal{W}_{sep}$, as these processes can violate causal inequalities which often correspond to advantages in communication tasks.

6.2.2 Different measures of signaling

Inspired by these numerical preliminary results suggesting a strong connection between the amount of signaling a process can encode and the nature of the causality structure that it requires, we have conducted more careful analyses, now using a proper measure for different classes of signaling.

In the same spirit of $\mathcal{R}_s$, a measure for signaling obtained by evaluating the distance of a given process to the set $\mathcal{W}_{par}$ of non-signaling processes, one can define different measures for other kinds of signaling. Following the steps laid out in in [194], one can analogously construct a measure for one-way signaling,

for instance, from Alice to Bob. This can be done by evaluating the distance of a process to the set $\mathcal{W}_{A\prec B}$ of processes where Alice's operations precede Bob's, and thus Bob cannot signal to Alice.

The quantity that results from this analysis measures how much signaling in only a given direction is encoded in a process. Like $\mathcal{R}_s$, this new object is a robustness measure against worst-case scenario noise, defined analogously as

$$\mathcal{R}_{A\prec B}(W) = \min_{T \in \mathcal{W}_{proc}} \left\{ s \geq 0 \, \middle| \, \frac{W + sT}{s + 1} \in \mathcal{W}_{A\prec B} \right\}. \tag{6.23}$$

Recall that, as argued in [194], any process in $\mathcal{W}_{A\prec B}$ must have a trivial output space for Bob, since he cannot signal to Alice by definition. Consequently, $\mathcal{R}_{A\prec B}$ can also be cast as an optimization task

$$
\begin{aligned}
\textbf{given} \quad & W \\
\textbf{minimize} \quad & s \\
\textbf{subject to} \quad & \frac{W + sT}{s + 1} = \Omega^{A\prec B}_{A_I A_O B_I} \otimes \mathbb{1}_{B_O} \\
& L_v[T] = T \\
& \text{Tr}[T] = d_{A_O} d_{B_O} \\
& \text{Tr}[\Omega^{A\prec B}_{A_I A_O B_I}] = d_{A_O} \\
& T \geq 0, \quad \Omega_{A_I A_O B_I} \geq 0, \quad s \geq 0.
\end{aligned}
\tag{6.24}
$$

To make this optimization suitable to an SDP formulation, we make the substitutions

$$
\begin{aligned}
\tilde{\Omega}^{A\prec B}_{A_I A_O B_I} &= (1 + s)\Omega^{A\prec B}_{A_I A_O B_I} \\
\tilde{T} &= Ts \\
\tilde{T} &= \tilde{\Omega}^{A\prec B}_{A_I A_O B_I} \otimes \mathbb{1}_{B_O} - W
\end{aligned}
\tag{6.25}
$$

which finally yield the SDP

$$
\begin{aligned}
\textbf{given} \quad & W \\
\textbf{minimize} \quad & \frac{\text{Tr}[\tilde{\Omega}^{A\prec B}_{A_I A_O B_I}]}{2} - 1 \\
\textbf{subject to} \quad & \tilde{\Omega}^{A\prec B}_{A_I A_O B_I} \otimes \mathbb{1}_{B_O} - W \geq 0 \\
& \tilde{\Omega}^{A\prec B}_{A_I A_O B_I} \geq 0.
\end{aligned}
\tag{6.26}
$$

A lengthy but straightforward evaluation of the Lagrangian of the problem above yields its dual formulation

$$
\begin{aligned}
\textbf{given} \quad & W \\
\textbf{minimize} \quad & \frac{\text{Tr}[WS]}{d_{A_O}} - 1 \\
\textbf{subject to} \quad & \mathbb{1}_{A_I A_O B_I} - \text{Tr}_{B_O}[S] \geq 0 \\
& S \geq 0.
\end{aligned}
\tag{6.27}
$$

What have done so far was to construct a measure for a specific kind of signaling encoded in a process: the signaling that can occur from Alice to Bob. By evaluating the distance between a process matrix W and $\mathcal{W}_{A\prec B}$, $\mathcal{R}_{A\prec B}(W)$ imposes restrictions on the geometry of the set of process matrices. As shown in [194], we know that $\mathcal{R}_s(W)$ is limited by the upper bound in eq. (6.15), and we now follow the same steps to show that a similar upper bound is imposed on $\mathcal{R}_{A\prec B}(W)$

$$\mathcal{R}_{A\prec B}(W) \leq d_O^2 - 1, \quad d_O := \max(d_{A_O} d_{B_O}). \tag{6.28}$$

The details of the calculation can be found in appendix G.

Given the intrinsic symmetry between the sets $\mathcal{W}_{A \prec B}$ and $\mathcal{W}_{B \prec A}$, as one is constituted by the processes where Bob cannot signal to Alice while the other consists of processes where Alice cannot signal to Bob, whatever results we have reached for $\mathcal{R}_{A \prec B}$ can be easily carried over to $\mathcal{R}_{B \prec A}$ by simply swapping Alice's spaces with those of Bob, so we can also conclude that

$$\mathcal{R}_{B \prec A}(W) \leq d_O^2 - 1. \tag{6.29}$$

These bounds are tight, and are saturated by processes that encode a perfect one-way channel, as the example provided in appendix G.

We can now analyze how these three measures for different kinds of signaling are interconnected.

6.2.3 Relation between the different robustness measures

It is fruitful to notice how the upper bounds for $\mathcal{R}_s$, $\mathcal{R}_{A \prec B}$ and $\mathcal{R}_{B \prec A}$ are consistent with each other. Indeed, the fact that the upper bound for $\mathcal{R}_s$ is not higher than those of $\mathcal{R}_{A \prec B}$ and $\mathcal{R}_{B \prec A}$ was to be expected, since $\mathcal{R}_s$ measures the distance to $\mathcal{W}_{par}$, which is, in turn, a subset of $\mathcal{W}_{A \prec B}$ and $\mathcal{W}_{A \prec B}$.

Though distinct concepts, one can clearly see, then, that these robustness measures are not completely independent, and whatever relationship there is between them helps constructing a geometrical structure of the set of process matrices. Though each of these measures is upper-bounded by the same limit, there must surely be a trade-off when all three of them are considered, and a single process cannot saturate all of these bounds.

If one want to go further and investigate the nature of the signaling encoded in a process, it is necessary to come up with a quantifier that combines the notions provided by $\mathcal{R}_s$, $\mathcal{R}_{A \prec B}$ and $\mathcal{R}_{B \prec A}$, that would, in turn, reflect a physical restriction of overall signaling that every process should obey.

In the next section, we introduce numerical results that have to be taken in consideration when looking for a physical restriction on the amount of signaling a process can encode.

6.3 Results and discussion

Let us start by defining some models that describe different classes of process matrices, with distinct physical properties. After that is done, we can evaluate the different values of signaling robustness that associated to these processes, and evaluate their joint behavior to try to comprehend what is the relation that they are obeying.

We already have two models available. The first one, in eq. (6.18), describes a class of separable process matrices, in terms of parameters p, q, constructed with a convex mixture of two perfect one-way signaling channels. We will dub the processes yielded by this model $W_{\Phi^+}(p, q)$. Similarly, the second model we already have at hand is the one in eq. (6.21), obtained as a generalization of W_{OCB}. We dub the processes described by it in terms of p, q as $W_{OCB}(p, q)$.

Some other models can be introduced. Let

$$W_{GYNI}(p, q) = \frac{1}{4} \left(\mathbb{1}^{\otimes 4} + p \, ZZZ\mathbb{1} + q \, Z\mathbb{1}XX \right), \tag{6.30}$$

once again with $p, q \in [0, 1]$. For the sake of keeping the expression above clean, we have dropped the tensor product $\otimes$ between the operators, so $ZZZ\mathbb{1}$ should be understood as $Z_{A_I} \otimes Z_{A_O} \otimes Z_{B_I} \otimes \mathbb{1}_{B_O}$, and so on.

This model is inspired by a process defined in [196], which violates a causal inequality derived from a communication task called "guess you neighbor's input", and the original process is recovered for $p = q = 1/\sqrt{2}$.

Finally, we introduce a particular process

$$\begin{aligned} W_{max} = \frac{1}{4} \left(\mathbb{1} + a_0 Z\mathbb{1}Z\mathbb{1} - a_1(Z\mathbb{1}\mathbb{1}\mathbb{1} + \mathbb{1}\mathbb{1}Z\mathbb{1}) - a_2(Z\mathbb{1}\mathbb{1}Z + \mathbb{1}ZZ\mathbb{1}) \right. \\ \left. + a_3(Z\mathbb{1}ZZ + ZZZ\mathbb{1}) + a_4(Z\mathbb{1}XX - Z\mathbb{1}YY + XXZ\mathbb{1} - YYZ\mathbb{1}) \right), \end{aligned} \tag{6.31}$$

with $a_0 = 0.2744$, $a_1 = 0.2178$, $a_2 = 0.3628$, $a_3 = 0.3114$ and $a_4 = 0.2097$. Here, we have also dropped the tensor product between operators.

This process was introduced in [196], where it was found to be the one that maximally violates the causal inequality obtained from the OCB game, described in section 6.1.1, a causally non-separable process.

We have also analyzed the robustness measures for signaling in a batch of 10.000 process matrices that we sampled[1]. We restricted ourselves to processes that, like W_{Φ^+}, W_{OCB} and W_{GYNI}, have $_{A_O B_O} W$ being the identity.

The following table summarizes our results, obtained numerically by running several SDPs to evaluate the different signaling robustness measures.

W	$\mathcal{R}_s$	$\mathcal{R}_{A \prec B}$	$\mathcal{R}_{B \prec A}$
$W_{\Phi^+}(p,q)$	3	$3q$	$3p$
$W_{OCB}(p,q), W_{GYNI}(p,q)$	1	q	p
W_{max}	1.1588	0.5794	0.5794
$W_{random}^{\mathbb{1}}$	< 1.2	< 0.8	< 0.8

Table 6.1: Table showing the robustness of different classes of process matrices.

Some things can be noted from this table, not all of them being intuitive. First of all, even though non-separable processes like $W_{OCB}(p,q), W_{GYNI}(p,q)$ were expected to encode more signaling than separable processes such as $W_{\Phi^+}(p,q)$, the robustness of these processes was lower for all three kinds of signaling. Second, W_{max} produces a larger violation of the OCB inequality than $W_{OCB}(p,q)$ for any value of p,q, and yet it is less robust according to $\mathcal{R}_{A \prec B}$ or $\mathcal{R}_{A \prec B}$ for a range of values for p,q. More surprising still, the robustness of W_{max} is surpassed even by random process matrices.

One can, however, see from the models of $W_{\Phi^+}(p,q)$, $W_{OCB}(p,q)$ and $W_{GYNI}(p,q)$ that, indeed, there is an interplay between the different types of robustness, and a trade-off must be obeyed (here made explicit by the fact that p and q in all of these models are not independent of each other).

These counter-intuitive behavior of robustness in these processes makes it hard to devise what is the rule determining how much signaling a process can encode, which would in turn reveal more about the geometry of the set of processes. A lengthy discussion is still needed in order to define what would even be a good measure for overall signaling.

The future of this project is still open, but we have many fronts to tackle. Our main goal is to find a relation between $\mathcal{R}_s$, $\mathcal{R}_{A \prec B}$ and $\mathcal{R}_{B \prec A}$ that is being obeyed, from which we could learn much about the nature of signaling in any process. To do that, some preliminary steps can be traced.

It would be great to obtain analytical results to extrapolate our numerical results. As $\mathcal{R}_s$, $\mathcal{R}_{A \prec B}$ and $\mathcal{R}_{B \prec A}$ are obtained from an SDP, this task goes through finding good guesses for optimal solutions and comparing them to the dual formulation of these problems. This is not an easy task, specially for the general case that we want to build.

It would also be interesting to find what is the process that encodes the most signaling. One could then compare it to the process that produces the maximal violation of causal inequalities, which is also unknown. This process would be the most resourceful process in terms of signaling, and could be explored in communication tasks with maximum advantage, perhaps.

Finally, it is known from [194] that the bound for $\mathcal{R}_s$ is saturated by processes of the form W_{sat}, but it is not known if this is the only process to achieve the bound. Given that W_{sat} is a causally separable, we wonder if no process that is not causally ordered can also saturate it.

So far, a main lesson we have learned from these analysis is that the interplay between different kinds of signaling is a complex one, and a good candidate for a measure of overall signaling must take these subtleties into account. Once this quantity has been established, it will be easier to identify what is the physical restriction on signaling that is being obeyed by all processes.

---

[1]This sampling process was not random, as there is no random measure for the set of process matrices, but we followed a procedure of randomly sampling unitary matrices and projecting them onto the space of processes with L_v. We then still had to check that the resulting matrix was still positive.

Concluding remarks

A famous quote, widely attributed to Richard Feynman, states that "if you think you understand quantum mechanics, you don't understand quantum mechanics" (similar quotes are attributed to Niels Bohr, John Wheeler, and surely many others outside my knowledge). Perhaps I can add to this piece of wisdom that, in fact, the more you learn about quantum mechanics the less you understand it, as this has been my own personal experience.

I say this in the most favorable way possible. The role of science in society is to provide an objective and reliable method to investigate phenomena, but, just like art, I believe science is a precious matter on its own. Beyond its usefulness, science has the power (and I dare say, duty) to instigate our minds and push the boundaries of human knowledge. What better medium to cultivate curiosity than a field populated by counter-intuitive phenomena, inaccessible regions and overall utter beauty?

Through the last four years, I have let myself be guided by this spark and actively sought "not understanding". "Not understanding" is not a bad thing, in fact "not understanding" is a great place to be. It means the possibilities are endless, and once one embraces the uncomfortable realization that maybe some things simply cannot be known, one can focus on the next step: determining what can be understood and what must remain a mystery.

I believe the quantum-to-classical transition can, indeed, be understood. The disparities between the behavior of systems on quantum and classical regimes are undeniable, but I do not see why they could not be bridged by a neat theory. Though there are many different aspects of the transition that need to be explained, I believe our works in part I are modest, yet valuable, contributions to this goal. In both chapters 1 and 2, the main point we make is that, in order to overcome the gap between microscopic and effective descriptions of a system, one must adopt realistic, physically motivated characterization of the scenario. We do so by employing coarse-graining maps, including imprecision into the measurements that model our limited access to information in the lab.

However, other areas of foundations of quantum mechanics will remain an enigma, and trying to "solve" non-locality, contextuality or steering by making it somehow fit our classical intuition is, in my opinion, a petty goal. Yet in part II, we are pushing the boundaries of what *can* be known in such counter-intuitive scenarios. In chapter 4, we address the issue of characterizing the set of d-quantum behaviors, by providing criteria for a behavior to admit a d-dimensional quantum realization. There, we also show how to evaluate contextuality inequalities when, similarly, we impose restrictions on the dimension of the physical system, proposing SDP implementations of the optimizations tasks that arise from both these queries. In chapter 5, we also devised criteria to ascertain that, in a one-side-device-independent approach to a bipartite steering scenario, Alice must have access to at least a given amount of incompatible measurements. In chapter 6, we explore how signaling determines what processes (in particular, those without causal order) are physical and how this resource shapes the geometry of the set of process matrices.

If you made it this far, I hope my work can be of some use to you. I would also be very satisfied if my work is completely useless for any practical reason but inspires a good conversation among colleagues with a moderate amount of alcohol nearby. I am always available to discussions.

I am happy that for every question I answered in this thesis, a couple new questions emerged. Most of these will certainly be answered in the future, either by me or by colleague scientists, but I wonder which will remain unanswered. As Tim Hickson put in an essay not at all related to quantum mechanics, "when we wonder about these questions, there's something left in that gap - wonder".

Bibliography

[1] Isadora Veeren and Fernando de Melo. Entropic uncertainty relations and the quantum-to-classical transition. *Physical Review A*, 102(2):022205, 2020.

[2] Xiao-Dong Yu, Isadora Veeren, and Otfried Gühne. Characterizing finite-dimensional quantum contextuality. *arXiv preprint arXiv:2212.11559*, 2022.

[3] Steven K Lamoreaux. The casimir force: background, experiments, and applications. *Reports on progress in Physics*, 68(1):201, 2004.

[4] Albert Einstein. The photoelectric effect. *Ann. Phys*, 17(132):4, 1905.

[5] Yaduvir Singh. *Semiconductor devices*. IK International Pvt Ltd, 2013.

[6] Anant V Narlikar. *Superconductors*. Oxford University Press, 2014.

[7] Erwin Schrödinger. Der stetige übergang von der mikro-zur makromechanik. *Naturwissenschaften*, 14(28):664–666, 1926.

[8] Stefan Gerlich, Sandra Eibenberger, Mathias Tomandl, Stefan Nimmrichter, Klaus Hornberger, Paul J Fagan, Jens Tüxen, Marcel Mayor, and Markus Arndt. Quantum interference of large organic molecules. *Nature communications*, 2(1):1–5, 2011.

[9] Ralf Riedinger, Andreas Wallucks, Igor Marinković, Clemens Löschnauer, Markus Aspelmeyer, Sungkun Hong, and Simon Gröblacher. Remote quantum entanglement between two micromechanical oscillators. *Nature*, 556(7702):473–477, 2018.

[10] Stéphane Barland, P Azam, GL Lippi, RA Nyman, and R Kaiser. Photon thermalization and a condensation phase transition in an electrically pumped semiconductor microresonator. *Optics Express*, 29(6):8368–8375, 2021.

[11] Tobias Bothwell, Dhruv Kedar, Eric Oelker, John M Robinson, Sarah L Bromley, Weston L Tew, Jun Ye, and Colin J Kennedy. Jila sri optical lattice clock with uncertainty of. *Metrologia*, 56(6):065004, 2019.

[12] Vojtěch Havlíček, Antonio D Córcoles, Kristan Temme, Aram W Harrow, Abhinav Kandala, Jerry M Chow, and Jay M Gambetta. Supervised learning with quantum-enhanced feature spaces. *Nature*, 567(7747):209–212, 2019.

[13] K Wright, KM Beck, S Debnath, JM Amini, Y Nam, N Grzesiak, J-S Chen, NC Pisenti, M Chmielewski, C Collins, et al. Benchmarking an 11-qubit quantum computer. *Nat. Commun.*, 10(1):1–6, 2019.

[14] Frank Arute, Kunal Arya, Ryan Babbush, Dave Bacon, Joseph C Bardin, Rami Barends, Rupak Biswas, Sergio Boixo, Fernando GSL Brandao, David A Buell, et al. Quantum supremacy using a programmable superconducting processor. *Nature*, 574(7779):505–510, 2019.

[15] Amir O Caldeira and Anthony J Leggett. Influence of dissipation on quantum tunneling in macroscopic systems. *Physical Review Letters*, 46(4):211, 1981.

[16] Maximilian A Schlosshauer. *Decoherence: and the quantum-to-classical transition*. Springer Science & Business Media, 2007.

[17] Wojciech Hubert Zurek. Decoherence and the transition from quantum to classical—revisited. In *Quantum Decoherence: Poincaré Seminar 2005*, pages 1–31. Springer, 2007.

[18] Wojciech Hubert Zurek. Quantum darwinism. *Nature physics*, 5(3):181–188, 2009.

[19] Fernando GSL Brandao, Marco Piani, and Paweł Horodecki. Generic emergence of classical features in quantum darwinism. *Nature communications*, 6(1):1–8, 2015.

[20] Roberto D Baldijão, Rafael Wagner, Cristhiano Duarte, Bárbara Amaral, and Marcelo Terra Cunha. Emergence of noncontextuality under quantum darwinism. *PRX Quantum*, 2(3):030351, 2021.

[21] Don N Page. Does decoherence make observations classical? *arXiv preprint arXiv:2108.13428*, 2021.

[22] Christopher A Fuchs and Rüdiger Schack. Bayesian conditioning, the reflection principle, and quantum decoherence. In *Probability in physics*, pages 233–247. Springer, 2011.

[23] Anthony J Leggett. Probing quantum mechanics towards the everyday world: where do we stand? *Physica Scripta*, 2002(T102):69, 2002.

[24] Anthony J Leggett. Testing the limits of quantum mechanics: motivation, state of play, prospects. *Journal of Physics: Condensed Matter*, 14(15):R415, 2002.

[25] Cristhiano Duarte, Gabriel Dias Carvalho, Nadja K Bernardes, and Fernando de Melo. Emerging dynamics arising from coarse-grained quantum systems. *Physical Review A*, 96(3):032113, 2017.

[26] David Poulin. Macroscopic observables. *Physical Review A*, 71(2):022102, 2005.

[27] Oleg Kabernik. Quantum coarse graining, symmetries, and reducibility of dynamics. *Physical Review A*, 97(5):052130, 2018.

[28] N David Mermin. Quantum mechanics vs local realism near the classical limit: A bell inequality for spin s. *Physical Review D*, 22(2):356, 1980.

[29] Hyunseok Jeong, Youngrong Lim, and MS Kim. Coarsening measurement references and the quantum-to-classical transition. *Physical review letters*, 112(1):010402, 2014.

[30] Johannes Kofler and Časlav Brukner. Conditions for quantum violation of macroscopic realism. *Physical review letters*, 101(9):090403, 2008.

[31] Sadegh Raeisi, Pavel Sekatski, and Christoph Simon. Coarse graining makes it hard to see micro-macro entanglement. *Physical review letters*, 107(25):250401, 2011.

[32] Tian Wang, Roohollah Ghobadi, Sadegh Raeisi, and Christoph Simon. Precision requirements for observing macroscopic quantum effects. *Physical Review A*, 88(6):062114, 2013.

[33] Pedro Silva Correia and Fernando de Melo. Spin-entanglement wave in a coarse-grained optical lattice. *Physical Review A*, 100(2):022334, 2019.

[34] Jiyong Park, Se-Wan Ji, Jaehak Lee, and Hyunchul Nha. Gaussian states under coarse-grained continuous variable measurements. *Physical Review A*, 89(4):042102, 2014.

[35] Iwo Bialynicki-Birula and Łukasz Rudnicki. Entropic uncertainty relations in quantum physics. *Statistical Complexity*, pages 1–34, 2011.

[36] xkcd - a webcomic of romance, sarcasm, math, and language. https://xkcd.com/824/. Accessed: 01-02-2023.

[37] Werner Heisenberg. Über den anschaulichen inhalt der quantentheoretischen kinematik und mechanik. In *Original Scientific Papers Wissenschaftliche Originalarbeiten*, pages 478–504. Springer, 1985.

[38] Howard Percy Robertson. The uncertainty principle. *Physical Review*, 34(1):163, 1929.

[39] J v Neumann. Beweis des ergodensatzes und desh-theorems in der neuen mechanik. *Zeitschrift für Physik*, 57(1):30–70, 1929.

[40] David Deutsch. Uncertainty in quantum measurements. *Physical Review Letters*, 50(9):631, 1983.

[41] Patrick J. Coles, Mario Berta, Marco Tomamichel, and Stephanie Wehner. Entropic uncertainty relations and their applications. *Rev. Mod. Phys.*, 89:015002, Feb 2017.

[42] Michael A Nielsen and Isaac L Chuang. Quantum computation and quantum information. *Phys. Today*, 54(2):60, 2001.

[43] Karl Kraus. Complementary observables and uncertainty relations. *Physical Review D*, 35(10):3070, 1987.

[44] Hans Maassen and Jos BM Uffink. Generalized entropic uncertainty relations. *Physical Review Letters*, 60(12):1103, 1988.

[45] Roy J Glauber. Coherent and incoherent states of the radiation field. *Physical Review*, 131(6):2766, 1963.

[46] FT Arecchi, Eric Courtens, Robert Gilmore, and Harry Thomas. Atomic coherent states in quantum optics. *Physical Review A*, 6(6):2211, 1972.

[47] Anthony J Leggett and Anupam Garg. Quantum mechanics versus macroscopic realism: Is the flux there when nobody looks? *Physical Review Letters*, 54(9):857, 1985.

[48] Ivan N Sanov. *On the probability of large deviations of random variables.* United States Air Force, Office of Scientific Research, 1958.

[49] Ludwig Boltzmann. *Über die Beziehung zwischen dem zweiten Hauptsatze des mechanischen Wärmetheorie und der Wahrscheinlichkeitsrechnung, respective den Sätzen über das Wärmegleichgewicht.* Kk Hof-und Staatsdruckerei, 1877.

[50] Imre Csiszár and János Körner. *Information theory: coding theorems for discrete memoryless systems.* Cambridge University Press, 2011.

[51] Linda E Reichl. A modern course in statistical physics, 1999.

[52] Álvaro M Alhambra, Lluis Masanes, Jonathan Oppenheim, and Christopher Perry. Fluctuating work: From quantum thermodynamical identities to a second law equality. *Physical Review X*, 6(4):041017, 2016.

[53] Leon Brillouin. *Science and information theory.* Courier Corporation, 2013.

[54] Arthur Eddington. *The nature of the physical world: THE GIFFORD LECTURES 1927*, volume 23. BoD–Books on Demand, 2019.

[55] William Thomson. Xv.—on the dynamical theory of heat, with numerical results deduced from mr joule's equivalent of a thermal unit, and m. regnault's observations on steam. *Earth and Environmental Science Transactions of The Royal Society of Edinburgh*, 20(2):261–288, 1853.

[56] Rudolf Clausius. Über eine veränderte form des zweiten hauptsatzes der mechanischen wärmetheorie. *Annalen der Physik*, 169(12):481–506, 1854.

[57] YVC Rao. *An introduction to thermodynamics.* Universities Press, 2004.

[58] Sheldon Goldstein, Joel L Lebowitz, Roderich Tumulka, and Nino Zanghì. Gibbs and boltzmann entropy in classical and quantum mechanics. In *Statistical mechanics and scientific explanation: Determinism, indeterminism and laws of nature*, pages 519–581. World Scientific, 2020.

[59] John Von Neumann. Thermodynamik quantenmechanischer gesamtheiten. *Nachrichten von der Gesellschaft der Wissenschaften zu Göttingen, Mathematisch-Physikalische Klasse*, 1927:273–291, 1927.

[60] M Grabowski and P Staszewski. On continuity properties of the entropy of an observable. *Reports on Mathematical Physics*, 11(2):233–237, 1977.

[61] Anatoli Polkovnikov. Microscopic diagonal entropy and its connection to basic thermodynamic relations. *Annals of Physics*, 326(2):486–499, 2011.

[62] JM Deutsch, Haibin Li, and Auditya Sharma. Microscopic origin of thermodynamic entropy in isolated systems. *Physical Review E*, 87(4):042135, 2013.

[63] Dominik Šafránek, JM Deutsch, and Anthony Aguirre. Quantum coarse-grained entropy and thermalization in closed systems. *Physical Review A*, 99(1):012103, 2019.

[64] Maciej Lewenstein, Anna Sanpera, and Veronica Ahufinger. *Ultracold Atoms in Optical Lattices: Simulating quantum many-body systems*. OUP Oxford, 2012.

[65] Pedro Silva Correia, Paola Concha Obando, Raúl O Vallejos, and Fernando de Melo. Macro-to-micro quantum mapping and the emergence of nonlinearity. *Physical Review A*, 103(5):052210, 2021.

[66] Christopher Jarzynski. Nonequilibrium equality for free energy differences. *Physical Review Letters*, 78(14):2690, 1997.

[67] Gavin E Crooks. Nonequilibrium measurements of free energy differences for microscopically reversible markovian systems. *Journal of Statistical Physics*, 90:1481–1487, 1998.

[68] Christopher Jarzynski. Equalities and inequalities: Irreversibility and the second law of thermodynamics at the nanoscale. *Annu. Rev. Condens. Matter Phys.*, 2(1):329–351, 2011.

[69] Francesco Buscemi and Valerio Scarani. Fluctuation theorems from bayesian retrodiction. *Physical Review E*, 103(5):052111, 2021.

[70] Hyukjoon Kwon and MS Kim. Fluctuation theorems for a quantum channel. *Physical Review X*, 9(3):031029, 2019.

[71] Gabriel T Landi and Mauro Paternostro. Irreversible entropy production: From classical to quantum. *Reviews of Modern Physics*, 93(3):035008, 2021.

[72] John Von Neumann. *Mathematical foundations of quantum mechanics: New edition*, volume 53. Princeton university press, 2018.

[73] Albert Einstein. Beiträge zur quantentheorie. *Physikalische Gesellschaft*, 16:820–828, 1914.

[74] Raúl O Vallejos, Pedro Silva Correia, Paola Concha Obando, Nina Machado O'Neill, Alexandre B Tacla, and Fernando de Melo. Quantum state inference from coarse-grained descriptions: Analysis and an application to quantum thermodynamics. *Physical Review A*, 106(1):012219, 2022.

[75] Alexander Streltsov, Hermann Kampermann, Sabine Wölk, Manuel Gessner, and Dagmar Bruß. Maximal coherence and the resource theory of purity. *New Journal of Physics*, 20(5):053058, 2018.

[76] Gilad Gour, Markus P Müller, Varun Narasimhachar, Robert W Spekkens, and Nicole Yunger Halpern. The resource theory of informational nonequilibrium in thermodynamics. *Physics Reports*, 583:1–58, 2015.

[77] Richard Bellman and Ky Fan. On systems of linear inequalities in hermitian matrix variables. *Convexity*, 7:1–11, 1963.

[78] CVX. http://web.cvxr.com/cvx/doc/intro.html#what-is-cvx. Accessed: 01-02-2023.

[79] YALMIP. https://sites.google.com/site/jamiesikora/teaching/semidefinite-programming-quantum-information?pli=1. Accessed: 01-02-2023.

[80] MATLAB. *version 7.10.0 (R2010a)*. The MathWorks Inc., Natick, Massachusetts, 2010.

[81] Steven Diamond and Stephen Boyd. CVXPY: A Python-embedded modeling language for convex optimization. *Journal of Machine Learning Research*, 17(83):1–5, 2016.

[82] Guido Van Rossum and Fred L Drake Jr. *Python reference manual*. Centrum voor Wiskunde en Informatica Amsterdam, 1995.

[83] SCS. https://github.com/cvxgrp/scs. Accessed: 01-02-2023.

[84] MOSEK. https://www.mosek.com/. Accessed: 01-02-2023.

[85] Nicolas Brunner, Daniel Cavalcanti, Stefano Pironio, Valerio Scarani, and Stephanie Wehner. Bell nonlocality. *Reviews of modern physics*, 86(2):419, 2014.

[86] Roope Uola, Ana CS Costa, H Chau Nguyen, and Otfried Gühne. Quantum steering. *Reviews of Modern Physics*, 92(1):015001, 2020.

[87] Costantino Budroni, Adán Cabello, Otfried Gühne, Matthias Kleinmann, and Jan-Åke Larsson. Quantum contextuality. *arXiv e-prints*, pages arXiv–2102, 2021.

[88] Paul Busch, Pekka J Lahti, and Peter Mittelstaedt. *The quantum theory of measurement*, volume 2. Springer Science & Business Media, 1996.

[89] Jon Dattorro. *Convex optimization & Euclidean distance geometry*. Lulu. com, 2010.

[90] Lieven Vandenberghe and Stephen Boyd. Semidefinite programming. *SIAM review*, 38(1):49–95, 1996.

[91] Daniel Cavalcanti and Paul Skrzypczyk. Quantum steering: a review with focus on semidefinite programming. *Reports on Progress in Physics*, 80(2):024001, 2016.

[92] John Watrous. Lecture notes on advanced topics in quantum information. `https://cs.uwaterloo.ca/~watrous/QIT-notes/`, 2020.

[93] Antonios Varvitsiotis. Lecture notes on Semidefinite Programming & Quantum Information. `https://sites.google.com/site/jamiesikora/teaching/semidefinite-programming-quantum-information?pli=1`, 2015.

[94] Sartaj Sahni. Computationally related problems. *SIAM Journal on computing*, 3(4):262–279, 1974.

[95] A Kamath and N Karmarkar. A continuous approach to compute upper bounds in quadratic maximization problems with integer constraints. In *Recent Advances in Global Optimization*, pages 125–140. 1992.

[96] Morton Slater. Lagrange multipliers revisited. In *Traces and emergence of nonlinear programming*, pages 293–306. Springer, 2013.

[97] D. Cavalcanti, L. Guerini, R. Rabelo, and P. Skrzypczyk. General method for constructing local hidden variable models for entangled quantum states. *Phys. Rev. Lett.*, 117:190401, Nov 2016.

[98] Flavien Hirsch, Marco Túlio Quintino, Tamás Vértesi, Matthew F. Pusey, and Nicolas Brunner. Algorithmic construction of local hidden variable models for entangled quantum states. *Phys. Rev. Lett.*, 117:190402, Nov 2016.

[99] Huan-Yu Ku, Shin-Liang Chen, Costantino Budroni, Adam Miranowicz, Yueh-Nan Chen, and Franco Nori. Einstein-podolsky-rosen steering: Its geometric quantification and witness. *Phys. Rev. A*, 97:022338, Feb 2018.

[100] Miguel Navascués, Stefano Pironio, and Antonio Acín. Bounding the set of quantum correlations. *Phys. Rev. Lett.*, 98:010401, Jan 2007.

[101] Xiao-Dong Yu, Timo Simnacher, Nikolai Wyderka, H Chau Nguyen, and Otfried Gühne. A complete hierarchy for the pure state marginal problem in quantum mechanics. *Nature communications*, 12(1):1–7, 2021.

[102] Maharshi Ray, Naresh Goud Boddu, Kishor Bharti, Leong-Chuan Kwek, and Adán Cabello. Graph-theoretic approach to dimension witnessing. *New Journal of Physics*, 23(3):033006, 2021.

[103] Michel X Goemans and David P Williamson. Improved approximation algorithms for maximum cut and satisfiability problems using semidefinite programming. *Journal of the ACM (JACM)*, 42(6):1115–1145, 1995.

[104] Miguel Navascués and Tamás Vértesi. Bounding the set of finite dimensional quantum correlations. *Phys. Rev. Lett.*, 115:020501, Jul 2015.

[105] Andrew C Doherty, Pablo A Parrilo, and Federico M Spedalieri. Complete family of separability criteria. *Physical Review A*, 69(2):022308, 2004.

[106] Nicolas Gisin. Bell's inequality holds for all non-product states. *Physics Letters A*, 154(5-6):201–202, 1991.

[107] Howard Wiseman, Steve Jones, and Doherty Andrew. Steering, entanglement, nonlocality, and the epr paradox. In *APS Division of Atomic, Molecular and Optical Physics Meeting Abstracts*, volume 38, pages R1–126, 2007.

[108] Leonid Gurvits. Classical deterministic complexity of edmonds' problem and quantum entanglement. In *Proceedings of the thirty-fifth annual ACM symposium on Theory of computing*, pages 10–19, 2003.

[109] Ties-A Ohst, Xiao-Dong Yu, Otfried Gühne, and H Chau Nguyen. Certifying quantum separability with adaptive polytopes. *arXiv preprint arXiv:2210.10054*, 2022.

[110] Miguel Navascués, Masaki Owari, and Martin B Plenio. Complete criterion for separability detection. *Physical review letters*, 103(16):160404, 2009.

[111] Fernando GSL Brandao and Reinaldo O Vianna. Robust semidefinite programming approach to the separability problem. *Physical Review A*, 70(6):062309, 2004.

[112] Antoine Girardin, Nicolas Brunner, and Tamás Kriváchy. Building separable approximations for quantum states via neural networks. *Physical Review Research*, 4(2):023238, 2022.

[113] Asher Peres. Separability criterion for density matrices. *Physical Review Letters*, 77(8):1413, 1996.

[114] Dariusz Chruściński and Gniewomir Sarbicki. Entanglement witnesses: construction, analysis and classification. *Journal of Physics A: Mathematical and Theoretical*, 47(48):483001, 2014.

[115] Ryszard Horodecki, Michał Horodecki, and Paweł Horodecki. Teleportation, bell's inequalities and inseparability. *Physics Letters A*, 222(1-2):21–25, 1996.

[116] David Gross, Yi-Kai Liu, Steven T. Flammia, Stephen Becker, and Jens Eisert. Quantum state tomography via compressed sensing. *Phys. Rev. Lett.*, 105:150401, Oct 2010.

[117] Xiao-Dong Yu, Timo Simnacher, H Chau Nguyen, and Otfried Gühne. Quantum-inspired hierarchy for rank-constrained optimization. *PRX Quantum*, 3(1):010340, 2022.

[118] Jessica Bavaresco, Marco Túlio Quintino, Leonardo Guerini, Thiago O Maciel, Daniel Cavalcanti, and Marcelo Terra Cunha. Most incompatible measurements for robust steering tests. *Physical Review A*, 96(2):022110, 2017.

[119] Tobias Moroder, Oleg Gittsovich, Marcus Huber, and Otfried Gühne. Steering bound entangled states: a counterexample to the stronger peres conjecture. *Physical review letters*, 113(5):050404, 2014.

[120] Tamás Vértesi and Nicolas Brunner. Disproving the peres conjecture by showing bell nonlocality from bound entanglement. *Nature communications*, 5(1):5297, 2014.

[121] Asher Peres. All the bell inequalities. *Foundations of Physics*, 29(4):589–614, 1999.

[122] Helle Bechmann-Pasquinucci and Asher Peres. Quantum cryptography with 3-state systems. *Physical Review Letters*, 85(15):3313, 2000.

[123] Alastair A Abbott, Cristian S Calude, Jonathan Conder, and Karl Svozil. Strong kochen-specker theorem and incomputability of quantum randomness. *Physical Review A*, 86(6):062109, 2012.

[124] Anatoly Kulikov, Markus Jerger, Anton Potočnik, Andreas Wallraff, and Arkady Fedorov. Realization of a quantum random generator certified with the kochen-specker theorem. *Physical Review Letters*, 119(24):240501, 2017.

[125] Mark Howard, Joel Wallman, Victor Veitch, and Joseph Emerson. Contextuality supplies the 'magic'for quantum computation. *Nature*, 510(7505):351–355, 2014.

[126] Sergey Bravyi, David Gosset, and Robert König. Quantum advantage with shallow circuits. *Science*, 362(6412):308–311, 2018.

[127] Sergey Bravyi, David Gosset, Robert Koenig, and Marco Tomamichel. Quantum advantage with noisy shallow circuits. *Nature Physics*, 16(10):1040–1045, 2020.

[128] E. Specker Simon Kochen. The problem of hidden variables in quantum mechanics. *Indiana Univ. Math. J.*, 17:59–87, 1968.

[129] CH BENNET. Quantum cryptography: Public key distribution and coin tossing. In *Proc. of IEEE Int. Conf. on Comp., Syst. and Signal Proc., Bangalore, India, Dec. 10-12, 1984*, 1984.

[130] Ekert. Quantum cryptography based on bell's theorem. *Physical review letters*, 67 6:661–663, 1991.

[131] Nicolas Brunner, Stefano Pironio, Antonio Acin, Nicolas Gisin, André Allan Méthot, and Valerio Scarani. Testing the dimension of hilbert spaces. *Physical review letters*, 100(21):210503, 2008.

[132] Adán Cabello, Simone Severini, and Andreas Winter. Graph-theoretic approach to quantum correlations. *Physical review letters*, 112(4):040401, 2014.

[133] Otfried Gühne, Costantino Budroni, Adán Cabello, Matthias Kleinmann, and Jan-Åke Larsson. Bounding the quantum dimension with contextuality. *Physical Review A*, 89(6):062107, 2014.

[134] Hamza Fawzi. Lecture notes on Topics in Convex Optimisation. `http://www.damtp.cam.ac.uk/user/hf323/M18-OPT/index.html`, 2018.

[135] L. Lov´asz and K. Vesztergombi. Lecture notes on Discrete Mathematics. `https://cims.nyu.edu/~regev/teaching/discrete_math_fall_2005/dmbook.pdf`, 1999.

[136] László Lovász. Semidefinite programs and combinatorial optimization. *Recent advances in algorithms and combinatorics*, pages 137–194, 2003.

[137] László Lovász. Lecture notes on Orthogonal representations: stability number and coloring. `https://www2.math.ethz.ch/t3/fileadmin/math/ndb/00238/07403/`, 2014.

[138] N. David Mermin. Simple unified form for the major no-hidden-variables theorems. *Phys. Rev. Lett.*, 65:3373–3376, Dec 1990.

[139] N. David Mermin. Hidden variables and the two theorems of john bell. *Rev. Mod. Phys.*, 65:803–815, Jul 1993.

[140] Asher Peres. Recursive definition for elements of reality. *Foundations of physics*, 22:357–361, 1992.

[141] Asher Peres. Incompatible results of quantum measurements. *Physics Letters A*, 151(3-4):107–108, 1990.

[142] Adán Cabello. Experimentally testable state-independent quantum contextuality. *Phys. Rev. Lett.*, 101:210401, Nov 2008.

[143] Adán Cabello, JoséM Estebaranz, and Guillermo García-Alcaine. Bell-kochen-specker theorem: A proof with 18 vectors. *Physics Letters A*, 212(4):183–187, 1996.

[144] Zhen-Peng Xu, Jing-Ling Chen, and Otfried Gühne. Proof of the peres conjecture for contextuality. *Phys. Rev. Lett.*, 124:230401, Jun 2020.

[145] Davide Poderini, Rafael Chaves, Iris Agresti, Gonzalo Carvacho, and Fabio Sciarrino. Exclusivity graph approach to instrumental inequalities. In *Uncertainty in Artificial Intelligence*, pages 1274–1283. PMLR, 2020.

[146] Anubhav Chaturvedi, Máté Farkas, and Victoria J Wright. Characterising and bounding the set of quantum behaviours in contextuality scenarios. *Quantum*, 5:484, 2021.

[147] László Lovász. On the shannon capacity of a graph. *IEEE Transactions on Information theory*, 25(1):1–7, 1979.

[148] P. Kurzyński and D. Kaszlikowski. Contextuality of almost all qutrit states can be revealed with nine observables. *Phys. Rev. A*, 86:042125, Oct 2012.

[149] Toby S. Cubitt, Debbie Leung, William Matthews, and Andreas Winter. Improving zero-error classical communication with entanglement. *Phys. Rev. Lett.*, 104:230503, Jun 2010.

[150] Ognyan Oreshkov, Fabio Costa, and Časlav Brukner. Quantum correlations with no causal order. *Nature Communications*, 3(1):1–8, 2012.

[151] A. Einstein, B. Podolsky, and N. Rosen. Can quantum-mechanical description of physical reality be considered complete? *Phys. Rev.*, 47:777–780, May 1935.

[152] J. S. Bell. On the einstein podolsky rosen paradox. *Physics Physique Fizika*, 1:195–200, Nov 1964.

[153] Jian-Wei Pan, Zeng-Bing Chen, Chao-Yang Lu, Harald Weinfurter, Anton Zeilinger, and Marek Żukowski. Multiphoton entanglement and interferometry. *Reviews of Modern Physics*, 84(2):777, 2012.

[154] Otfried Gühne and Géza Tóth. Entanglement detection. *Physics Reports*, 474(1-6):1–75, 2009.

[155] Ryszard Horodecki, Paweł Horodecki, Michał Horodecki, and Karol Horodecki. Quantum entanglement. *Rev. Mod. Phys.*, 81:865–942, Jun 2009.

[156] Hartmut Häffner, Wolfgang Hänsel, CF Roos, Jan Benhelm, D Chek-al Kar, M Chwalla, T Körber, UD Rapol, M Riebe, PO Schmidt, et al. Scalable multiparticle entanglement of trapped ions. *Nature*, 438(7068):643–646, 2005.

[157] Reinhard F Werner. Quantum states with einstein-podolsky-rosen correlations admitting a hidden-variable model. *Physical Review A*, 40(8):4277, 1989.

[158] Erwin Schrödinger. Discussion of probability relations between separated systems. In *Mathematical Proceedings of the Cambridge Philosophical Society*, volume 31, pages 555–563. Cambridge University Press, 1935.

[159] E. Schrödinger. Probability relations between separated systems. *Mathematical Proceedings of the Cambridge Philosophical Society*, 32(3):446–452, 1936.

[160] Cyril Branciard, Eric G Cavalcanti, Stephen P Walborn, Valerio Scarani, and Howard M Wiseman. One-sided device-independent quantum key distribution: Security, feasibility, and the connection with steering. *Physical Review A*, 85(1):010301, 2012.

[161] Yun Zhi Law, Jean-Daniel Bancal, Valerio Scarani, et al. Quantum randomness extraction for various levels of characterization of the devices. *Journal of Physics A: Mathematical and Theoretical*, 47(42):424028, 2014.

[162] Yu Xiang, Ioannis Kogias, Gerardo Adesso, and Qiongyi He. Multipartite gaussian steering: Monogamy constraints and quantum cryptography applications. *Physical Review A*, 95(1):010101, 2017.

[163] Marco Túlio Quintino, Tamás Vértesi, and Nicolas Brunner. Joint measurability, einstein-podolsky-rosen steering, and bell nonlocality. *Physical review letters*, 113(16):160402, 2014.

[164] Teiko Heinosaari, Takayuki Miyadera, and Mário Ziman. An invitation to quantum incompatibility. *Journal of Physics A: Mathematical and Theoretical*, 49(12):123001, 2016.

[165] P Kruszyński and WM De Muynck. Compatibility of observables represented by positive operator-valued measures. *Journal of mathematical physics*, 28(8):1761–1763, 1987.

[166] Teiko Heinosaari, Daniel Reitzner, and Peter Stano. Notes on joint measurability of quantum observables. *Foundations of Physics*, 38:1133–1147, 2008.

[167] Arthur Fine. Hidden variables, joint probability, and the bell inequalities. *Physical Review Letters*, 48(5):291, 1982.

[168] Teiko Heinosaari, Jukka Kiukas, Daniel Reitzner, and Jussi Schultz. Incompatibility breaking quantum channels. *Journal of Physics A: Mathematical and Theoretical*, 48(43):435301, 2015.

[169] Francesco Buscemi, Eric Chitambar, and Wenbin Zhou. Complete resource theory of quantum incompatibility as quantum programmability. *Physical review letters*, 124(12):120401, 2020.

[170] Valerio Scarani, Sofyan Iblisdir, Nicolas Gisin, and Antonio Acín. Quantum cloning. *Rev. Mod. Phys.*, 77:1225–1256, Nov 2005.

[171] Wayne C Myrvold, Joy Christian, and Paul Busch. "no information without disturbance": quantum limitations of measurement. *Quantum Reality, Relativistic Causality, and Closing the Epistemic Circle: Essays in Honour of Abner Shimony*, pages 229–256, 2009.

[172] Claudio Carmeli, Teiko Heinosaari, Daniel Reitzner, Jussi Schultz, and Alessandro Toigo. Quantum incompatibility in collective measurements. *Mathematics*, 4(3):54, 2016.

[173] Paul Busch. Unsharp reality and joint measurements for spin observables. *Physical Review D*, 33(8):2253, 1986.

[174] Leonardo Guerini, Jessica Bavaresco, Marcelo Terra Cunha, and Antonio Acín. Operational framework for quantum measurement simulability. *Journal of Mathematical Physics*, 58(9):092102, 2017.

[175] Michał Oszmaniec, Leonardo Guerini, Peter Wittek, and Antonio Acín. Simulating positive-operator-valued measures with projective measurements. *Phys. Rev. Lett.*, 119:190501, Nov 2017.

[176] Erkka Haapasalo, Teiko Heinosaari, and Juha-Pekka Pellonpää. Quantum measurements on finite dimensional systems: relabeling and mixing. *Quantum Information Processing*, 11:1751–1763, 2012.

[177] D Bohm. Quantum theory prentice-hall. *Englewood Cliffs, NJ*, 1951.

[178] Eric Gama Cavalcanti, Steve J Jones, Howard M Wiseman, and Margaret D Reid. Experimental criteria for steering and the einstein-podolsky-rosen paradox. *Physical Review A*, 80(3):032112, 2009.

[179] Bernhard Wittmann, Sven Ramelow, Fabian Steinlechner, Nathan K Langford, Nicolas Brunner, Howard M Wiseman, Rupert Ursin, and Anton Zeilinger. Loophole-free einstein–podolsky–rosen experiment via quantum steering. *New Journal of Physics*, 14(5):053030, 2012.

[180] Dylan John Saunders, Steve J Jones, Howard M Wiseman, and Geoff J Pryde. Experimental epr-steering using bell-local states. *Nature Physics*, 6(11):845–849, 2010.

[181] Adam Joseph Bennet, David Andrew Evans, Dylan John Saunders, Cyril Branciard, Eric Gama Cavalcanti, Howard Mark Wiseman, and Geoff J Pryde. Arbitrarily loss-tolerant einstein-podolsky-rosen steering allowing a demonstration over 1 km of optical fiber with no detection loophole. *Physical Review X*, 2(3):031003, 2012.

[182] Sania Jevtic, Michael JW Hall, Malcolm R Anderson, Marcin Zwierz, and Howard M Wiseman. Einstein–podolsky–rosen steering and the steering ellipsoid. *JOSA B*, 32(4):A40–A49, 2015.

[183] H Chau Nguyen and Thanh Vu. Nonseparability and steerability of two-qubit states from the geometry of steering outcomes. *Physical Review A*, 94(1):012114, 2016.

[184] H Chau Nguyen, Huy-Viet Nguyen, and Otfried Gühne. Geometry of einstein-podolsky-rosen correlations. *Physical review letters*, 122(24):240401, 2019.

[185] Matthew F Pusey. Negativity and steering: A stronger peres conjecture. *Physical Review A*, 88(3):032313, 2013.

[186] Roope Uola, Costantino Budroni, Otfried Gühne, and Juha-Pekka Pellonpää. One-to-one mapping between steering and joint measurability problems. *Physical review letters*, 115(23):230402, 2015.

[187] Otfried Gühne, Erkka Haapasalo, Tristan Kraft, Juha-Pekka Pellonpää, and Roope Uola. Incompatible measurements in quantum information science. *arXiv preprint arXiv:2112.06784*, 2021.

[188] Ingemar Bengtsson. Three ways to look at mutually unbiased bases. In *AIP Conference Proceedings*, volume 889, pages 40–51. American Institute of Physics, 2007.

[189] William K Wootters and Brian D Fields. Optimal state-determination by mutually unbiased measurements. *Annals of Physics*, 191(2):363–381, 1989.

[190] Sébastien Designolle, Paul Skrzypczyk, Florian Fröwis, and Nicolas Brunner. Quantifying measurement incompatibility of mutually unbiased bases. *Physical review letters*, 122(5):050402, 2019.

[191] Charles H Bennett, Gilles Brassard, Claude Crépeau, Richard Jozsa, Asher Peres, and William K Wootters. Teleporting an unknown quantum state via dual classical and einstein-podolsky-rosen channels. *Physical review letters*, 70(13):1895, 1993.

[192] Charles H Bennett and Stephen J Wiesner. Communication via one-and two-particle operators on einstein-podolsky-rosen states. *Physical review letters*, 69(20):2881, 1992.

[193] Eric G Cavalcanti and Howard M Wiseman. Implications of local friendliness violation for quantum causality. *Entropy*, 23(8):925, 2021.

[194] Simon Milz, Jessica Bavaresco, and Giulio Chiribella. Resource theory of causal connection. *Quantum*, 6:788, 2022.

[195] Mateus Araújo, Cyril Branciard, Fabio Costa, Adrien Feix, Christina Giarmatzi, and Časlav Brukner. Witnessing causal nonseparability. *New Journal of Physics*, 17(10):102001, 2015.

[196] Cyril Branciard, Mateus Araújo, Adrien Feix, Fabio Costa, and Časlav Brukner. The simplest causal inequalities and their violation. *New Journal of Physics*, 18(1):013008, 2015.

[197] Eric Chitambar and Gilad Gour. Quantum resource theories. *Reviews of modern physics*, 91(2):025001, 2019.

[198] Bob Coecke, Tobias Fritz, and Robert W Spekkens. A mathematical theory of resources. *Information and Computation*, 250:59–86, 2016.

[199] Marcel Riesz. Sur les maxima des formes bilinéaires et sur les fonctionnelles linéaires. *Acta mathematica*, 49(3):465–497, 1927.

[200] Wolfram Research, Inc. Mathematica, Version 13.2. Champaign, IL, 2022.

[201] John B Bronzan. Parametrization of su (3). *Physical Review D*, 38(6):1994, 1988.

[202] Lina Vandré and Marcelo Terra Cunha. Quantum sets of the multicolored-graph approach to contextuality. *Physical Review A*, 106(6):062210, 2022.

[203] Rafael Rabelo, Cristhiano Duarte, Antonio J López-Tarrida, Marcelo Terra Cunha, and Adán Cabello. Multigraph approach to quantum non-locality. *Journal of Physics A: Mathematical and Theoretical*, 47(42):424021, 2014.

[204] Barbara Amaral and Marcelo Terra Cunha. *On graph approaches to contextuality and their role in quantum theory.* Springer, 2018.

[205] JOHN S. BELL. On the problem of hidden variables in quantum mechanics. *Rev. Mod. Phys.*, 38:447–452, Jul 1966.

[206] John F. Clauser, Michael A. Horne, Abner Shimony, and Richard A. Holt. Proposed experiment to test local hidden-variable theories. *Phys. Rev. Lett.*, 23:880–884, Oct 1969.

[207] Boris S Cirel'son. Quantum generalizations of bell's inequality. *Letters in Mathematical Physics*, 4:93–100, 1980.

Appendix A

Proof of the entropic uncertainty relation in eq. (1.10)

In this appendix, we provide a proof for the entropic uncertainty relation we are going go use throughout our work, namely

$$H(A|\psi) + H(B|\psi) \geq -2 \log \max_{j,k} |\langle a_j | b_k \rangle|, \tag{A.1}$$

where $H(A|\psi)$ is the Shannon entropy of measuring an observable A with eigenvectors $\{a_j\}$ on a state ψ.

Let us start by simply writing out the explicit expression for the l.h.s. of this inequality. For a system of dimension N, it reads

$$
\begin{aligned}
H(A|\psi) + H(B|\psi) &= -\sum_{j=1}^{N} |\langle\psi|a_j\rangle|^2 \log|\langle\psi|a_j\rangle|^2 - \sum_{k=1}^{N} |\langle\psi|b_k\rangle|^2 \log|\langle\psi|b_k\rangle|^2 \\
&= \sum_{j,k} |\langle\psi|a_j\rangle|^2 |\langle\psi|b_k\rangle|^2 \left(-\log|\langle\psi|a_j\rangle|^2 - \log|\langle\psi|b_k\rangle|^2\right).
\end{aligned}
\tag{A.2}
$$

Here, we have used the fact that $\sum_j |\langle\psi|a_j\rangle|^2 = 1$, and similarly for $|b_k\rangle$. Since we want to achieve a state independent relation, we will minimize the r.h.s. of the expression above. As argued in [35], the symmetries in this expression between the eigenvectors of A and B ensure that the maximum value that the term in parenthesis can achieve will be given for a state state lying midway between $|a_j\rangle$ and $|b_k\rangle$, which we will call $|\phi_{jk}\rangle$. Following their calculations, to find the explicit form of this state one must evaluate the expression

$$\frac{\delta}{\delta |\phi_{jk}\rangle} \left(-\log|\langle\phi_{ij}|a_j\rangle|^2 - \log|\langle\phi_{ij}|b_k\rangle|^2 + \kappa \langle\phi_{jk}|\phi_{jk}\rangle\right) = 0, \tag{A.3}$$

where κ is a Lagrange multiplier. This means $|\phi_{jk}\rangle$ must obey

$$|\phi_{jk}\rangle = \frac{1}{\kappa}\left(\frac{|a_j\rangle}{\langle\phi_{jk}|a_j\rangle} + \frac{|b_k\rangle}{\langle\phi_{jk}|b_j\rangle}\right) = \frac{1}{2}\left(\frac{|a_j\rangle}{\langle\phi_{jk}|a_j\rangle} + \frac{|b_k\rangle}{\langle\phi_{jk}|b_j\rangle}\right), \tag{A.4}$$

and we set $\kappa = 2$ such that the state is normalized. To solve this equation, we multiply it by $\langle a_j|$. For simplicity, we identify $a = \langle\phi_{jk}|a_j\rangle$ and $b = \langle\phi_{jk}|b_k\rangle$, such that

$$
\begin{aligned}
\langle a_j|\phi_{jk}\rangle &= \frac{1}{2}\left(\frac{1}{\langle\phi_{jk}|a_j\rangle} + \frac{\langle a_j|b_k\rangle}{\langle\phi_{jk}|b_k\rangle}\right), \\
a^* &= \frac{1}{2}\left(\frac{1}{a} + \frac{\langle a_j|b_k\rangle}{b}\right).
\end{aligned}
\tag{A.5}
$$

Following a similar calculation for $|b_k\rangle$, we arrive at

$$|a|^2 = \frac{1}{2}\left(1 + \frac{a\langle a_j|b_k\rangle}{b}\right), \quad |b|^2 = \frac{1}{2}\left(1 + \frac{b\langle b_k|a_j\rangle}{a}\right). \tag{A.6}$$

Notice that $\dfrac{a\langle a_j|b_k\rangle}{b}$ must be real, since $|a|^2$ is also real, and the same goes for $\dfrac{b\langle b_k|a_j\rangle}{a}$. Because of that, combining these two equations we get

$$\frac{|a|^2}{|b|^2} - 1 = \frac{a}{b}\langle a_j|b_k\rangle - \frac{a^*}{b^*}\langle a_j|b_k\rangle^* = 0, \tag{A.7}$$

meaning $|a| = |b|$. Using this result in eq. (A.6), one gets

$$|a|^2 = |\langle\phi_{jk}|a_j\rangle|^2 = \frac{1}{2}(1 + \langle a_j|b_k\rangle), \tag{A.8}$$

which means $|\phi_{jk}\rangle$ must be

$$|\phi_{jk}\rangle = \frac{1}{\sqrt{2(1+|\langle a_j|b_k\rangle|)}}\left(|a_j\rangle + e^{-i\arg\langle a_j|b_k\rangle}|b_k\rangle\right). \tag{A.9}$$

Now that we have an expression for the state that maximizes the term in parenthesis in eq. (A.2), we can simply plug it back to find the inequality

$$
\begin{aligned}
H(A|\psi) + H(B|\psi) &\geq -\sum_{j,k} |\langle\psi|a_j\rangle|^2 |\langle\psi|b_k\rangle|^2 \left(\log|\langle\phi_{jk}|a_j\rangle|^2\log|\langle\phi_{jk}|b_k\rangle|^2\right) \\
&= -2\sum_{j,k} |\langle\psi|a_j\rangle|^2 |\langle\psi|b_k\rangle|^2 \log\frac{1}{2}(1 + |\langle a_j|b_k\rangle|) \\
&= 2\sum_{j,k} |\langle\psi|a_j\rangle|^2 |\langle\psi|b_k\rangle|^2 \log\frac{2}{(1 + |\langle a_j|b_k\rangle|)}.
\end{aligned}
\tag{A.10}
$$

The r.h.s. of this inequality sets a lower bound to the l.h.s. Thus, the inequality will still be valid if we take the highest possible value for $|\langle a_j|b_k\rangle|$, by substituting it for $\max_{jk}\{|\langle a_j|b_k\rangle|\}$. Then, by summing over j,k one arrives at the inequality obtained in [40],

$$H(A|\psi) + H(B|\psi) \geq 2\log\frac{2}{1 + \max_{jk}\{|\langle a_j|b_k\rangle|\}}. \tag{A.11}$$

It was then conjectured in [43] and finally proven in [44] that this inequality could be further improved to the final form of eq. (A.1), in a direct application of Riesz theorem [199]:

Theorem (Riesz Theorem). *Let $x = \{x_1,\ldots,x_N\}$ be a string of complex numbers and T a matrix with elements T_{jk}, so that $(Tx)_j = \sum_k T_{jk}x_k$ and $\sum_j|(Tx)_j|^2 = \sum_k|x_k|^2 \ \forall x$, then*

$$c^{1/a'}\left(\sum_j|(Tx)_j|^{a'}\right)^{1/a'} \leq c^{1/a}\left(\sum_k|x_k|^a\right)^{1/a}, \tag{A.12}$$

where $c = \max_{jk}|T_{jk}|$, for $1 \leq a \leq 2$ and $1/a + 1/a' = 1$.

To apply this theorem, we start by associating $x_k = \langle a_k|\psi\rangle$ and $T_{jk} = \langle b_j|a_k\rangle$. Consequently,

$$(Tx)_j = \sum_k \langle b_j|a_k\rangle\langle a_k|\psi\rangle = \langle b_j|\psi\rangle. \tag{A.13}$$

We then make a change of variables $a = 2(1+r)$ and $a' = 2(1+s)$. With this, we can rearrange the inequality above to read

$$\left(\sum_j|\langle b_j|\psi\rangle|^{2(1+s)}\right)^{1/2(1+s)}\left(\sum_k|\langle a_k|\psi\rangle|^{2(1+r)}\right)^{-1/2(1+r)} \leq c^{\frac{s-r}{2(1+r)(1+s)}}. \tag{A.14}$$

To simplify the process, we can identify $P_j = |\langle b_j|\psi\rangle|^2$ and $Q_k = |\langle a_k|\psi\rangle|^2$ with probability distributions. Moreover, the relation between a and a' implies

$$r = -\frac{s}{2s+1}, \tag{A.15}$$

such that the power on the r.h.s. of the inequality (A.14) can be simplified to

$$\frac{s-r}{2(1+r)(1+s)} = \frac{s}{s+1}. \tag{A.16}$$

Now we can update (A.14) to

$$\left(\sum_j P_j^{(1+s)}\right)^{1/2(1+s)} \left(\sum_k Q_k^{(1+r)}\right)^{-1/2(1+r)} \leq c^{s/(s+1)}. \tag{A.17}$$

Now, we make one final substitution of $\Pi_s = \left(\sum_j P_j^{(1+s)}\right)^{1/s}$ and $\Theta_r = \left(\sum_k Q_k^{(1+r)}\right)^{1/r}$, so

$$\Pi_s^{s/2(s+1)} \Theta_r^{-r/2(r+1)} \leq c^{s/(s+1)}. \tag{A.18}$$

Recalling that $r = -\dfrac{s}{2s+1}$,

$$\Pi_s^{s/2(s+1)} \Theta_r^{s/2(s+1)} \leq c^{s/(s+1)}$$
$$\Pi_s \Theta_r \leq c^2. \tag{A.19}$$

Let us plug the values of Π_s and Θ_r back in, and take the logarithm on both sides.

$$\frac{1}{s} \log \sum_j P_j^{1+s} + \frac{1}{r} \sum_k Q_k^{1+r} \leq 2 \log c. \tag{A.20}$$

Relabel $s' = 1 + s$ and $r' = 1 + r$ to get

$$-\frac{1}{1-s'} \log \sum_j P_j^{s'} - \frac{1}{1-r'} \sum_k Q_k^{r'} \leq 2 \log c. \tag{A.21}$$

The r.h.s. of this inequality is simply the sum of Renyi entropies, and we can recover the Shannon entropy of probability distributions P and Q by taking the limit $s' \to 1$ and $r' \to 1$. Since $P_j = |\langle b_j|\psi\rangle|^2$ and $Q_k = |\langle a_k|\psi\rangle|^2$, we finally arrive at the final form of the entropic uncertainty relation

$$H(A|\psi) + H(B|\psi) \geq -2 \log c, \tag{A.22}$$

where we recall that $c = \max_{jk}\{|\langle a_j|b_k\rangle|\}$.

Appendix B

Calculation leading to eqs. (1.13) and (1.17)

In this appendix we show the calculations that yield the probability distributions necessary to obtain the Shannon entropy of measuring Z_N and $\tilde{Z}_N$ on a spin coherent state.

To obtain these probabilities, is is useful to first get the explicit expression for the density matrix of a spin-coherent state. Recall that for N particles these states are defined as

$$|\Psi_N\rangle = |\Psi_1\rangle^{\otimes N}, \tag{B.1}$$

where $|\Psi_1\rangle = \sqrt{p}\,|0\rangle + e^{i\phi}\sqrt{1-p}\,|1\rangle$, parameterized by $p \in [0,1]$ and $\phi \in [0, 2\pi[$. So,

$$|\Psi_N\rangle\langle\Psi_N| = \underbrace{\left((\sqrt{p}\,|0\rangle + \sqrt{1-p}\,e^{i\phi}\,|1\rangle)\dots(\sqrt{p}\,|0\rangle + \sqrt{1-p}\,e^{i\phi}\,|1\rangle)\right)}_{\text{N times}} \times(\text{c.c.}), \tag{B.2}$$

where c.c. denotes the complex conjugate of the first term. Notice that there will be a pattern to the coefficient multiplying each term of this product.

For instance, the coefficient to the term $|0\dots0\rangle\langle0\dots0|$, the state with no spin-down particles, is clearly p^N. Now considering the state $|0\dots01\rangle\langle0\dots01|$ (or any state with a single spin-down particle), one can see that the corresponding coefficient is $p^{N-1}(1-p)$. We can follow the same line of thought for every possible spin configuration and conclude that

$$
\begin{aligned}
|\Psi_N\rangle\langle\Psi_N| = p^N &\underbrace{(|0\dots0\rangle\langle0\dots0|)}_{\text{1 state with 0 spin-down particles}} \\
+ p^{N-1}(1-p) &\underbrace{(|0\dots01\rangle\langle0\dots01|) + (|0\dots10\rangle\langle0\dots10|) + \dots(|10\dots0\rangle\langle10\dots0|)}_{\text{N states with 1 spin-down particles}} \\
+ \dots & \\
+ p(1-p)^{N-1} &\underbrace{(|1\dots10\rangle\langle1\dots10|) + (|1\dots01\rangle\langle1\dots01|) + \dots(|01\dots1\rangle\langle01\dots1|)}_{\text{N states with N-1 spin-down particles}} \\
+ (p-1)^N &\underbrace{(|1\dots1\rangle\langle1\dots1|)}_{\text{1 state with N spin-down particles}} .
\end{aligned}
\tag{B.3}
$$

In general, the term corresponding k spin-down particles will have the coefficient $p^{N-k}(1-p)^k$ multiplying its $\binom{N}{k}$ states.

To obtain eq. (1.13), we must also define the POVM elements associated to each possible outcome of Z_N. This measurement in fact has access to the complete spin configuration of a N-particle state, so it has N^2 possible outcomes. We have labeled by $s_z = 1, \dots, 2^N$, so the POVM elements $Z_N^{s_z}$ are

$$Z_N^1 = |0\ldots0\rangle\langle0\ldots0|,$$
$$Z_N^2 = |0\ldots1\rangle\langle0\ldots1|,$$
$$Z_N^3 = |0\ldots10\rangle\langle0\ldots10|,$$
$$\ldots$$
$$Z_N^{2^N-1} = |1\ldots10\rangle\langle1\ldots10|,$$
$$Z_N^{2^N} = |1\ldots1\rangle\langle1\ldots1|.$$

(B.4)

Now, it is easy to see that $\Pr(s_z|\Psi_N)$ will be the same for every outcome with the same total magnetization, regardless of the individual spin configuration it refers to. Indeed, in terms of the number k of spin-down particles, it reads

$$\Pr(k|\Psi_N) = p^{N-k}(1-p)^k. \tag{B.5}$$

As already discussed, $\binom{N}{k}$ outcomes will have this same probability associated to it. Plugging these results in the definition of the Shannon entropy, one gets eq. (1.13). One can go further and notice that eq. (1.13) can be expanded as

$$H(Z_N|\Psi_N) = -\sum_{k=1}^{N}\binom{N}{k}p^k(1-p)^{N-k}\log p^k(1-p)^{N-k} \tag{B.6}$$

$$= -\underbrace{\sum_{k=1}^{N}\binom{N}{k}p^k(1-p)^{N-k}k\log p}_{Np}$$

$$-\underbrace{\sum_{k=1}^{N}\binom{N}{k}p^k(1-p)^{N-k}N\log(1-p)}_{1} \tag{B.7}$$

$$+\underbrace{\sum_{k=1}^{N}\binom{N}{k}p^k(1-p)^{N-k}k\log(1-p)}_{Np}$$

$$=N\left(-p\log p-(1-p)\log(1-p)\right) \tag{B.8}$$
$$=Nh(p), \tag{B.9}$$

which is precisely eq. (1.15), where $h(p) = -p\log p - (1-p)\log(1-p)$ is Shannon's binary entropy for p.

To obtain eq. (1.17), half of the path has already been traced and we must simply define the POVM elements of $\tilde{Z}_N$. We recall that these observables explore the inherent degeneracy of the measurement, being simply the projectors onto subspaces of same total magnetization. Thus, its $N+1$ POVM elements Z_N^k can be labeled by the number $k = 0, 1, \ldots, N$ of spin-down particles to yield

$$\tilde{Z}_N^0 = |00\ldots00\rangle\langle00\ldots00|,$$
$$\tilde{Z}_N^1 = |00\ldots01\rangle\langle00\ldots01| + |00\ldots10\rangle\langle00\ldots10| + \cdots + |10\ldots00\rangle\langle10\ldots00|,$$
$$\ldots$$
$$\tilde{Z}_N^{N-1} = |11\ldots10\rangle\langle11\ldots10| + |11\ldots01\rangle\langle11\ldots01| + \cdots + |01\ldots1\rangle\langle01\ldots11|,$$
$$\tilde{Z}_N^N = |1\ldots1\rangle\langle1\ldots1|.$$

(B.10)

If we want to express, now, the probability of obtaining outcome j_z/N when measuring $\tilde{Z}_N$, we must simply notice that $k = \dfrac{N}{2} - j_z$. This way, using the already established of for $|\Psi_N\rangle\langle\Psi_N|$, one can easily see that

$$\Pr(j_z|\Psi_N) = \binom{N}{\frac{N}{2}+j_z}p^{\frac{N}{2}+j_z}(1-p)^{\frac{N}{2}-j_z}. \tag{B.11}$$

Appendix C

Calculation leading to $\mathcal{A}_{\Lambda_D}(\rho)$

In this section we will obtain eq. (2.15), which we re-state here for clarity

$$
\mathcal{A}_{\Lambda_D}(\rho) = \begin{bmatrix} \rho_{00} & \rho_{01}/\sqrt{2} & \rho_{01}/\sqrt{2} \\ \rho_{01}^*/\sqrt{2} & \rho_{11}/2 & \frac{|\rho_{01}|^2}{\rho_{00}} - \frac{\rho_{11}}{2} \\ \rho_{01}^*/\sqrt{2} & \frac{|\rho_{01}|^2}{\rho_{00}} - \frac{\rho_{11}^*}{2} & \rho_{11}/2 \end{bmatrix}. \tag{C.1}
$$

We want to find the state $\mathcal{A}_{\Lambda_D}(\rho)$ resulting from averaging over the pure microscopic states that are compatible with an effective description ρ. The expression we want to evaluate is

$$
\mathcal{A}_{\Lambda_D}(\rho) = \int d\mu_\psi \mathrm{Pr}_{\Lambda_D}(\psi|\rho)\psi. \tag{C.2}
$$

In order to do that, we will follow the steps laid out in [65], where the authors find the general form of the average assigned state for two different coarse-graining maps.

We start by calling attention to the fact that $\mathrm{Pr}_{\Lambda_D}(\psi|\rho)$ must be such that it only assumes non-zero values for $\psi \in \Omega_{\Lambda_D}(\rho)$. This is of course because $\Omega_{\Lambda_D}(\rho)$ is precisely the set of states that are assigned to ρ through the coarse-graining map. To states that do not belong to $\Omega_{\Lambda_D}(\rho)$ one must assign null probability. This can be conveyed by demanding that this probability distribution obeys the proportionality

$$
\mathrm{Pr}_{\Lambda_D}(\psi|\rho) \propto \delta(\Lambda_D[\psi] - \rho). \tag{C.3}
$$

Thus, the probability distribution $\mathrm{Pr}_{\Lambda_D}(\psi|\rho)$ will be invariant under transformations that respect this symmetry above. In words, these are the transformations that take states in $\Omega_{\Lambda_D}(\rho)$ into other states also in $\Omega_{\Lambda_D}(\rho)$. In appendix D we show that these operators can be parameterized by $\alpha \in [0, 2\pi]$ as

$$
U_1(\alpha) = \frac{1}{2} \begin{pmatrix} 2e^{-i\alpha} & 0 & 0 \\ 0 & (1 + e^{i\alpha}) & (1 - e^{i\alpha}) \\ 0 & (1 - e^{i\alpha}) & (1 + e^{i\alpha}). \end{pmatrix} \tag{C.4}
$$

This means that

$$
\mathrm{Pr}_{\Lambda_D}(\psi|\rho) = \mathrm{Pr}_{\Lambda_D}(U_1(\alpha)\psi U_1^\dagger(\alpha)|\rho). \tag{C.5}
$$

If we recall that the Haar measure is invariant under unitary transformations, we can make the change of variables $|\psi\rangle \to U_1(\alpha)|\psi\rangle$, such that equation eq. (C.2) reads

$$
\mathcal{A}_{\Lambda_D}(\rho) = \int d\mu_\psi \, \mathrm{Pr}_{\Lambda_D}(\psi|\rho) \, U_1(\alpha)\psi U_1^\dagger(\alpha). \tag{C.6}
$$

We can choose any $U_1(\alpha)$ above, as long as it respects the parametrization in eq. (C.4), so we can in fact average over all such unitary transformations to yield

$$
\mathcal{A}_{\Lambda_D}(\rho) = \int d\mu_\psi \, \mathrm{Pr}_{\Lambda_D}(\psi|\rho) \, \overline{U_1(\alpha)\psi U_1^\dagger(\alpha)}, \tag{C.7}
$$

where

$$\overline{U_1(\alpha)\psi U_1^\dagger(\alpha)} = \frac{1}{2\pi}\int_0^{2\pi} d\alpha \; U_1(\alpha)\psi U_1^\dagger(\alpha). \tag{C.8}$$

The result of this integration is obtained after some straight-forward calculation. Let ψ be represented by a density matrix with elements

$$\psi = \begin{pmatrix} \chi_1\chi_1^* & \chi_1\chi_2^* & \chi_1\chi_3^* \\ \chi_2\chi_1^* & \chi_2\chi_2^* & \chi_2\chi_3^* \\ \chi_3\chi_1^* & \chi_3\chi_2^* & \chi_3\chi_3^*, \end{pmatrix} \tag{C.9}$$

such that eq. (C.8) yields

$$\overline{U_1(\alpha)\psi U_1^\dagger(\alpha)} = \frac{1}{2}\begin{pmatrix} 2|\chi_1|^2 & \chi_1(\chi_2^*+\chi_3^*) & \chi_1(\chi_2^*+\chi_3^*) \\ \chi_1^*(\chi_2+\chi_3) & |\chi_2|^2+|\chi_3|^2 & \chi_2\chi_3^*+\chi_2^*\chi_3 \\ \chi_1^*(\chi_2+\chi_3) & \chi_2\chi_3^*+\chi_2^*\chi_3 & |\chi_2|^2+|\chi_3|^2. \end{pmatrix} \tag{C.10}$$

We want the final expression for $\mathcal{A}_{\Lambda_D}[\rho]$ to be expressed in terms of ρ instead of ψ. In that direction, we have to use the information that $\rho = \Lambda_D[\psi]$. Using the Kraus operators for Λ_D from eq. (2.9), we have an expression in terms of elements of density matrices

$$\begin{pmatrix} \rho_{11} & \rho_{12} \\ \rho_{21} & \rho_{22} \end{pmatrix} = \begin{pmatrix} |\chi_1|^2 & \frac{1}{\sqrt{2}}\chi_1(\chi_2^*+\chi_3^*) \\ \frac{1}{\sqrt{2}}\chi_1^*(\chi_2+\chi_3) & |\chi_2|^2+|\chi_3|^2. \end{pmatrix} \tag{C.11}$$

Some further rearranging of variables yields, finally,

$$\overline{U_1(\alpha)\psi U_1^\dagger(\alpha)} = \frac{1}{2}\begin{pmatrix} \rho_{00} & \rho_{01}/\sqrt{2} & \rho_{01}/\sqrt{2} \\ \rho_{01}^*/\sqrt{2} & \rho_{11}/2 & \frac{|\rho_{01}|^2}{\rho_{00}}-\frac{\rho_{11}}{2} \\ \rho_{01}^*/\sqrt{2} & \frac{|\rho_{01}|^2}{\rho_{00}}-\frac{\rho_{11}}{2} & \rho_{11}/2 \end{pmatrix} \tag{C.12}$$

Notice that this result no longer depends on ψ. Back to the main expression eq. (C.13), we then have

$$\mathcal{A}_{\Lambda_D}(\rho) = \frac{1}{2}\begin{pmatrix} \rho_{00} & \rho_{01}/\sqrt{2} & \rho_{01}/\sqrt{2} \\ \rho_{01}^*/\sqrt{2} & \rho_{11}/2 & \frac{|\rho_{01}|^2}{\rho_{00}}-\frac{\rho_{11}}{2} \\ \rho_{01}^*/\sqrt{2} & \frac{|\rho_{01}|^2}{\rho_{00}}-\frac{\rho_{11}^*}{2} & \rho_{11}/2 \end{pmatrix}\underbrace{\int d\mu_\psi \; \mathrm{Pr}_{\Lambda_D}(\psi|\rho)}_{1}, \tag{C.13}$$

from which we finally obtaineq. (2.15).

Appendix D

Finding the unitary evolutions in eqs. (2.39), (2.40) and (2.41)

In this appendix we will show how to obtain the unitary evolutions that yield reversible effective dynamics. We start by the simplest case, where the observed dynamics is trivial, and the microscopic evolution must be given by operators that obey eq. (2.34). Denote by U_1 the unitaries that yield such trivial effective dynamics, and we now that

$$\Lambda_D[\psi] = \Lambda_D[U_1\psi U_1^\dagger] \tag{D.1}$$

must hold for every microscopic state ψ.

Let us start by parameterizing a general microscopic state ψ as

$$\psi = \begin{pmatrix} a & e+if & g+ih \\ e-if & b & k+im \\ g-ih & k-im & 1-a-b. \end{pmatrix} \tag{D.2}$$

Then, using the Kraus operators for Λ_D given in eq. (2.9), we have that

$$\Lambda_D[\psi] = \begin{pmatrix} a & \frac{e+if+g+ih}{\sqrt{2}} \\ \frac{e-if+g-ih}{\sqrt{2}} & 1-a. \end{pmatrix} \tag{D.3}$$

In order to evaluate eq. (D.1), we must now compute $\Lambda_D[U_1\psi U_1^\dagger]$. Let us parameterize U_1 as

$$U_1 = \begin{pmatrix} u_{11} & u_{12} & u_{13} \\ u_{21} & u_{22} & u_{23} \\ u_{31} & u_{32} & u_{33}. \end{pmatrix} \tag{D.4}$$

Then, we have that

$$\Lambda_D[U_1\psi U_1^\dagger] = \sum_{i=1}^{2} K_i U_1 \psi U_1^\dagger K_i^\dagger, \tag{D.5}$$

where K_i are the Kraus operators of Λ_D, and U_1 and ψ are given by eqs. (D.4) and (D.2) respectively. We spare the reader from the hideous output of this calculation, which we simply dub

$$\Lambda_D[U_1\psi U_1^\dagger] = \begin{pmatrix} \gamma_{11} & \gamma_{12} \\ \gamma_{21} & \gamma_{22} \end{pmatrix} \tag{D.6}$$

, The actual elements of this matrix are easily found with numerical computational tools such as Mathematica [200], expressed in terms of the parameters of U_1 and ψ.

Now, we must impose that $\Lambda_D[\psi] - \Lambda_D[U_1\psi U_1^\dagger]$ is zero. This equality must be evaluated element-wise, i.e., every element of the resulting 2×2 matrix must be zero. Let us consider the first element of the first row, which we write out explicitly

$$a - \gamma_{11} = a(u_{11}u_{11}^* - u_{13}u_{13}^* - 1) + b(u_{12}u_{12}^* - u_{13}u_{13}^*) + e(u_{12}u_{11}^* + u_{11}u_{12}^*) + f(iu_{11}u_{12}^* - iu_{12}u_{11}^*)$$
$$+ g(u_{13}u_{11}^* + u_{11}u_{13}^*) + h(iu_{11}u_{13}^* - iu_{13}u_{11}^*) + k(u_{13}u_{12}^* + u_{12}u_{13}^*) + m(iu_{12}u_{13}^* - iu_{13}u_{12}^*) + u_{13}u_{13}^*. \tag{D.7}$$

Since eq. (D.1) must be valid for any microscopic state, the expression above will only equal zero if the coefficients of a, b, e, f, g, h, k, m are zero, which imposes the restrictions on the elements of U_1

$$u_{11}u_{11}^* - u_{13}u_{13}^* - 1 = 0 \tag{D.8}$$
$$u_{12}u_{12}^* - u_{13}u_{13}^* = 0 \tag{D.9}$$
$$u_{12}u_{11}^* + u_{11}u_{12}^* = 0 \tag{D.10}$$
$$iu_{11}u_{12}^* - iu_{12}u_{11}^* = 0 \tag{D.11}$$
$$u_{13}u_{11}^* + u_{11}u_{13}^* = 0 \tag{D.12}$$
$$iu_{11}u_{13}^* - iu_{13}u_{11}^* = 0 \tag{D.13}$$
$$u_{13}u_{12}^* + u_{12}u_{13}^* = 0 \tag{D.14}$$
$$iu_{12}u_{13}^* - iu_{13}u_{12}^* = 0 \tag{D.15}$$
$$u_{13}u_{13}^* = 0 \tag{D.16}$$

From these restrictions combined, we conclude that $u_{12} = u_{13} = u_{21} = u_{31} = 0$. Without loss of generality we set $u_{11} = 1$, and find that

$$u_{22} + u_{31} = u_{23} + u_{33} = 1. \tag{D.17}$$

Finally, all these constraints can be expressed in terms of a parameter $\alpha \in [0, 2\pi]$ such that we reach eq. (2.39).

$$U_1(\alpha) = \frac{1}{2} \begin{pmatrix} 2e^{-i\alpha} & 0 & 0 \\ 0 & (1 + e^{i\alpha}) & (1 - e^{i\alpha}) \\ 0 & (1 - e^{i\alpha}) & (1 + e^{i\alpha}). \end{pmatrix} \tag{D.18}$$

This process that was carried out above sets the path that we will follow to obtain eqs. (2.40) and (2.41): state an equation that imposes the relevant condition on the microscopic evolution and parameterize U and ψ to impose such condition.

Let us now do the same to obtain U_2, the unitary operators that describe microscopic evolutions yielding single-shot reversible effective dynamics. We want condition in eq. (2.33) to be satisfied, which we re-state in a similar way

$$\begin{aligned} &\text{if} \quad \Lambda_D[\psi_1] = \Lambda_D[\psi_1], \quad \text{then} \\ &\Lambda_D[U_2\psi_1 U_2^\dagger] = \Lambda_D[U_2\psi_2 U_2^\dagger]. \end{aligned} \tag{D.19}$$

for any microscopic states ψ_1, ψ_2. Recall the meaning of this expression: it sets the condition for U_2 to generate effective dynamics that always recover the state that was prepared initially, on every realization of the experiment, not just on average. These unitary operators must be such that they don't "split" microscopic states assigned to the same effective description. We can re-write this condition as

$$\begin{aligned} &\text{if} \quad \Lambda_D[\underbrace{\psi_1 - \psi_2}_{\chi}] = 0, \quad \text{then} \\ &\Lambda_D[U_2(\underbrace{\psi_1 - \psi_2}_{\chi})U_2^\dagger] = 0, \end{aligned} \tag{D.20}$$

with χ, then, being some Hermitian matrix with null trace. Let it be parameterized as

$$\chi = \begin{pmatrix} k_{11} & k_{12} & k_{13} \\ k_{12}^* & k_{22} & k_{23} \\ k_{13}^* & k_{23}^* & k_{33}. \end{pmatrix} \tag{D.21}$$

Then, the action of the coarse-graining map is given by the Kraus operators of Λ_D

$$\Lambda_D[\chi] = \begin{pmatrix} k_{11} & \frac{k_{12}+k_{13}}{\sqrt{2}} \\ \frac{k_{12}^*+k_{13}^*}{\sqrt{2}} & k_{22} + k_{33}. \end{pmatrix} \tag{D.22}$$

Following the condition in eq. (D.20), for $\Lambda_D[\chi] = 0$ we must impose $k_{11} = k_{22} + k_{33} = k_{12} + k_{13} = 0$.

Now, let U_2 be parameterized the same way as U_1, so we can compute $\Lambda_D[U_2\chi U_2^\dagger]$ and impose it to be zero. Just like before, we will not explicitly write the result of this calculation because it would be counter-productive. To impose $\Lambda_D[U_2\chi U_2^\dagger] = 0$, we demand that each of its elements is null, which yield the following conditions:

$$k_{12}^* u_{11}^* (u_{12} - u_{13}) + k_{12}(u_{11}u_{12}^* - u_{11}u_{13}^*) + k_{22}(u_{12}u_{12}^* - u_{13}u_{13}^*) + u_{13}k_{23}^*u_{12}^* + k_{23}u_{12}u_{13}^* = 0 \tag{D.23}$$

$$k_{12}^* (u_{21}^*(u_{22} - u_{23}) + u_{31}^*(u_{32} - u_{33})) + k_{12}(u_{21}u_{22}^* - u_{21}u_{23}^* + u_{31}u_{32}^* - u_{31}u_{33}^*) + \tag{D.24}$$

$$k_{22}(u_{22}u_{22}^* - u_{23}u_{23}^* + u_{32}u_{32}^* - u_{33}u_{33}^*) + k_{23}(u_{22}u_{23}^* + u_{32}u_{33}^*) + u_{23}k_{23}^*u_{22}^* + u_{33}k_{23}^*u_{32}^* = 0$$

$$k_{12}(u_{11}u_{22}^* - u_{11}u_{23}^* + u_{11}u_{32}^* - u_{11}u_{33}^*) + k_{12}^*(u_{12} - u_{13})(u_{21}^* + u_{31}^*) + k_{22} \tag{D.25}$$

$$(u_{12}u_{22}^* + u_{12}u_{32}^* - u_{13}u_{23}^* - u_{13}u_{33}^*) + k_{23}(u_{12}u_{23}^* + u_{12}u_{33}^*) + u_{13}k_{23}^*u_{22}^* + u_{13}k_{23}^*u_{32}^* = 0.$$

From these equations we learn that $u_{12} = u_{13} = 0$ and that $u_{22} + u_{32} = u_{23} + u_{33}$. Finally, we arrive at a possible parameterization of U_2 in terms of $\alpha, \beta \in [0, 2\pi]$

$$U_2(\alpha, \beta) = \frac{1}{2} \begin{pmatrix} 2e^{-i(\alpha+\beta)} & 0 & 0 \\ 0 & (e^{i\alpha} + e^{i\beta}) & -(e^{i\alpha} - e^{i\beta}) \\ 0 & -(e^{i\alpha} - e^{i\beta}) & (e^{i\alpha} + e^{i\beta}) \end{pmatrix}. \tag{D.26}$$

Lastly, let us derive eq. (2.41), the unitaries that generate reversible effective evolutions. They arise from a similar method where we impose the condition expressed in eq. (2.32), so we are looking for transformations U_3 that take average assigned states into average assigned states, or mathematically

$$\begin{aligned} &\text{if} \quad (\mathcal{A}_{\Lambda_D} \circ \Lambda_D)[\psi] = \psi, \quad \text{then} \\ &(\mathcal{A}_{\Lambda_D} \circ \Lambda_D)[U_3\psi U_3^\dagger] = U_3\psi U_3^\dagger. \end{aligned} \tag{D.27}$$

We can follow a perfectly analogous process as the ones before, only now demanding the following: for any microscopic state ψ in the form of eq. (2.15) (that is, for any average assigned state), U_3 must transform it into another microscopic state $U_3\psi U_3^\dagger$ that also has form given by eq. (2.15) (that it, it is also an average assigned state).

With the aid of mathematical tools, we find that the constraints that the elements of U_3 must obey are

$$u_{21} = u_{31} \tag{D.28}$$
$$u_{12} = u_{13} \tag{D.29}$$
$$u_{22} = u_{33} \tag{D.30}$$
$$u_{23} = u_{32}. \tag{D.31}$$

To find a form for U_3 that satisfies these conditions, we start by presenting the parametrization of SU(3) introduced in [201]

$$U_3(\theta_1, \theta_2, \theta_3, \phi_1, \phi_2, \phi_3, \phi_4, \phi_5) = \frac{1}{2} \begin{pmatrix} \chi_{11} & \chi_{12} & \chi_{13} \\ \chi_{21} & \chi_{22} & \chi_{23} \\ \chi_{31} & \chi_{32} & \chi_{33} \end{pmatrix}, \tag{D.32}$$

with

$$\chi_{11} = \cos\theta_1 \cos\theta_2 e^{i\phi_1}, \tag{D.33}$$

$$\chi_{12} = \sin\theta_1 e^{i\phi_3}, \tag{D.34}$$

$$\chi_{13} = \cos\theta_1 \sin\theta_2 e^{i\phi_4}, \tag{D.35}$$

$$\chi_{21} = \sin\theta_2 \sin\theta_3 e^{-i\phi_4-i\phi_5} - \sin\theta_1 \cos\theta_2 \cos\theta_3 e^{i\phi_1+i\phi_2-i\phi_3}, \tag{D.36}$$

$$\chi_{22} = \cos\theta_1 \cos\theta_3 e^{i\phi_2}, \tag{D.37}$$

$$\chi_{23} = -\cos\theta_2 \sin\theta_3 e^{-i\phi_1-i\phi_5} - \sin\theta_1 \sin\theta_2 \cos\theta_3 e^{i\phi_2-i\phi_3+i\phi_4}, \tag{D.38}$$

$$\chi_{31} = -\sin\theta_1 \cos\theta_2 \sin\theta_3 e^{i\phi_1-i\phi_3+i\phi_5} - \sin\theta_2 \cos\theta_3 e^{-i\phi_2-i\phi_4}, \tag{D.39}$$

$$\chi_{32} = \cos\theta_1 \sin\theta_3 e^{-i\phi_5}, \tag{D.40}$$

$$\chi_{33} = \cos\theta_2 \cos\theta_3 e^{-i\phi_1-i\phi_2} - \sin\theta_1 \sin\theta_2 \sin\theta_3 e^{-i\phi_3+i\phi_4+i\phi_5}. \tag{D.41}$$

where $\theta_1, \theta_2, \theta_3 \in [0, \pi/2]$ and $\phi_1, \phi_2, \phi_3, \phi_4, \phi_5 \in [0, 2\pi]$.

All that is left is to find the values for which the parameters satisfy conditions in eqs. (D.28), (D.29), (D.30) and (D.31). With enough brute force, one can obtain the values

$$0 \geq \frac{\sin\phi_5 - \phi_2}{\sin\phi_1 + \phi_2 + \phi_5} \geq 1 \tag{D.42}$$

$$\frac{\sin\phi_1 + 2\phi_2}{\sin\phi_1 + \phi_2 + \phi_5} \leq 0 \tag{D.43}$$

$$\phi_4 = \phi_3 \tag{D.44}$$

$$\frac{\theta_1}{\cos 2\theta_1} = \cos^2 2\theta_1 \left(\frac{\sin\phi_5 - \phi_2}{\sin\phi_1 + \phi_2 + \phi_5} \right) \tag{D.45}$$

$$\theta_2 = \arcsin\tan\theta_1, \quad 0 \leq \theta_1 \leq \pi/4 \tag{D.46}$$

$$\tan\theta_3 = -\cot^2\theta_1 \csc\phi_1 + \phi_2 + \phi_5 \sin\phi_1 + 2\phi_2. \tag{D.47}$$

As a final note, we point out that U_2 can be recovered by U_3 by setting $\theta_1 = \theta_2 = 0$, which yields

$$\begin{pmatrix} e^{i\phi_1} & 0 & 0 \\ 0 & \cos\theta_3 e^{-i\phi_1/2} & \sin\theta_3 e^{-i(\phi_1-\pi)/2} \\ 0 & \sin\theta_3 e^{-i(\phi_1-\pi)/2} & \cos\theta_3 e^{-i\phi_1/2} \end{pmatrix}. \tag{D.48}$$

If we make the change of variables $\phi_1 = -(\alpha + \beta)$ and $\theta_3 = (\alpha + \beta)/2$, we get

$$\frac{1}{2} \begin{pmatrix} 2e^{-i(\alpha+\beta)} & 0 & 0 \\ 0 & (e^{i\alpha} + e^{i\beta}) & -(e^{i\alpha} - e^{i\beta}) \\ 0 & -(e^{i\alpha} - e^{i\beta}) & (e^{i\alpha} + e^{i\beta}) \end{pmatrix}, \tag{D.49}$$

which is precisely U_2.

Appendix E

Volume of uncertainty for Λ_D

To obtain eq. (2.76), we will follow calculations completely analogous to the one found in [74], letting the software Mathematica do the brute-force evaluations.

Let us start by decomposing a given effective state $\rho \in \mathcal{L}(\mathcal{H}_2)$ as

$$\rho = \begin{pmatrix} \rho_{00} & 0 \\ 0 & \rho_{11} \end{pmatrix} + \frac{1}{2}(x\sigma_x + y\sigma_y), \tag{E.1}$$

where $x = \text{Tr}[\rho\sigma_x]$, $y = \text{Tr}[\rho\sigma_y]$, ρ_{ij} with $i,j \in \{0,1\}$ being the matrix coefficients of ρ. Let us parameterize the matrix elements of microscopic pure states $\psi \in \mathcal{L}(\mathcal{L}_3)$ as $\psi_{ij} = c_i c_j^*$, $i,j \in \{1,2,3\}$, such that $\psi = cc^\dagger$. We can write the action of Λ_D on a generic state as

$$\Lambda_D[\psi] = \begin{pmatrix} c_0 c_0^* & c_0(c_1^* + c_2^*)/\sqrt{2} \\ c_0^*(c_1 + c_2)/\sqrt{2} & c_1 c_1^* + c_2 c_2^* \end{pmatrix}, \tag{E.2}$$

where have simply applied the Kraus operators defined in eq. (2.9). In terms of these parameters, we can write the volume of $\Omega_{\Lambda_D}(\rho)$ as

$$\mathcal{V}_{\Lambda_D}(\rho) = \int d\mu_\psi \delta(c_0 c_0^* - \rho_{00})\delta(c_1 c_1^* + c_2 c_2^* - \rho_{11})\delta(\text{Tr}[\Lambda_D[\psi]\sigma_x] - x)\delta(\text{Tr}[\Lambda_D[\psi]\sigma_y] - y) \tag{E.3}$$

where simply used eqs. (E.1) and (E.2) to impose the constraint $\Lambda_D[\psi] = \rho$.

The trick now is to consider the Laplace or Fourier transformations of these objects, perform some calculations on the results, and subsequently evaluate the corresponding inverse transformation. The advantage of this method is that, between applying the integral transformation and its inverse, the expression will be independent of ρ, which will greatly simplify calculations.

We can re-write each term in parenthesis as follows

$$\begin{aligned} \delta(c_0 c_0^* - \rho_{00}) &= \mathfrak{L}^{-1}\{\mathfrak{L}\{\delta(c_0 c_0^* - \rho_{00})\}(s_0)\}(\rho_{00}) \\ &= \mathfrak{L}^{-1}\{\int_0^\infty d\rho_{00} e^{-s_0\rho_{00}}\delta(c_0 c_0^* - \rho_{00})\}(\rho_{00}) \\ &= \mathfrak{L}^{-1}\{e^{-s_0 c_0 c_0^*}\}(\rho_{00}), \end{aligned} \tag{E.4}$$

and similarly

$$\delta(c_1 c_1^* + c_2 c_2^* - \rho_{11}) = \mathfrak{L}^{-1}\{e^{-s_1 c_1 c_1^* + c_2 c_2^*}\}(\rho_{11}), \tag{E.5}$$

where $\mathfrak{L}$ is the Laplace transform. Furthermore,

$$\begin{aligned} \delta(\text{Tr}[\Lambda_D[\psi]\sigma_x] - x) &= \mathfrak{F}^{-1}\{\mathfrak{F}\{\delta(\text{Tr}[\Lambda_D[\psi]\sigma_x] - x)\}(k_x)\}(x) \\ &= \mathfrak{L}^{-1}\{\int_{-\infty}^{+\infty} dx e^{-ik_x x}\delta(\text{Tr}[\Lambda_D[\psi]\sigma_x] - x)\}(x) \\ &= \mathfrak{F}^{-1}\{e^{-ik_x \text{Tr}[\Lambda_D[\psi]\sigma_x]}\}(x) \\ &= \mathfrak{F}^{-1}\{e^{-ik_x c\Lambda_D'[\sigma_x]c^\dagger}\}(x), \end{aligned} \tag{E.6}$$

where Λ'_D is the dual of the map Λ_D, and similarly

$$\delta(\text{Tr}[\Lambda_D[\psi]\sigma_y] - y) = \mathfrak{F}^{-1}\{e^{-ik_y c\Lambda'_D[\sigma_y]c^\dagger}\}(y), \tag{E.7}$$

where $\mathfrak{F}$ is the Fourier transform (which we perform here instead of the Laplace transform because x, y can assume negative values).

Now, denote this intermediate object that we obtain after applying the integral transform by $\mathcal{I}$, and we re-write it as

$$\mathcal{I}[s_0, s_1, k_x, k_y] = \int d(c)e^{-c^\dagger Ac}, \tag{E.8}$$

with

$$A = \text{diag}(s_0, s_1, s_1) + i\Lambda'_D[k_x\sigma_x + k_y\sigma_y] \tag{E.9}$$

$$= \begin{pmatrix} s_0 & \frac{ik_x+k_y}{\sqrt{2}} & \frac{ik_x+k_y}{\sqrt{2}} \\ \frac{ik_x-k_y}{\sqrt{2}} & s_1 & 0 \\ \frac{ik_x-k_y}{\sqrt{2}} & 0 & s_1 \end{pmatrix}. \tag{E.10}$$

Mathematica can evaluate $\mathcal{I}$

$$\mathcal{I}[s_0, s_1, k_x, k_y] = \frac{\pi^4}{\det A}. \tag{E.11}$$

One can now consider ψ to be mixed, and let it be purified by an auxiliary space of dimension d_B. Then, perfectly similar calculations would yield

$$\mathcal{I}_{d_B}[s_0, s_1, k_x, k_y] = \frac{\pi^{4d_B}}{(\det A)^{d_B}}. \tag{E.12}$$

All that is left is to perform the inverse transforms, such that we recover the volume of uncertainty of ρ. Once again, with the aid of Mathematica, we get the final expression in terms of the Bloch vector of ρ:

$$\mathcal{V}_{\Lambda_D}(\rho) = \frac{2^{4-3d_B}\pi^{1+4d_B}(1+z)^{-d_B}(1-x^2-y^2-z^2)^{2(d_B-1)}}{\Gamma[d_B]\Gamma[2d_B-1]}. \tag{E.13}$$

Appendix F

The weighted Lovász number and maximum violation of inequalities

In this appendix we want to explore the relation between the weighted Lovász number of an exclusivity graph $\vartheta(\mathcal{G}_{ex}, w)$ and the maximum value one can achieve when evaluating the expectation value of some operator. We will follow the approach introduced in [132] and further explored, for instance, in [202, 203]. We suggest seeing [204] for in-depth discussions.

The paradigmatic example of a Bell inequality [152, 205], the CHSH inequality [206] describes a two-party scenario where Alice and Bob share a common bipartite quantum state, upon which they perform local measurements. Alice can choose to apply one out of two dichotomic observables $\{A_0, A_1\}$, with possible outcomes $\{-1, +1\}$. Bob, on his side, can perform $\{B_0, B_1\}$ with outcomes $\{-1, +1\}$. The CHSH inequality states that, for classical theories,

$$S_{CHSH} = \langle A_0 B_0 + A_0 B_1 + A_1 B_0 - A_1 B_1 \rangle \leq 2, \tag{F.1}$$

where the braket notation $\langle M \rangle$ denotes the expectation value of the measurement M on some given quantum state. Notoriously, this upper bound can be violated in quantum theories up to the value of $2\sqrt{2}$, the famous Tsirelson bound [207].

We will now present the approach to obtaining the maximum violation of eq. (F.1) using graph theory, a method extensible to any linear inequality.

What one wants to find out is what is the maximum value that a given function (in this case, S_{CHSH}) can achieve while obeying a set of restrictions. S_{CHSH} is a function of the outcome probabilities of measurements $\{A_i B_j\}_{i,j=0,1}$, and the restrictions arise from the fact that these probabilities are not independent. In fact, they must obey exclusivity relations among them, such that they cannot simply assume any value regardless of their context.

One might already foresee how $\vartheta(\mathcal{G}_{ex}, w)$ comes into the scene. The task we are trying to perform is precisely the definition of the weighted Lovász number: what is the maximum value a function of probabilities $\{p_i\}$ can assume, given that they must arise from a valid quantum realization compatible with exclusivity relations between the given measurements.

Let us take another look at eq. (F.1). Denote by $p(xy|XY)$ the probability associated to event $(xy|XY)$, where one measures XY and obtains outcomes x, y. We can rewrite the CHSH inequality as

$$
\begin{aligned}
S_{CHSH} = &\underbrace{p(00|00) - p(01|00) - p(10|00) + p(11|00)}_{\langle A_0 B_0 \rangle} \\
&+ \underbrace{p(00|01) - p(01|01) - p(10|01) + p(11|01)}_{\langle A_0 B_1 \rangle} \\
&+ \underbrace{p(00|10) - p(01|10) - p(10|10) + p(11|10)}_{\langle A_1 B_0 \rangle} \\
&- \underbrace{p(00|11) - p(01|11) - p(10|11) + p(11|11)}_{\langle A_1 B_1 \rangle}.
\end{aligned}
\tag{F.2}
$$

Notice, additionally, that these probabilities can be further simplified, since $\sum_{ij} p(ij|A_i B_j) = 1$. This yields

$$S_{CHSH} = 2(p(00|00) + p(11|00) + p(00|01) + p(11|01)$$
$$+ p(00|10) + p(11|10) + p(01|11) + p(10|11)) - 4 \leq 2. \tag{F.3}$$

If we let

$$\tilde{S}_{CHSH} = p(00|00) + p(11|00) + p(00|01) + p(11|01) + p(00|10) + p(11|10) + p(01|11) + p(10|11), \tag{F.4}$$

then we have a simpler and yet equivalent expression

$$\tilde{S}_{CHSH} \leq 3. \tag{F.5}$$

To find the maximum violation of this inequality, we must first establish the exclusivity graph associated to these probabilities, which results in G_{CHSH} portrayed in fig. 4.1. Now, we can compute the weighted Lovász number of this graph, that we re-state here for convenience

$$
\begin{aligned}
\textbf{given} \quad & \{w_i\}_{i=1}^8, G_{CHSH} \\
\textbf{maximize} \quad & \sum_{i=1}^8 w_i |X_{0i}|^2 \\
\textbf{subject to} \quad & X_{ii} = 1, \quad i = 0, \ldots, n \\
& X_{ij} = 0, \quad \text{if } (i,j) \in E \\
& X \geq 0 \,.
\end{aligned}
\tag{F.6}
$$

By choosing $w_i = 1$, $\forall i$ we make the objective function reflect $\tilde{S}_{CHSH}$ and the solution to this optimization gives us precisely the maximum violation of eq. (F.5). As expected, by computing this SDP we get $\vartheta(G_{CHSH}, 1) = 2 + \sqrt{2}$, which corresponds to the Tsirelson bound for eq. (F.1).

Notice that for this specific case we ended up evaluating the regular Lovász number $\vartheta(G_{CHSH})$. This happened because the structure of the CHSH inequality attributed equal weights to the probabilities we must consider, but this is a mere coincidence. When evaluating the maximum violation of other Bell inequalities one might have to choose more complex sets of weights $\{w_i\}$ to reflect them.

Appendix G

Calculations leading to the upper bound on $\mathcal{R}_{A \prec B}$

In this section we will show that the robustness of one-way signaling from Alice to Bob, denoted by $\mathcal{R}_{A \prec B}$, must obey the bound

$$\mathcal{R}_{A \prec B}(W) \leq d_O^2 - 1, \quad d_O := \max(d_{A_O} d_{B_O}). \tag{G.1}$$

We will follow the same steps carried out in [194] to find the upper bound for $\mathcal{R}_s$, only applied to a different set of processes: $\mathcal{R}_s$ measures the distance to $\mathcal{W}_{par}$ (the set of processes where no signaling takes place), while $\mathcal{R}_{A \prec B}$ measures the distance to $\mathcal{W}_{A \prec B}$ (the set of processes where Alice's actions precede those of Bob, so there can be no signaling from Bob to Alice).

Let us first show a relevant property of process matrices. Define the channel D acting on a process W as

$$D[W] = d \operatorname{Tr}[W]\mathbb{1} - W, \tag{G.2}$$

where d is the dimension of W, that is, $d = d_{A_I} d_{A_O} d_{B_I} d_{B_O}$, and $\mathbb{1}$ is the identity in the same space of W.

Notice that this map is completely positive. Indeed, all processes obey $W \geq 0$, and since $\operatorname{Tr}[W] = d_{A_O} d_{B_O}$ it is clear that its largest eigenvalue can be at most $d_{A_O} d_{B_O}$, so $D[W] \geq 0$. This means that applying D to only a part of W still yields a positive result, and

$$D^{B_O}[W] = d_{B_O} \operatorname{Tr}_{B_O}[W] \otimes \mathbb{1}_{B_O} - W \geq 0. \tag{G.3}$$

Recall the definition of the trace-and-replace operation, and realize that exchanging d_{B_O} for $max(d_{A_O}, d_{B_O})$ will not affect the positivity of $D^{B_O}[W]$. One can then conclude that

$$d_{O B_O}^2 W - W \geq 0. \tag{G.4}$$

Now, we want to evaluate an upper bound for $\mathcal{R}_{A \prec B}$, which can be determined from its dual formulation eq. (6.27) as

$$\mathcal{R}_{A \prec B}(W) = \max \frac{\operatorname{Tr}[WS]}{d_{A_O}} - 1. \tag{G.5}$$

Using eq. (G.4), we have

$$\mathcal{R}_{A \prec B}(W) \leq \max \frac{d_O^2}{d_{A_O}} \operatorname{Tr}[_{B_O} WS] - 1 \tag{G.6}$$

$$= \max \frac{d_O^2}{d_{A_O}} \operatorname{Tr}[W_{B_O} S] - 1 \tag{G.7}$$

$$= \max \frac{d_O^2}{d_{A_O} d_{B_O}} \operatorname{Tr}[W \operatorname{Tr}_{B_O} S \otimes \mathbb{1}_{B_O}] - 1, \tag{G.8}$$

where we have used the fact that the trace-and-replace operation is self-dual. Then, from the dual formulation of $\mathcal{R}_{A \prec B}$ we also know that $\text{Tr}_{B_O}[S] \leq \mathbb{1}_{A_I A_O B_I}$, so

$$\mathcal{R}_{A \prec B}(W) \leq \max \frac{d_O^2}{d_{A_O} d_{B_O}} \text{Tr}[W \mathbb{1}_{A_I A_O B_I B_O}] - 1. \tag{G.9}$$

Finally, since $\text{Tr}[W] = d_{A_O} d_{B_O}$,

$$\mathcal{R}_{A \prec B}(W) \leq d_O^2 - 1. \tag{G.10}$$

This bound is also tight, and can be saturated by any process where Alice can signal perfectly to Bob, such as the identity channel. An example is

$$W_{A \to B} = \mathbb{1}_{A_I} \Phi^+_{A_O B_I} \mathbb{1}_{B_O}, \tag{G.11}$$

which is a particular case of the model in eq. (6.18), with $p = 1$ and $q = 0$.